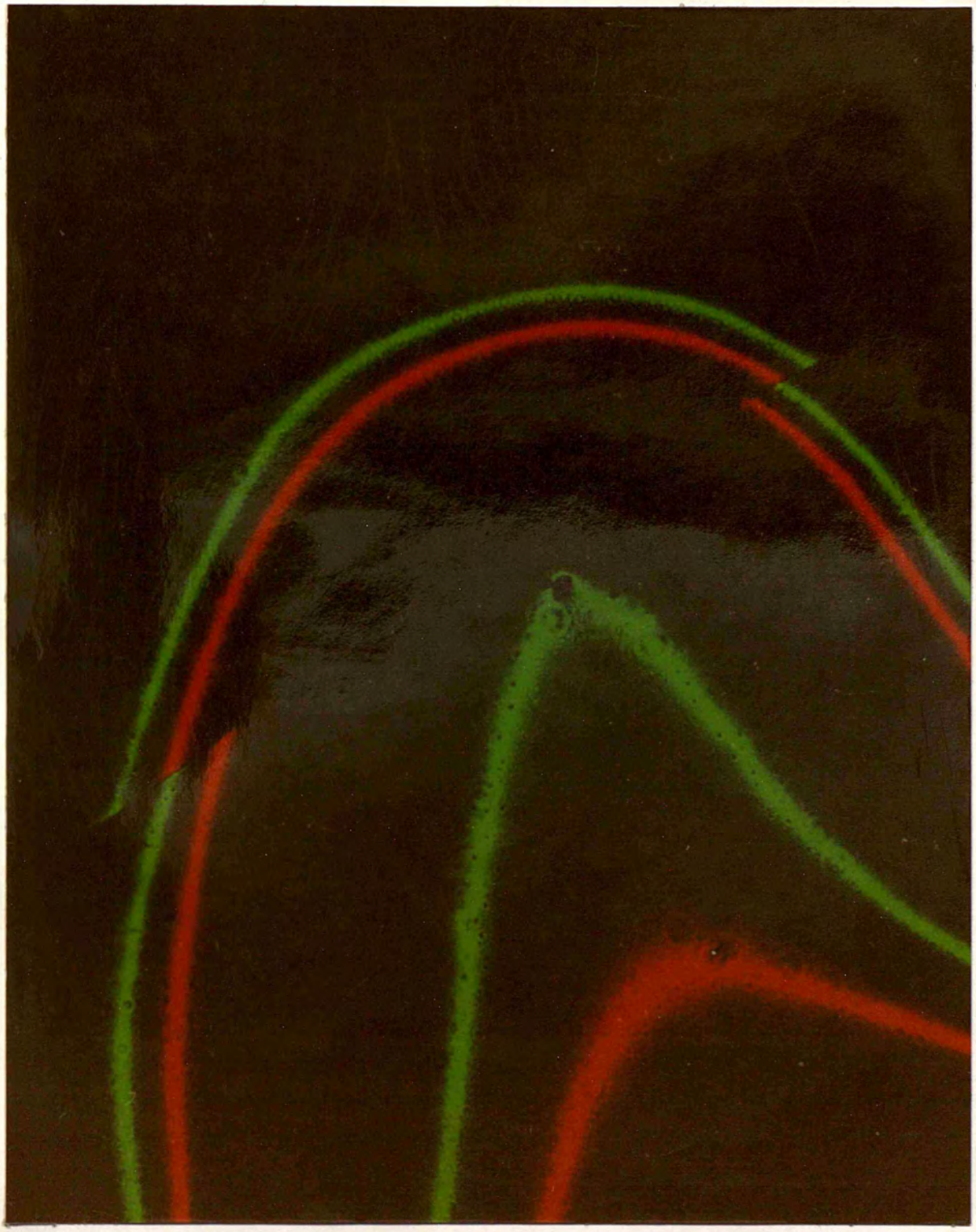

MULTIPLE BEAM FIZEAU FRINGES IN THE FIRST ORDER OBTAINED ON A SILVERED MICA SURFACE FEATURING A CLEAVAGE STEP OF 315 Å

OPTICAL AND INTERFEROMETRIC INVESTIGATIONS OF SOME METALLIC THIN FILMS

MOHAMED SAFI-EL-DIN SHAALAN

Royal Holloway College

This thesis is submitted for the Degree of
Doctor of Philosophy in the University of London

April, 1975

TO MY PARENTS

CONTENTS

CONTENTS
(continued)

C O N T E N T S
(continued)

ACKNOWLEDGEMENTS

I wish to express my deep sense of sadness at the loss of my teacher and supervisor, the late Prof. S. Tolansky. I am indebted to him for suggesting the subject investigated here and for his continuous guidance, interest and warm care, which he always gave me until his untimely death in March, 1973.

- - - - - - - - - - -

I would like to thank Dr V.I. Little to whom I am grateful for encouragement and guidance throughout the last two years. My thanks are also due to friends and colleagues at the Physics Department of Royal Holloway College especially Dr A.J. Taylor for help and advice on computing, and for many useful discussions. I would like to thank the technical staff of the department for help in constructing apparatus and evaporation techniques. In particular Mr M. Thyer, Mr G. Hayward and Mr J. Williams. I would like to thank Ina Godwin for the able typing.

This work was made possible through maintenance grants from the British Council and the Egyptian Government.

ABSTRACT

A sensitivity study is conducted on the polarimetric measurable $\Delta = (\delta_p - \delta_s)$, the differential change of phase on reflection air/metallic film. A computer aided study shows the quantity Δ to be sensitive to the extinction coefficient k and to film thickness. It is only sensitive to the refractive index n in certain ranges of n, k and for certain d values. For films of $d \geq 200$ Å, Δ becomes insensitive to n but maintains high sensitivity to k, while for $d \leq 200$ Å it shows some sensitivity to n as well as k in certain ranges of lower values of $k \leq 2.5$.

An interferometric technique due to Tolansky (1944), is used to determine Δ as a function of θ, the angle of incidence for films of Ag, Au and Aℓ at different wavelengths in the visible region of the spectrum. It is shown that this interferometric technique, when critically applied, is capable of an accuracy of $\pm 0.003\pi$.

The extinction coefficients of films investigated are found from curves of Δ vs n for constant values of k. They are shown to be accurate to ± 0.03 when Δ is accurate to $\pm 0.003\pi$ thus rendering a simple and inexpensive technique an accurate and effective method for the determination of the extinction coefficient of highly reflecting metallic films.

A new optical system to produce multiple beam interference fringes of variable chromaticity in the first order is described. The system enables the surveying of features within the order. It also removes the

ambiguity met in conventional monochromatic interferometry concerning the order of interference to which a fringe may belong. White light multiple fringes are obtained first and the orders are recognized.

Some outlines are projected for investigating the sensitivity of the optical phase properties of metallic films, namely the phase changes on reflection air/metallic film β, dielectric substrate/metallic film β' and in transmission γ, at normal incidence, to n, k and d. It is proposed to try to explain and link the behaviour of these phase quantities with thickness for $d \leq 200$ Å in terms of n and k. Also a compact new monochromator to produce fringes of variable chromaticity for surface microtopography studies is projected.

GENERAL INTRODUCTION

In trying to open this general introduction to this thesis there was nothing more expressive of what one may say in introducing interferometry than the first few lines Tolansky wrote in the preface of his Introduction to Interferometry[34]

> ".... Interferometry is an elegant branch of optics. It is elegant because of it's economy of means. With little more than two slits or two mirrors one can, on the one hand, plumb the depth of space to measure the diameter of a star or, on the other hand, the heart of a crystal to measure the sizes of molecules ... . The essential success with interferometry lies not so much in the means at disposal but in the critically correct use of these simple means. The subject therefore constitute an admirable exercise in discretionary application ... "

Two main areas where interferometric techniques proved to be a powerful and versatile tool are thin film optics and surface microtopography. Many of the significant developments in these two areas were originated in this department during the last three decades. Tolansky's application of multiple-beam Fizeau fringes and fringes of equal chromatic order to measure the thickness of thin films[39,8], remains the most widely used. The applications of interferometry to topographical studies are too numerous to be mentioned here. However the extensive number of studies carried out on mica and diamonds would illustrate the point[39]. In this thesis it is sought to further develop the use of interferometric techniques in these two areas of thin film optics and surface microtopography. As for the first field we deal here with a physical quantity essential for the determination of optical constants. This quantity is the change of phase at reflection at the boundary between two optically different media. In thin film optics the quantity usually determined is $\Delta = (\delta_p - \delta_s)$ the differen- change of phase at reflection, i.e. the difference in phase upon reflection, at angles other than normal, between the light vibrating parallel and perpendicular to the plane of incidence. A technique first reported by

Tolansky[5] and later used and developed by Avery[7] and Barakat and Shaalan[33], for the determination of Δ as functions of θ the angle of incidence, is optimized and used together with computer prepared graphs to extract the extinction coefficient of thin highly reflecting films. Thus rendering multiple beam interferometry useful for the determination of the optical constant k. As will be shown in the following chapters, the method is capable of accuracy comparable to those achieved by other methods with the added advantages of economy and simplicity. The computer study of the properties of the quantity Δ yielded some interesting points useful in designing experimental set-ups and explains the poor sensitivity of some methods used to find Δ in certain regions of n and k values.

In the second area dealt with in this thesis, namely surface micro-topography, a new optical set-up is used to produce 'fringes of variable chromaticity in the first order'. These are observed for the first time. The idea is that if and when white light multiple beam fringes are obtained between two surfaces, only the first and second orders are clearly seen because overlapping occurs for higher orders. The order of interference therefore, that is first or second, is never in doubt. In multiple-beam fringes with monochromatic light, one has no idea as to what order of interference the observed fringe belongs. To determine the order of interference it is necessary to produce f.e.c.o. fringes and resort to some calculations. In white-light multiple beam fringes the ambiguity is totally removed. In the first order one has a pure spectrum from the blue to the red. The blue fringe is surrounded by a 'black fringe' at the point of contact, i.e. at the edge of the wedge. However the white-light pattern remains only a beautiful descriptive pattern without means of yielding information about the surface it contours in a quantitative manner. Tolansky[58], produced such fascinating patterns on mica surfaces. He noted that if the first order spectrum could be divided into a hundred

parts, this division would correspond to dividing the height of the wedge enclosing the first order spectrum into 13 Å steps or thereabouts, i.e. a chromatic change of about 25 Å. In this thesis we shall describe an optical monochromator set-up capable of producing a chromatic change of ~20 Å resulting in height changes of the order of 10 Å in the part of the wedge enclosing the first order fringes. The system is capable of yielding a topographical map representative of the space within the known order in the up and down directions.

Now, as for interferometric determination of the extinction coefficient of highly reflecting thin films, we note that the three parameters which define a thin absorbing film at a certain wavelength are d the thickness, n 'the refractive index' and k 'the extinction coefficient" where $\hat{n} = n - ik$ is the 'complex refractive index'. The term constants is somewhat misleading, specially when applied to films with $d \leq \lambda$ since the structure of the film plays a dominant role in determining its properties. However, for films of thickness sufficient to ignore the effects of multiple reflections within them, the constants approach stable values characterizing the bulk material. the constants n and k are not directly measurable quantities. They cou ' be found from measurements performed to determine quantities that are related to them by formulae based on the electromagnetic theory. In a broad sense, these quantities could be divided into two categories, reflected and transmitted intensities of light falling onto the surface of the specimen, and phase changes upon reflection and in transmission. The combination to be used will depend upon the nature of the problem at hand. In the general case of an absorbing film on a non-absorbing substrate, and for thick films where multiple reflections within them could be ignored, the following set of equations[1] hold and could be used to determine the optical constants:

$$n^2 - k^2 = t^2 \frac{(\cos^2 2\psi - \sin^2 2\psi \sin^2 \Delta)}{(1 + \sin 2\psi \cos \Delta)^2} + \sin^2 \theta$$

$$2nk = \frac{\sin 4\psi \sin \Delta}{(1 + \sin 2\psi \cos \Delta)^2}$$

$$t = \sin \theta \tan \theta$$

$$-\cot \Delta = (p^2 + q^2 - t^2)/2qt$$

$$\sec 2\psi = (p^2 + q^2 + t^2)/2qt$$

where

$$2p^2 = n^2 - k^2 - \sin^2\theta + \left[(n^2 - k^2 - \sin^2\theta)^2 + 4n^2k^2\right]^{\frac{1}{2}}$$

$$2q^2 = -n^2 + k^2 + \sin^2\theta + \left[(n^2 - k^2 - \sin^2\theta)^2 + 4n^2k^2\right]^{\frac{1}{2}}.$$

In the above formulae,

$\Delta = \delta_p - \delta_s$ the differential change of phase on reflection air/metallic surface.

$\psi = \tan^{-1} \frac{\rho_p}{\rho_s}$ where ρ_p and ρ_s are the reflected amplitudes for the $\parallel$ and $\perp$ components.

θ is the angle of incidence.

The previous set of equations are, perhaps, best dealt with using Drude's[2] polarimetric techniques. Measurements are made at reflection and at oblique incidence. When $d \leq \lambda$ expressions which take into account multiple reflections within the film must be used. However, there exist many variations on this general technique to suit certain applications and sometimes to suit some research budgets! The different approaches to the problem of the choice of a method to determine the optical constants of absorbing films are discussed in reviews by Abele's[3] and Heaven's[4].

Tolansky[5] used multiple beam fringes, formed in transmission using a lens-plate interferometer, to determine $\Delta = (\delta_p - \delta_s)$ as a function of the angle of incidence. The film coating the interferometer's plates was a silver film of about 500 Å. This approximates very closely to the case of bulk silver since the optical constants of silver films of $d \geq 200$ Å

are nearly those of the bulk metal[6]. Avery[7] used the technique together with measuring the ratio of the reflected amplitudes to deduce the optical constants of silver, copper and tin films. A survey of literature on the techniques for determining the measurable quantities leading to n, k and d would reveal that interferometric techniques are only largely used for determining d using Tolansky's method[8]. They are also used in determining phase changes at reflection and in transmission[9,10,11,12]. Schulz[13] used an interferometric assembly to determine k the extinction coefficient of silver films. This was based on determining the phase change at reflection dielectric/metallic film interface at normal incidence.

In this thesis the quantity Δ is determined interferometrically as a function of θ for films of silver, gold and aluminium at different wavelengths. This is done in the light of a computer analysis of the dependence of Δ on the parameters n, k and d. A preliminary investigation showed two cases of principal interest for films of thickness above and below 200 Å. For the thicker films Δ is insensitive to n but k the extinction coefficient could be found to ± 0.025 when Δ is measured to $\pm 0.0025\,\pi^{\circ}$ at the highest possible angle of incidence. For films of $d \leq 200$ Å, Δ shows some dependence on n as well as k. This increases as the film thickness decreases, and in the lower range of $k \leq 2.5$. Also the dependence on n is more pronounced in the higher ranges of n where n is in the neighbourhood of 2.0.

The first case is fully investigated here using interferometric methods. The second case of $d \leq 200$ Å could be investigated using special interferometers, e.g. koster interference comparator at normal incidence. Outlines for further work in this direction are given at the end of this present work. In the case when the highly reflecting film is of thickness $d \geq 200$ Å, the experimental arrangement is to deposit

such a film on two high grade optical flats which will constitute the two plates of a coated air wedge interferometer in transmission.

Multiple beam Fizeau fringes are first secured at normal incidence. In transmission they are bright, straight line fringes on a dark background, they run parallel to the edge of the wedge. As the incidence changes from normal, the fringes get broader, and for $\theta \geq 20^{\circ}$, depending on the original shrpness of the fringes, each splits in two components. It can be shown that the two components belong to light vibrating parallel and perpendicular to the plane of incidence with the outer fringe, belonging to the perpendicular component, moving away and becoming progressively sharper and weaker. The difference in path resulting from the phase difference at reflection for the two light components, parallel and perpendicular to the plane of incidence, shows itself as a finge separation, allowing Δ to be measured as a fraction of the interferometric order separation. This permits Δ to be expressed as a fraction of λ the wavelength of light used to illuminate the interferometer, since a path difference of $\lambda/2$ is equivalent to difference in phase of π°. A Δ vs θ curve is obtained experimentally and the value of k, the extinction coefficient, is deduced from computed curves of Δ vs n with k as a parameter.

In the surface microtopography area, experiments were performed to show the possibility of achieving a scanning fringe set-up of variable chromaticity. White-light multiple beam fringes were obtained on mica surfaces. Observed under proper optical conditions, the first order fringes, of pure spectrum colours, are clearly seen. They are followed by second and higher orders where overlapping takes place. A simple calculation would show that the first order fringes do enclose between their blue and red ends, a topographical height interval of the order of 1500 Å.

In monochromatic multiple beam interferometry, the topographical height enclosed between any two successive fringes is $\lambda/2$. This is 2730 Å in the case of the mercury green line. Thus when working inside one single order we have a greatly enhanced topographical sensitivity with the added knowledge of the order of interference. However, to estimate the topographical changes, one must either measure the changes in wavelength and relate them to the corresponding height changes, or measure the height changes in step forms, and relate them to the wavelength at which they occur. The latter case is the conventional chromatic multiple beam interferometric procedure. To achieve the first goal, the first order fringes must be divided in spectral steps of the order of 20 Å, corresponding to some 10 Å in height changes. This end was realized in this work, by setting up a monochromator system with a constant deviation prism as its dispersing element.

The system, to be described later in detail, has the following main features:

(1) a white light source

(2) a multichromatic line source

(3) a monochromatic source

(4) a constant deviation spectrometer with its telescope removed.

Light from the white light and multichromatic sources is, simultaneously, focused down onto the entrance slit of the spectrometer. Parallel rays fall on the constant deviation prism. The dispersed rays are collected by a 100 cm focal length lens at the focal point of which a narrow slit is placed. The lens produces a strip of dispersed white light spectrum from the deep blue to the deep red, with a line spectrum clearly imposed upon it.

The length of the spectrum strip and the width of the slit is such that it makes it possible to select narrow bands of spectrum, 10 Å - 20 Å

are typical values. The imposed line spectrum serves the purpose of calibrating the white light spectrum strip. Now the wavelength selected by the exit slit could be varied at will by turning the prism table drum. The calibrated drum could read to 1.0 Å. The third source, a filtered monochromatic spectral lamp, provides a one fixed wavelength focused onto the exit slit through the same 100 cm focal length lens, replacing the spectrometers telescope arm but not via the prism. The mixture of light emerging from the exit slit is rendered parallel and allowed to fall onto the test piece interferometer. A microscope with a camera attachment, permit photographic recordings of the interference fringes. When white light interference bands are obtained and first order spectrum clearly seen, light from the fixed wavelength is allowed to fall on the test piece and one would observe the monochromatic fringes contouring the features of the surface. Now obscuring the calibration spectrum and allowing the white light spectrum through the exit slit, one observes (i) the fixed wavelength fringe of the first order, and (ii) the variable chromaticity fringe formed by light selected by the slit from the white light spectrum strip. If the feature contoured by the first order fringes is, say, a step of 50 Å in height, one would obtain a coincidence, across the step, between the fringe belonging to the fixed wavelength λ_1 and a fringe belonging to a wavelength $(\lambda_1 + 100)$Å, read on the spectrometers drum (see front piece photograph). The height of the step $[(\lambda_1 + 100) - \lambda_1]/2$ thus obtained. However, since the fringes are formed in transmissions, the phase change at reflection inside the wedge gab would affect the step height calculated from the above formula. This problem needs knowledge of values of the phase change at reflection at the air/silver interface, for the particular wavelengths involved. Alternatively the whole experiment could be performed in reflection, i.e. having a reflected fringe system[8,39]. This point will be taken up later in greater detail.

To investigate the topographical details of the first order enclave, different filters may be used to produce different fixed wavelength fringes, while the spectrometers drum provides the variable element. In this way the first order, or any other, span could be scanned to produce a topographical map describing the surface under examination. The set-up could be improved, e.g. by the use of two grating monochromators moving against each other, providing greater dispersion and higher accuracy. This will be mentioned at the end of this thesis. The above described method seems to achieve the goal of 'within the order', 'inch-by-inch' survey of surface micritopography with the minimum calculation, and with both ease of experimentation and elegance of interference techniques.

Chapter I of this thesis states the Maxwell equations, and defines the optical constants of an absorbing medium. It also reviews methods and techniques employed to determine the optical constants n and k. In Chapter II, a computer aided study of the dependence of the quantity Δ on thickness, wavelength, angle of incidence, and the constants n and k are also presented. Chapter III describes the experimental arrangements used to determine Δ as a function of θ and the interferometric thickness determination. In Chapter IV the intensity properties of multiple beam Fizeau fringes at oblique incidence are discussed. It is shown that the difference in intensity between fringes, belonging to the perpendicular and parallel components, could be accounted for in terms of interferometric properties of the system, as well as the optical properties of the interferometer coating layers. Chapter V contains experimental results on Ag, Au and Al films, presented and compared with previous work. The values of k for these films at different wavelengths, are given in Chapter VI.

The principles and experimentation involved in the production of the fringes of variable chromaticity and their applications, are contained in Chapters VII and VIII. Chapter IX projects some ideas for future work both on sensitivity studies of phase changes and on developing the microtopographic techniques described in Chapters VII and VIII.

CHAPTER I

DEFINITIONS AND REVIEW OF METHODS USED TO DETERMINE THE PARAMETERS OF THIN ABSORBING FILMS

I.1 THE WAVE EQUATION AND THE OPTICAL CONSTANTS

It can be shown[14-16] that when the equations for wave propagation in an absorbing medium are developed, reflection and refraction at the boundary between absorbing and transparent media can be completely described. The theory of the propagation of electromagnetic waves in a conducting medium is based on Maxwell's field equations, which may be written as:

$$\text{curl } \hat{E} = -\mu\mu_o \frac{\partial \hat{H}}{\partial t} \quad \ldots (I.1)$$

$$\text{div } \hat{H} = 0 \quad \ldots (I.2)$$

$$\text{curl } \hat{H} = \sigma\hat{E} + \epsilon\,\epsilon_o \frac{\partial \hat{E}}{\partial t} \quad \ldots (I.3)$$

$$\text{div } \hat{E} = 0 \,, \quad \ldots (I.4)$$

where ϵ_o and μ_o are the permittivity and permeability of free space, and μ and ϵ are the specific permeability and relative permittivity of the medium, and the other symbols have their usual meaning. Equation (I.4) is taken as zero since in a conducting medium there can be no permanent free charge density. Hence:

$$\text{curl curl } \hat{E} = -\mu\mu_o \left(\sigma \frac{\partial \hat{E}}{\partial t} + \epsilon\,\epsilon_o \frac{\partial^2 \hat{E}}{\partial t^2}\right),$$

but

$$\text{curl curl } \hat{E} = \text{grad div } \hat{E} - \nabla^2 \hat{E} \,,$$

therefore

$$\nabla^2 \hat{E} - \sigma\mu\mu_o \frac{\partial \hat{E}}{\partial t} - \mu\mu_o\,\epsilon\,\epsilon_o \frac{\partial^2 \hat{E}}{\partial t^2} = 0 \,. \quad \ldots (I.5)$$

A similar equation for $\hat{H}$ can be obtained. As a solution for equation (I.5) we write,

$$E_x = E_o\, e^{i\omega(t - x/v)} \quad \ldots (I.6)$$

or

$$E_x = E_o\, e^{i\omega t} \cdot e^{-i2\pi/\lambda \cdot c/v \cdot x} \,. \quad \ldots (I.7)$$

This solution satisfies equation (I.5) provided

$$\frac{1}{v^2} = \mu\epsilon\mu_o\,\epsilon_o - i\,\sigma\mu_o\,\mu/\omega \,. \quad \ldots (I.8)$$

In equation (I.7) the ratio c/v is the refractive index of the absorbing medium. From equation (I.5) it is obvious that the ratio c/v is complex, hence $N = \frac{c}{v} = n - ik$ is the 'complex refractive index' of the medium,

where n and k are the 'optical constants'. $k = (nk)$ is the extinction coefficient. Equation (I.7) becomes:

$$E_x = E_0 \, e^{i\omega t} \cdot e^{-i2\pi/\lambda \cdot N \cdot x}$$
$$= E_0 \, e^{i\omega t} \cdot e^{-i2\pi/\lambda \cdot (n - ik) \cdot x}$$

$$\therefore \quad E = E_0 \cdot e^{-2\pi/\lambda \cdot k \cdot x} \cdot e^{-i2\pi/\lambda \cdot n \cdot x} \cdot e^{i2\pi/\lambda \cdot c \cdot t} \qquad \ldots (I.9)$$

In equation (I.9) the real exponential function represents an exponential damping of the amplitude of a wave travelling in an absorbing medium. Multiplying (I.9) by the complex conjugate gives the intensity and leads to the well known absorption law. Hence:

$$I = I_0 \cdot e^{-4\pi/\lambda \cdot k \cdot x} \qquad \ldots (I.10)$$

where I_0 is the intensity of the incident light, and I is the intensity after the wave has travelled a distance x in the medium. It seems useful, at this stage, to emphasize that the foregoing description of the propagation of a monochromatic wave in an absorbing medium assumes the following assumptions:

(a) The wave falls normally on the surface of the absorbing medium.

(b) The medium is isotropic.

(c) The thickness of the medium is $>>> \lambda$ the wavelength of the incident wave.

I.2 THE REFLECTED AMPLITUDES AND ACCOMPANING PHASE CHANGE

Consider the reflection of a beam of light polarized either parallel or perpendicular to the plane of incidence, at the boundary between a transparent medium and an absorbing medium; let n_1 be the refractive index of the transparent medium, and the incident wavefront be plane, of unit amplitude and zero phase immediately before reflection, and let θ be the angle of incidence. The angle of refraction into the absorbing medium η is given by Snell's law:

$$n_1 \sin\theta = N \sin\eta \, , \qquad \ldots (I.11)$$

and since we have seen that N is a complex quantity for an absorbing

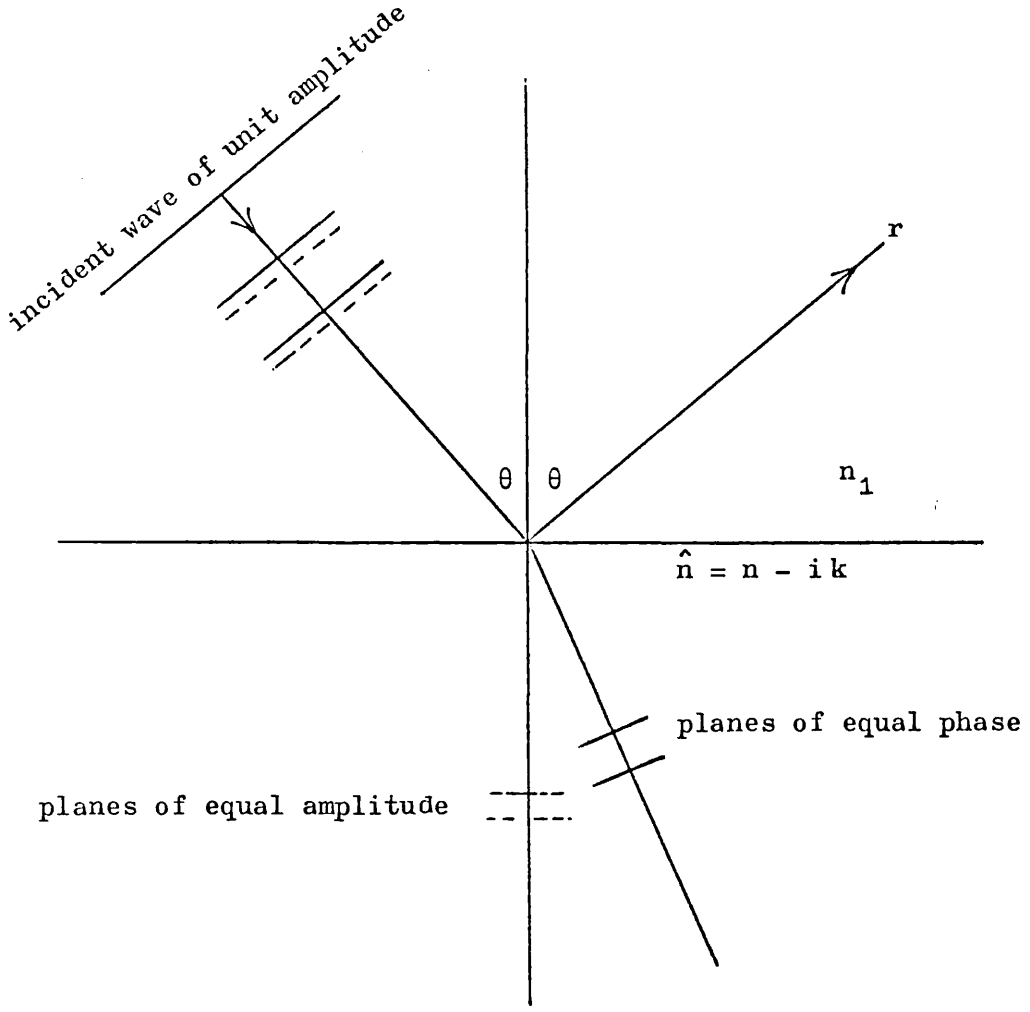
incident wave of unit amplitude
r
θ
θ
n_1
$\hat{n} = n - ik$
planes of equal phase
planes of equal amplitude

Fig.I.1

medium, it follows that the angle of refraction η must also be complex. When an electromagnetic disturbance is travelling in a non-absorbing medium, the wave fronts, i.e. the planes of equal phase are also planes of equal amplitudes. When the wave is travelling in an absorbing medium, however, the planes of equal phase remain perpendicular to the direction of propagation of the wave, but the planes of equal amplitude are not necessarily coincident with them. A vector representing the direction of maximum damping of the vibration is not necessarily parallel to the vector representing the direction of propagation of the vibration in an absorbing medium.

In the case of refraction into an absorbing medium as shown in Fig.I.1, the planes of equal phase remain perpendicular to the direction of propagation, this direction varying with the angle of incidence. Hence they are only coincident with the planes of equal phase when light is incident normally on the surface of the absorbing medium. The reflected beam in Fig.I.1, can be described by a complex quantity r, related to the angles of incidence and refraction by Fresnel's equations. If r is expressed as $r = \rho e^{i\delta}$, then the amplitude factor is ρ and δ is the phase change. If the incident light has equal components perpendicular and parallel to the plane of incidence, these can be taken, each, as unity, and the reflected beam has two components given by,

For the parallel component $$r_p = \rho_p e^{i\delta_p} = \frac{N\cos\theta - n_0\cos\eta}{N\cos\theta + n_0\cos\eta} \quad \ldots (I.12)$$

For the perpendicular component $$r_s = \rho_s e^{i\delta_s} = \frac{-N\cos\eta + n_0\cos\theta}{N\cos\eta + n_0\cos\theta} \quad \ldots (I.13)$$

Both the amplitudes and the phases of the components of the incident light polarized parallel and perpendicular to the plane of incidence, are changed upon reflection, the amount of change in each varying with θ the angle of incidence. Two important quantities are:

$$\tan \psi = \frac{\rho_p}{\rho_s} \quad , \quad \Delta = (\delta_p - \delta_s) \qquad \ldots (I.14)$$

The azimuth and the differential change of phase on reflection. These two quantities are of fundamental importance in the determination of the optical constants n and k. They are related by the set of equations stated on page 12.

I.3 THE CHARACTERISTIC PARAMETERS OF A THIN ABSORBING FILM

The optical properties of absorbing media, in bulk or thin form, depend primarily on their optical constants at a particular wavelength. The third parameter for a thin film is its thickness. Here the concept of a thickness is one which, to have a physical meaning, has to be linked to the wavelength of the incident radiation. So it is the d/λ ratio which is of a physical significance.

A more coherent description of a thin film is that which transmits a significant portion of incident light allowing multiple reflections to take place within the film itself. For highly absorbing media with $k \geq 1.0$, d may have to reach a few hundred angstroms before the case of a single reflection is reached, enabling one to ignore the contribution of multiply reflected beams inside the film to its apparent optical properties. In this case, e.g. a silver film of 300 Å at λ5461 Å, would show insignificant variation of its optical constants with thickness and its computed properties; assuming bulk constants, are usually, subject to the conditions of preparation, in agreement with those experimentally measured. However as shown in the study of the effect of varying the rate of evaporation on the optical properties of silver films by Sennett and Scott[17], the absorption of a 300 Å film of Ag at λ6500 Å could vary considerably with the rate at which it was deposited under vacuum. The more rapidly condensed films show much lower absorption.

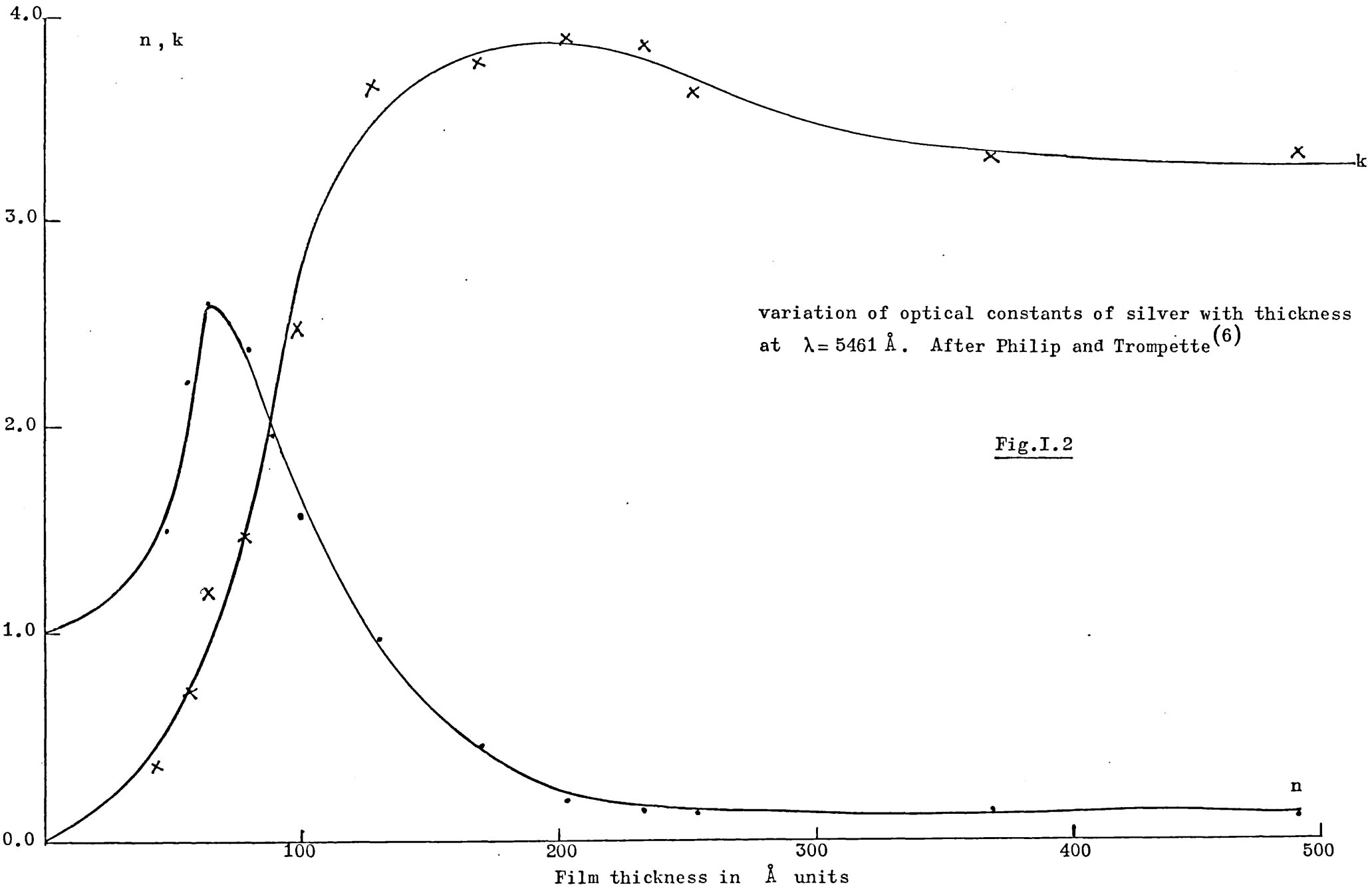

variation of optical constants of silver with thickness at $\lambda = 5461$ Å. After Philip and Trompette[6]

Fig.I.2

For films of thickness $300 \geq d \leq 200$ Å, there are indications that values of n and k do vary in a slow manner with thickness. However, for many a purpose, the bulk values of n and k may give a good approximation to experimentally determined properties. It is for films of thickness ≤ 200 Å that variation of the optical constants with thickness is comparatively rapid, and differences between computed and experimental results would be expected and indeed take place[18]. Fig.I.2 shows the variation of n and k with thickness d for silver films at $\lambda 5462$ Å by Philip and Trompette[6]. Films studied in this thesis are in the thickness range $d \geq 200$ Å. Formulae by Hadley and Dennison[19], and by Born and Wolf[16] are used to compute the optical properties of the films. This leaves the category of films where the structure plays a dominant role in their properties out of the scope of the present work. Specifically out of the interferometric application with which this thesis is concerned. However, as will be explained later, the technique can be applied to films of $d \leq 200$ Å but this will necessitate the use of ellipsometry or other techniques concerned with measuring the phase change at reflection at normal incidence[12].

The accuracy with which the optical constants of an absorbing film need to be known depends on the use to which they may be put. Needless to say that for band structure calculations, the highest possible accuracy is needed. However, if the purpose is to calculate the apparent optical properties R, T and A, for e.g. the design of a metal-dielectric-metal type of interference filter, it is hardly justifiable to use elaborate expensive techniques to obtain highly accurate values for the constants. For such an application R, T and A, important as they may be for the quality of the device, do not constitute the only parameters to be considered. A compromise has to be struck between the transmission and the half-width at the peak wavelengths. The highest transmission value may

not give the desired reflection factor crucial for a narrow-band width. Also it may be noted that variations in k are more likely to produce significant variations in R, T and A when $k \gg n$ which is the case for metals in the visible region of the spectrum.

The technique presented later in this work, makes it possible with minimum apparatus and computing, to produce values of k to within ± 0.025. This is ten times less than the 10% scatter in the values of n and k reported in the literature, e.g. silver films[20].

To sum-up this section, films dealt with here are of thicknesses such that complications arising from structure are avoided, and, since k is the dominant constant in determining the apparent optical properties of metals in the visible, the interferometric technique presented in this thesis was investigated and developed.

I.4 METHODS AND TECHNIQUES USED TO DETERMINE THE OPTICAL PARAMETERS OF A THIN ABSORBING FILM

There are several methods available for the determination of the optical constants and thickness of an absorbing thin film. Since the vast majority of measurements are made on films deposited in vacuum, the accuracy of results are critically dependent on the conditions of preparation. Also the method to be adopted depends on the nature of work at hand. Therefore the approach required for fundamental investigation on solid-state thin film physics will not necessarily be suitable for studying and designing interference filters.

Historically, methods involving the analysis of the state of polarization of reflected light constitute the first category of the methods available for the determination of the optical constants. Photometric methods involving intensity measurements of reflected light do constitute the other major category. Combinations of photometric and polarimetric

measurements are possible and useful to compensate for defects in either, or to serve certain applications. A survey of all methods is beyond the scope of this thesis. However, the purpose of this section is to present a general picture of the basis and limits of the two major groups of techniques mentioned above. This will enable us, in a later stage, to fit the new interferometric technique proposed in this thesis in its proper place, and to show its relative ease and accuracy.

I.4.1 Methods Based on Analysis of the State of Polarization of Reflected Light

When plane polarized light falls on a plane boundary between two dielectrics, e.g. air and glass, the reflected light is also plane polarized. If a thin superficial film is present on the glass, the reflected light is elliptically polarized. In the case of reflection of plane polarized light from a metallic surface, the reflected light is elliptically polarized. The measure of this ellipticity is the angle ψ determined by the ratio of the minor to major axes. The incident light is usually polarized at 45° to the plane of incidence, where the amplitudes of the two components, parallel and perpendicular to the plane of incidence, are in phase and of equal magnitude. Upon reflection from a perfectly clean metallic surface, each component suffers a change of phase δ_p and δ_s respectively, and the ratio of their amplitude, $\tan\psi$, is decreased.

Reflection polarimetry or ellipsometry, is that art concerned with measuring $\Delta = \delta_p - \delta_s$ and $\tan\psi = \frac{r_p}{r_s}$, two quantities related to the optical constants n and k of the clean metallic surface. But the practical application is not easy. It is often the case that the metallic surface is contaminated with a surface film. This could be simply an oxide layer or still more complicated, an absorbing film. The formation of surface films on top of the clean metallic interface, introduces changes in the two quantities Δ and $\tan\psi$. It was Drude's work seventy years

ago[2] which related the change, due to surface films, in Δ and $\tan\psi$ to the optical constants of the clean metal, the refractive index of a non-absorbing surface film and the film thickness. According to Vasicek[21] these relations could take the following form:

$$\Delta - \bar{\Delta} = -\frac{4\pi d}{\lambda}\,\frac{\cos\theta\sin^2\theta(n_1^2 - n_o^2)}{(\cos^2\theta - n_o^2 a)^2 + n_o^4 a'^2} \times \left[\left(\cos^2\theta - n_o^2 a\right)\left(\frac{1}{n_1^2} - a\right) + n_o^2 a'^2\right] \qquad \ldots (I.15)$$

$$2\psi - 2\bar{\psi} = \sin 2\bar{\psi}\,\frac{4\pi d}{\lambda}\,\frac{\cos\theta\sin^2\theta(n_1^2 - n_o^2)}{(\cos^2\theta - n_o^2 a)^2 + n_o^4 a'^2} \times \left[n_1^2 a'\left(\frac{1}{n_1^2} - a\right) - \left(\cos^2\theta - n_o^2 a\right)a\right] \qquad \ldots (I.16)$$

where $\bar{\psi}$ indicates the azimuth, $\bar{\Delta}$ the phase difference measured on a clean metal surface, ψ and Δ the same quantities measured on a metal with a thin superficial transparent (non-absorbing) film. d denotes the thickness of the film, n_1 its refractive index, n_o that of the incidence medium (usually air). These formulae also include θ the angle of incidence, and λ the wavelength of the monochromatic light falling onto the specimen. The terms a and a' are simple functions of the optical constants n and k.

Formulae (I.15) and (I.16) may be written in the form,

$$\Delta - \bar{\Delta} = -\,c\,d \qquad \ldots (I.17)$$

$$2\psi - 2\bar{\psi} = c'\,d\ . \qquad \ldots (I.18)$$

It is evident that with increasing thickness of the surface film the measured azimuth increases linearly, but the phase difference decreases linearly. According to Vasicek in the same reference, and Heavens[4] that the preceding formulae, which are the approximate Drude's equations, are valid for the thinnest of surface films up to about 100 Å. As for the case of a thin weakly absorbing film on a metal substrate, the formulae are more complicated; they are discussed by Vasicek in reference (21). In

the forgoing presentation the optical constants of the clean metal substrate are assumed to be known. The formulae mentioned in page 12, are applicable to clean metallic surfaces. The expression, clean metallic surface, is assumed to be that of a bulk specimen or a very thick non-transmitting film deposited on a dielectric substrate where the assumption of a single reflection is sufficient to describe the reflected light.

The case of a highly absorbing, e.g. metallic, partially transmitting film on a dielectric substrate must be dealt with using formulae which would take into consideration the multiple reflections within the film, and reflection from the film-substrate interface. Equations for Δ and ψ can be formed explicitly as functions of θ, λ, n, k, n_3 and d. The resulting equations are arithmetically complicated, but the use of digital computers could make it easier to handle. To extract n and k, sets of curves of Δ vs ψ must be prepared for a number of possible combinations of n and k for given values of θ, λ, n_3 and d. This technique has been used for weakly absorbing films ($k \simeq 0.05$) on a silicon substrate, Archer[1].

The order of precision to be expected from polarimetric analysis may be illustrated by the work of Meyer[22] on films of iron prepared by electron bombardment at a pressure of 2×10^{-6} torr. Opaque layers of $d > 1000$ Å were used. The optical measurements were made with Soleil-Babinet comansator at an angle of incidence $50^\circ - 70^\circ$. Visual observations enables Δ to be determined to $\pm 20'$ and 2ψ to $\pm 6'$. For annealed films, the optical constants at $\lambda = 5890$ Å are found to be $(2.56 - i\,3.02)$ with uncertainty of $0.02 - 0.03$.

Ellipsometric techniques are very often applied to three main cases:

(a) study of surface of non-absorbing films on absorbing substrates,

(b) weakly absorbing films on absorbing substrates, and

(c) opaque highly absorbing thick clean films on dielectric substrates.

In the first two cases the substrate constants must be known and the surface film thickness could be obtained together with its constants. The method is sensitive for the thinnest of surface films where $d \leq 100$ Å and for k values $0 - 1.0$. In the case of such thin films the geometry and structure of the film plays an important role in shaping ellipsometric results, Berreman[23,24] has shown how Δ and Ψ for a given material can vary for a variety of thin film geometries, from ideal flat films to films assumed to consist of a flat area having half submerged spherical particles embedded. In the case of a Ag_2S ($\hat{n} = 3.0 + i.0.45$) on a bulk silver substrate, large errors ($\sim 100\%$) in the deduced optical constants for the film could arise if the effect of the film structure was ignored. For thin metal films ($d \leq 100$ Å) on a flat dielectric substrate, Berreman concludes that Drude's equations giving the thickness of such films may be inaccurate when the films are not planar and continuous. The particles shape must be known and corrections applied for cases such as mentioned. In the third case the constant n and k are directly related to Δ and Ψ and the thickness is not relevant since it is almost a bulk case, or the thickness, if need be known, could be obtained independently, e.g. by interferometric techniques. Experimental arrangements for carrying out ellipsometric measurements are discussed and described by Bennet and Bennet[25] and Archer[1]. Some computational procedures and techniques are discussed by McCrackin and Colson[26].

I.4.2 Methods Based on Measurement of Light Intensities

This is the other major group of methods generally employed to obtain the optical constants of an absorbing film. They could be subclassified in more than one way. They could employ polarized or unpolarized light, they may be performed at normal or oblique incidence,

Measurements can be carried out at reflection or transmission. There are a number of combinations involving reflection coefficients and incidence angles, or transmission coefficients and thicknesses. Any combination chosen for obtaining the constants will depend on the problem investigated and its requirements. However, the sensitivity of a particular combination to the constants at a certain wavelength, is a factor of paramount importance. Humphreys-Owen[27] studied the sensitivites of a number of possible methods. Heavens[4] gives a good summary of his work. Humphreys-Owen's work is mainly concerned with measuring reflectance coefficients. It is therefore suitable for thick films where the effect of multiple reflections within the film could be ignored. The measurements are divided into two general classes. In the first of these, two reflectance measurements are made, in the second one, reflectance measurements is made and the Brewster angle determined. Heavens, in reference (4), discusses the merits of the different possibilities in Humphreys-Owen's work. Ward and Nag[28,29], studied the sensitivies of a range of possible measurements designed to extract the optical constants and thickness of thin absorbing films. For the case of normal incidence they deal with six quantities. They are:

(1) The reflectance R at the vacuum-film interface;

(2) The reflectance R' at the substrate-film interface;

(3) The transmittance T;

(4) The phase change β on reflection at the vacuum-film interface;

(5) The phase change β' on reflection at the substrate-film interface; and

(6) The phase change γ on transmission.

These six quantities were used in pairs (x, y) and for each pair, graphs were plotted of x against y for (i) constant d/λ, (ii) constant k and (iii) constant n. These were found to be consisting of two families of intersecting curves. Quantitative judgement was based on

the changes produced in n, k or d/λ by a change in R, R' or T of ± 0.01, or a change in β, β' or γ of $\pm 1.0^{o}$ $(0.0055\ \pi)$. These changes were read off the graphs. If the change in n or k was less than 0.15 or that in d/λ was less than 0.003 (if $\lambda = 6000$ this is 18 Å) the region was regarded as one of high sensitivity. It was concluded that, in order to obtain n, k and d/λ, the combination of (R, T, γ) would be that giving the highest overall sensitivity in a region covering the cases of a number of metals, e.g. Ag, Aℓ, Cu, in the visible spectrum. In their second paper[29] Ward and Nag extended their study to the case of non-normal incidence. They performed sensitivity studies on pairs of the photometric quantities R, T $\theta = 30^{o}, 45^{o}, 60^{o}, 75^{o}$. The diagrams for (T_p, T_s) and (R_p, R_s) at $\theta = 45^{o}, 60^{o}$ and 75^{o} show over all high sensitivity over the region $0 < n < 3.0$, $0 < k < 3.0$, $0 < d/\lambda < 0.02$. For all combinations except (R_p, R_s) the sensitive region decreased with d/λ. No combination was found to be of high sensitivity in the region $n > 3.0$, $k > 3.0$. No consideration, though, was given to polarimetric quantities. Shaalan and Taylor[30] conducted a preliminary investigation on the sensitivity of Δ the differential change of phase at reflection to n, k, θ and d. The study was applied to extract the extinction coefficient of thin films of Ag.

Chapter II and subsequent chapters contain a more detailed and extended study of both the theoretical and experimental aspects.

CHAPTER II

THE DIFFERENTIAL CHANGE OF PHASE ON REFLECTION AIR/ABSORBING FILM. A STUDY OF THE DEPENDENCE OF Δ ON SEVERAL PARAMETERS

II.1 INTRODUCTION

It has been shown in the previous chapter that several methods and techniques do serve the purpose of determining the optical constants of an absorbing film, all of which are subject to inherent or external limitations. However, sensitivity studies have been largely applied to the photometric measurables. No such studies have been performed on the polarimetric quantities[31]. The two polarimetric measurables are

$$\Delta = (\delta_p - \delta_s) \quad \text{and} \quad \psi = \tan^{-1} \frac{\rho_p}{\rho_s} .$$

In this chapter the first of these two quantities is studied in depth and its dependence on several factors demonstrated. The choice of Δ for this study was promoted mainly because it could be measured, in certain cases, interferometrically, thus achieving the target of this present work, i.e. to widen further the use of interferometric techniques as a tool in thin film optics. This is made possible by extracting the optical constants, or either of them, from the measurement of Δ as a function of θ the angle of incidence, at a certain wavelength and thickness. Also an insight in the properties of the quantity Δ could lead to an assessment of the worthiness of pursuing this kind of investigation on the quantities β, β' and γ mentioned in the last chapter, since all of them are readily determined interferometrically. The variation of these quantities with d and with the optical constants, could help establish interferometry as a sensitive, accurate and inexpensive method to determine the optical constants. In fact this is intended for later work and will be mentioned again at the end of this thesis.

The study of Δ presented in this chapter, is concerned with establishing its variation with θ, d, and λ in a range of n and k which would include most of the highly reflecting films in the visible part of the spectrum. The range of n and k investigated is $0.05 \leq n \leq 3.0$ and $2.0 \leq k \leq 5.0$, while d ranges from 50 to 500 Å. The angle of incidence

varied between 30° and 70°. However, only graphs at $\theta = 45^{\circ}$ and $\theta = 70^{\circ}$ are presented here, since it was found that the higher the incidence the higher is the sensitivity of Δ to all other factors, and consequently graphs at those two angles are presented to show the difference in sensitivity at the regions of low and high incidence. In the following the conclusions of this study will be presented separately for each of the following sub-ranges of n values, (a) $0.05 \leq n \leq 1.0$, (b) $1.0 \leq n \leq 2.0$ and (c) $2.0 \leq n \leq 3.0$; k was varied in the range $2.0 \leq k \leq 5.0$ in steps of 0.5. Also the study showed that one can distinguish between two ranges of thickness, over and below 200 Å. Therefore the graphs will be grouped in these two ranges separately.

This way of presenting the properties of the quantity Δ is probably laborious and yields many graphs. But, on the other hand, it provides clear presentation of each case bringing out clearly the physical meaning of each graph and a direct visual assessment of the properties of Δ in each range of n and k for a particular thickness at an angle of incidence. This was convenient in assessing the experimental prospects.

II.2 THE PROPERTIES OF THE POLARIMETRIC MEASURABLE $\Delta = (\delta_p - \delta_s)$

Ward and Nag[28,29] adopted a criterion for sensitivity. If a change of ± 0.01 in the photometric measurables or $\pm 1.0^{\circ} \approx 0.006\,\pi$ in the phase measurables would result in a change less than 0.15 in the constants, the region was regarded as one of high sensitivity. This appears to be a generous criterion. The photometric measurables could be measured to ± 0.001 and the phase changes could be measured to better than $\pm 0.003\,\pi$. However, for the sake of some unified approach and to facilitate comparison, Ward and Nag's criterion will be adopted here, bearing in mind that experimentally speaking, one can afford to be a bit more demanding.

GROUP 1 GRAPHS OF Δ vs n

(a) $0.05 \leq n \leq 1.0$

(b) $1.0 \leq n \leq 2.0$

(c) $2.0 \leq n \leq 3.0$

$2.0 \leq k \leq 5.0$ $\quad \theta = 70^{\circ}$

$0.01 \leq d/\lambda \leq 0.04$ $\quad \theta = 45^{\circ}$

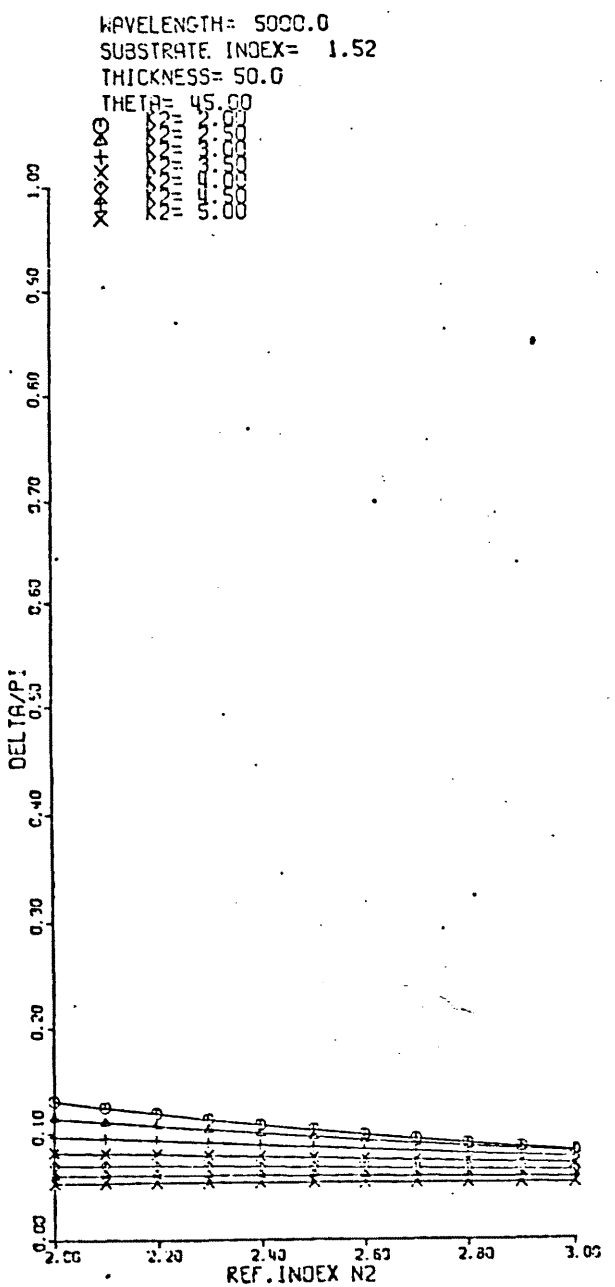
WAVELENGTH= 5000.0
SUBSTRATE INDEX= 1.52
THICKNESS= 50.0
THETA= 45.00
K2= 2.00
K2= 2.50
K2= 3.00
K2= 3.50
K2= 4.00
K2= 4.50
K2= 5.00
DELTA/PI
REF.INDEX N2
0.00
0.10
0.20
0.30
0.40
0.50
0.60
0.70
0.80
0.90
1.00
2.00
2.20
2.40
2.60
2.80
3.00

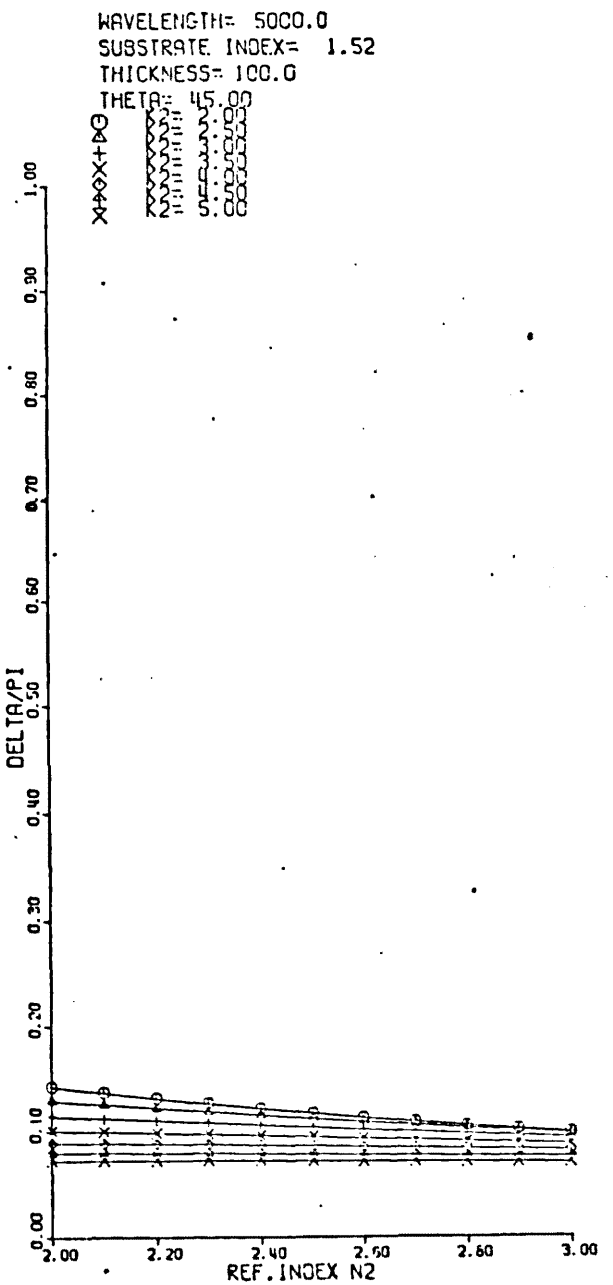
WAVELENGTH= 5000.0
SUBSTRATE INDEX= 1.52
THICKNESS= 100.0
THETA= 45.00
K2= 2.00
K2= 2.50
K2= 3.00
K2= 3.50
K2= 4.00
K2= 4.50
K2= 5.00
DELTA/PI
REF.INDEX N2
0.00
0.10
0.20
0.30
0.40
0.50
0.60
0.70
0.80
0.90
1.00
2.00
2.20
2.40
2.60
2.80
3.00

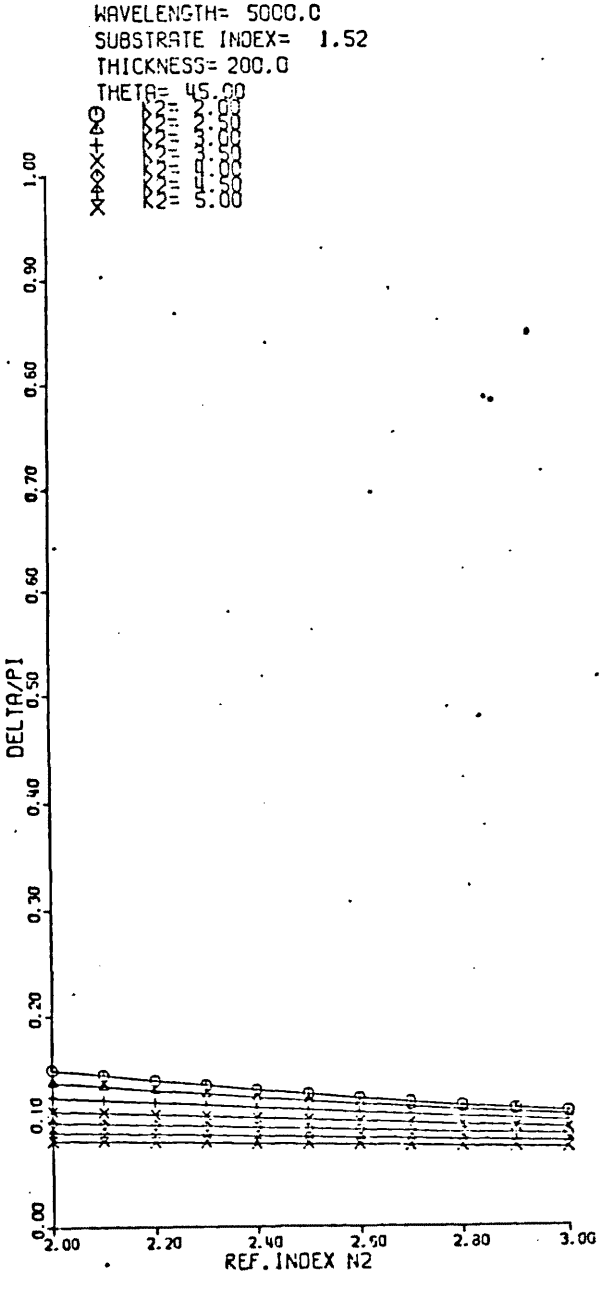
WAVELENGTH= 5000.0
SUBSTRATE INDEX= 1.52
THICKNESS= 200.0
THETA= 45.00
K2= 2.00
K2= 2.50
K2= 3.00
K2= 3.50
K2= 4.00
K2= 4.50
K2= 5.00
DELTA/PI
REF.INDEX N2
0.00
0.10
0.20
0.30
0.40
0.50
0.60
0.70
0.80
0.90
1.00
2.00
2.20
2.40
2.60
2.80
3.00

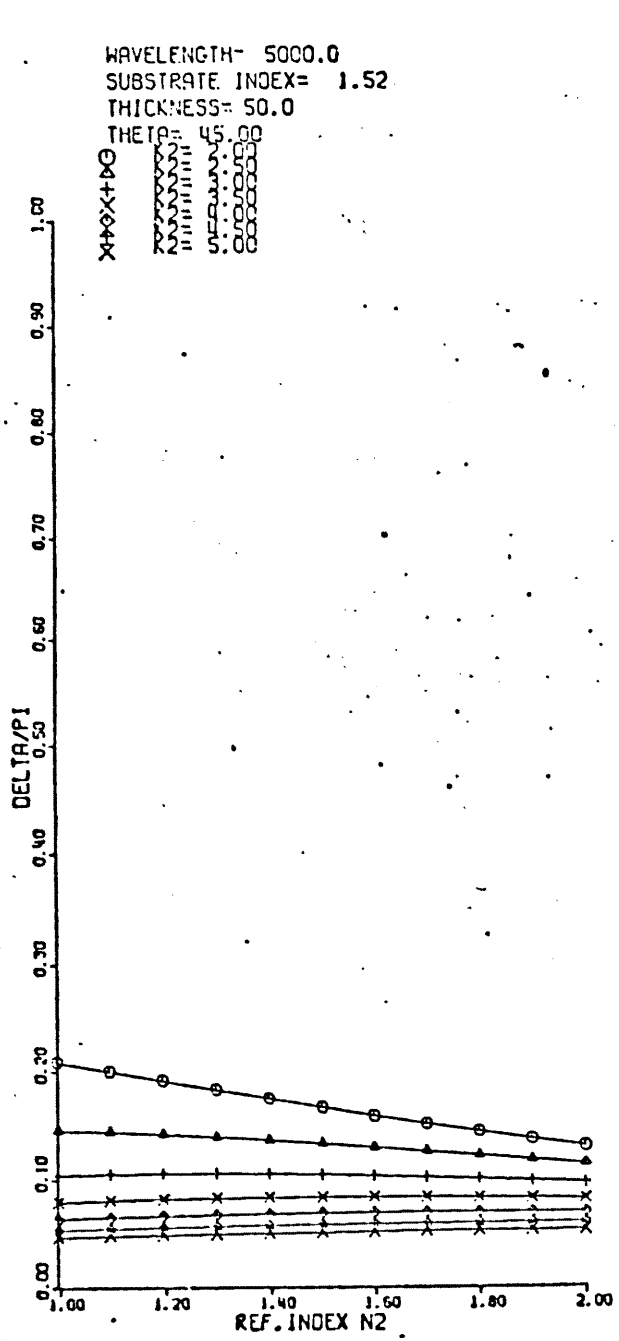
WAVELENGTH= 5000.0
SUBSTRATE INDEX= 1.52
THICKNESS= 50.0
THETA= 45.00
K2= 2.00
K2= 3.00
K2= 4.00
K2= 5.00
DELTA/PI
REF.INDEX N2
1.00
1.20
1.40
1.60
1.80
2.00

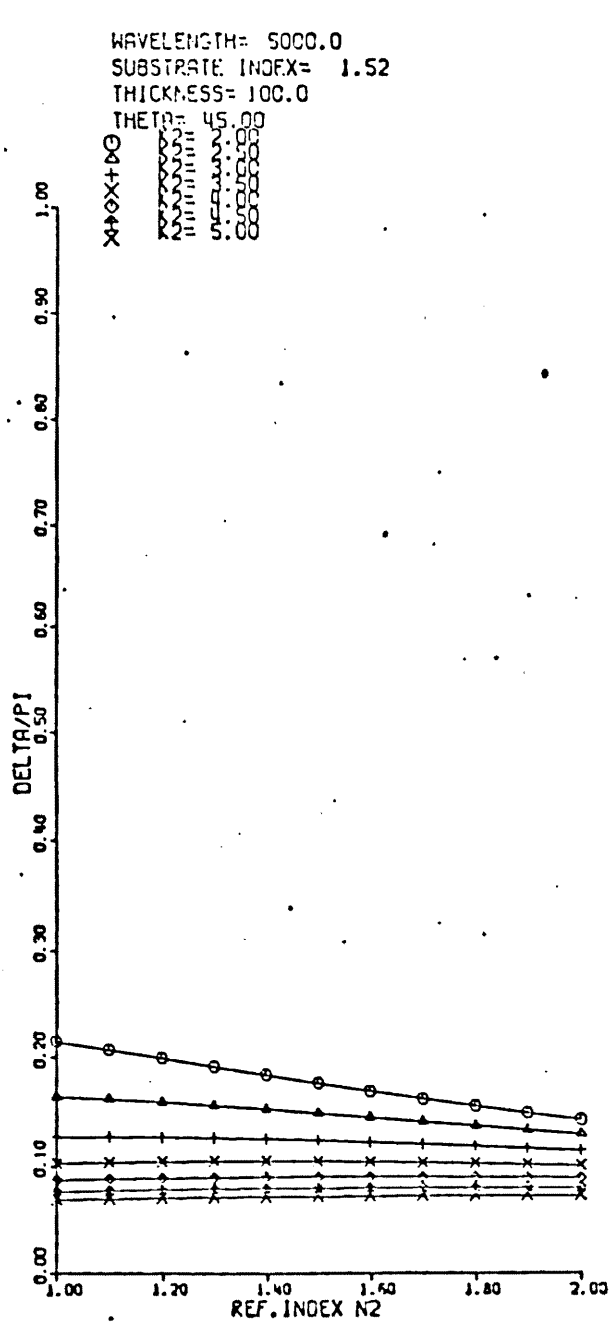
WAVELENGTH= 5000.0
SUBSTRATE INDEX= 1.52
THICKNESS= 100.0
THETA= 45.00
K2= 2.00
K2= 3.00
K2= 4.00
K2= 5.00
DELTA/PI
REF.INDEX N2
1.00
1.20
1.40
1.60
1.80
2.00

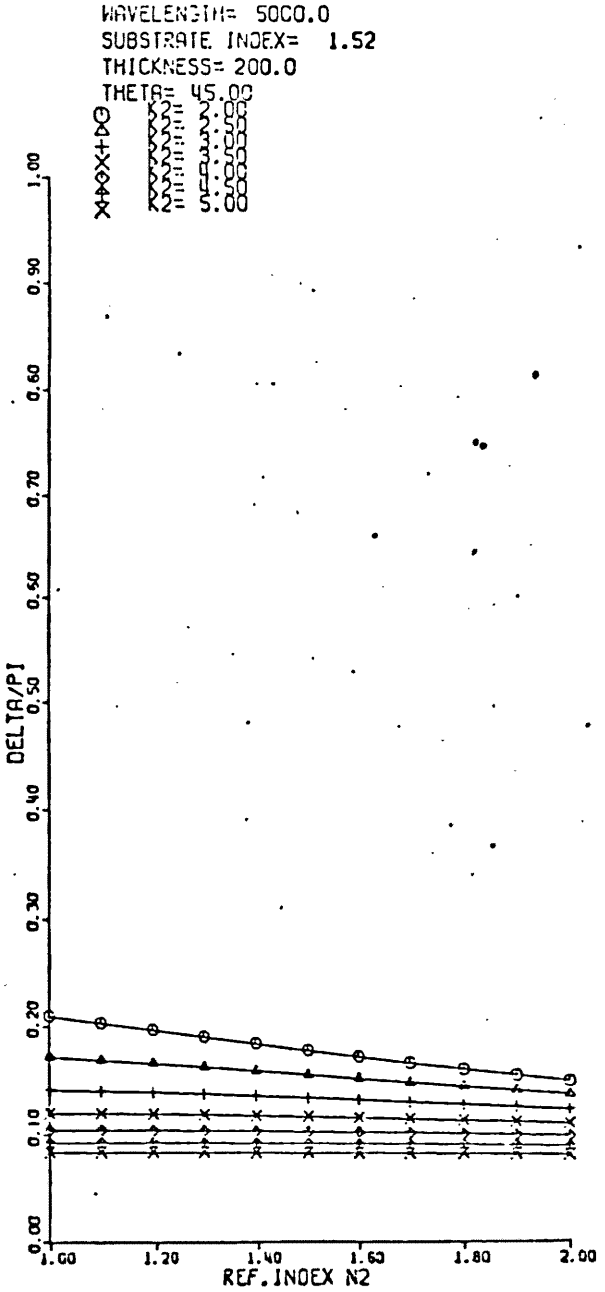
WAVELENGTH= 5000.0
SUBSTRATE INDEX= 1.52
THICKNESS= 200.0
THETA= 45.00
K2= 2.00
K2= 3.00
K2= 4.00
K2= 5.00
DELTA/PI
REF.INDEX N2
1.00
1.20
1.40
1.60
1.80
2.00

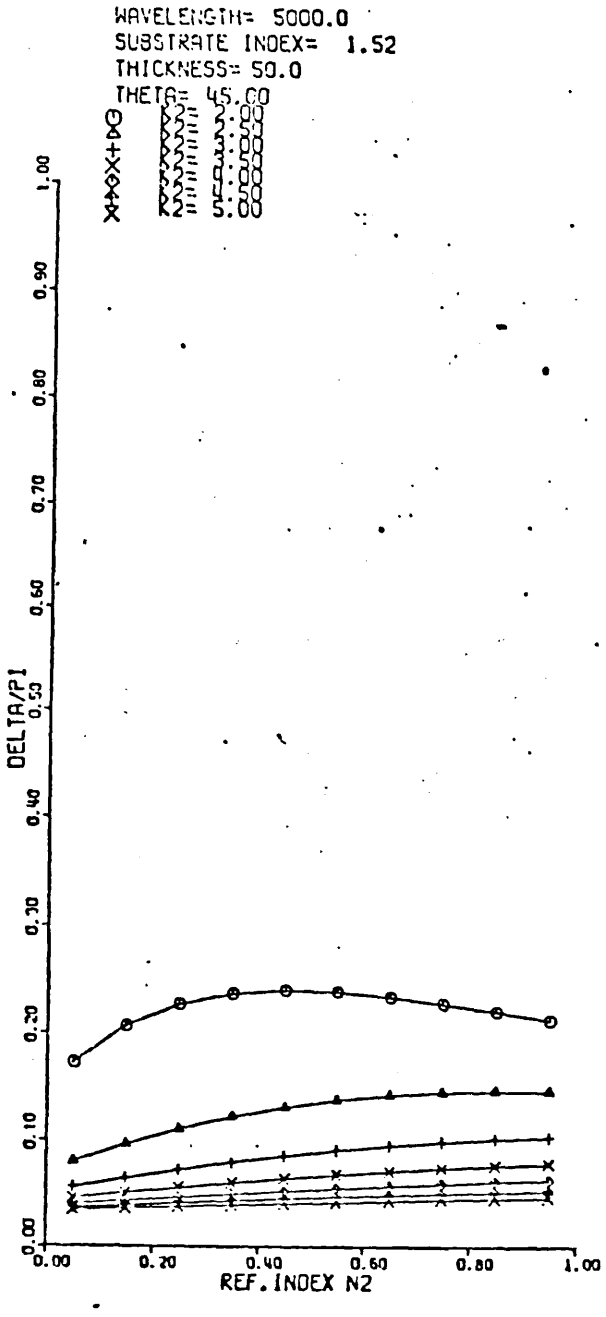
WAVELENGTH= 5000.0
SUBSTRATE INDEX= 1.52
THICKNESS= 50.0
THETA= 45.00
K2= 2.00
K2= 2.50
K2= 3.00
K2= 4.00
K2= 5.00
DELTA/PI
REF.INDEX N2
0.00
0.10
0.20
0.30
0.40
0.50
0.60
0.70
0.80
0.90
1.00

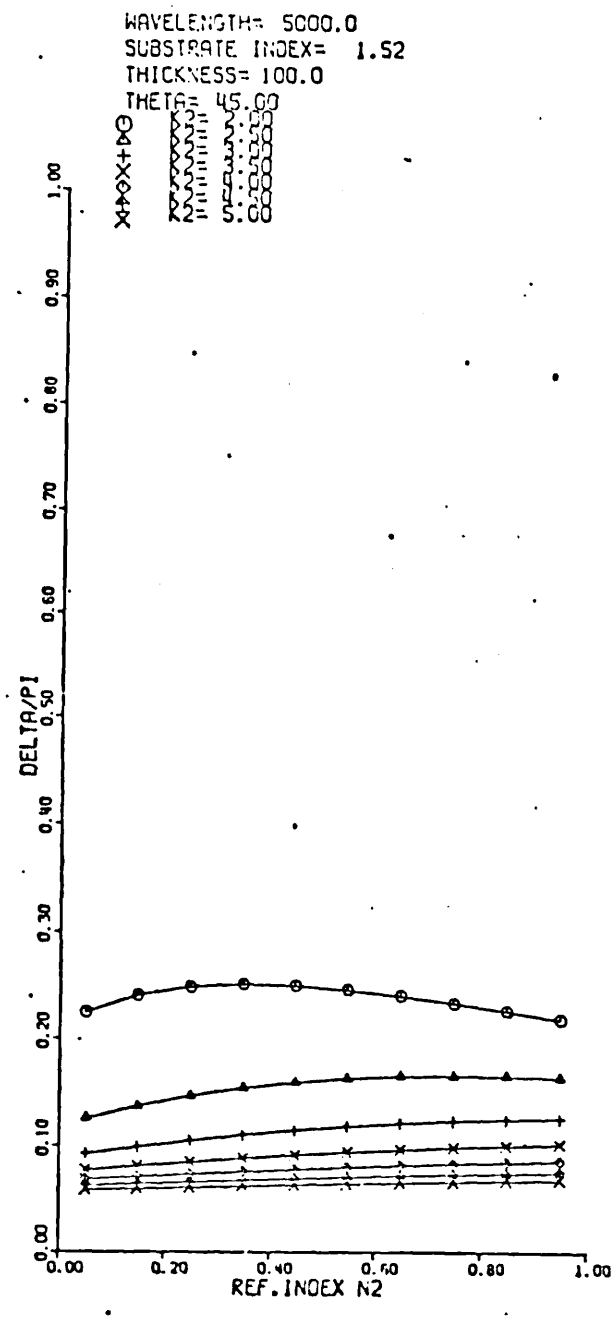
WAVELENGTH= 5000.0
SUBSTRATE INDEX= 1.52
THICKNESS= 100.0
THETA= 45.00
DELTA/PI
REF.INDEX N2
0.00
0.10
0.20
0.30
0.40
0.50
0.60
0.70
0.80
0.90
1.00

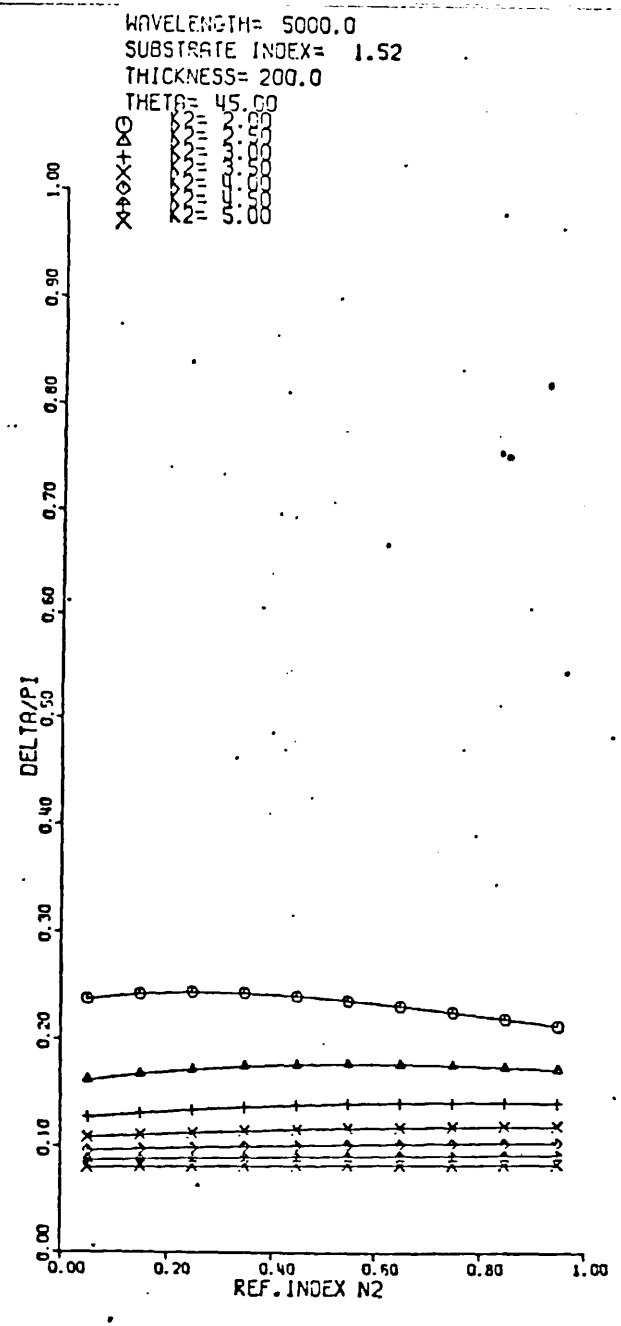
WAVELENGTH= 5000.0
SUBSTRATE INDEX= 1.52
THICKNESS= 200.0
THETA= 45.00
K2= 2.00
K2= 5.00
DELTA/PI
REF.INDEX N2
0.00
0.10
0.20
0.30
0.40
0.50
0.60
0.70
0.80
0.90
1.00

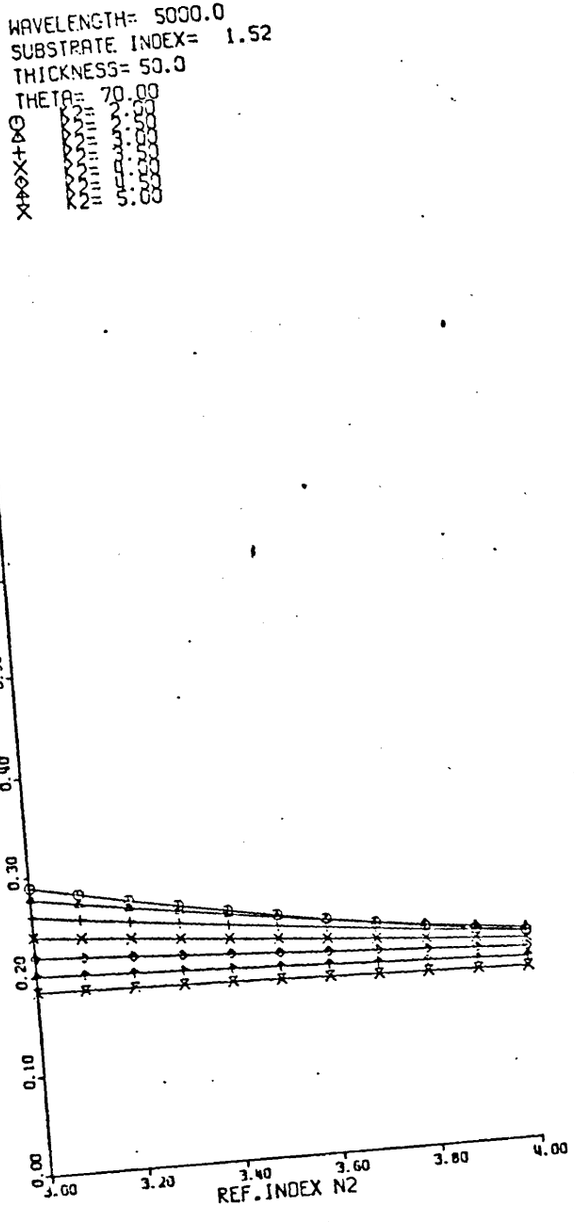
WAVELENGTH= 5000.0
SUBSTRATE INDEX= 1.52
THICKNESS= 50.0
THETA= 70.00
DELTA/PI
REF.INDEX N2
1.00
0.90
0.80
0.70
0.60
0.50
0.40
0.30
0.20
0.10
0.00
3.00
3.20
3.40
3.60
3.80
4.00

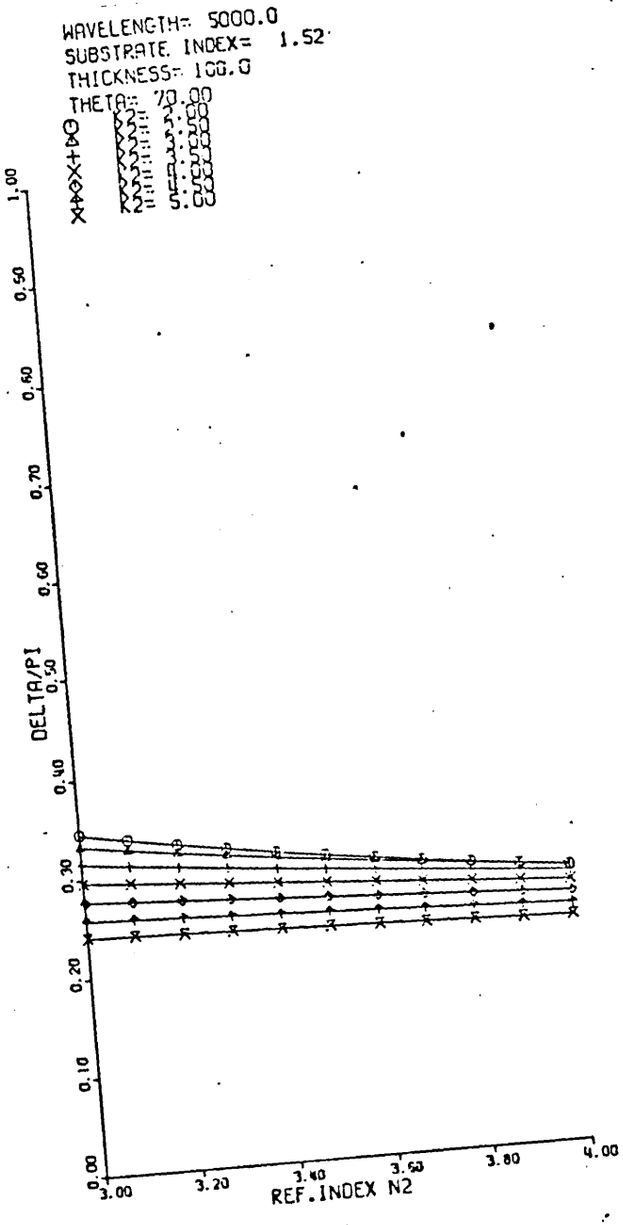
WAVELENGTH= 5000.0
SUBSTRATE INDEX= 1.52
THICKNESS= 100.0
THETA= 70.00
DELTA/PI
REF.INDEX N2
1.00
0.90
0.80
0.70
0.60
0.50
0.40
0.30
0.20
0.10
0.00
3.00
3.20
3.40
3.60
3.80
4.00

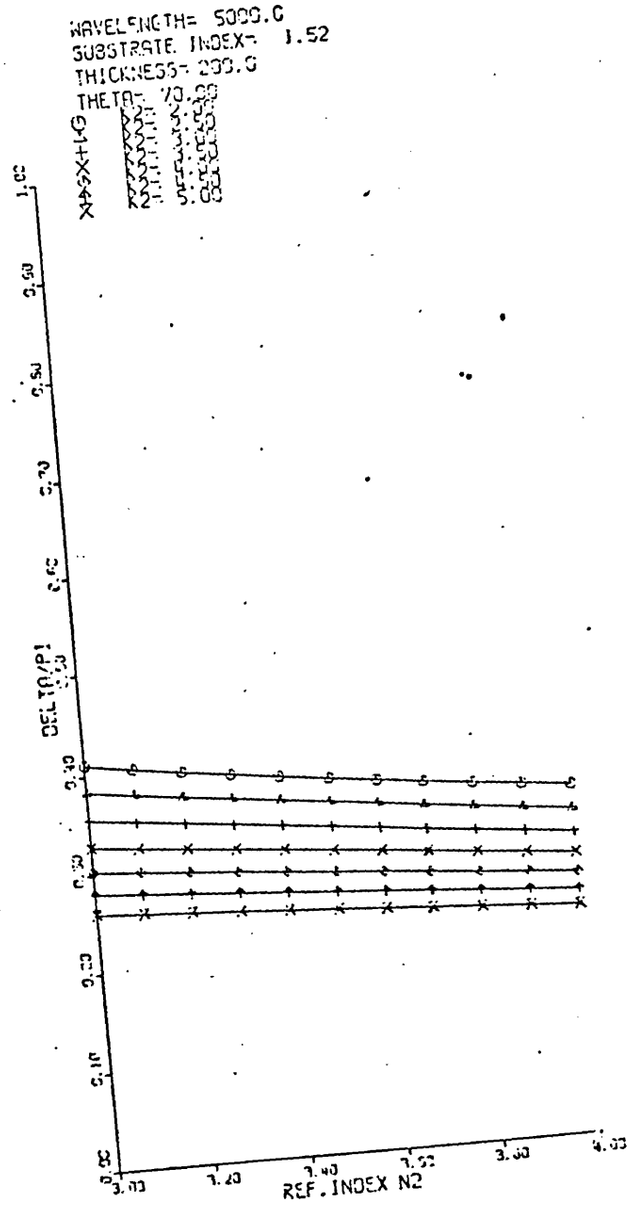
WAVELENGTH= 5000.0
SUBSTRATE INDEX= 1.52
THICKNESS= 200.0
THETA= 70.00
REF.INDEX N2

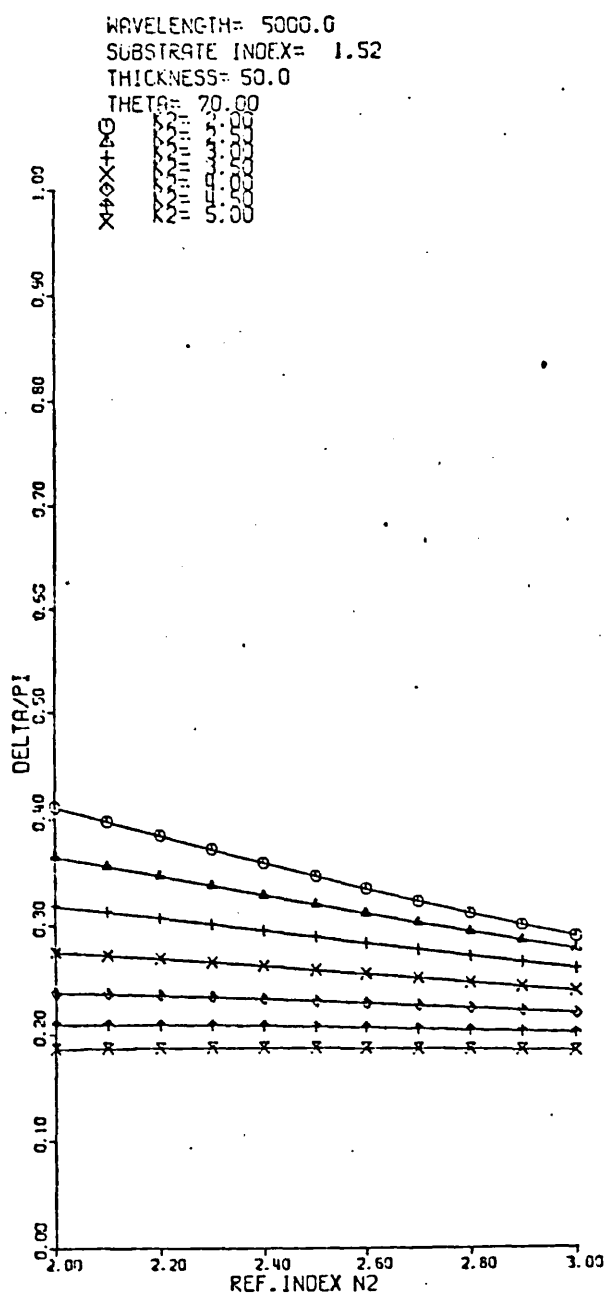
WAVELENGTH= 5000.0
SUBSTRATE INDEX= 1.52
THICKNESS= 50.0
THETA= 70.00
DELTA/PI
REF. INDEX N2
2.00
2.20
2.40
2.60
2.80
3.00

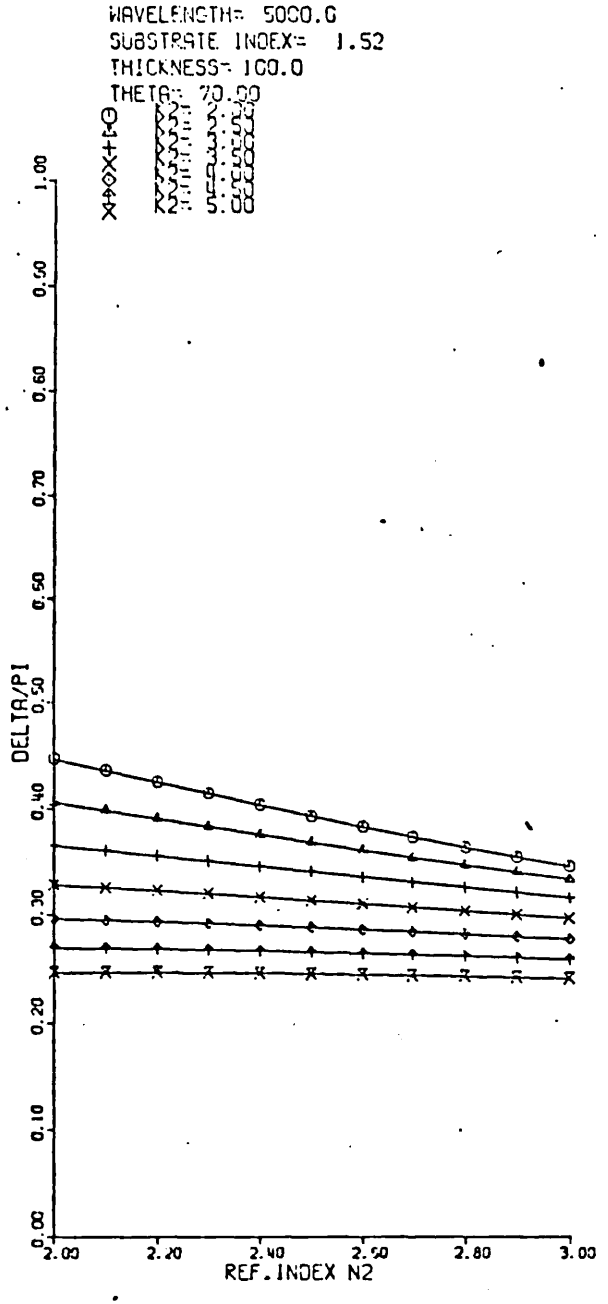
WAVELENGTH= 5000.0
SUBSTRATE INDEX= 1.52
THICKNESS= 100.0
THETA= 70.00
DELTA/PI
REF. INDEX N2
2.00
2.20
2.40
2.60
2.80
3.00

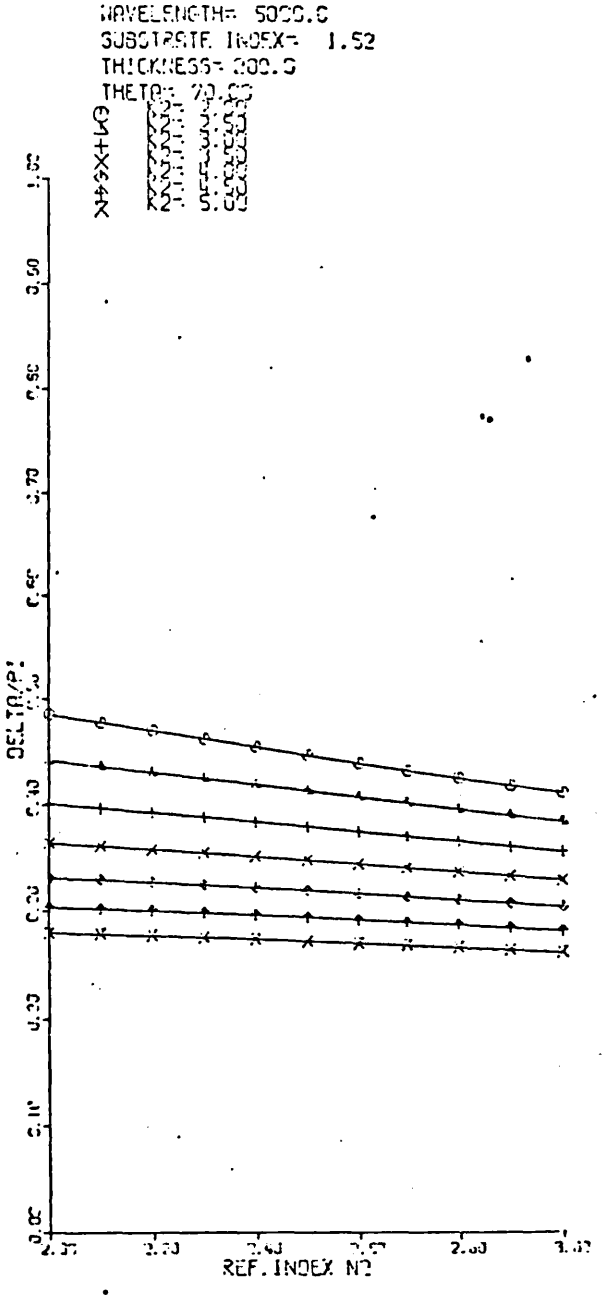
WAVELENGTH= 5000.0
SUBSTRATE INDEX= 1.52
THICKNESS= 200.0
THETA= 70.00
DELTA/PI
REF. INDEX N2

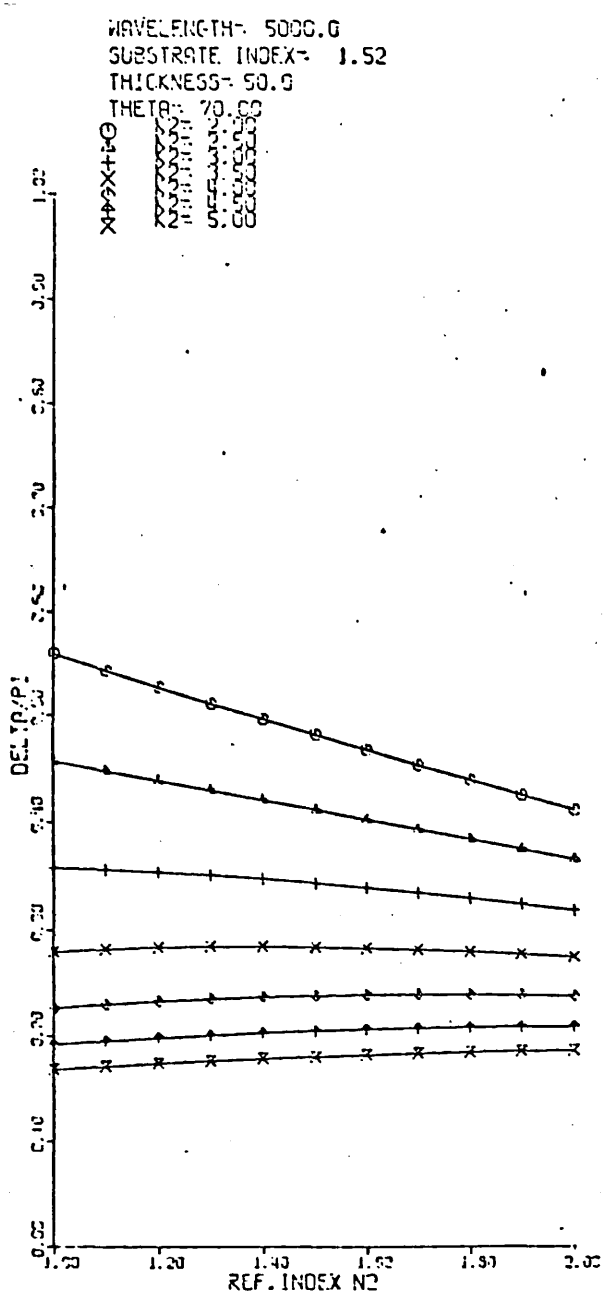
WAVELENGTH= 5000.0
SUBSTRATE INDEX= 1.52
THICKNESS= 50.0
THETA= 70.00
DELTA/PI
REF.INDEX N2

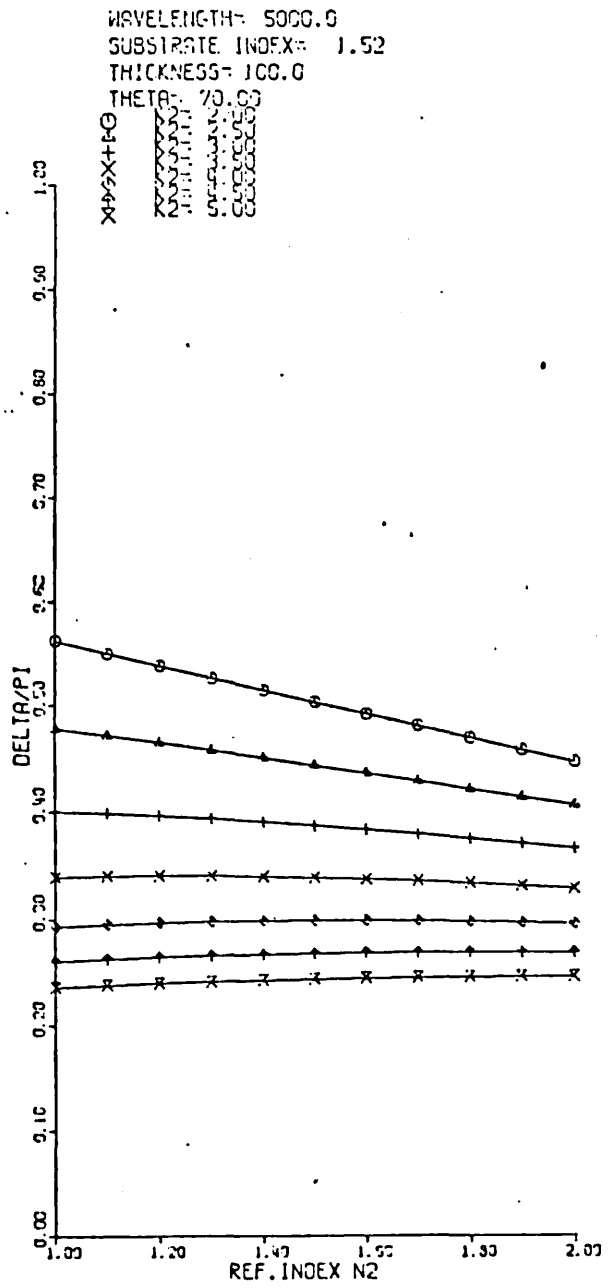
WAVELENGTH= 5000.0
SUBSTRATE INDEX= 1.52
THICKNESS= 100.0
THETA= 70.00
DELTA/PI
REF.INDEX N2

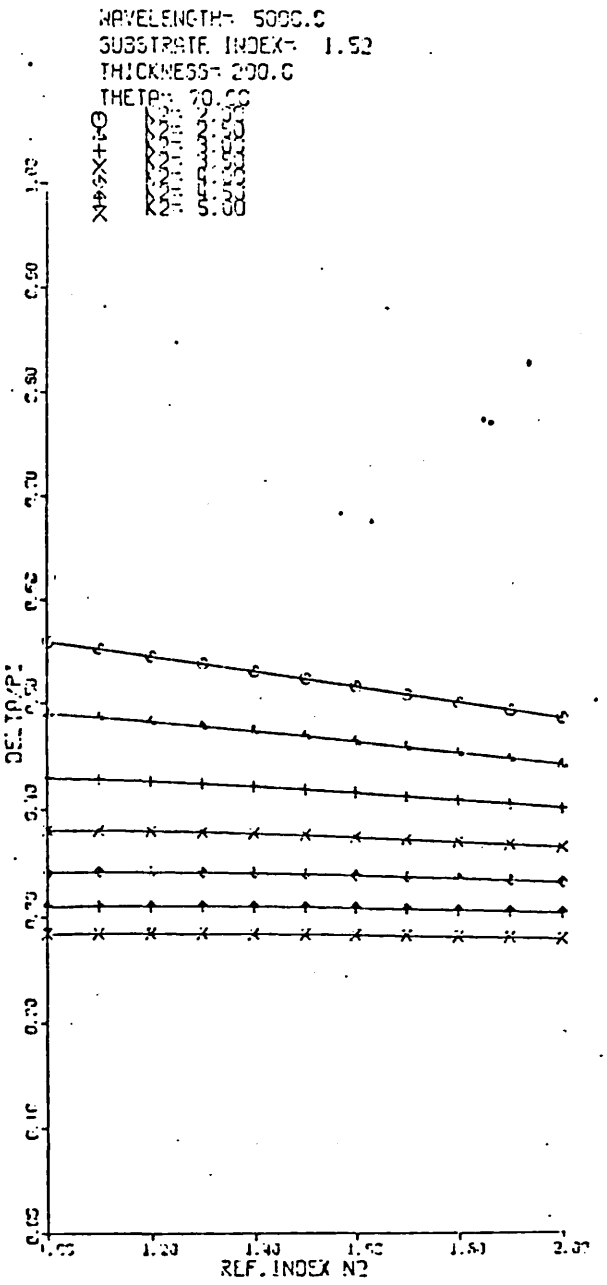
WAVELENGTH= 5000.0
SUBSTRATE INDEX= 1.52
THICKNESS= 200.0
THETA= 70.00
DELTA/PI
REF.INDEX N2

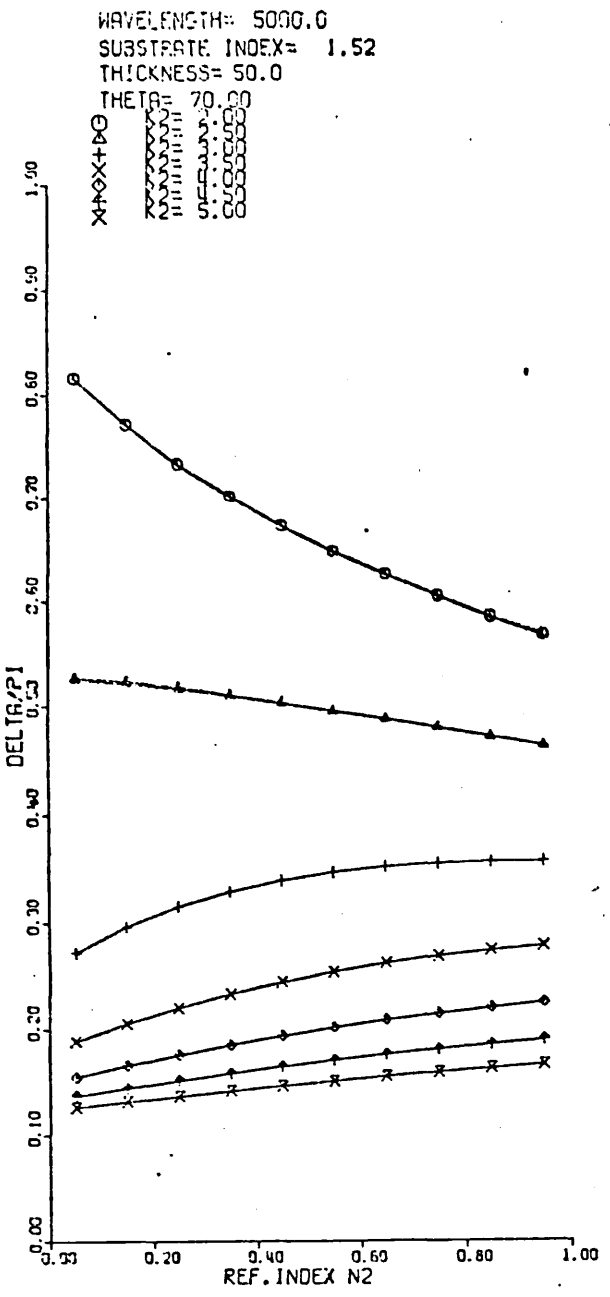
WAVELENGTH= 5000.0
SUBSTRATE INDEX= 1.52
THICKNESS= 50.0
THETA= 70.00
K2= 5.00
DELTA/PI
REF. INDEX N2
0.00
0.20
0.40
0.60
0.80
1.00

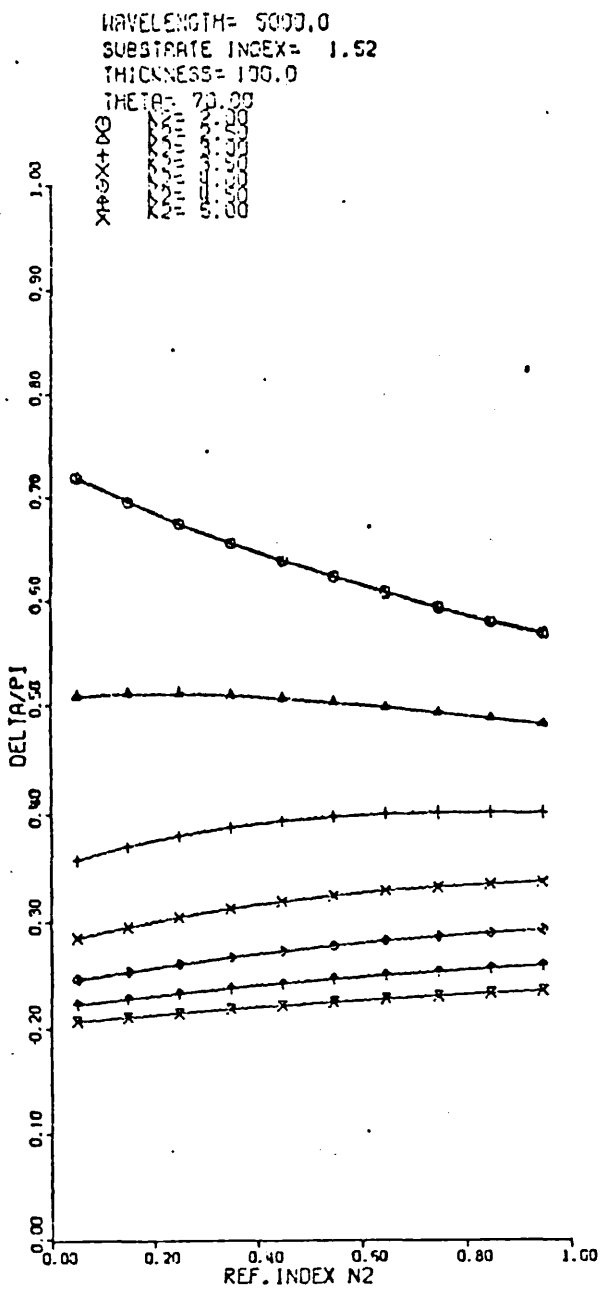
WAVELENGTH= 5000.0
SUBSTRATE INDEX= 1.52
THICKNESS= 100.0
THETA= 70.00
K2= 5.00
DELTA/PI
REF. INDEX N2
0.00
0.20
0.40
0.60
0.80
1.00

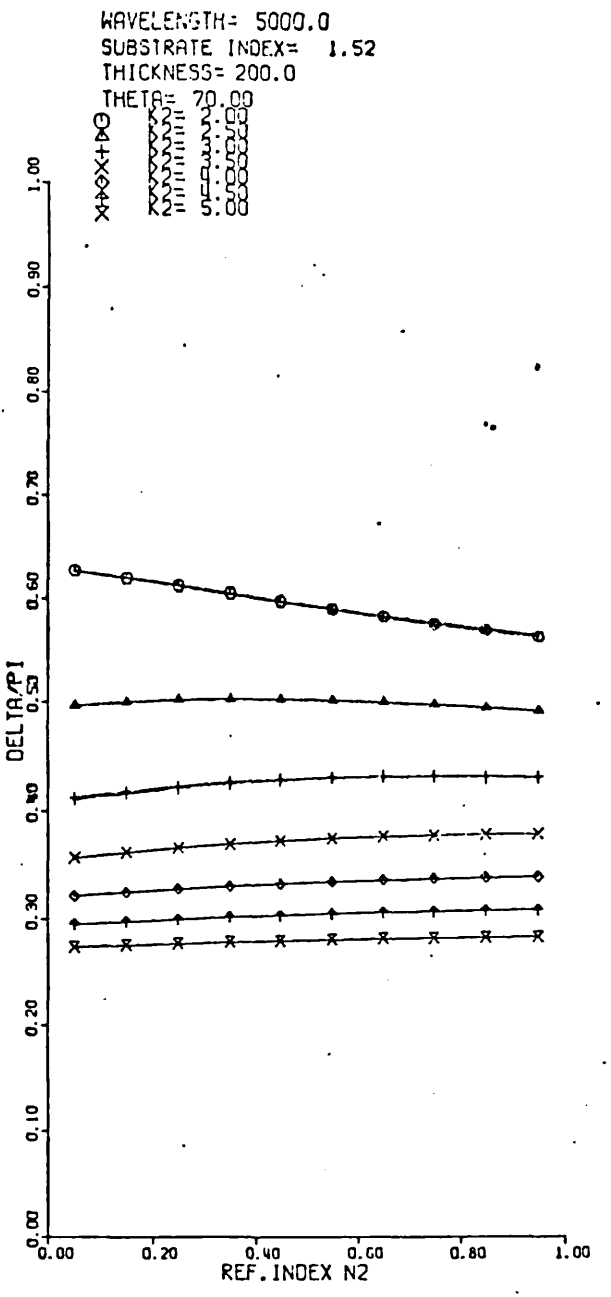
WAVELENGTH= 5000.0
SUBSTRATE INDEX= 1.52
THICKNESS= 200.0
THETA= 70.00
K2= 5.00
DELTA/PI
REF. INDEX N2
0.00
0.20
0.40
0.60
0.80
1.00

II.2.1 The Sensitivity of Δ to k in the n Range of 0.05 to 3.00 and for $0.01 \leq d/\lambda \leq 0.04$ at an Angle of Incidence $\theta = 70^{\circ}$

In this section we will try to establish how sensitive is the quantity Δ, the differential change of phase at reflection, to the optical constants n and k of thin absorbing films in the thickness and constants ranges indicated above.

In Group 1 of the graphs presented in this chapter, each is a family of curves of Δ vs n, and each curve is at a constant value of k. The values of k increase from 2.00 to 5.00 in steps of 0.5. The change in Δ corresponding to a change in k is read directly from the graph at two points, the lowest and highest values of n. The following tables give the change in k, $\Delta(k)$, corresponding to a change of Δ, $\Delta(\Delta)$, equal to $0.006\,\pi$. This is in line with Ward and Nag's[28,29] criterion mentioned earlier. Also included in the tables is a column showing the change in k corresponding to a change in Δ of $0.003\,\pi$. Two tables are given for each range of n corresponding to $d/\lambda = 0.01$ and 0.04 respectively. It has already been mentioned that the quantity Δ could be determined to $\pm\, 0.003\,\pi$ by interferometric techniques, while ellipsometric determination could lead to an accuracy of the order $0.0006\,\pi$, Avery[32]. The experimental details of the interferometric technique and results on some thin metallic films will be discussed in the following chapters.

TABLE II.1

$d/\lambda = 0.01$, $n = 0.05$, $\theta = 70^{\circ}$		
Range of k	$\Delta(k) \equiv \Delta(\Delta)$ of $0.006\,\pi$	$\Delta(k) \equiv \Delta(\Delta)$ of $0.003\,\pi$
4.5 - 5.0	0.300	0.150
4.0 - 4.5	0.150	0.075
3.5 - 4.0	0.120	0.060
3.0 - 3.5	0.030	0.015
2.5 - 3.0	0.012	0.006
2.0 - 2.5	0.010	0.005

TABLE II.2

$d/\lambda = 0.04$, $n = 0.05$, $\theta = 70^\circ$		
Range of k	$\Delta(k) \equiv \Delta(\Delta)$ of $0.006\,\pi$	$\Delta(k) \equiv \Delta(\Delta)$ of $0.003\,\pi$
4.5 - 5.0	0.150	0.075
4.0 - 4.5	0.100	0.050
3.5 - 4.0	0.075	0.037
3.0 - 3.5	0.054	0.027
2.5 - 3.0	0.038	0.019
2.0 - 2.5	0.023	0.011

TABLE II.3

$d/\lambda = 0.01$, $n = 1.0$, $\theta = 70^\circ$		
Range of k	$\Delta(k) \equiv \Delta(\Delta)$ of $0.006\,\pi$	$\Delta(k) \equiv \Delta(\Delta)$ of $0.003\,\pi$
4.5 - 5.0	0.120	0.060
4.0 - 4.5	0.080	0.040
3.5 - 4.0	0.054	0.027
3.0 - 3.5	0.038	0.019
2.5 - 3.0	0.038	0.019
2.0 - 2.5	0.023	0.011

TABLE II.4

$d/\lambda = 0.04$, $n = 1.0$, $\theta = 70^\circ$		
Range of k	$\Delta(k) \equiv \Delta(\Delta)$ of $0.006\,\pi$	$\Delta(k) \equiv \Delta(\Delta)$ of $0.003\,\pi$
4.5 - 5.0	0.100	0.050
4.0 - 4.5	0.100	0.050
3.5 - 4.0	0.100	0.050
3.0 - 3.5	0.050	0.025
2.5 - 3.0	0.054	0.027
2.0 - 2.5	0.035	0.017

TABLE II.5

$d/\lambda = 0.01$, $n = 2.0$, $\theta = 70^\circ$		
Range of k	$\Delta(k) \equiv \Delta(\Delta)$ of $0.006\ \pi$	$\Delta(k) \equiv \Delta(\Delta)$ of $0.003\ \pi$
4.5 - 5.0	0.120	0.060
4.0 - 4.5	0.100	0.050
3.5 - 4.0	0.080	0.040
3.0 - 3.5	0.066	0.033
2.5 - 3.0	0.065	0.032
2.0 - 2.5	0.066	0.033

TABLE II.6

$d/\lambda = 0.04$, $n = 2.0$, $\theta = 70^\circ$		
Range of k	$\Delta(k) \equiv \Delta(\Delta)$ of $0.006\ \pi$	$\Delta(k) \equiv \Delta(\Delta)$ of $0.003\ \pi$
4.5 - 5.0	0.120	0.060
4.0 - 4.5	0.107	0.053
3.5 - 4.0	0.093	0.046
3.0 - 3.5	0.085	0.042
2.5 - 3.0	0.066	0.033
2.0 - 2.5	0.073	0.036

TABLE II.7

$d/\lambda = 0.01$, $n = 3.0$, $\theta = 70^\circ$		
Range of k	$\Delta(k) \equiv \Delta(\Delta)$ of $0.006\ \pi$	$\Delta(k) \equiv \Delta(\Delta)$ of $0.003\ \pi$
4.5 - 5.0	0.200	0.100
4.0 - 4.5	0.150	0.075
3.5 - 4.0	0.150	0.075
3.0 - 3.5	0.150	0.075
2.5 - 3.0	0.190	0.095
2.0 - 2.5	0.210	0.105

TABLE II.8

$d/\lambda = 0.01$, $n = 3.0$, $\theta = 70^{\circ}$		
Range of k	$\Delta(k) \equiv \Delta(\Delta)$ of $0.006\,\pi$	$\Delta(k) \equiv \Delta(\Delta)$ of $0.003\,\pi$
4.5 - 5.0	0.150	0.075
4.0 - 4.5	0.120	0.060
3.5 - 4.0	0.120	0.060
3.0 - 3.5	0.120	0.060
2.5 - 3.0	0.100	0.050
2.0 - 2.5	0.111	0.055

It is clear from the tables just presented that the quantity $\Delta = (\delta_p - \delta_s)$ does in fact meet the sensitivity requirement of the Ward and Nag's criterion in almost all the regions considered. However, it was noticed that Δ becomes insensitive in the regions (a) $4.5 \leq k \leq 5.0$, $n = 0.05$ and $d/\lambda \leq 0.02$; (b) $2.0 \leq k \leq 5.0$, $n = 5.0$ and $d/\lambda \leq 0.02$. At $3.5 \leq n \leq 4.0$ and for $d/\lambda \leq 0.02$ multiple solutions occur, and one is facing the situation where a certain value of Δ could result from one value of n and two or more values of k. This situation is, probably, of theoretical interest, but could be experimentally confusing and could lead to significantly wrong answers.

From the second column of the previous tables it could be concluded that the accuracy with which k could be determined ranges from ± 0.09 to ± 0.005, a typical accuracy would be of the order ± 0.03. This considering that Δ could be determined to $\pm 0.003\,\pi$. If Δ is determined to $\pm 0.0006\,\pi$ [32] the accuracy for k could be still higher. As mentioned before, the sensitivity of Δ increases with higher incidence and this is evident by comparing graphs at 70° to those at 45°. This was found to be generally the case.

II.2.2 The Sensitivity of Δ to n in the k Range of 2.0 to 5.0 and for $0.01 \leq d/\lambda \leq 0.04$ at an Angle of Incidence $\theta = 70^{\circ}$

As for the sensitivity of Δ to n in the above mentioned ranges of k and d/λ, two points of importance emerge from examining the graphs of Δ vs n at $\theta = 70^{\circ}$:

(1) The variation of Δ with n becomes more considerable in the regions of $k \leq 3.0$ and for lower values of $n \leq 2.0$.

(2) The higher the d/λ value the less noticeable is the variation of Δ with n.

In the following some tables illustrating these points will be presented. In these tables $\Delta(n) \equiv \Delta(\Delta)$ of $0.006\,\pi$ will be given at specific values of k, d/λ and $\theta = 70^{\circ}$.

It is to be emphasized here that all the figures appearing in tables contained in this chapter are derived from readings taken off the graphs directly. This, inevitably, introduces some inaccuracies, and they should be taken as a guide to the changes in n and k corresponding to changes in the measurable Δ. Specific cases would have to be treated separately, and accurate readings could be made off suitably scaled graphs over the desired ranges of variables.

TABLE II.9

$d/\lambda = 0.01$, $k = 2.00$, $\theta = 70^\circ$		
Range of n	$\Delta(n) \equiv \Delta(\Delta)$ of $0.006\ \pi$	$\Delta(n) \equiv \Delta(\Delta)$ of $0.003\ \pi$
0.05 - 1.00	ranges from 0.015 to 0.03	ranges from 0.007 to 0.015
2.00 - 3.00	approx. 0.06	approx. 0.03

TABLE II.10

$d/\lambda = 0.01$, $k = 5.00$, $\theta = 70^\circ$		
Range of n	$\Delta(n) \equiv \Delta(\Delta)$ of $0.006\ \pi$	$\Delta(n) \equiv \Delta(\Delta)$ of $0.003\ \pi$
0.05 - 1.00	more than 0.20	more than 0.10
2.00 - 3.00	Undetectable	Undetectable

TABLE II.11

$d/\lambda = 0.04$, $k = 2.00$, $\theta = 70^\circ$		
Range of n	$\Delta(n) \equiv \Delta(\Delta)$ of $0.006\ \pi$	$\Delta(n) \equiv \Delta(\Delta)$ of $0.003\ \pi$
0.05 - 1.00	0.06	0.03
2.00 - 3.00	approx. 0.12	approx. 0.06

TABLE II.12

$d/\lambda = 0.04$, $k = 5.00$, $\theta = 70^\circ$		
Range of n	$\Delta(n) \equiv \Delta(\Delta)$ of $0.006\ \pi$	$\Delta(n) \equiv \Delta(\Delta)$ of $0.003\ \pi$
0.05 - 1.00	over 0.30	over 0.15
2.00 - 3.00	approx. 0.20	approx. 0.10

II.2.3 The Sensitivity of Δ to k in the n Range of 0.05 to 3.00 and for $0.06 \leq d/\lambda \leq 0.10$ at an Angle of Incidence $\theta = 70^{\circ}$

Here we continue to assess the sensitivity of the differential change $\Delta = (\delta_p - \delta_s)$ to the extinction coefficient k in the higher range of thickness where d/λ ranges between 0.06 and 0.10. The important features of this region can be summarized as follows:

(1) The quantity Δ remains sensitive to k in this region, and, generally speaking, this sensitivity is increased with the increase of thickness. This is evident from comparing corresponding figures in Tables II.2 - II.9 and II.14 - II.21.

(2) The sensitivity of Δ to n in general is decreasing with higher thicknesses and higher values of n and k ($n \geq 2.0$ and $k \geq 3.0$).

(3) Multiple solutions do occur at values of $n \geq 3.2$.

However it should be emphasized here that specific cases for certain applications must be treated on their own in the regions of interest. This will be shown in Chapter VI for the cases of films of Ag, Au and Aℓ.

GROUP 2 GRAPHS OF Δ vs n

(a) $0.05 \leq n \leq 1.0$

(b) $1.0 \leq n \leq 2.0$

(c) $2.0 \leq n \leq 3.0$

$2.0 \leq k \leq 5.0$ $\quad \theta = 70^\circ$

$0.06 \leq d/\lambda \leq 0.10$ $\quad \theta = 45^\circ$

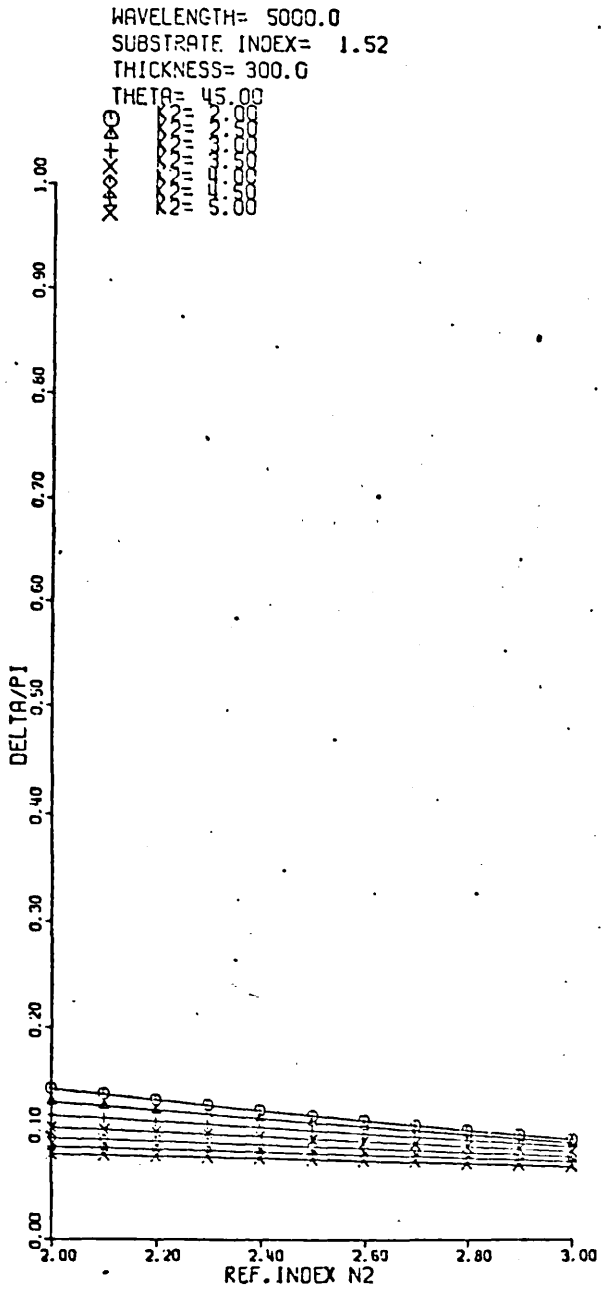
WAVELENGTH= 5000.0
SUBSTRATE INDEX= 1.52
THICKNESS= 300.0
THETA= 45.00
DELTA/PI
REF.INDEX N2
2.00
2.20
2.40
2.60
2.80
3.00
0.00
0.10
0.20
0.30
0.40
0.50
0.60
0.70
0.80
0.90
1.00

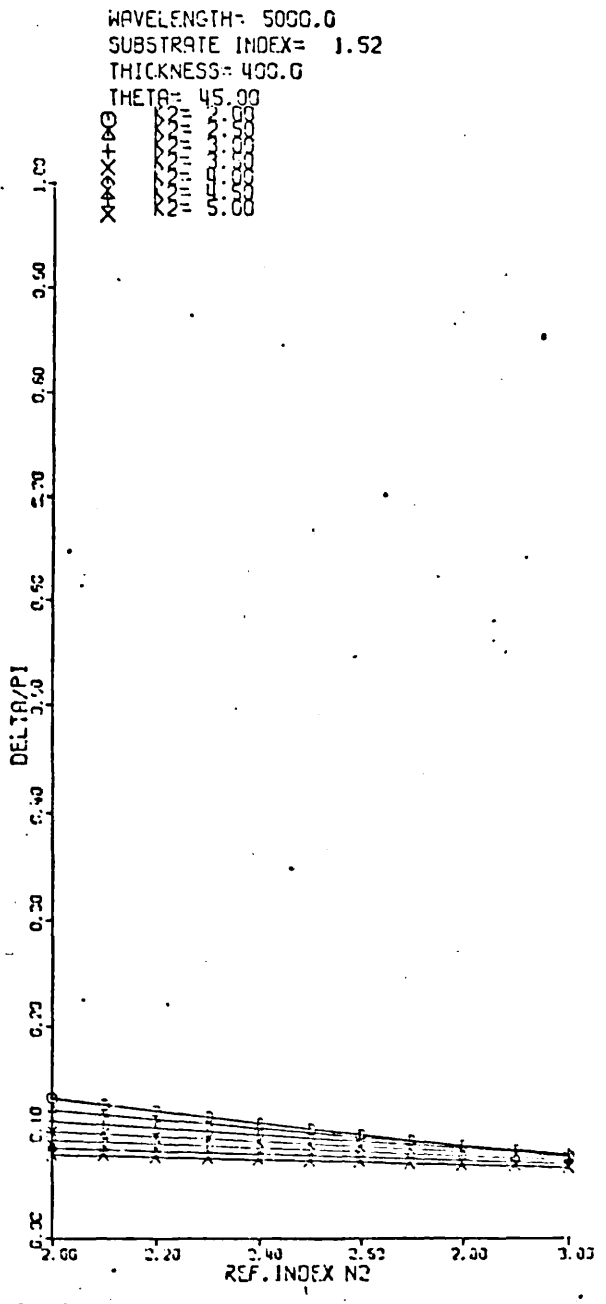
WAVELENGTH= 5000.0
SUBSTRATE INDEX= 1.52
THICKNESS= 400.0
THETA= 45.00
DELTA/PI
REF.INDEX N2

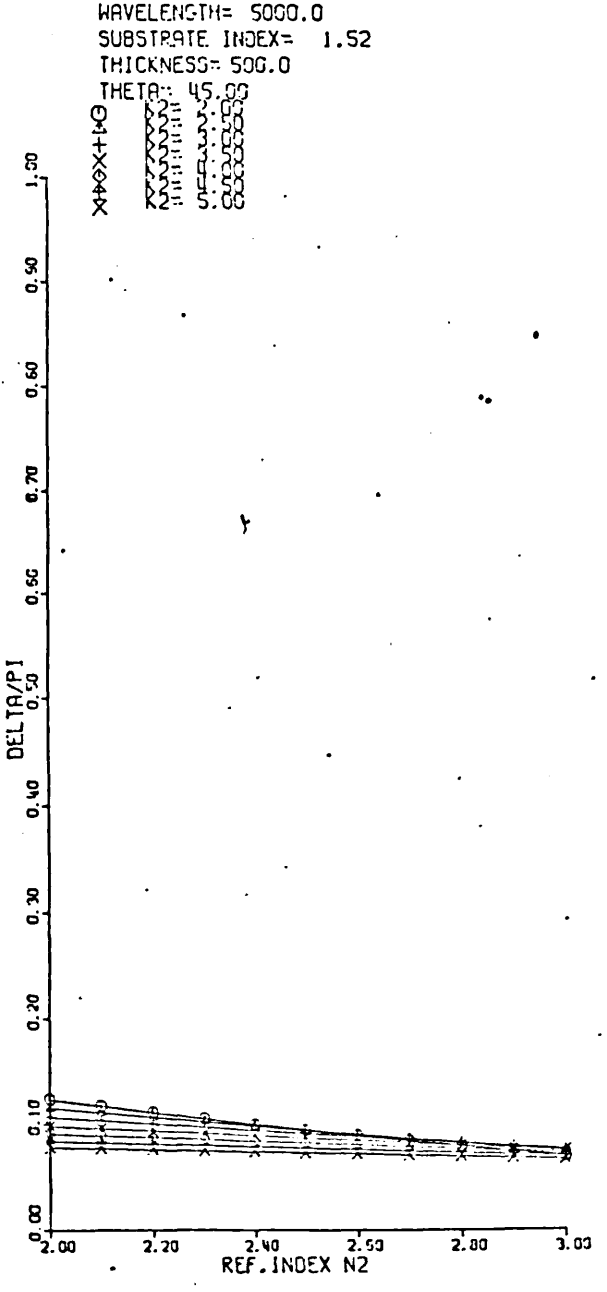
WAVELENGTH= 5000.0
SUBSTRATE INDEX= 1.52
THICKNESS= 500.0
THETA= 45.00
DELTA/PI
REF.INDEX N2

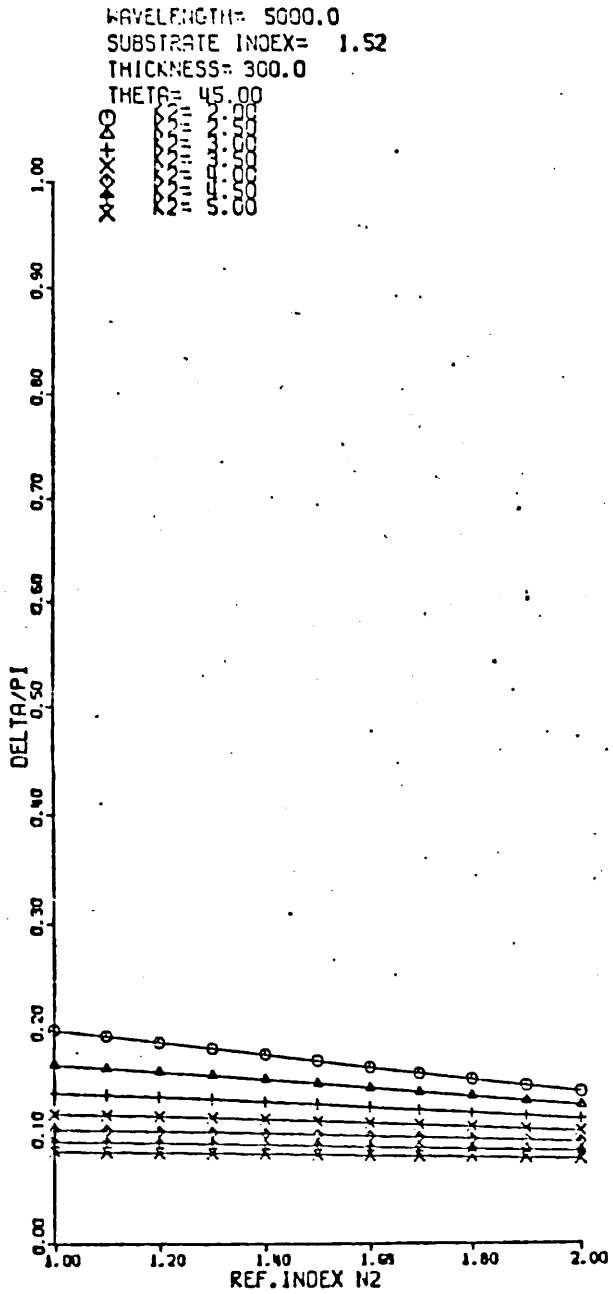
WAVELENGTH= 5000.0
SUBSTRATE INDEX= 1.52
THICKNESS= 300.0
THETA= 45.00
K2
2.50
5.00
DELTA/PI
0.00
0.10
0.20
0.30
0.40
0.50
0.60
0.70
0.80
0.90
1.00
1.00
1.20
1.40
1.60
1.80
2.00
REF.INDEX N2

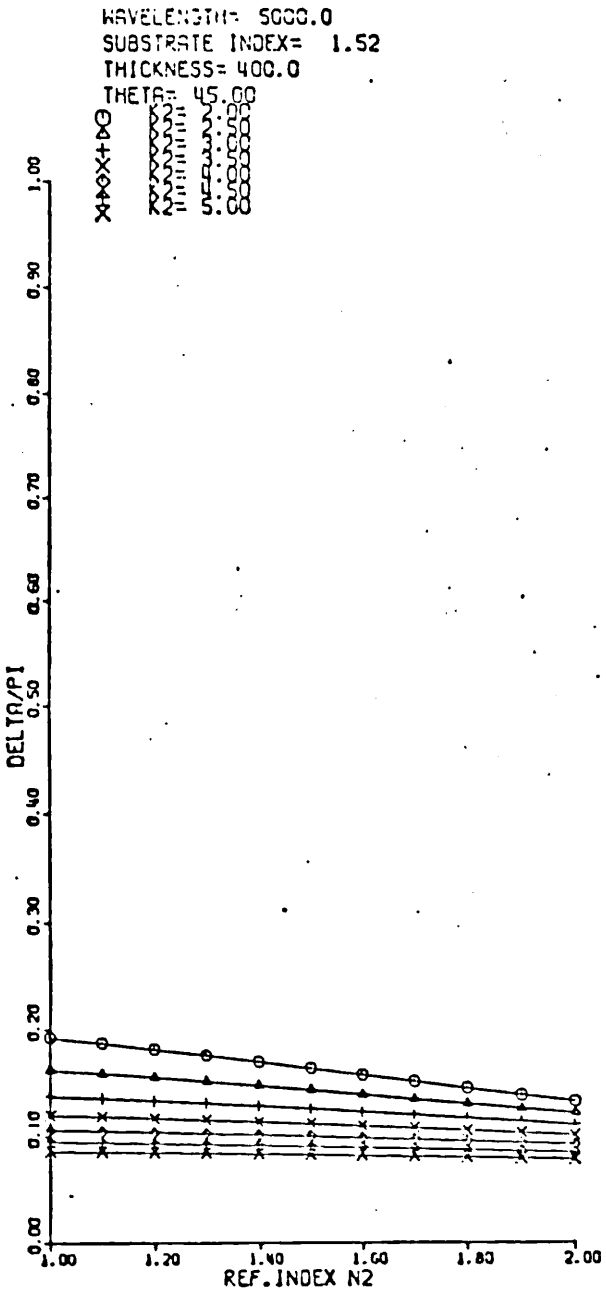
WAVELENGTH= 5000.0
SUBSTRATE INDEX= 1.52
THICKNESS= 400.0
THETA= 45.00
K2
2.50
5.00
DELTA/PI
0.00
0.10
0.20
0.30
0.40
0.50
0.60
0.70
0.80
0.90
1.00
1.00
1.20
1.40
1.60
1.80
2.00
REF.INDEX N2

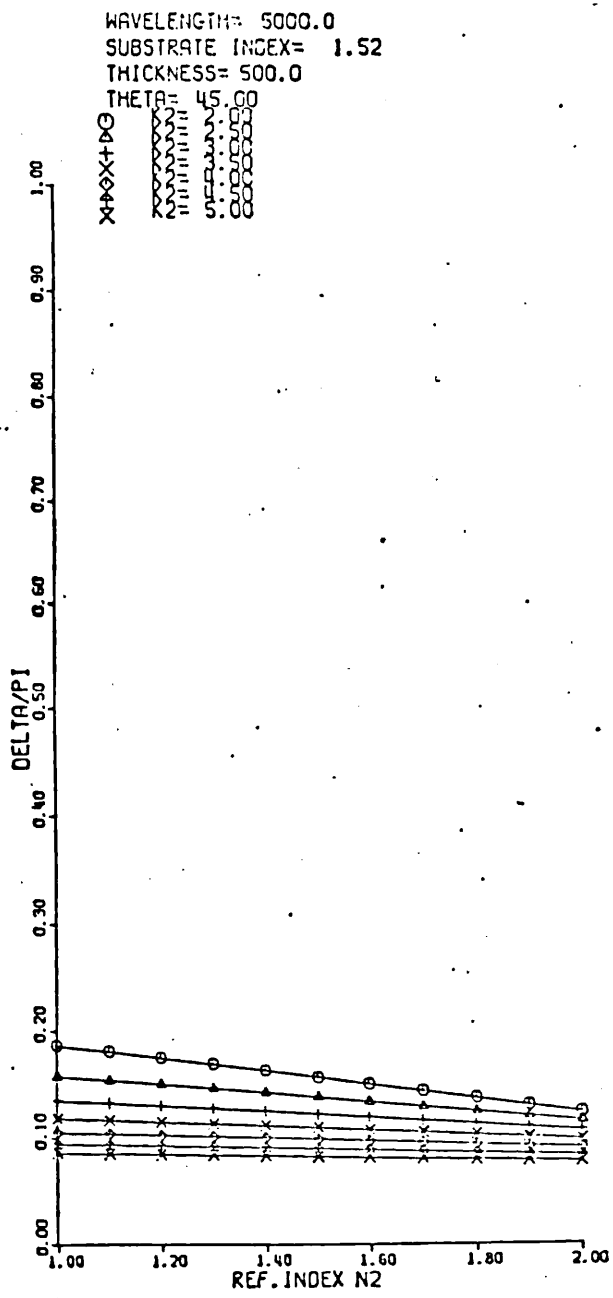
WAVELENGTH= 5000.0
SUBSTRATE INDEX= 1.52
THICKNESS= 500.0
THETA= 45.00
K2
2.50
5.00
DELTA/PI
0.00
0.10
0.20
0.30
0.40
0.50
0.60
0.70
0.80
0.90
1.00
1.00
1.20
1.40
1.60
1.80
2.00
REF.INDEX N2

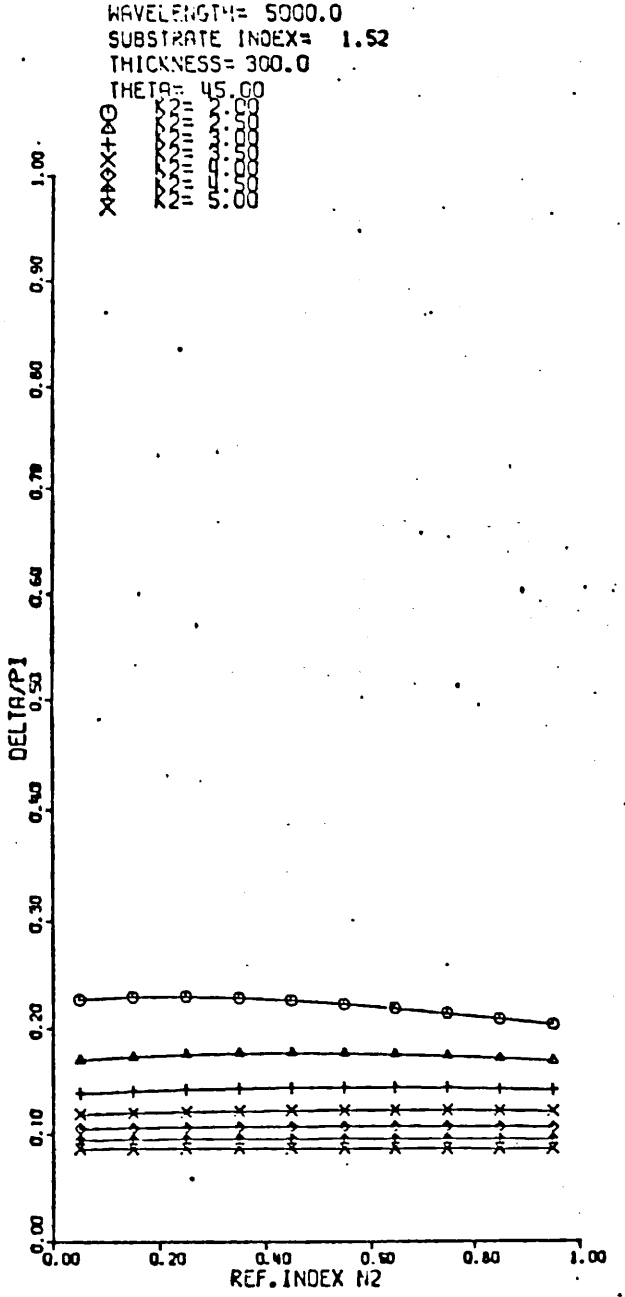
WAVELENGTH= 5000.0
SUBSTRATE INDEX= 1.52
THICKNESS= 300.0
THETA= 45.00
K2= 2.00
K2= 2.50
K2= 3.00
K2= 3.50
K2= 4.00
K2= 4.50
K2= 5.00
DELTA/PI
REF.INDEX N2
0.00
0.20
0.40
0.60
0.80
1.00

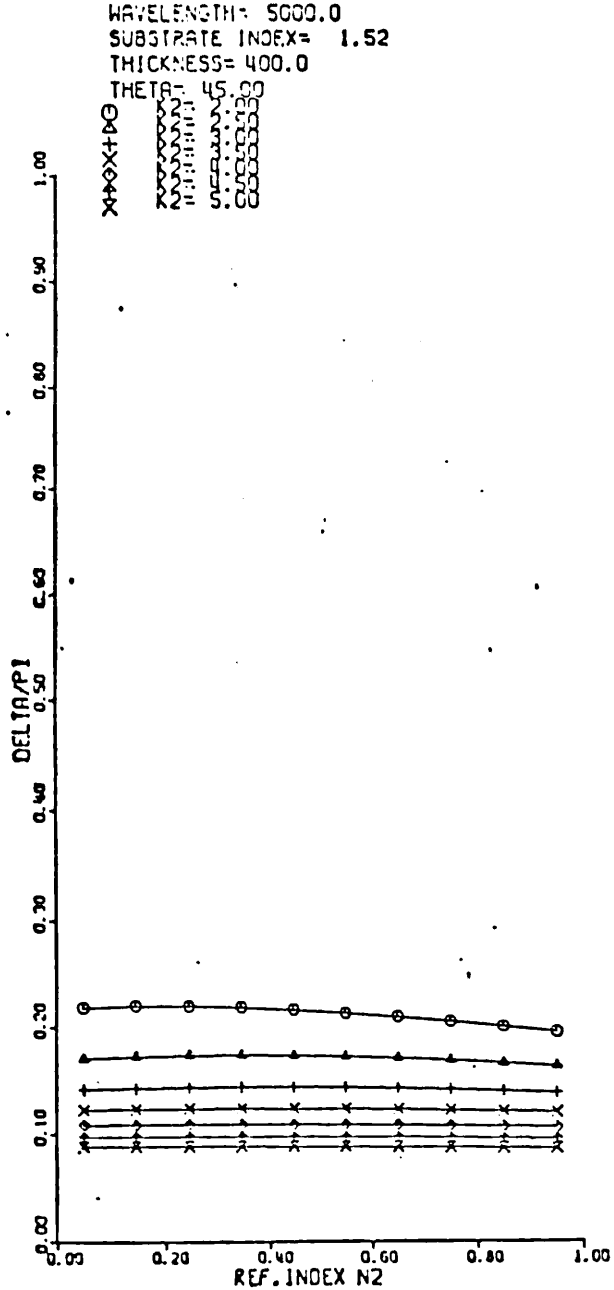
WAVELENGTH= 5000.0
SUBSTRATE INDEX= 1.52
THICKNESS= 400.0
THETA= 45.00
K2= 5.00
DELTA/PI
REF.INDEX N2
0.00
0.20
0.40
0.60
0.80
1.00

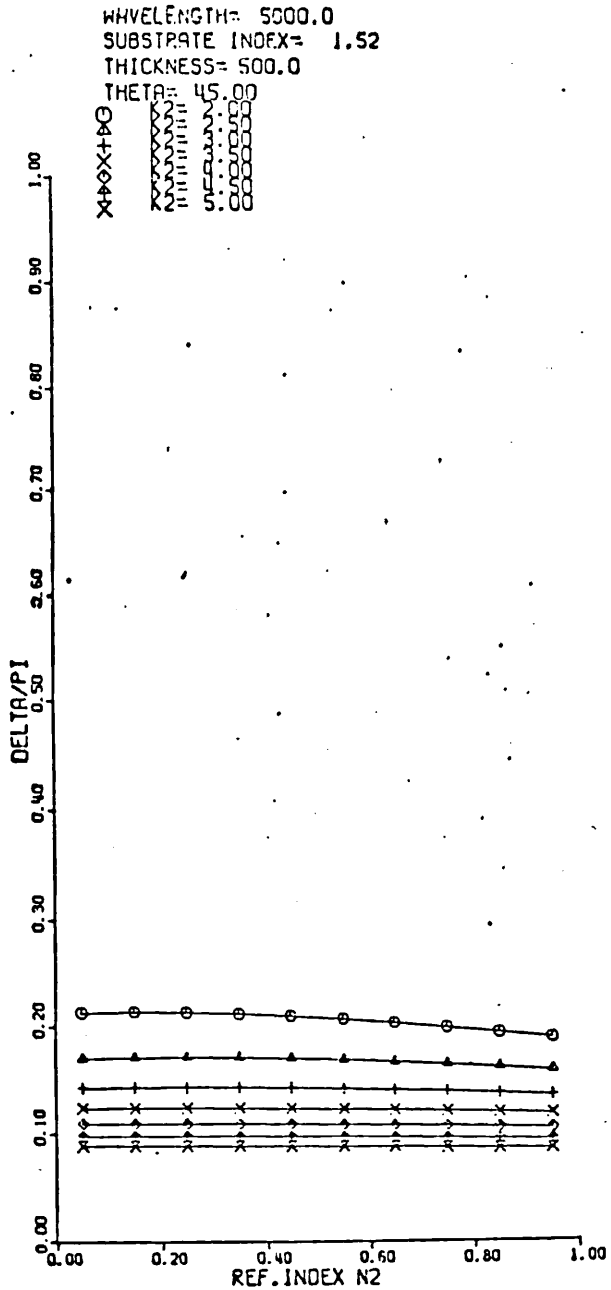
WAVELENGTH= 5000.0
SUBSTRATE INDEX= 1.52
THICKNESS= 500.0
THETA= 45.00
K2= 5.00
DELTA/PI
REF.INDEX N2
0.00
0.20
0.40
0.60
0.80
1.00

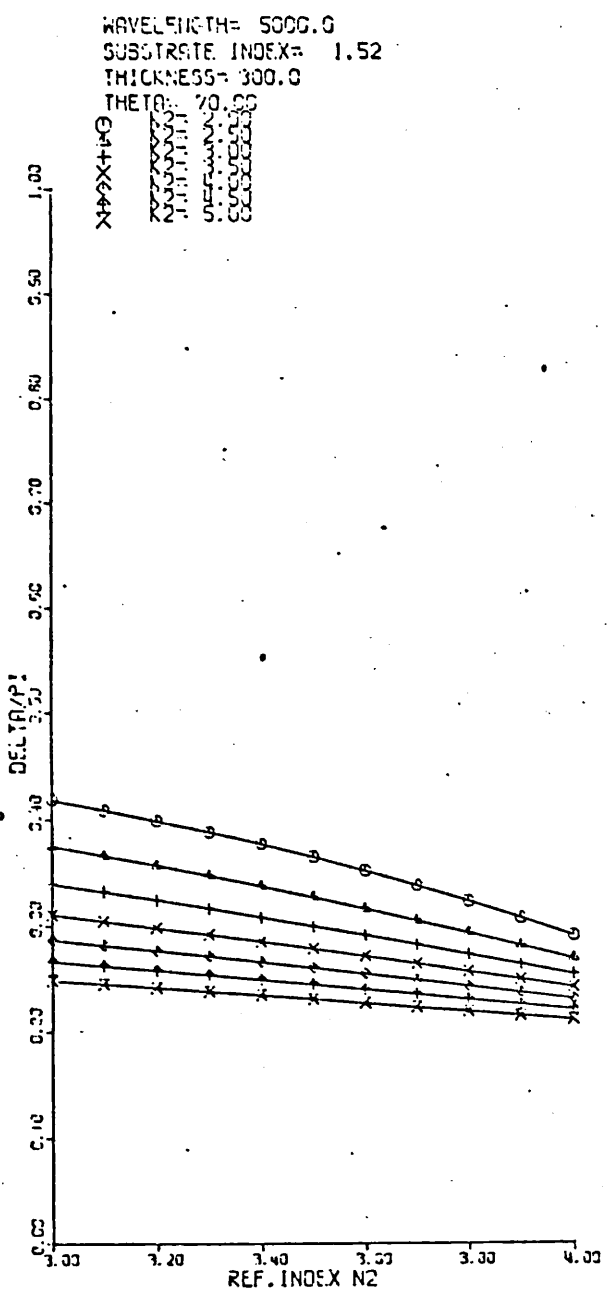
WAVELENGTH= 5000.0
SUBSTRATE INDEX= 1.52
THICKNESS= 300.0
THETA= 70.00
DELTA/PI
REF.INDEX N2

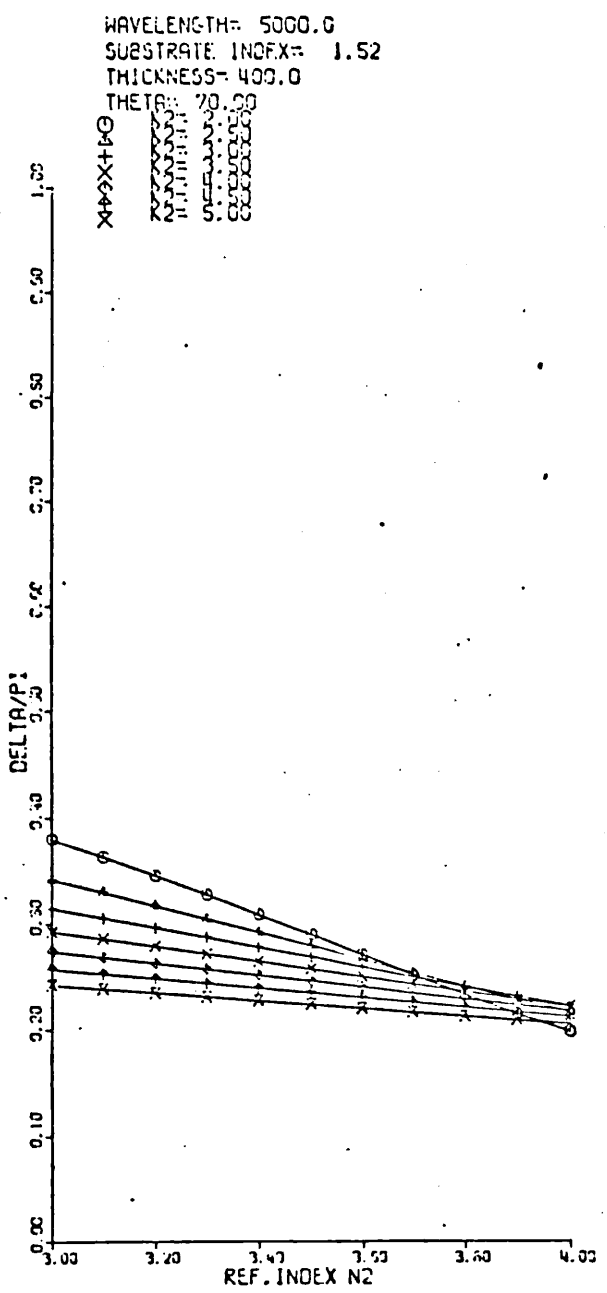
WAVELENGTH= 5000.0
SUBSTRATE INDEX= 1.52
THICKNESS= 400.0
THETA= 70.00
DELTA/PI
REF.INDEX N2

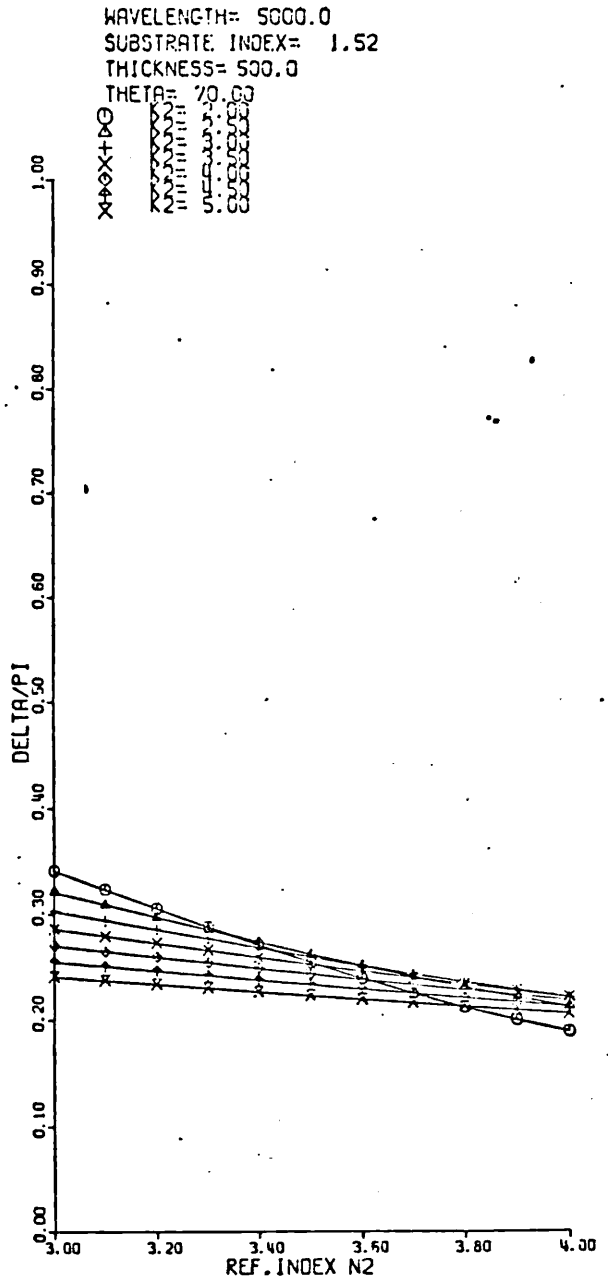
WAVELENGTH= 5000.0
SUBSTRATE INDEX= 1.52
THICKNESS= 500.0
THETA= 70.00
DELTA/PI
REF.INDEX N2

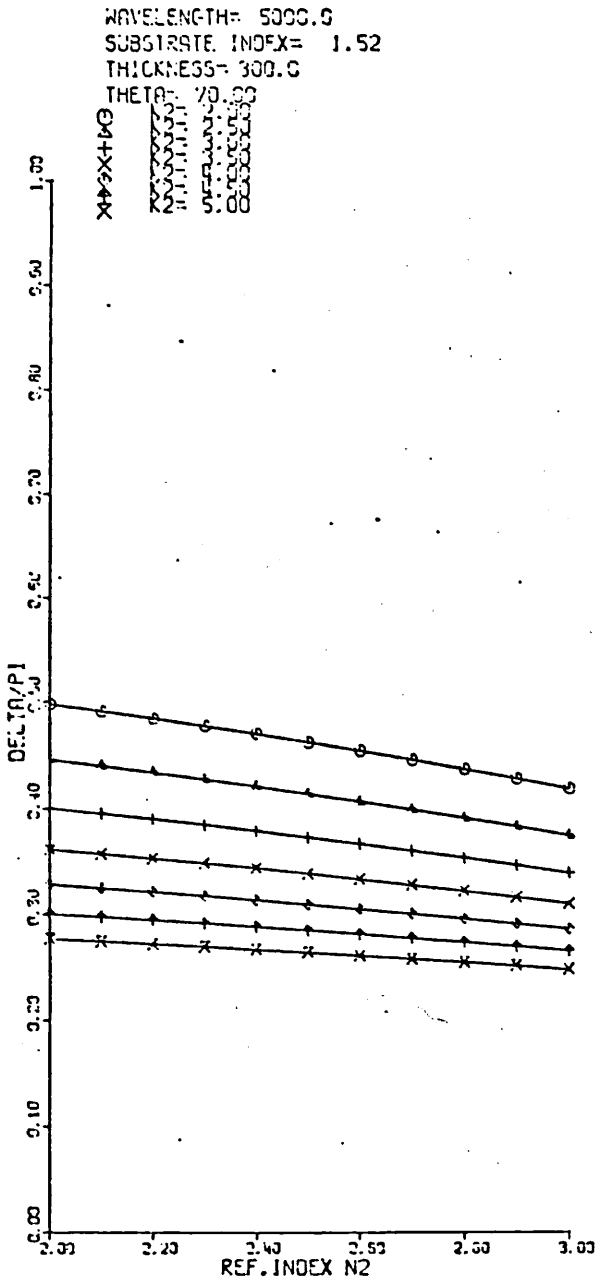
WAVELENGTH= 5000.0
SUBSTRATE INDEX= 1.52
THICKNESS= 300.0
THETA= 70.00
DELTA/PI
REF.INDEX N2

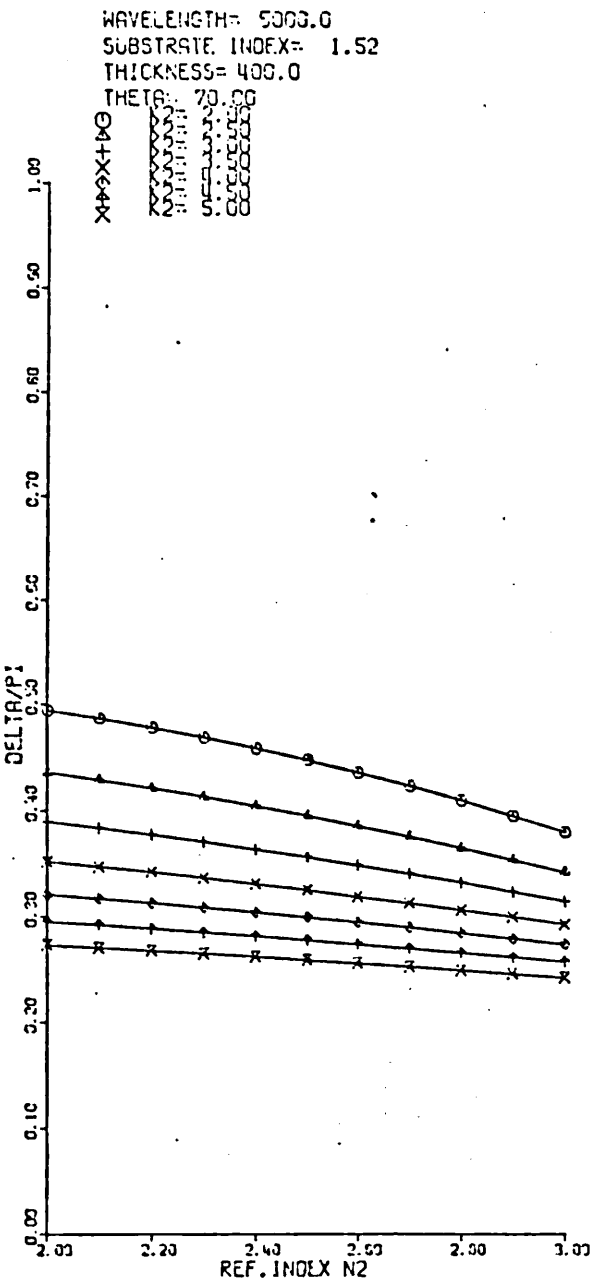
WAVELENGTH= 5000.0
SUBSTRATE INDEX= 1.52
THICKNESS= 400.0
THETA= 70.00
DELTA/PI
REF.INDEX N2

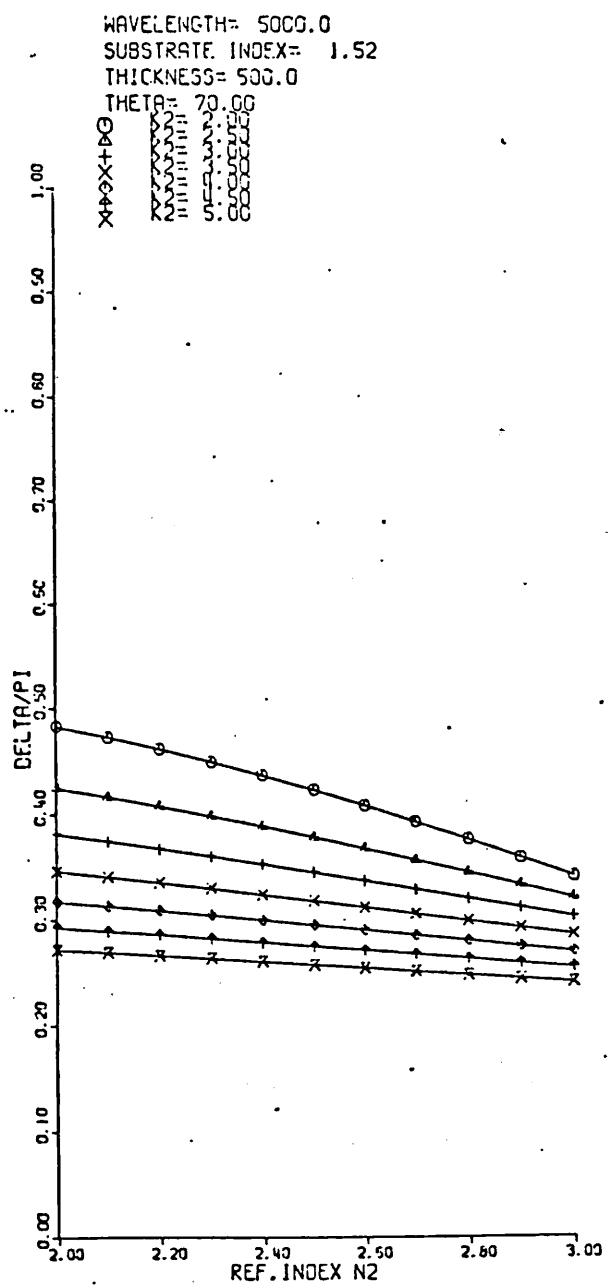
WAVELENGTH= 5000.0
SUBSTRATE INDEX= 1.52
THICKNESS= 500.0
THETA= 70.00
DELTA/PI
REF.INDEX N2

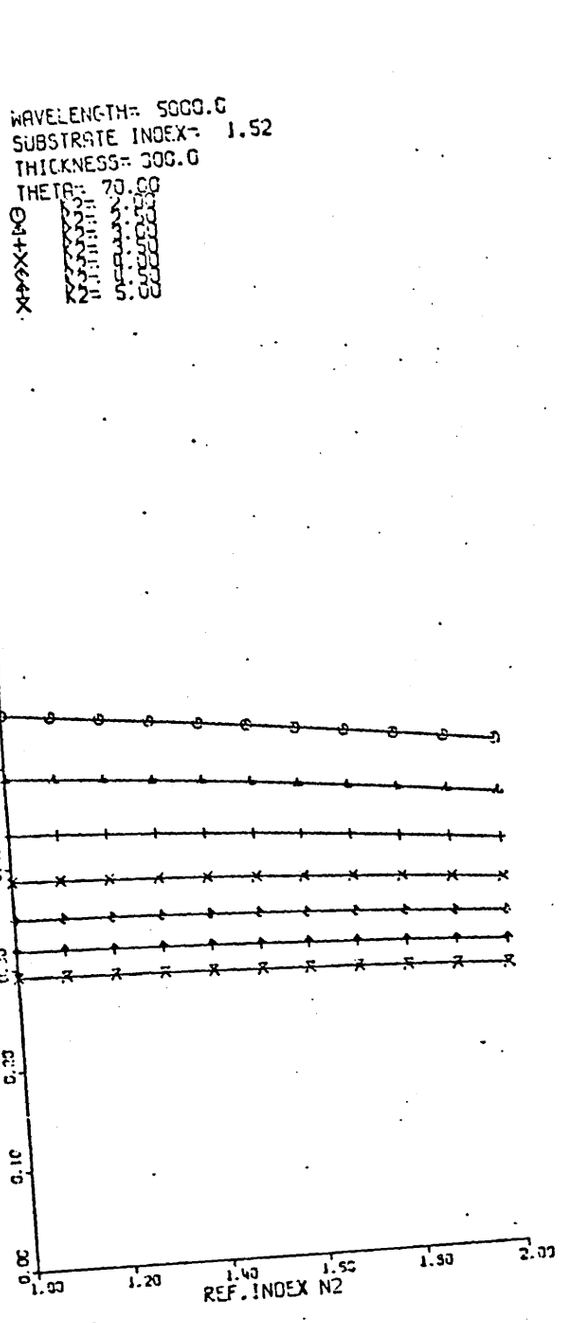
WAVELENGTH= 5000.0
SUBSTRATE INDEX= 1.52
THICKNESS= 300.0
THETA= 70.00
DELTA/PI
REF.INDEX N2
1.00
1.20
1.40
1.60
1.80
2.00
0.00
0.10
0.20
0.30
0.40
0.50
0.60
0.70
0.80
0.90
1.00

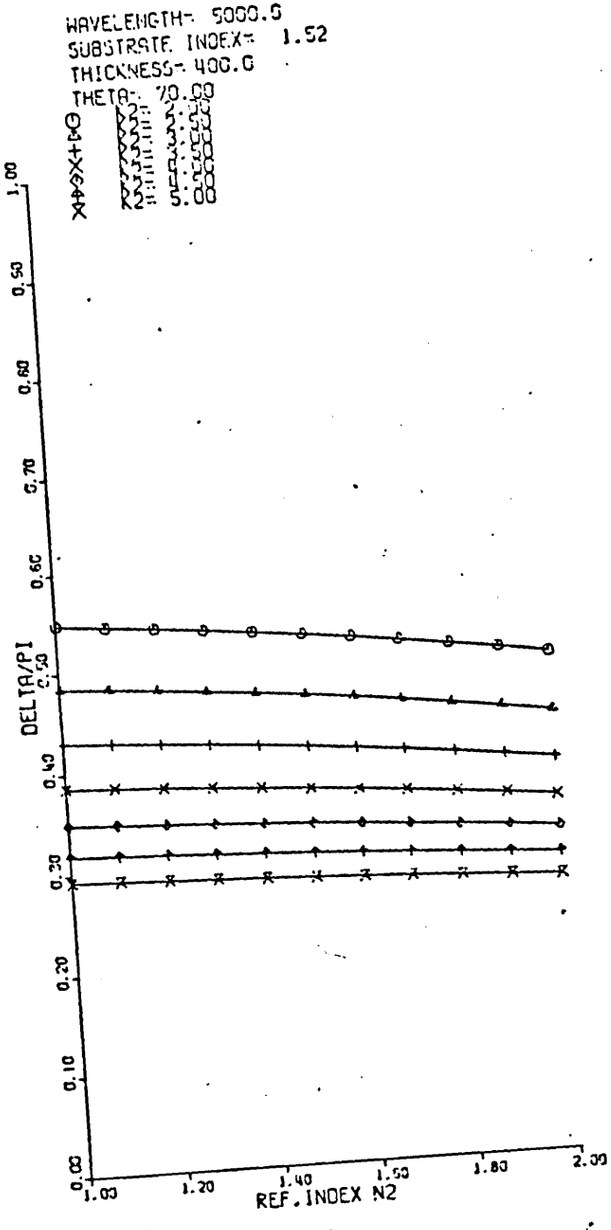
WAVELENGTH= 5000.0
SUBSTRATE INDEX= 1.52
THICKNESS= 400.0
THETA= 70.00
DELTA/PI
REF.INDEX N2
1.00
1.20
1.40
1.60
1.80
2.00
0.00
0.10
0.20
0.30
0.40
0.50
0.60
0.70
0.80
0.90
1.00

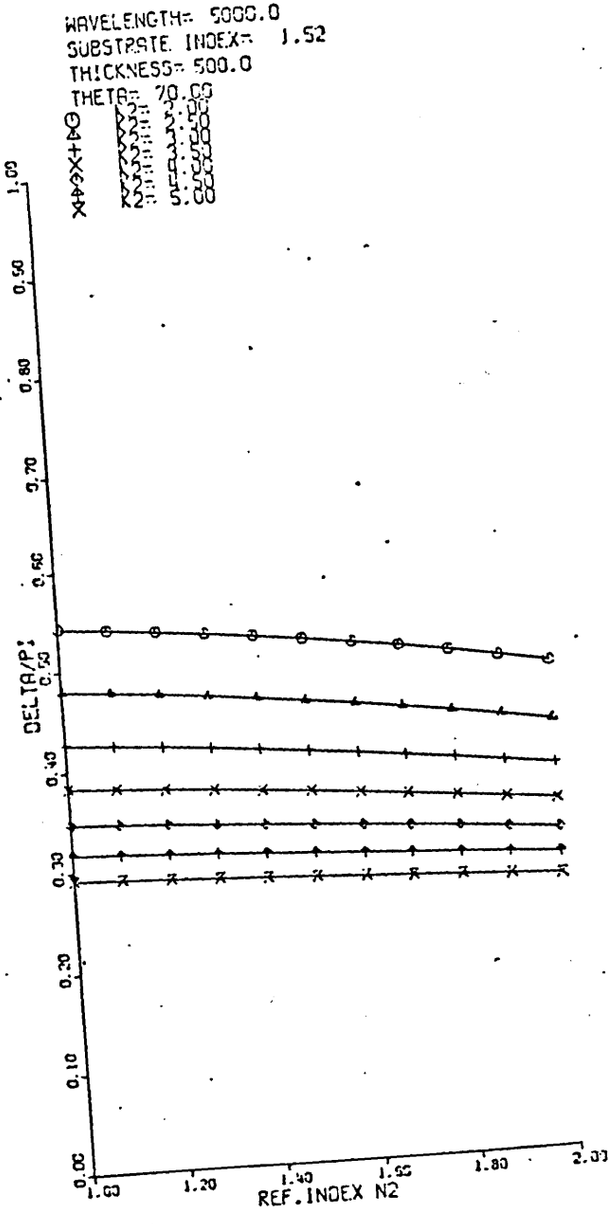
WAVELENGTH= 5000.0
SUBSTRATE INDEX= 1.52
THICKNESS= 500.0
THETA= 70.00
DELTA/PI
REF.INDEX N2
1.00
1.20
1.40
1.60
1.80
2.00
0.00
0.10
0.20
0.30
0.40
0.50
0.60
0.70
0.80
0.90
1.00

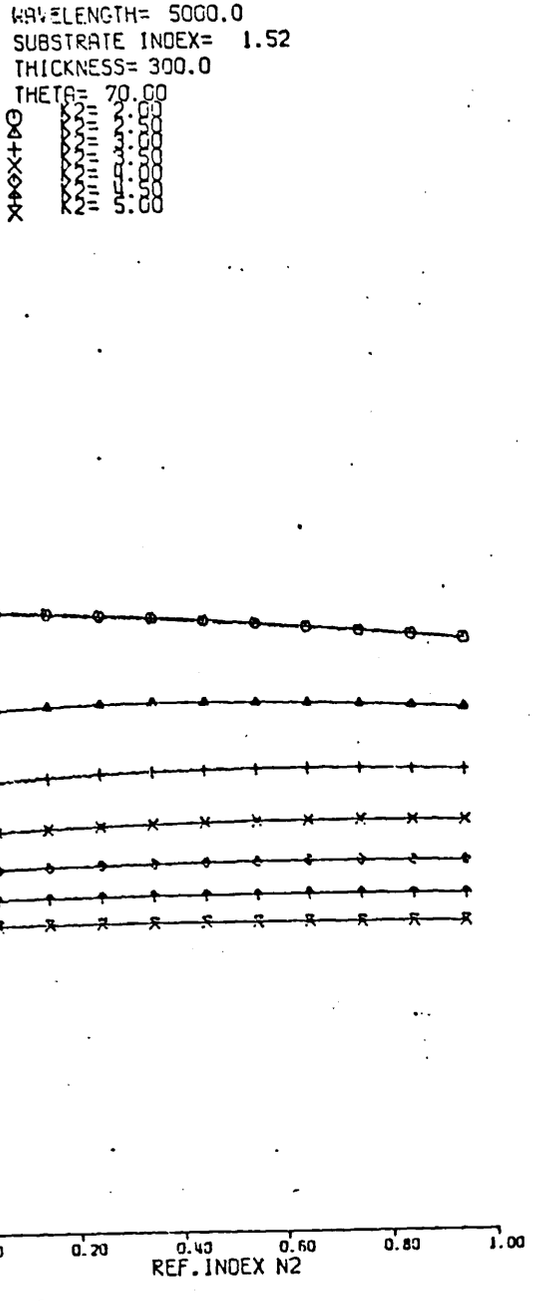
WAVELENGTH= 5000.0
SUBSTRATE INDEX= 1.52
THICKNESS= 300.0
THETA= 70.00
K2= 2.00
K2= 5.00
DELTA/PI
REF.INDEX N2
0.00
0.10
0.20
0.30
0.40
0.50
0.60
0.70
0.80
0.90
1.00

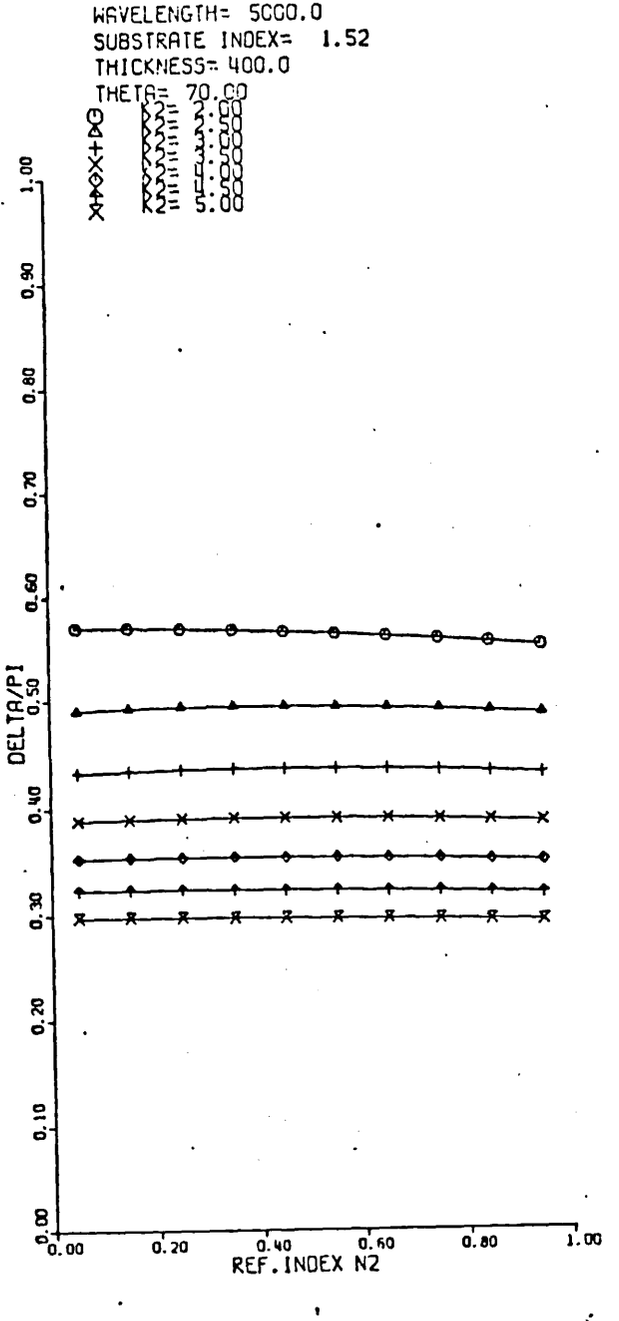
WAVELENGTH= 5000.0
SUBSTRATE INDEX= 1.52
THICKNESS= 400.0
THETA= 70.00
K2= 2.00
K2= 5.00
DELTA/PI
REF.INDEX N2
0.00
0.10
0.20
0.30
0.40
0.50
0.60
0.70
0.80
0.90
1.00

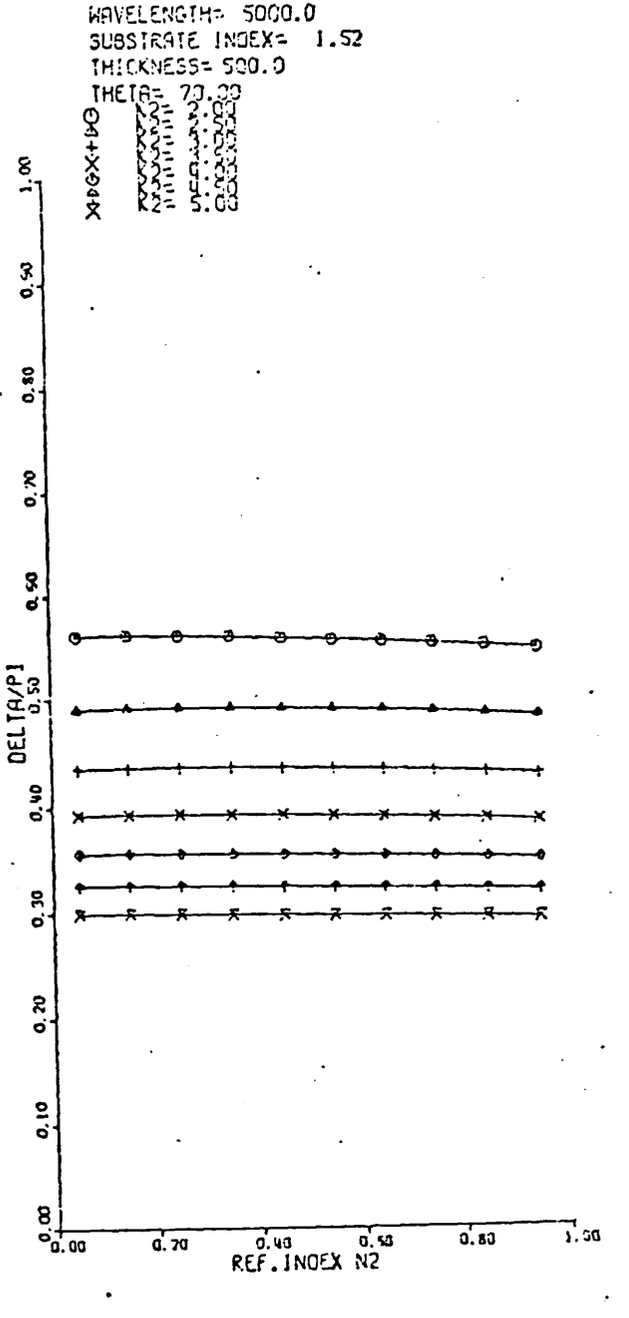
WAVELENGTH= 5000.0
SUBSTRATE INDEX= 1.52
THICKNESS= 500.0
THETA= 70.00
DELTA/PI
REF.INDEX N2
0.00
0.10
0.20
0.30
0.40
0.50
0.60
0.70
0.80
0.90
1.00

TABLE II.13

$d/\lambda = 0.06$, $n = 0.05$, $\theta = 70^\circ$		
Range of k	$\Delta(k) \equiv \Delta(\Delta)$ of $0.006\ \pi$	$\Delta(k) \equiv \Delta(\Delta)$ of $0.003\ \pi$
4.5 - 5.0	0.135	0.067
4.0 - 4.5	0.100	0.050
3.5 - 4.0	0.085	0.042
3.0 - 3.5	0.060	0.030
2.5 - 3.0	0.048	0.024
2.0 - 2.5	0.035	0.017

TABLE II.14

$d/\lambda = 0.10$, $n = 0.05$, $\theta = 70^\circ$		
Range of k	$\Delta(k) \equiv \Delta(\Delta)$ of $0.006\ \pi$	$\Delta(k) \equiv \Delta(\Delta)$ of $0.003\ \pi$
4.5 - 5.0	0.120	0.060
4.0 - 4.5	0.100	0.050
3.5 - 4.0	0.085	0.042
3.0 - 3.5	0.066	0.033
2.5 - 3.0	0.054	0.027
2.0 - 2.5	0.042	0.021

TABLE II.15

$d/\lambda = 0.06$, $n = 1.0$, $\theta = 70^\circ$		
Range of k	$\Delta(k) \equiv \Delta(\Delta)$ of $0.006\ \pi$	$\Delta(k) \equiv \Delta(\Delta)$ of $0.0\ 3\ \pi$
4.5 - 5.0	0.110	0.055
4.0 - 4.5	0.100	0.050
3.5 - 4.0	0.066	0.033
3.0 - 3.5	0.060	0.030
2.5 - 3.0	0.054	0.027
2.0 - 2.5	0.046	0.023

TABLE II.16

$d/\lambda = 0.10$, $n = 1.0$, $\theta = 70^\circ$		
Range of k	$\Delta(k) \equiv \Delta(\Delta)$ of $0.006\ \pi$	$\Delta(k) \equiv \Delta(\Delta)$ of $0.003\ \pi$
4.5 - 5.0	0.110	0.055
4.0 - 4.5	0.105	0.052
3.5 - 4.0	0.080	0.040
3.0 - 3.5	0.070	0.035
2.5 - 3.0	0.055	0.027
2.0 - 2.5	0.045	0.022

TABLE II.17

$d/\lambda = 0.06$, $n = 2.0$, $\theta = 70^\circ$		
Range of k	$\Delta(k) \equiv \Delta(\Delta)$ of $0.006\ \pi$	$\Delta(k) \equiv \Delta(\Delta)$ of $0.003\ \pi$
4.5 - 5.0	0.135	0.067
4.0 - 4.5	0.100	0.050
3.5 - 4.0	0.090	0.045
3.0 - 3.5	0.080	0.040
2.5 - 3.0	0.063	0.031
2.0 - 2.5	0.060	0.030

TABLE II.18

$d/\lambda = 0.10$, $n = 2.0$, $\theta = 70^\circ$		
Range of k	$\Delta(k) \equiv \Delta(\Delta)$ of $0.006\ \pi$	$\Delta(k) \equiv \Delta(\Delta)$ of $0.003\ \pi$
4.5 - 5.0	0.135	0.067
4.0 - 4.5	0.125	0.062
3.5 - 4.0	0.100	0.050
3.0 - 3.5	0.085	0.042
2.5 - 3.0	0.070	0.035
2.0 - 2.5	0.050	0.025

TABLE II.19

$d/\lambda = 0.06$, $n = 3.0$, $\theta = 70^\circ$		
Range of k	$\Delta(k) \equiv \Delta(\Delta)$ of $0.006\ \pi$	$\Delta(k) \equiv \Delta(\Delta)$ of $0.003\ \pi$
4.5 - 5.0	0.150	0.075
4.0 - 4.5	0.130	0.065
3.5 - 4.0	0.110	0.055
3.0 - 3.5	0.100	0.050
2.5 - 3.0	0.085	0.042
2.0 - 2.5	0.070	0.035

TABLE II.20

$d/\lambda = 0.10$, $n = 3.0$, $\theta = 70^\circ$		
Range of k	$\Delta(k) \equiv \Delta(\Delta)$ of $0.006\ \pi$	$\Delta(k) \equiv \Delta(\Delta)$ of $0.003\ \pi$
4.5 - 5.0	in this region the sensitivity of Δ to k drops beyond the values in the tables above and also multiple roots occur for values of $n \geq 3.2$.	
4.0 - 4.5		
3.5 - 4.0		
3.0 - 3.5		
2.5 - 3.0		
2.0 - 2.5		

II.2.4 Conclusions

In this chapter it was attempted to explore and investigate the sensitivity of the polarimetric measurable Δ, to the optical constants n and k and to d/λ and θ. It is hoped that Δ has been shown to be sensitive to k over a wide range of n and thickness ($0.005 \leq n \leq 3.0$ and $0.01 \leq d/\lambda \leq 0.1$). However, the sensitivity to n is limited to certain cases and these are mostly in the lower ranges of thickness. As for suitable incidence it was found that the highest possible incidence is required.

It is fair to say that, experimentally, probably ellipsometry is the most universal technique for the determination of $\Delta = (\delta_p - \delta_s)$. However it remain a basic aim of this thesis to exploit, more fully, interferometry to determine the optical constants of thin metallic films. The interferometric technique, described in the next chapter, is capable of dealing with highly reflecting films of thicknesses over 200 Å. This would restrict the exercise to determining k only since in the higher thickness range, and for metallic films, e.g. Ag, Au, Aℓ of low n values, Δ becomes insensitive to n. On the other hand the investigation of the properties of Δ presented in this chapter could be used for designing a range of experimental techniques aiming at determining the constants n and k accurately, and over a wide range of variables.

CHAPTER III

THE INTERFEROMETRIC DETERMINATION OF THE DIFFERENTIAL CHANGE OF PHASE ON REFLECTION AT AN AIR/METALLIC FILM INTERFACE

III.1 INTRODUCTION

This chapter is concerned with describing the interferometric method for the determination of the differential change of phase on reflection at an air/metallic film interface. The technique, first described by Tolansky[5] and later used by Avery[7], was applied in a modified form by Barakat and Shaalan[33]. It is based on observing multiple-beam interference fringes at non-normal incidence. As the incidence increases beyond 20° the fringes start splitting into doublets polarised perpendicular and parallel to the plane of incidence. The separation between the two components of each doublet increases as the incidence increases. The separation of the perpendicular and parallel components is due to a path difference introduced by the differential change of phase when light is reflected at the air/interferometer's coating interface. The path difference could be measured as a fraction of an order separation, i.e. as a fraction of λ. This could be easily translated to a phase difference reading, since a path difference of $\lambda/2$ is equivalent to a phase difference of π°.

In general the technique depends on the quality of the fringes, i.e. their sharpness and visibility. This in turn depends on the apparent optical properties of the interferometer coating layers, i.e. R, T and A. Thus the thickness of the layers deposited on the interferometer plates is of critical importance. Avery[7] claimed that measurable displacements between resolved components for R as low as 30% at high angles of incidence were possible. Barakat and Shaalan[33] modulated the first beam contributing to the formation of multiple beam Fizeau fringes for coatings of $R \leq 0.6$. The result was a reflection-like pattern of fringes of superior visibility to the original transmitted system. This permitted the determination of Δ as a function of θ for films of $d \leq 200$ Å. However, the technique could not be successfully applied to films of $d < 100$ Å.

Fig.III.1

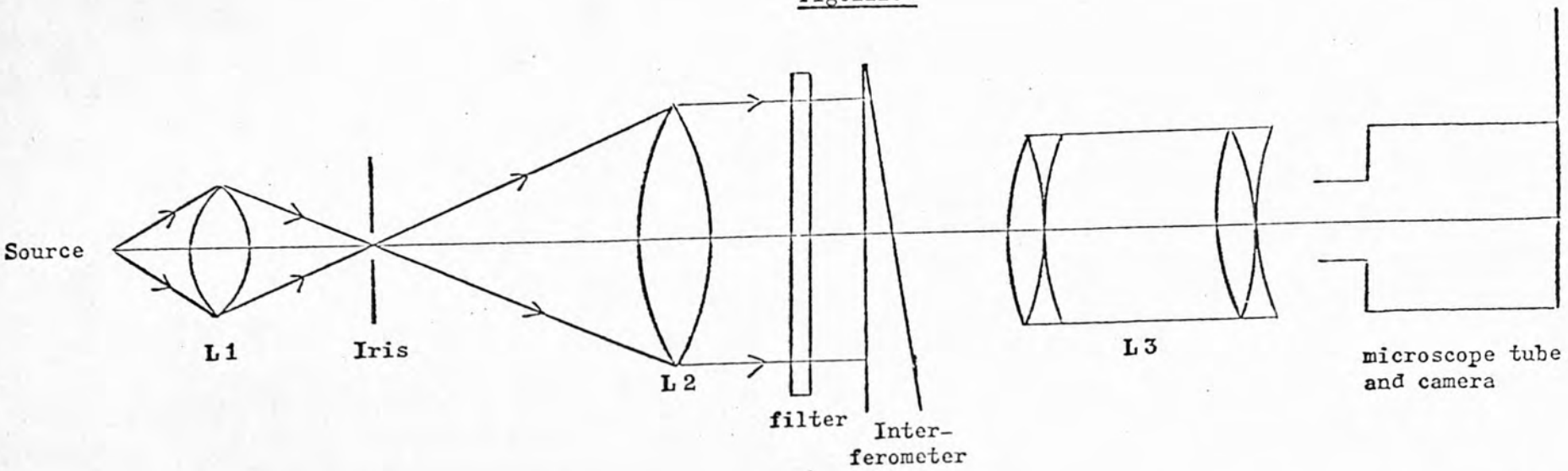

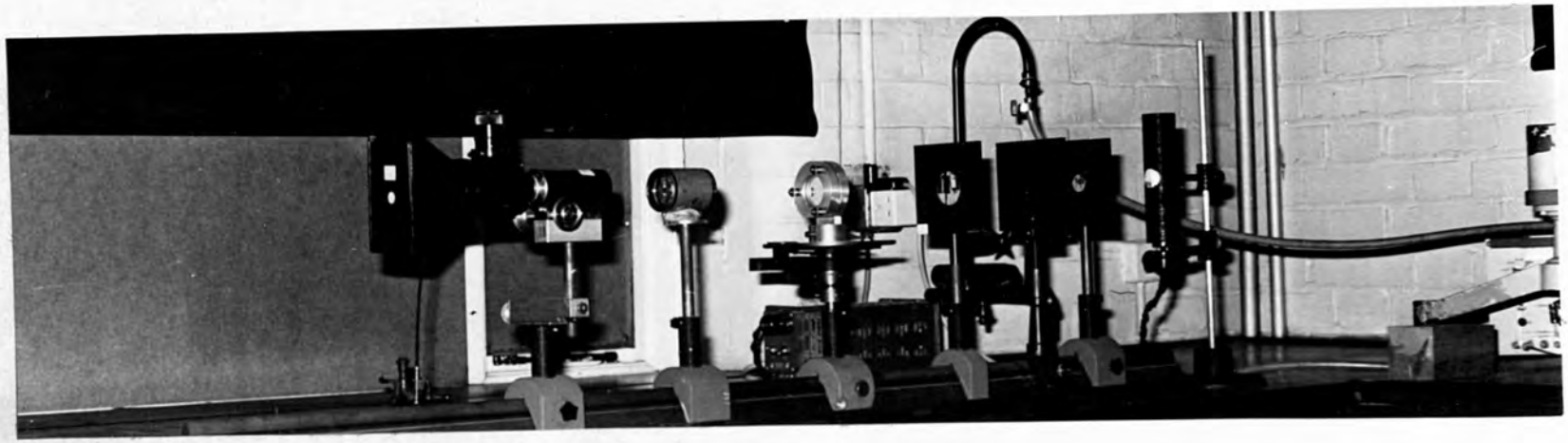

PLATE (1)

Only in the case of Avery[32] the quantity Δ, determined interferometrically was used to extract the optical constants. In his case he used Δ together with some photometric measurables. There was no attempt to analyse and map the properties, and dependencies of Δ itself. This as we showed in the last chapter, is sensitive to n and k, but more to k than n, in a wide range.

In the following sub-chapters the experiment is described. This involves the optical arrangement to determine how Δ varies with θ. The preparation of specimens and the measurement of their thicknesses are discussed. The method and theory of calculating Δ as a fraction of λ are also given. Finally the limits of the technique and the sources of errors are discussed.

III.2 THE OPTICAL SET-UP FOR THE DETERMINATION OF $\Delta = (\delta_p - \delta_s)$ AS A FUNCTION OF θ THE ANGLE OF INCIDENCE

The optical arrangement is simple and can be divided in the following components:

1. The Source

This is a cd-Hg high pressure spectral lamp by Philips operated from the mains via a suitable transformer. It provided mono-chromatic radiation at different wavelengths. The ones used in this work are

cd - red 6438 Å, Hg - green 5461 Å, Hg - blue 4358 Å.

2. Collimation

Light from the source (see Fig.III.1) is condensed and focused by means of a lens L 1 of short focal length f_1 onto an iris diaphragm of approximately 2 mm diameter. Rays diverging from the iris diaphragm are then rendered parallel by means of a lens L 2, the distance between L 2 and the iris being f_2 the focal length of this lens where $f_2 = 2 f_1$. When the system was correctly levelled and heights adjusted, the beam was parallel to ± 0.5 cm at a distance of about 3 metres.

PLATE (2)

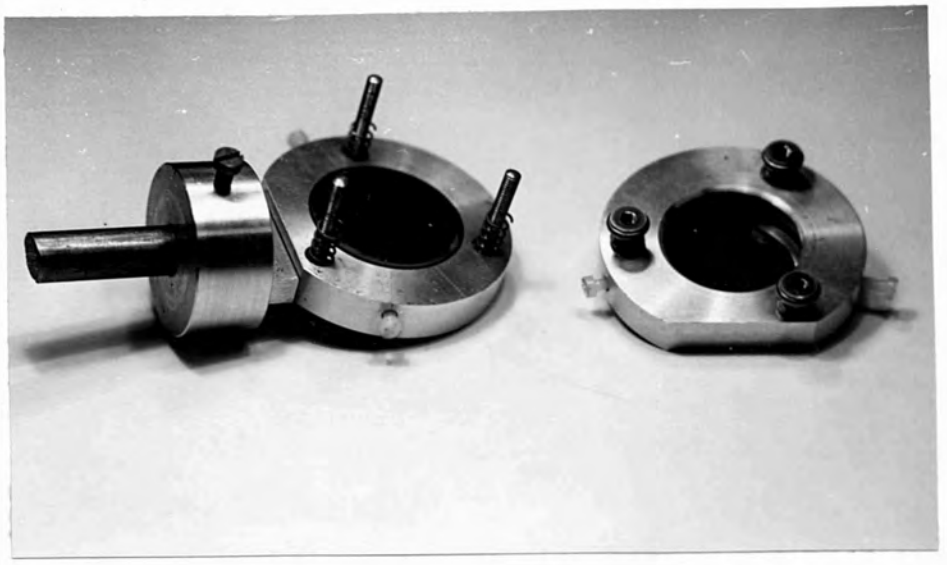

INTERFEROMETER COMPONENTS

PLATE (3)

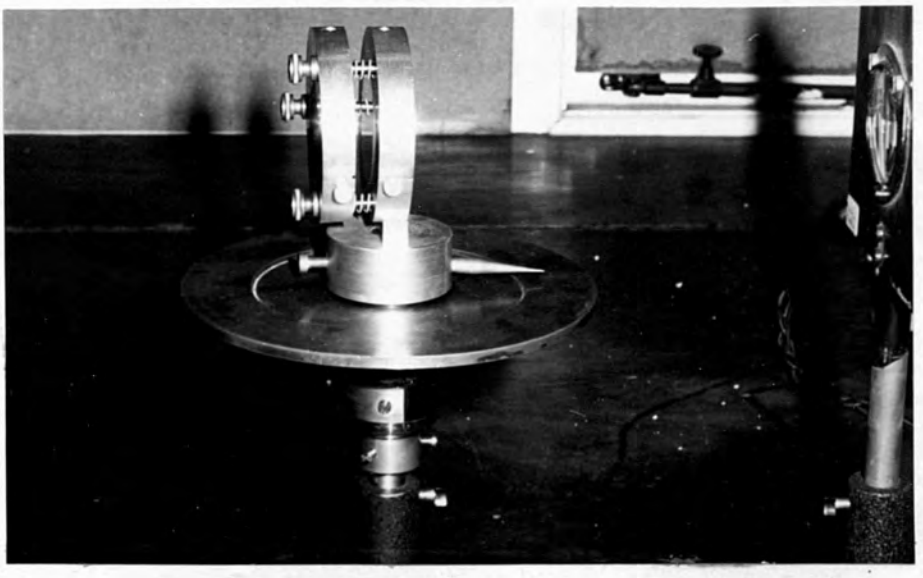

INTERFEROMETER ON SPECTROMETER TABLE

3. Spectral Isolation

This was realized by placing a monochromatic all dielectric interference filter behind lens L 2. The filters used were by Barr and Stroud and had the following characteristics.

TABLE III.1

λ_{peak}	$T_{\lambda_{peak}}$	Half-Width	Remarks
6440	35%	60 Å	T at λ 6438 = 30%
5475	54%	60 Å	T at λ 5461 = 50.5%
4386	49%	31 Å	T at λ 4358 = 44%

4. The Interferometer

This was made up of two high grade glass optical flats by Zeiss-Jena of the following specifications

TABLE III.2

Diameter mm	Thickness mm	Flatness Tolerance
45	11	0.1 μ

The two optical flats were placed, after coating, in a jig specially constructed to contain them. It had three screws as shown in Plate (2). They allowed the control of the spacing of the flats and the precise adjustment of the wedge angle. The surface area of the flats was such as to allow a very close experimental approximation to the requirements of the Airy summation formula governing the intensity distribution in a multiple beam interference pattern, Tolansky[34]. The jig was supported on a spectrometer table slightly modified to accommodate the jig mounting. Fig.III.1 shows a schematic diagram of the optical system. Plate (1) shows the actual experimental set-up and Plate (3) shows the complete interferometer supported on the spectrometer table. The interferometer moved freely around the central axis allowing variation of the angle of incidence.

5. Viewing and Recording the Fringes

This was done, see Fig.III.1, by placing a projecting lens L 3 behind the interferometer which projected the image of the fringes formed on the zero surface of localization, onto the photographic plate through the microscope eyepiece and the camera lens. The camera was attached to the microscope tube after removing its objective. This arrangement proved satisfactory since magnification could be altered by moving only the projection lens L 3 between the interferometer and the microscope tube while the camera assembly stayed in position. Fringes could be viewed in the side eyepiece attached to the camera body. The interferometer was adjusted so that eight fringes appeared in the field of view.

The optimum conditions to produce multiple beam Fizeau fringes were analysed by Tolansky[35], Brassel[36] and Barakat and Mokhtar[37].

The fringes, produced for angles of incidence varying from normal to 70° at intervals of 2.5° (some time at 5° intervals), were recorded on Ilford HP 3 photographic plates. These high speed plates, ASA 400, permitted short exposures and were developed and fixed according to standard procedure. The same exposure and developing conditions were followed in each series of plates relating to a certain film thickness at a certain wavelength.

III.3 THE SPECIMENS PREPARATION AND THICKNESS DETERMINATION

In this section a brief account is given of the techniques and conditions of preparing the metallic thin films investigated together with their thickness determination. The thin films of Ag, Au and Aℓ were prepared by thermal evaporation under vacuum of the order 10^{-6} torr or better. Their thickness was determined by initially weighing the material and later by interferometric methods.

PLATE (4)

EVAPORATION PLANT

PLATE (5a)

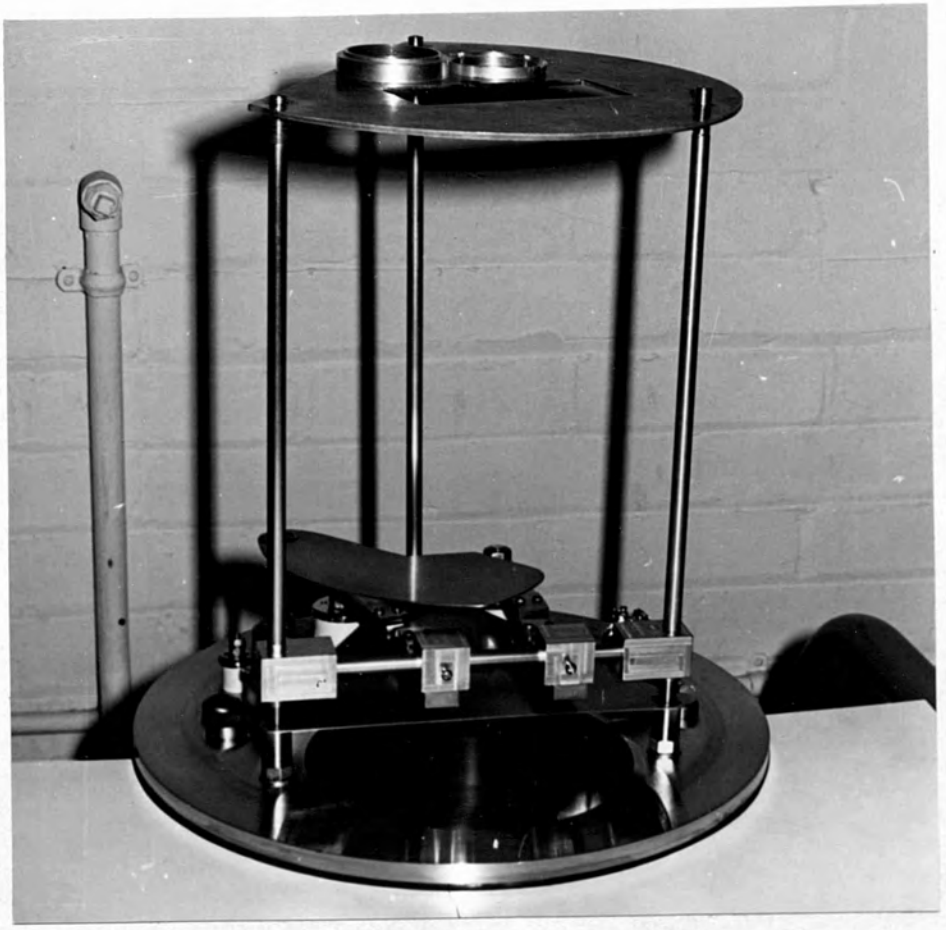

THE WORK CHAMBER

III.3.1 Vacuum Deposition of Thin Metallic Films

1. The Vacuum Plant

Plate (4) shows the 12 inch pumping system used. This consisted of a 5 inch diffusion pump backed by an E 250 Edwards rotary pump. The rotary was capable of extracting 250 litres/minute, reaching an ultimate pressure of 5×10^{-3} torr, without gas ballast. The maximum water vapour that could be pumped was 0.63 kG/hour. The rotary pump was connected to the diffusion pump through a Saunders vacuum valve.

The diffusion pump was capable of extracting 650 litres/sec. It was a Birvac TD 125A. The ultimate pressure reached by the total system was of the order of 2×10^{-7} torr. The diffusion pump working oil was silicone 704. The bell jar was connected to the diffusion pump via a high vacuum valve and a demountable liquid nitrogen trap. This was necessary to condense as many of the pumped vapours as possible. The whole system was fitted in a Birvac frame along with ancillary equipment such as Pirani and Penning gauges. The system pumped down to 10^{-5} torr in about ten minutes. When clean and allowing more time for pumping down, it could reach better than 3×10^{-6} torr in about half an hour. All parts of the working chamber, Plate (5a), and the bell jar were thoroughly cleaned after each evaporation, thus maintaining the efficiency of the system.

Molybdenum boats were used to contain the vapour source and a high current was used to heat them. A value of 90 amps was typical, it was derived from a specially constructed power supply. A shutter was used to regulate the evaporation.

PLATE (5b)

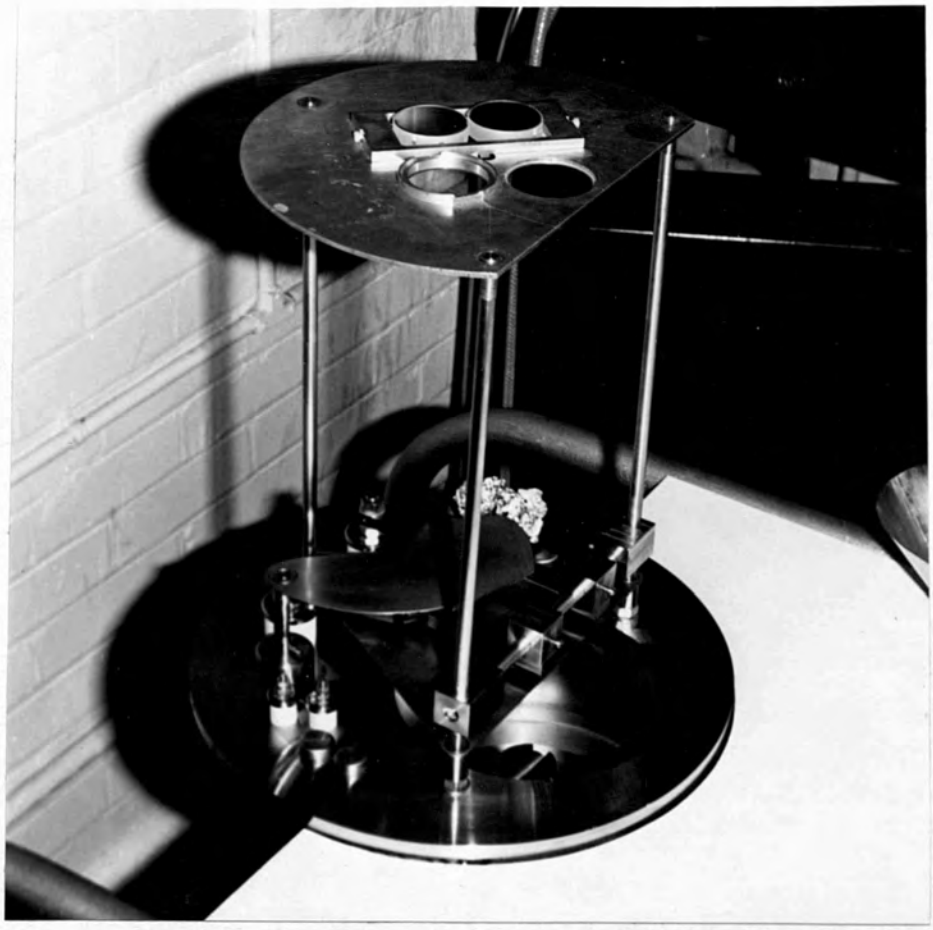

OPTICAL FLATS MOUNTED IN VACUUM CHMABER

2. Substrate Preparation

The optical flats were cleaned by removing the layer deposited previously on them using H_2O_2 solution. Then by rinsing them in distilled water. They were dried and rubbed using soft cotton wool until such time when they responded to the simple breathing test. When breathed upon, the surface, if free from contamination, did not hold the water vapour layer for more than a fraction of a second. This simple procedure of cleaning was safer than using nitric acid to remove the metallic layer to start with. The acid would attack the surface and scratch it causing damage to the flatness of the surface and probably affecting the atmosphere inside the working chamber. The two flats, constituents of the interferometer, together with one other flat were mounted in the chamber at a distance of 30 cm from the source. The third flat was half masked with a freshly cleaved sheet of mica with a sharp edge. The unmasked half received the same amount of metal vapour as the interferometer plates. The flat was later over coated with an opaque layer of silver to form the lower component of a reflection system used to determine the stop height. This procedure will be described later. Plate 5(b) shows how the flats were placed inside the chamber.

3. The Vacuum Materials

The metals used were all spectroscopically pure and supplied by Johnson and Matthey.

The silver was in the form of wires of diameter 0.5 mm. Gold wires were of comparable diameter, but the aluminium was supplied in the form of rods of a diameter 1.5 mm. Silver and gold were evaporated from molybdenum boats, but the aluminium was evaporated from helical coils[38]. The metal was allowed to melt first and, keeping the shutter in position, the rate of evaporation was stabilised first. Then, removing the shutter, the vapour was allowed to reach the substrate surface for a suitable

length of time. This operation, while lasting for only a few seconds, ended by moving back the shutter to its initial position.

III.3.2 Thickness Determination

The term thickness is one which, in the context of thin film optics, needs to be taken with some caution. Now, after three decades of mounting work on the optical properties of thin solid films, we tend to connect the term thickness more closely with the structural properties of the film and the conditions under which it was prepared. However, in analysing most optical measurements on thin films, it is necessary to assign a value to film thickness. This is because the ratio d/λ appears in almost all the formulae which are used to analyse the measurements. It is safe to say that, excluding the cases of discontinuous films of very small 'thickness', the interferometric technique as developed by Tolansky[8,39], is a simple and accurate way of finding d, the metric thickness of the film.

The interferometric method is of limited use for films of 'thickness' under 50 Å. This is so for two main reasons, (a) the variation in the structure of such films would lead to widely differing values for the step height, and (b) a step height of that order will cause a very small fringe shift making it difficult to observe and measure.

The type of film which we are concerned with here, is that deposited on a substrate and therefore could form a step, the height of which could be measured. Other methods for evaluating thickness were surveyed by Bennet and Bennet[25].

As for the interferometric technique, it is based on the fact that interference fringes formed between an optical flat and a surface having irregularities, will contour these surface features and render them available for measurement. This was realized as early as 1892 by

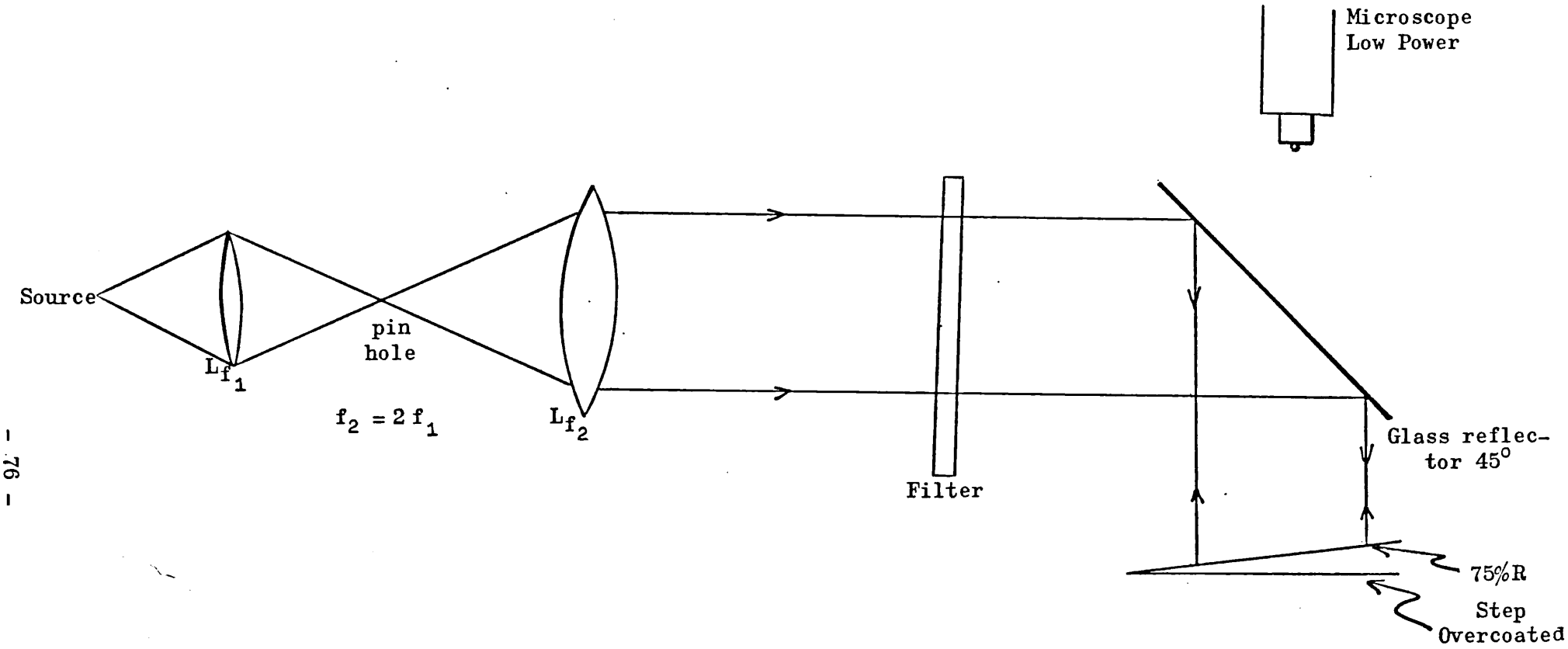

Fig.III.2

Optical set up for thickness determination

Laurent[40]. The experimental conditions for obtaining sharp and well defined multiple beam Fizeau fringes are well discussed and expertly written by Tolansky[34,35,39]. It is to be mentioned here that in the case of a wedge interferometer viewed at reflection with an overcoated step on the lower component, (a) the fringes must be perpendicular to the step; (b) the reflectivity of the upper component is critical, since it affects the visibility of the fringe pattern, and (c) photographing the fringes and measuring the displacement with a comparator is far safer than using a micrometer eyepiece. This eliminates any errors due to the 'moving' of the fringes. The procedure of alignment of the interferometer is described adequately, though very detailed and unnecessarily lengthy, in reference (25). From experience the process is very delicate indeed, but with care and practice, it becomes a second nature to one's fingers!

The experimental set-up is shown in Fig.III.2. The microscope is a low-power magnification, objective $\times 3$ and eyepiece $\times 6$, this is further reduced by the camera lens magnification of $\times \frac{1}{2}$. Low order interference fringes are employed, up to the twentieth order. This depends on the size of the optical flats and the way the edge of the wedge is adjusted. To point out the steps in simple terms, they are as follows:

(1) An additional optical flat is introduced in the chamber to be coated in the same time as those of the interferometer. It will be half masked with a freshly cleaved mica sheet having a sharp edge. The use of mica will prevent damaging the flat surface.

(2) The mask is removed and the step formed previously is overcoated with an opaque film of silver.

(3) A reference flat is coated with a silver film of reflectivity of about 75%. This will serve as the upper component of the interferometer. The value of 75% is critical for the visibility of the reflected fringe system;

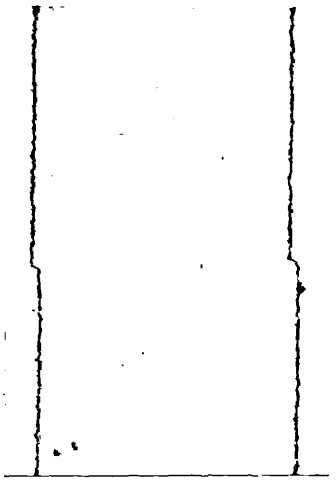

PLATE (6)

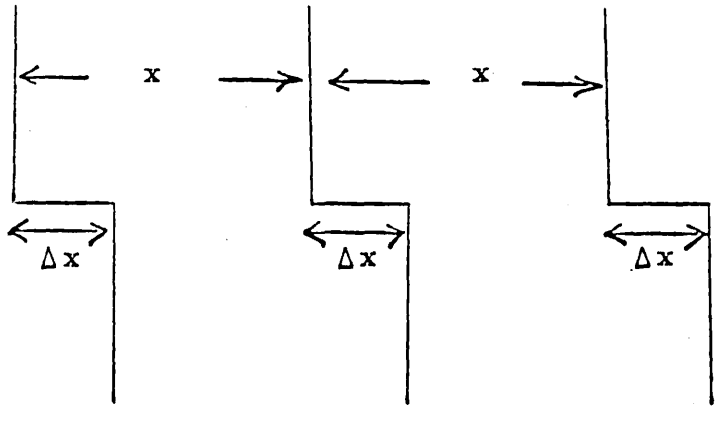

Fig.III.3
Thickness calculation from interferogram

(4) The two flats are placed in a jig similar to that described on page 68, and the jig screws used to adjust the dispersion of the fringes and their position perpendicularly to the step.

(5) When the fringes stop 'moving' they are photographed. Plate (6) shows their appearance. The step height is found from the simple equation $d = \frac{\Delta x}{x} \times \lambda/2$, Fig.III.3.

$\lambda/2$ is the order separation, and x is the distance between any two successive fringes, Δx being the displacement caused by the step.

This method is capable of an accuracy of $\pm$ 10 Å.

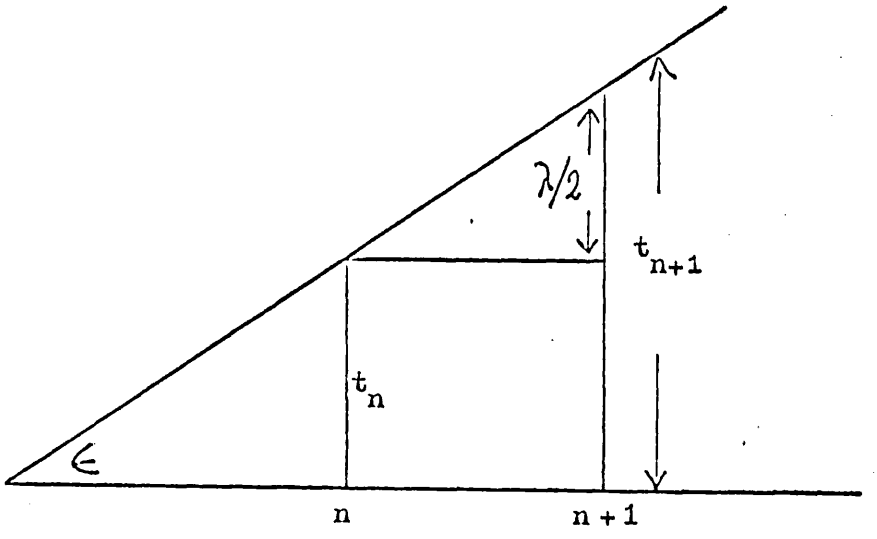

Fig.III.5
Formation of fringes of equal thickness

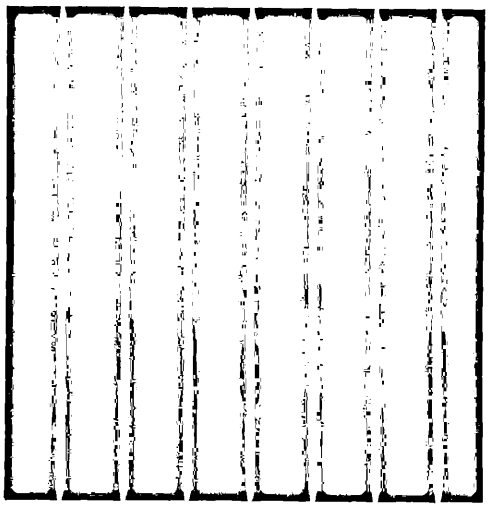

PLATE (7)
Transmitted fringes
at $\theta = 0^{\circ}$

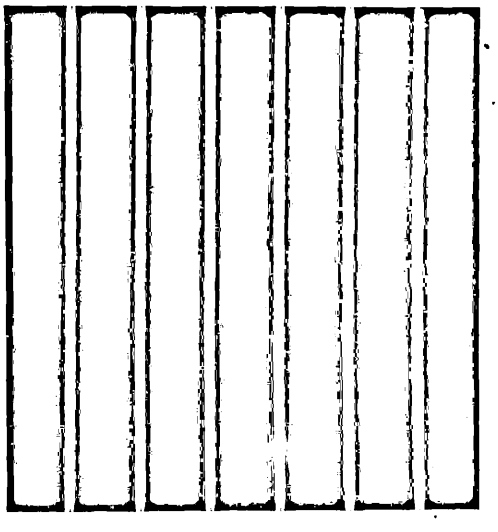

PLATE (8)
Transmitted fringes
at $\theta = 30^{\circ}$

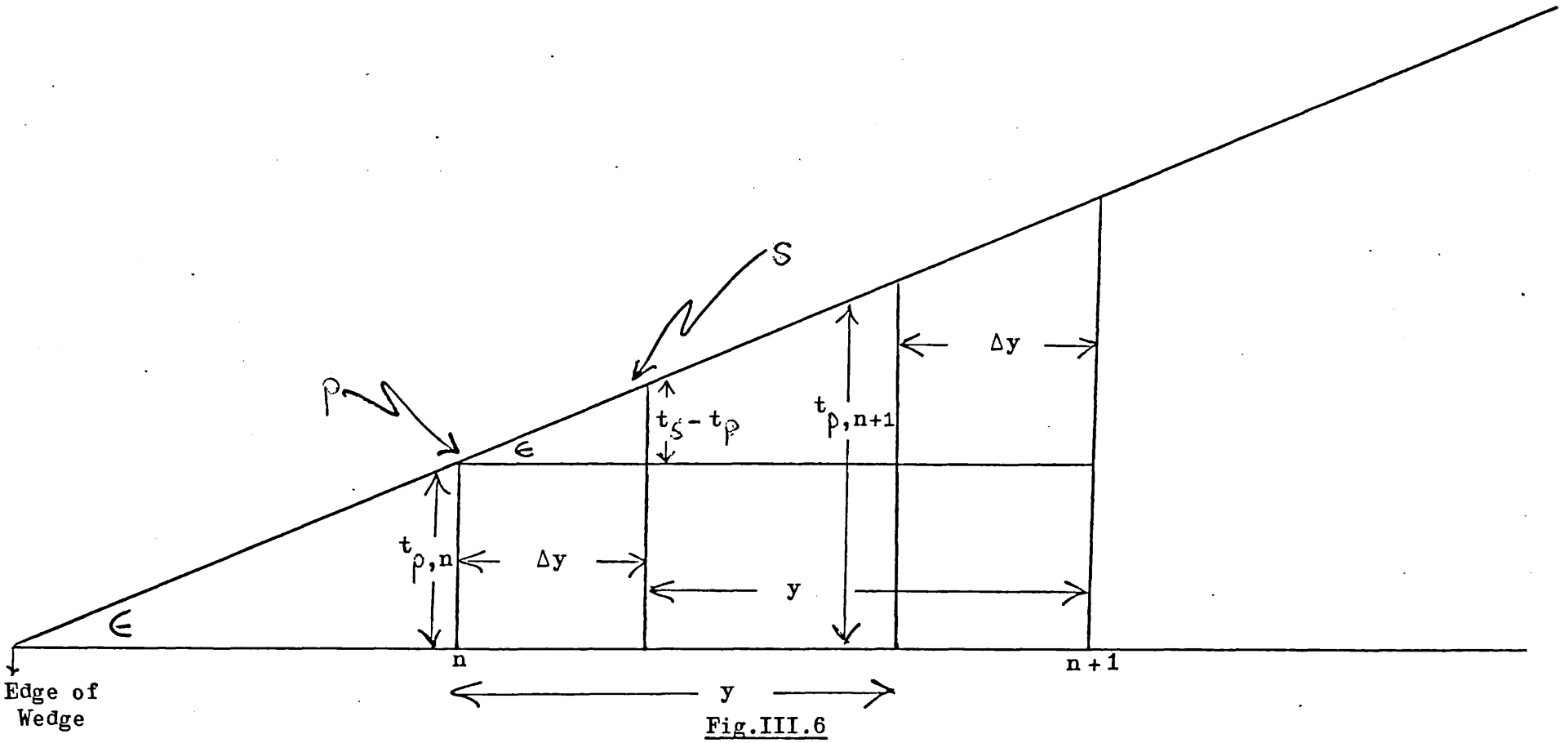

Fig.III.6

Fringes of equal thickness at non-normal incidence

III.4 THE CALCULATION OF $\Delta = (\delta_p - \delta_s)$ AS A FRACTION OF λ FROM A TRANSMITTED FRINGE PATTERN AT AN ANGLE OF INCIDENCE θ

In almost all measurements made from interferograms a fringe shift is being determined. This is a measurement of distance. However, this distance in itself is of no physical meaning unless it is related to the order separation of the fringe pattern. In the case of transmitted fringe system the order separation is $\lambda/2$. This is the path difference required to produce the next fringe as it were. Fig.III.5 shows how fringes of equal thickness are produced by an air metal coated wedge. Plate (7) shows the transmitted fringes of equal thickness produced by such an arrangement at normal incidence. They are equally spaced. Plate (8) shows the same transmitted system viewed and recorded at an angle of incidence of 30 degrees to the normal. There are two systems of fringes belonging to the perpendicular and parallel components of incident radiation. The difference in phase between the two components resulting from the non-normal incidence is translated into a path difference showing itself as a relative fringe shift. When the phase difference reaches π the path difference would be $\lambda/2$ and the two systems of fringes would fall onto each other. This would take place when the incidence is 90° and is impractical to record. However, Fig.III.6 shows how the path difference, as a fraction λ, could be found from such an interferogram.

The condition of interference is

$$n\lambda = 2t + 2\delta_\lambda \cdot \lambda, \qquad \ldots \text{(III.1)}$$

where δ_λ is the change of phase at reflection for the electromagnetic radiation incident at the air/metallic layer interface. This equation gives the condition of interference for bright fringes in transmission at normal incidence.

For non-normal incidence the condition is

$$n\lambda = 2t\cos\theta + 2\delta_{\lambda,\theta,\eta}\cdot\lambda \qquad \ldots \text{(III.2)}$$

where θ is the angle of incidence and $\delta_{\lambda,\theta,\eta}$ is the phase change at reflection, δ is a function of the angle of incidence, the wavelength and the state of polarization. In the case of non-normal incidence the phase change depends on the relation of the plane of polarization to the plane of incidence. Accordingly, two fringe systems occur for the two light vibrations and the following relations describe them:

$$n\lambda = 2t_{\perp}\cos\theta + 2\delta_{\lambda,\theta,\perp}\cdot\lambda \qquad \ldots \text{(III.3)}$$

$$n\lambda = 2t_{\parallel}\cos\theta + 2\delta_{\lambda,\theta,\parallel}\cdot\lambda \qquad \ldots \text{(III.4)}$$

Also for the same component the following relations hold

$$n\lambda = 2t_{n}\cos\theta + 2\delta_{\lambda,\theta,\eta}\cdot\lambda \qquad \ldots \text{(III.5)}$$

$$(n+1)\lambda = 2t_{n+1}\cos\theta + 2\delta_{\lambda,\theta,\eta}\cdot\lambda \qquad \ldots \text{(III.6)}$$

Subtracting the last two equations and from the geometry of Fig.III.6

$$\lambda = 2(t_{n+1} - t_{n})\cos\theta \qquad \ldots \text{(III.7)}$$

$$\therefore \qquad \frac{\lambda}{2\cdot\cos\theta} = (t_{n+1} - t_{n}) \qquad \ldots \text{(III.8)}$$

and

$$\tan\epsilon = \frac{(t_{n+1} - t_{n})}{y} \qquad \ldots \text{(III.9)}$$

Thus

$$\tan\epsilon = \frac{\lambda}{2y\cos\theta} \qquad \ldots \text{(III.10)}$$

where ϵ is the wedge angle, n is the order of a particular fringe, and y is the separation between any two successive fringes belonging to the same component. It could be concluded that, at a certain θ, y is the same for either components and as θ increases, $\cos\theta$ decreases and since ϵ is the same, y should increase leading to fewer number of fringes in the field of view,

From Fig.III.6 it is clear that

$$\tan \epsilon = \frac{t_s - t_p}{\Delta y} \qquad \ldots \text{(III.11)}$$

By subtracting equation (III.4) from (III.3) we get

$$(\delta_p - \delta_s) = \frac{\cos \theta \, (t_s - t_p)}{\lambda} \qquad \ldots \text{(III.12)}$$

From equations (III.10), (III.11) and (III.12)

$$(\delta_p - \delta_s) = \frac{\Delta y}{2y} = \frac{\Delta y}{y} \cdot \frac{1}{2} \, . \qquad \ldots \text{(III.13)}$$

This equation gives $\Delta = (\delta_p - \delta_s)$ as a fraction of λ. it could be translated to a phase angle since a path difference of $\lambda/2$ is equivalent to phase difference of π .

III.5 AN ANALYSIS OF THE SOURCES OF ERRORS INVOLVED IN THE INTERFEROMETRIC DETERMINATION OF Δ AND THEIR EFFECT ON THE ACCURACY OF THE TECHNIQUE

The interferometric technique for the determinatin of the differential change of phase is mainly dependent on the quality of the multiple beam fringes it employs. This quality in turn is a function of two main aspects: (a) the reflection coefficient of the interferometer coatings, and (b) the fulfilment of the optimum conditions for the production of multiple beam interference fringes. The first of these two aspects is the one which sets the limit to the ability of an observer, to extract the most accurate possible results from a certain fringe system. The sharper the fringe, the easier the focusing on the photographic plate, and the easier it is to bring the cross wires of the measuring instrument into coincidence with it.

In Tolansky's original experiments, the Newton's rings were fringes of equal thickness, and at normal incidence were localized in or very near to the air gap of the interferometer. At non-normal incidence, however, the fringes are no longer localized in the gap but on a curved surface in space near the interferometer. This surface is not perpendicular to the

PLATE (9)

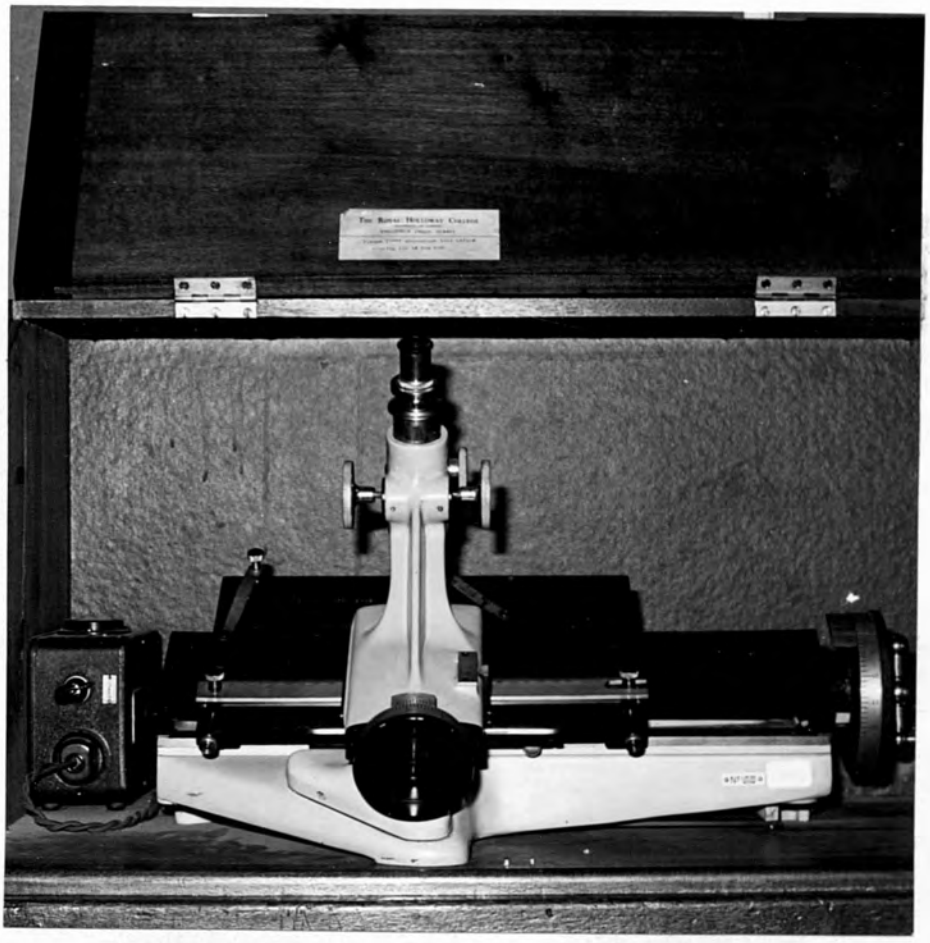

MEASURING COMPARATOR

optical axis of the system and as a result only part of the field of view can be secured in focus at any one time. In the wedge interferometer, ideally, the fringes are localized in a plane perpendicular to the optical axis of the system, and so all the fringes should be in focus at any given moment. In practice the interferometer plates may, to a small extent, bend or curve and the surface of localization is not plane any more. This introduces an apparent change in the spacing of the doublets. This could lead to false results. The effect could be minimized if the plates used were of such thickness as to make any bending of the surface insignificantly small. In this work, this is achieved by using optical flats 45 mm in diameter and 11 mm thick as mentioned earlier in this chapter. Also this effect is least when the angle of the wedge and the interferometric gap are both very small. When the fringes are sharp, resulting from coatings of high reflectivities, the error in focusing on the photographic plate is minimum.

Another source of error arises from the inconsistency in the measured values of y, the distance between any two successive fringes measured on the photographic plate. The measurement of these distances is made on a Hilger comparator, Plate (9), which gives its readings to ± 0.001 mm. If the interferometer plates are of such dimensions that bending of the surface introduces significant changes in the interferometric gap along the interferometer, the distance y will suffer accordingly and again a false result may be obtained. This is largely avoided by using flats of the size mentioned above, and by taking readings over a fixed number of fringes throughout one set of plates.

In one set of plates taken at intervals of 2.5° of incidence, each plate contained an average of 6 - 8 doublets, y was consistent to ± 0.01 mm. In measuring y and Δy another difficulty arises when the reflection coefficient of the interferometer coatings is such that it

PLATE (10)

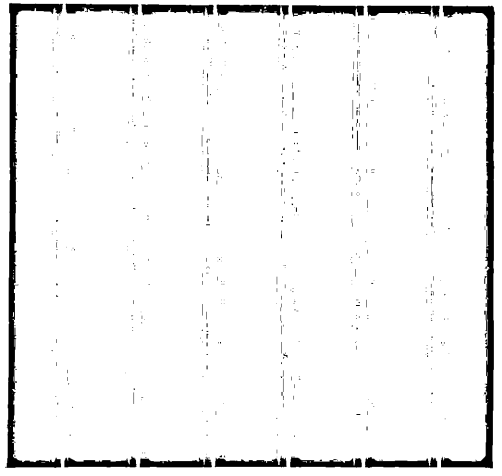

Ag

d = 600 Å

R ≃ 0.8

λ = 5461 Å

θ = 45°

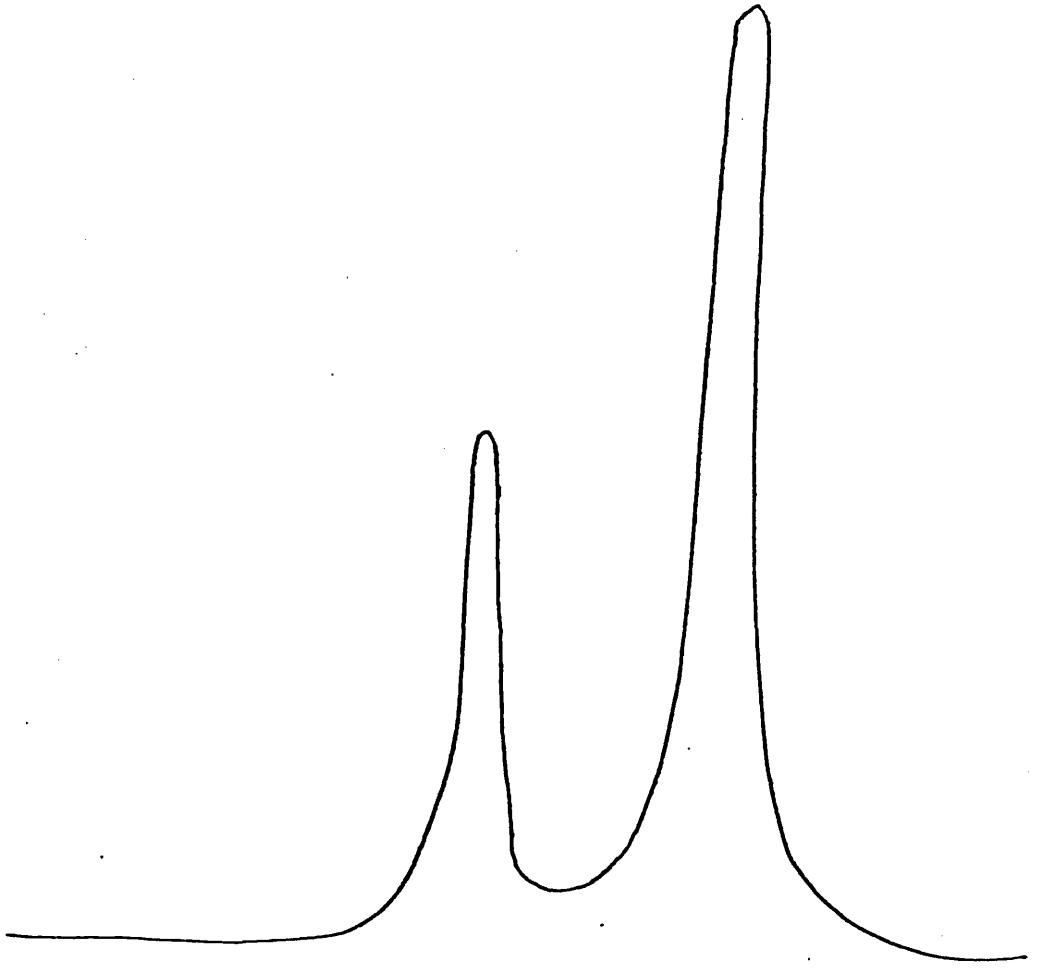

Fig.III.7

PLATE (11)

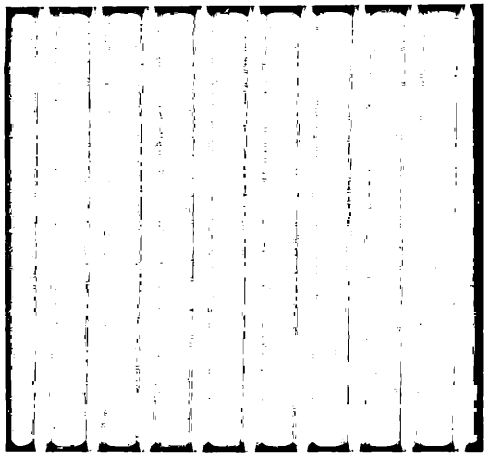

Ag
d = 250 Å
R = 0.65
λ = 6438 Å
θ = 45°

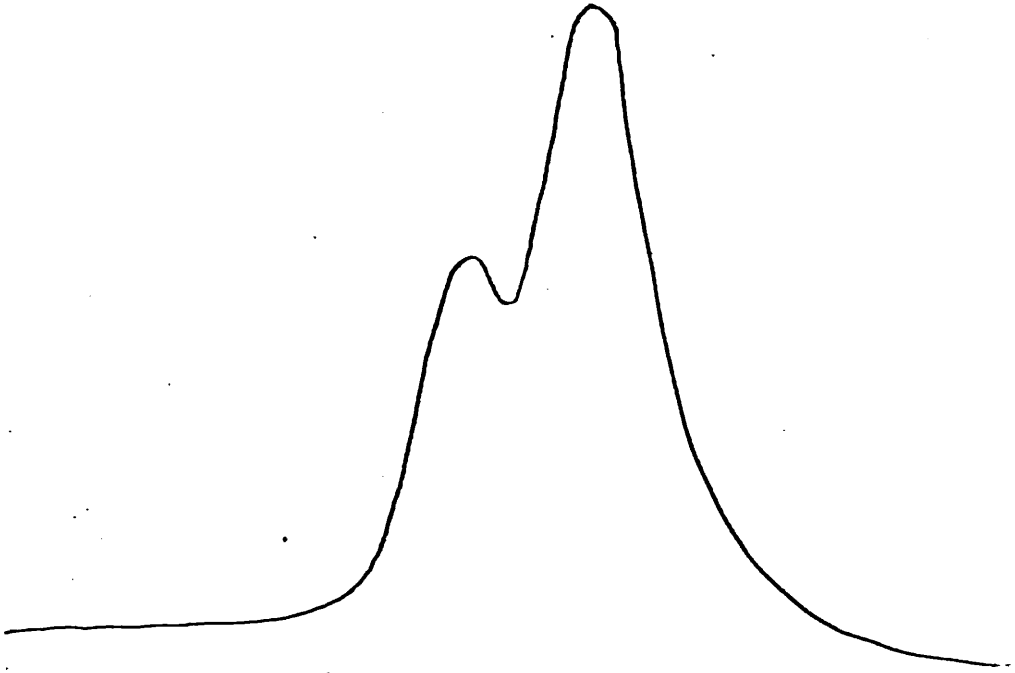

Fig.III.8

produced broad fringes. On the one hand, the doubling due to the difference in phase starts to be observable only at medium angles of incidence (40° for $R = 40\%$), and on the other hand, even at higher incidence, the broad fringe tends to overshadow the sharper but less intense component belonging to the perpendicularly polarized light vibration. Inevitably when recorded on photographic plates one of the two components, in this situation, will have to suffer according to the type of plates used, and the exposure time given. However, if a good compromise is struck between all these factors in the case of low reflecting films, e.g. $R \leq 0.5$, the measurement could still suffer inaccuracies because of the difficulty in locating the maximum of the broad fringe using the cross wires of the measuring comparator. Plate (10) shows the doublets resulting from an interferometer coatings of $R \simeq 0.8$ at $\theta = 45^\circ$, Fig.III.7 shows a microdensitometer trace of the same set of fringes. Plate (11) shows the doublets belonging to coating of $R \simeq 0.65$ at the same incidence and Fig.III.8 shows the microdensitometer trace in this case. The difficulties mentioned above become immediately clear.

It is obvious that the interferometric technique is most suited to films which have high reflecting power. In the case of silver this corresponds to film thickness of 200 Å and more. As a technique for the measurement of Δ it provides an inexpensive and simple way, both from the point of view of apparatus and of operation. As against this the technique suffers from some limitations, the most important being the loss of accuracy with lower reflection coefficients. Another factor arises from the fact that measurements have to be made in air outside the vacuum chamber, thus risking contamination of the films and consequent possible unrepresentative results. However, as for the contamination risk, this is important mainly in the case of reactive metals.

For many metals it is fair to assume that results are representative if measurements are made and carried out within a short time of deposition. In this work it was possible to complete the experiment for determining Δ vs θ within less than one hour. As for the use of the results obtained to deduce one or more of the optical constants, the accuracy will depend on sensitivity factors discussed in Chapter II. It could be fairly said that determining Δ using the interferometric technique in more than 100 measurements performed in the course of this work, the experimental error was $\pm 0.0025\,\pi$ in the optimum case to $\pm 0.006\,\pi$ in the worst case. The polarimetric determination of Δ in the work of Meyer[22] was accurate to $\pm 20'$ or $\pm 0.002\,\pi$.

The comparison between experimental results and theoretical values is a matter which depends on which values of n and k one takes to compute a theoretical curve. In this work values of n and k produced by Schulz[20] and recommended by Heavens[41] are used to compute the theoretical curves of Δ vs θ. Any one set would produce a theoretical curve in the light of which an experimentally determined one might appear to be unreasonable or in straight disagreement. Schulz[20] found that values of n and k for certain metals reported in literature, vary in a 10% range.

CHAPTER IV

THE PROPERTIES OF MULTIPLE-BEAM FIZEAU FRINGES AT NON-NORMAL INCIDENCE

IV.1 INTRODUCTION

The properties of multiple-beam Fizeau fringes can be divided into (a) intensity properties, and (b) phase properties. The two are related. The value of intensity at any point in the fringe pattern is the result of a number of beams interfering according to the condition of interference at reflection or in transmission as the case may be. The phase relation between the interfering beams at any point determines the location of this point from the peak to the minimum intensities.

In this chapter we shall state and analyse the factors affecting the intensity and phase properties of multiple-beam Fizeau fringes in transmission at non-normal incidence. For this to be understood, it must be looked at in the light of the properties of the F-P and Fizeau fringes at normal incidence. It will be shown that the properties of an air coated wedge fringe are not only dependent on the optical properties of the coatings but also on the geometry of the interferometer.

IV.2 THE DIFFERENCE BETWEEN THE MAXIMUM INTENSITIES OF FRINGES BELONGING TO THE PARALLEL AND PERPENDICULAR VIBRATIONS

A striking feature of a non-normal incidence system of Fizeau multiple-beam fringes is the difference in maximum intensity for fringes formed by light vibrating parallel and perpendicular to the plane of incidence, see Plates (10),(11). As the incidence increases and the fringes split in parallel and perpendicular components, the fringe belonging to the perpendicular component becomes progressively sharper and weaker in intensity, while the change in sharpness and intensity is not as noticeable in the case of the parallel component fringe. At high angles of incidence $\theta \geq 70$ and for highly reflecting thick films of $d \geq 300$ Å the perpendicular component fringe is hardly visible. Tolansky[5] suggested that this was due to a differential absorption effect where by the film absorbs the perpendicular component much more readily than the

parallel one. Avery[32], briefly, touched on the problem and suggested that the difference in intensity could be accounted for in two ways: (a) the difference in behaviour of the optical properties R, T and A with the angle of incidence for the two vibrations polarized parallel and perpendicular to the plane of incidence, and (b) the effect of the glass substrate when it reflects and transmits differently the two polarizations.

However, there are more factors than those mentioned by Avery which govern the intensity of a multiple-beam Fizeau fringe system. These are the number of effective beams emerging from the second component of the interferometer and the phase difference between any two successive beams contributing to any one point on the intensity distribution curve. Tolansky's suggestion of a differential absorption effect is ambiguous. Either we assume that each component would have a different absorption index $(k_\perp)_\theta$ and $(k_\parallel)_\theta$ varying with the angle of incidence, or simply interpret the 'differential effect' as the variation of the ratio of $A_\perp/A_\parallel$ with the angle of incidence.

The first assumption is evidently a serious one. The second does not explain the difference between the peak intensities of the two fringes. A third assumption, which was not considered either by Tolansky or Avery, is that the difference between the maximum intensity of fringes belonging to the parallel and perpendicular components of light falling at non-normal incidence onto the interferometer coating, is in fact a consequence of 'interferometric considerations' rather than merely 'film properties considerations'. In the following we shall try and explain this.

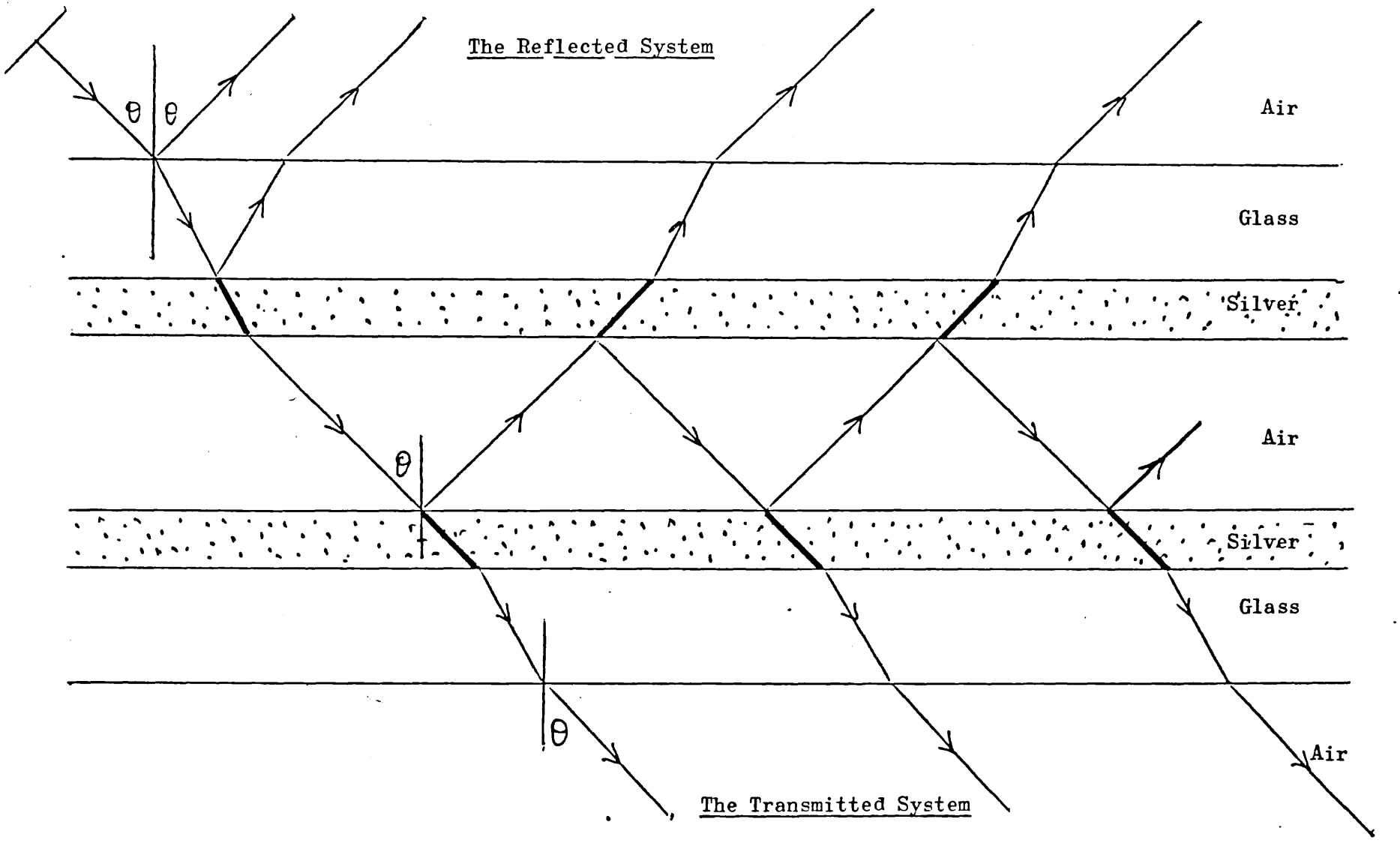
The Reflected System
θ
θ
Air
Glass
Silver
θ
Air
Silver
Glass
θ
Air
The Transmitted System

Fig.IV.1

IV.3 THE CASE OF PARALLEL PLATE, F-P FRINGES

Figure IV.1 shows the passage of light in a parallel plate interferometer, coated with a highly reflecting film. The emerging beams in transmission would have the following amplitudes:

$$T\ ,\ TR\ ,\ TR^2\ ,\ TR^3\ ,\ TR^4\ ,\ \ldots$$

and their intensities are simply the squares of these amplitudes, i.e.

$$T^2\ ,\ T^2R^2\ ,\ T^2R^4\ ,\ T^2R^6\ ,\ T^2R^8\ ,\ \ldots$$

the path difference between any two successive beams is constant and is given by $(2\,\mu t\cos\theta) = N\lambda$ where T and R are the fractions of light intensity transmitted and reflected by a single film. R is the reflectivity at the medium/film interface, as shown in Fig.IV.1, μ is the refractive index of the medium between the interferometer plates, N is the order of interference, and λ is the wavelength of light illuminating the interferometer.

The fringes resulting from such a system are fringes of equal inclination localized at infinity and the intensity at any point in the fringe pattern is given by the Airy summation where:

$$I = \frac{T^2}{(1-R)^2}\ \frac{1}{1+\dfrac{4R}{(1-R)^2}\sin^2\delta/2} \times I_o \qquad \ldots\ (IV.1)$$

where δ is the phase difference between any two successive beams and is given by $\delta = \frac{2\pi}{\lambda}(2\,\mu t\cos\theta)$ and I_o is the incident intensity equal to unity if we consider an incident plane wave of unit amplitude.

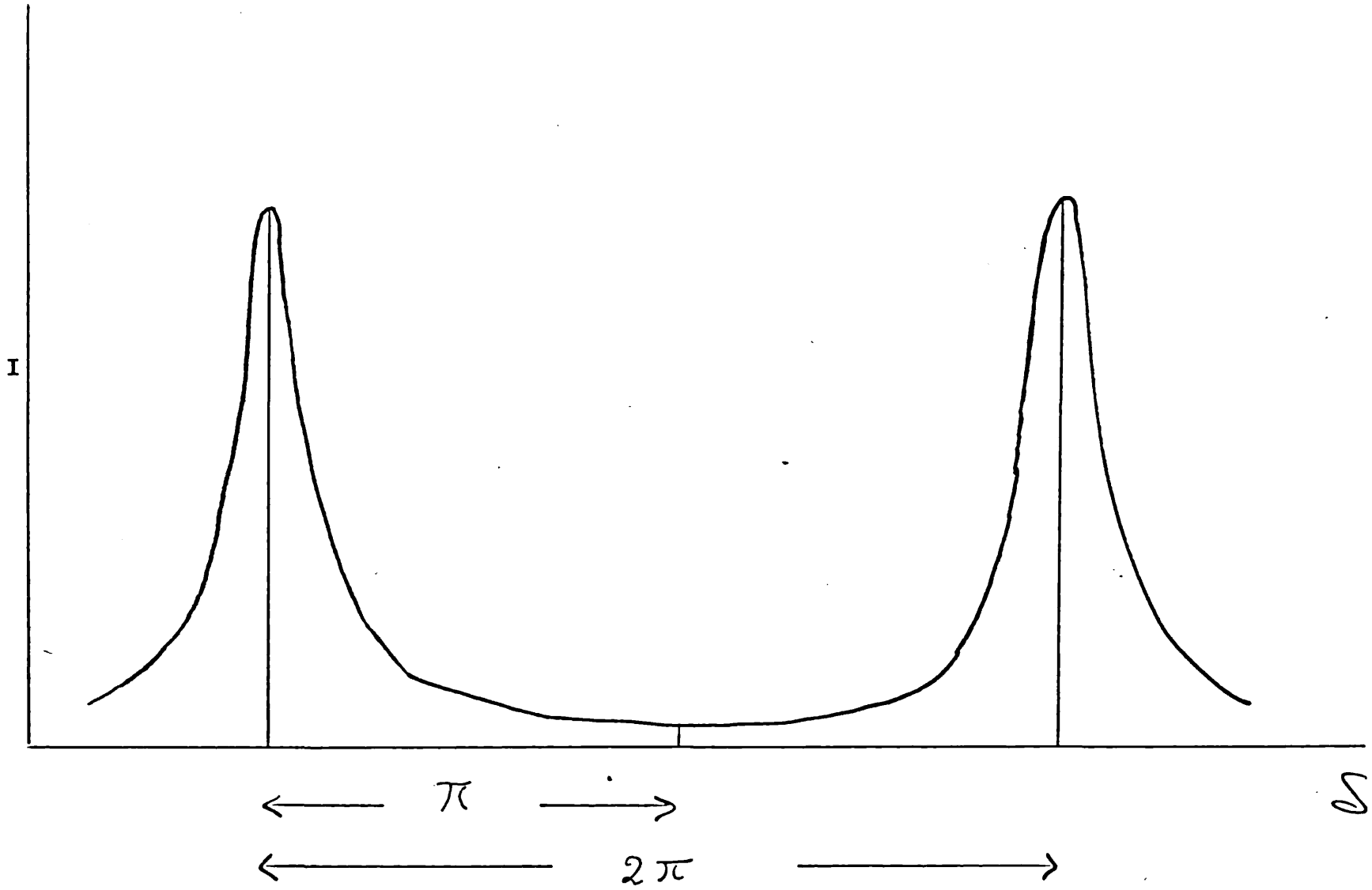

Fig.IV.2

Figures IV.2 shows a schematic variation of I vs δ for a parallel plate interferometer with a highly reflecting coating. The maximum intensity occurs at $\delta = 2m\pi$ and the minimum at $\delta = (2m+1)\pi$.

However, it is assumed, in formula (IV.1) that an infinite number of beams is being collected. This means that we are dealing with the case where the interferometer's aperture is infinite. This is only an approximation to practical reality. An infinite number of beams is never created nor collected. Also the transmission of the two glass substrates is not considered.

Now, if we consider that only a finite number of beams is collected and also account for the glass substrates transmission we would re-write formula (IV.1) as follows:

$$I = Tg^2 \times T^2 \times \frac{(1-R^{M+1})^2 + 4R^{M+1} \sin^2(M+1)\ \delta/2}{(1-R)^2 + 4R \sin^2\ \delta/2} \quad \ldots \text{(IV.2)}$$

In this formula Tg^2 is an intensity reducing factor due to the transmission of the glass substrates and it is assumed that a number of beams $(M+1)$ is collected. This is based on calling the first transmitted beam of amplitude $T\,Tg$ the zero order beam. The case for a finite number of beams was first dealt with by Gehrcke[42].

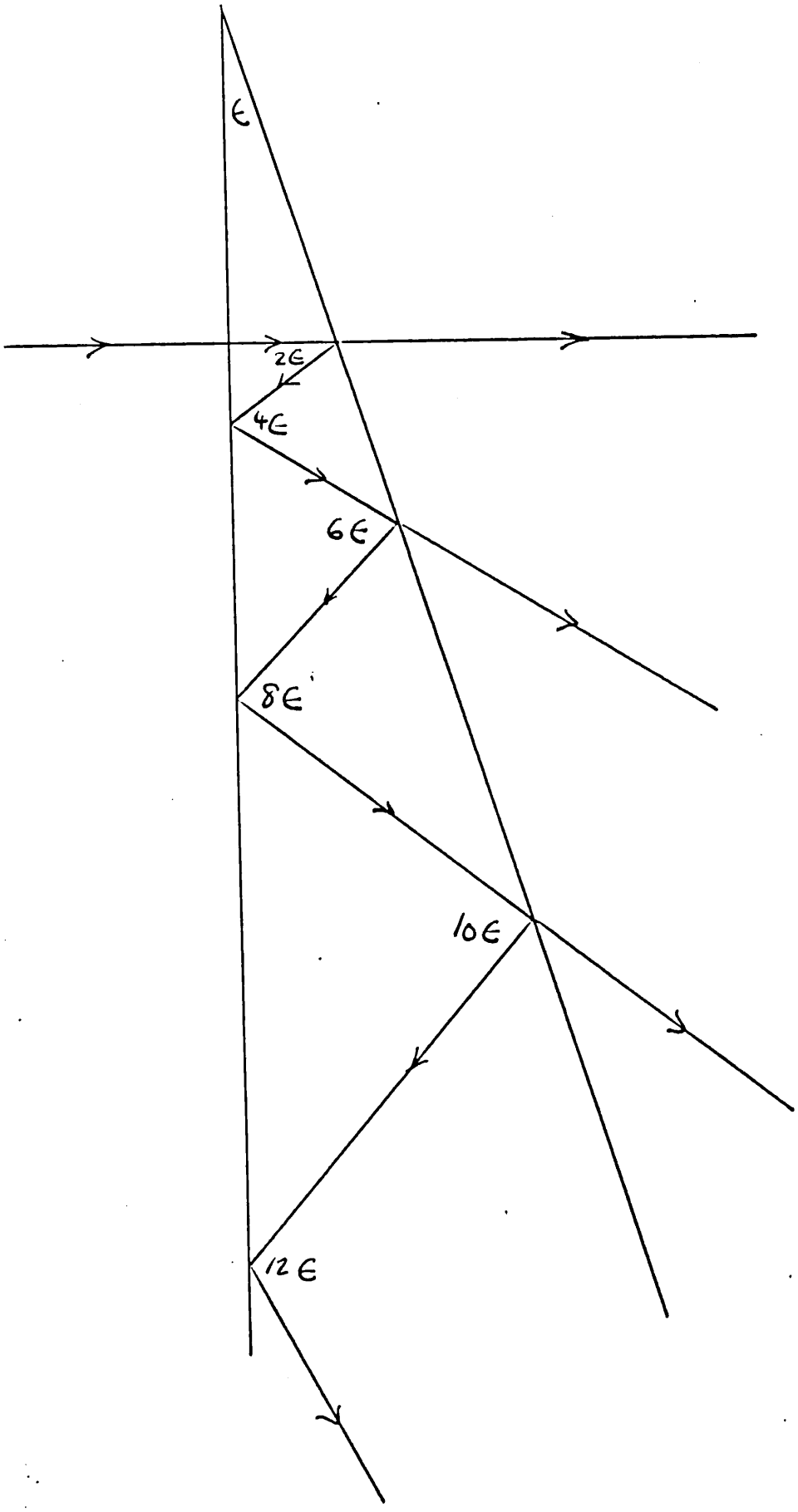

Fig.IV.3

IV.4 THE CASE OF FIZEAU – MULTIPLE BEAM FRINGES AT NORMAL INCIDENCE

In this case the plates of the interferometer are inclined to each other forming a wedge of small angle ϵ. Fig.IV.3 shows the passage of light in such an interferometer. Although the emerging beams in transmission would have the same amplitude as in the case of F-P, the path difference between any two successive beams is not constant. There is a phase lag w.r.t. the zeroth beam increasing with the order of the beam. The fringes produced by such a set-up will have an intensity distribution curve similar in shape to that produced by the F-P arrangement. But they will be fringes of equal thickness parallel to the edge of the wedge as shown in Fig.III.3. The comparison with the formula (IV.1) is rather formal. In the F-P case the variation of the $\sin^2$ term is produced by variation of θ while t, the interferometer gap, and λ are kept constant. But the same intensity distribution will result with t variable and θ, λ constant because what determines the intensity is a combination of these quantities $\delta = \frac{2\pi}{\lambda}(2\mu t \cos\theta)$.

Tolansky[34,35], Brossel[36], Holden[43], Kinosita[44] and Barakat and Mokhtar[37] studied the factors affecting the intensity in multiple beam Fizeau fringes at normal incidence. The point of maximum intensity on the intensity distribution curve is produced by a certain number of beams where the phase difference between the M^{th} beam suffering $2M$ reflections and the direct zeroth order beam is

$$2m\pi - \frac{4}{3}\pi M^3 \epsilon^2 N \qquad \ldots (IV.3)$$

where M is the order of the last beam of effective amplitude contributing to the point of peak intensity, ϵ is the wedge angle and N is the order of interference. If the reflectivity of the two surfaces is so poor that contributions of beams other than the zeroth and few following beams could be neglected and considering that ϵ is an experimentally adjustable

variable, and N could therefore be made small enough, the phase lag term becomes very small and could be neglected. This approximation is valid only for qualitative purposes, i.e. when intensity measurements are not desired. If intensity considerations are sought, it is in fact fatal to take the above mentioned approximation as valid. Equation (IV.3) could be written as follows:

$$2m\pi - z\pi M^3 \qquad \text{where} \qquad z = \frac{4}{3}\epsilon^2 N .$$

Now it is clear that even in the case of a wedge interferometer with highly reflecting surfaces, the maximum intensity is determined, for a certain value of ϵ and N, by the number of beams collected and the magnitude of the quantity $z\pi$. Barakat and Mokhtar[37] considered the case of a wedge interferometer of $\epsilon = 31 \times 10^{-5}$ rad, $R = 0.9$. They calculated I_{max} for different values of $z\pi$ and the phase lag of the last contributing beam with respect to the beam suffering no reflections, i.e. zeroth order. As evident from their table, below, the number of effective beams depends critically on the quantity $z\pi$, as it increases the number of effective beams decreased, bringing the resultant I_{max} down. Also the phase lag of the last contributing beam w.r.t. the first transmitted beam of zeroth order increases. This means if the $z\pi$ value is large, the number of effective beams is limited, and the phase lag of the last beam is large, in effect opposing the summation instead of adding to it, and the resultant I_{max} is brought down drastically.

$z\pi$	number of beams collected	I_{max}	phase lag of last beam
3 sec	47	0.968	86° 31 min
12 sec	30	0.873	90°
30 sec	23	0,760	101° 23 min
2 min	15	0.540	112° 30 min

Now, as Tolansky[34] pointed out if ϵ is kept very small, i.e. t the interferometric gap is kept small, the term $z\pi M^3 = \frac{4}{3}\pi\epsilon^2 M^3 N$ will be negligible and for highly reflecting wedge interferometer with a large number of effective beams contributing to the point of peak intensity on the intensity distribution curve, the value of I_{max} will approximate to that of the F-P set up value. We will show that in case of non-normal incidence these considerations of approximation are still less valid when it comes to intensity considerations rather than qualitative fringe definition.

IV.5 THE CASE OF FIZEAU – MULTIPLE BEAM FRINGES AT OBLIQUE INCIDENCE

We have already shown that the value of peak intensity of a multiple beam Fizeau fringe is not simply a function of the transmission and reflection coefficients of the coating layers. The most important factors emerging from the foregoing discussion are:

(1) The creation of beams depending on the reflection coefficient of the coating layers. The higher R is the higher the number of beams created and the higher the value of I_{max}.

(2) The collection of beams depending on the aperture of the interferometer, the wedge angle and the numerical aperture of the microscope objective.

(3) The intensity of the first transmitted beam determines the intensity of the peak point on the intensity distribution curve. Also the transmission of the two glass subtrates must be taken into account.

(4) The phase lag between the M^{th} beam suffering $2M$ reflections and the zeroth order beam. This together with the above mentioned factors sets the limit to the number of effective beams and determines the order of that beam which, due to all these factors, will start seriously opposing the summation bringing the I_{max} value considerably below the simple value calculated from formulae ignoring the effect of interferometric considerations.

Now, the question is how these factors would work for a system of multiple beam Fizeau fringes viewed in transmission and at oblique incidence. The following points could describe the situation then:

(1) As the reflection coefficients of the parallel and perpendicular components differ, the number of effective beams created by either component is different depending on the values of $R_{\perp}$ and $R_{\parallel}$ at a particular angle of incidence θ. The number of beams created by the perpendicular component is the larger but less intense.

(2) For both polarizations the aperture of the interferometer, wedge angle and the numerical aperture of the microscope objective are the same. However, the interferometric gap t is not the same for both components due to differing values of phase change at reflection at the medium/metallic coating interface.

(3) The intensity of the first transmitted beam is different for both vibrations. This takes into account the combined effect of transmission through the glass substrates and film at an incidence θ.

(4) The phase lag of the M^{th} beam undergoing 2M reflections w.r.t. the first zeroth order beam, is different for both polarizations. The value of $z_{\pi M}$ will be different for both directions. This together with differing values of T and R will determine the number of effective beams belonging to either component and also the order of the beam which will oppose the summation of beams contributing to $(I_{max})_{\perp}$ and $(I_{max})_{\parallel}$.

(5) Another factor is that at high angles of incidence the number of beams created and collected for either vibration will significantly decrease. This is because the interferometer aperture becomes very small and the beams reflecting inside the interferometer undergo severe angles of $\theta + 2\epsilon$ at each reflection which increases the linear displacement of the emerging beams allowing the objective to collect fewer beams for either component.

Now we will consider two examples to illustrate the preceeding arguments. We shall consider an air silvered wedge interferometer where the reflecting silver layers are of identical thickness and properties and deposited on glass substrates. The substrates are of index 1.52 and of high optical quality. In one instance the silver layer will be of thickness 500 Å , and in another it will be 205 Å

In each case, using a simple computer program, the amplitudes and intensities of the emerging beams contributing to the point of peak intensity for the parallel and perpendicular component fringes were computed from the optical properties of the film and the glass substrates. Also $(I_{max})_{\perp}$ and $(I_{max})_{\parallel}$ were computed. This was carried out for incidence 70°. The last two quantities are given below as functions of the number of beams $M+1$, where $M = 0, 1, 2, 3, \ldots$ etc. Figures are given to the fourth decimal place. It is, in fact, unlikely that intensities beyond this accuracy are of any practical significance. The following tables give the results of the calculations.

Case (1) $R_{\perp} = 0.984$ $R_{\parallel} = 0.902$ Case (2) $R_{\perp} = 0.792$ $R_{\parallel} = 0.422$

$T_{\perp} = 0.009$ $T_{\parallel} = 0.062$ $T_{\perp} = 0.192$ $T_{\parallel} = 0.544$

For both cases $T_{g\perp} = 0.710$ and $T_{g\parallel} = 0.968$.

For Case (1) we have

M+1	$(I_{max})_{\perp}$	$(I_{max})_{\parallel}$	M+1	$(I_{max})_{\perp}$	$(I_{max})_{\parallel}$
1	0.41×10^{-4}	0.36×10^{-2}	37	0.327×10^{-1}	0.3587
2	0.16×10^{-3}	0.130×10^{-1}	38	0.340×10^{-1}	0.3603
3	0.36×10^{-3}	0.266×10^{-1}	39	0.353×10^{-1}	0.36
4	0.63×10^{-3}	0.429×10^{-1}	40	0.365×10^{-1}	0.3630
5	0.97×10^{-3}	0.609×10^{-1}	41	0.379×10^{-1}	0.3642
6	0.14×10^{-2}	0.799×10^{-1}	42	0.392×10^{-1}	0.3653
7	0.18×10^{-2}	0.992×10^{-1}	43	0.405×10^{-1}	0.3662
8	0.24×10^{-2}	0.1184	44	0.418×10^{-1}	0.3671
9	0.30×10^{-2}	0.1372	45	0.431×10^{-1}	0.3678
10	0.36×10^{-2}	0.1553	46	0.444×10^{-1}	0.3686
11	0.43×10^{-2}	0.1726	47	0.457×10^{-1}	0.3692
12	0.50×10^{-2}	0.1890	48	0.470×10^{-1}	0.3698
13	0.58×10^{-2}	0.2045	49	0.483×10^{-1}	0.3763
14	0.66×10^{-2}	0.2189	50	0.496×10^{-1}	0.3707
15	0.75×10^{-2}	0.2324	51	0.509×10^{-1}	0.3712
16	0.84×10^{-2}	0.2448	52	0.521×10^{-1}	0.3715
17	0.93×10^{-2}	0.2564	53	0.534×10^{-1}	0.3719
18	0.102×10^{-1}	0.2670	54	0.547×10^{-1}	0.3722
19	0.113×10^{-1}	0.2768	55	0.559×10^{-1}	0.3725
20	0.123×10^{-1}	0.2858	56	0.572×10^{-1}	0.3727
21	0.134×10^{-1}	0.2940	57	0.585×10^{-1}	0.3730
22	0.144×10^{-1}	0.3015	58	0.597×10^{-1}	0.3732
23	0.155×10^{-1}	0.3083	59	0.609×10^{-1}	0.3733
24	0.167×10^{-1}	0.3146	60	0.622×10^{-1}	0.3735
25	0.178×10^{-1}	0.3203	61	0.634×10^{-1}	0.3737
26	0.190×10^{-1}	0.3255	62	0.646×10^{-1}	0.3738
27	0.201×10^{-1}	0.3302	63	0.658×10^{-1}	0.3739
28	0.214×10^{-1}	0.3344	64	0.670×10^{-1}	0.3740
29	0.266×10^{-1}	0.3383	65	0.682×10^{-1}	0.3741
30	0.238×10^{-1}	0.3418	66	0.694×10^{-1}	0.3742
31	0.250×10^{-1}	0.3450	67	0.706×10^{-1}	0.3743
32	0.263×10^{-1}	0.3479	68	0.717×10^{-1}	0.37440
33	0.276×10^{-1}	0.3505	69	0.729×10^{-1}	0.37440
34	0.288×10^{-1}	0.3529	70	0.740×10^{-1}	0.37450
35	0.301×10^{-1}	0.3550	71	0.752×10^{-1}	0.37460
36	0.314×10^{-1}	0.3570	72	0.763×10^{-1}	0.37460

For Case (2) we have

M+1	$(I_{max})_{\perp}$	$(I_{max})_{\parallel}$	M+1	$(I_{max})_{\perp}$	$(I_{max})_{\parallel}$
1	0.188×10^{-1}	0.2773	37	0.43540	0.8300
2	0.605×10^{-1}	0.5607	38	0.43550	
3	0.1103	0.7099	39	0.43550	
4	0.1603	0.7782	40	0.43550	
5	0.2064	0.8079	41	0.43550	
6	0.2471	0.8207	42	0.43560	
7	0.2819	0.8261	43	0.43560	
8	0.3112	0.8284	44	0.43560	
9	0.3353	0.8293	45	0.43560	
10	0.3551	0.8297	46	0.43560	
11	0.3712	0.8299	47	0.43560	
12	0.3842	0.83000	48	0.43560	
13	0.3946	0.83000	49	0.43560	
14	0.4030		50		constant at 0.8300
15	0.4096		51		
16	0.4150		52		
17	0.4192		53		
18	0.4226		54		
19	0.4253		55		
20	0.4274		56		
21	0.4291	constant at 0.8300	57	constant at 0.4356	
22	0.4305		58		
23	0.4315		59		
24	0.4324		60		
25	0.4330		61		
26	0.4336		62		
27	0.4340		63		
28	0.4343		64		
29	0.4346		65		
30	0.4348		66		
31	0.4350		67		
32	0.4351		68		
33	0.4352		69		
34	0.4353		70		
35	0.4354		71		
36	0.43540		72		

From the above calculations the following remarks could be made:

(a) In Case (1) where the wedge coatings are highly reflecting and when 72 beams are considered, $(I_{max})_{\perp} = 0.0763$ and $(I_{max})_{\parallel} = 0.3746$ with their ratio $(I_{max})_{\perp}/(I_{max})_{\parallel} = 0.20$.

(b) In Case (2) where the wedge coatings are of low reflectivity and when 72 beams are considered, $(I_{max})_{\perp} = 0.4356$ and $(I_{max})_{\parallel} = 0.8300$ with a ratio $(I_{max})_{\perp}/(I_{max})_{\parallel} = 0.52$.

However, these figures are not quite what they appear to be! Taken as they are, still does not explain the experimentally observed values for the ratio $(I_{max})_{\perp}/(I_{max})_{\parallel}$. In the original experiment of Tolansky[5], he reports a visually estimated value of about 0.05 for the ratio of intensities in a case of a highly reflecting coating. As for the second case of low reflectivity the ratio determined in the course of this work is of the order 0.20. The explanation seemed to lie in the answer to a main question, discussed earlier, namely, how many beams of effective amplitudes are actually collected of either polarization at a particular angle of incidence and at a very narrow interferometer aperture. To find the answer to this question, a simple experimental test was performed. An optical set-up similar to that shown in Fig.III.1 was employed. The iris diaphragm behind the condenser was replaced with a rectangular slit. The multiple images of the slit could be clearly observed in a focal plane some few millimeters before that of the fringes. The multiple images are of intensities proportional to the amplitudes of the beams contributing to the formation of the fringes. The plates of the interferometer were coated with a silver film of low reflectivity of the order of 0.50.

When the multiple images of the slit were viewed at normal incidence one could count no more than five images. The first is the most intense with the other four diminishing in intensity. The last two were very feeble. When the interferometer was turned into 70° with the

incident beam, the number of images was three. On the introduction of a polaroid sheet in the path of the incident beam such as we had only the perpendicular component passing the intensity of all images dropped but since the reflectivity is higher for this component one could still count three images in spite of their very low intensties. Turning the polaroid 90° now only the parallel component could pass, and two relatively bright images could be seen.

Now considering the factors discussed earlier concerning the effects of creating beams and collecting them on the (I_{max}) value of a Fizeau fringe, and taking into account the calculations performed in the second table, it is clear that for the case studied above, the ratio $(I_{max})_{\perp} / (I_{max})_{\parallel}$ is of the order of 0.21, a value which agrees well with experimentally determined ratio. Thus the difference in the peak intensities of fringes belonging to the parallel and perpendicular components in a multiple beam Fizeau fringe pattern in transmission received a satisfactory explanation.

CHAPTER V

EXPERIMENTAL DETERMINATION OF Δ AS A FUNCTION OF θ FOR Ag, Au AND Al FILMS IN THE THICKNESS RANGE $d \geq 200$ Å

V.1 INTRODUCTION

This chapter presents experimental results obtained on films of Ag, Au and Aℓ. The results shown here give Δ, the differential change of phase, as a function of θ the angle of incidence for a film thickness d at a wavelength λ. The wavelengths at which measurements were carried out were chosen to represent the two ends of the visible spectrum beside one at the middle of this spectrum. However, it was not always possible to carry out measurements at all three wavelengths for each film. This was so because of limitations imposed by the response of photographic plates available, and sometimes because of the low transmitted intensities exhibited by a film at a certain wavelength. This does not mean that the technique is not capable of dealing with such situations.

The use of different types of photographic plates would, almost, solve the problem, and indeed, may help to extend the applicability of the method to the invisible parts of the spectrum. However, when ordered, the required plates arrived too late to be used. In the case of each metal, relevant results were processed using a computer program which produced a computed curve, using Schulz[20] constants, and a group of experimental crosses from fed-in values of fringe shift measured on a Hilger comparator as explained in Chapter III. The program produced Δ as a fraction of π. Also photographically recorded fringes at varying incidence are presented with the relevant curves.

V.2 PREVIOUS WORK

It may be useful here to present a short survey of some earlier work on Δ for the metals mentioned earlier. It would be rather optimistic to try and compare values of Δ produced on films prepared in different vacuum systems and on subtrates of different nature. However, it is useful to point out the differences between observations and sets of measurements.

Previous work on phase changes, as it appears from the ever increasing volume of literature, could be grouped into the following:

(a) Computations and theoretical calculations. In most cases these are done using approximations and constants determined on samples approaching bulk characteristics. However, MacLaurin[45], and, forty years later, Scandone and Ballerini[46], gave calculations of Δ as a function of the angle of incidence for thin films The constants used were those of the bulk.

(b) Experimental determinations of Δ at certain angles of incidence as one of the factors needed to determine the optical constants, but not as curves of Δ vs θ. Avery's[32] and Clegg's[47] work are examples.

(c) Much work has been done on the experimental determination of the phase change at reflection air/metallic interface, or at the dielectric substrate/metallic interface at normal incidence. The quantity, as Heavens[41] remarks, reveals a highly complex variation with film thickness and wavelength. The phase properties of silver and aluminium are of importance to interferometry and its applications in many fields, e.g. wavelength measurements and length metrology. These phase properties were studied by many workers. Since 1950, Schulz[48,49], Koehler[50], Koester[51], Weaver et al[52], Bruce and Ciddor[53], Ciddor[54], Barakat et al[12,33,55], and Philip[56] all tackled the problem of measureing the quantities β and β' the change of phase at reflection at the air/film and sub/film interfaces respectively. However, in this thesis we are concerned with the quantity Δ the differential change of phase. In the end chapter some ideas for furthering work on β and β' for thin films of metals will be put forward.

V.3 EXPERIMENTAL RESULTS ON SILVER FILMS

Measurements of Δ as a function of the angle of incidence θ were carried out at three wavelengths. At $\lambda_1 = 4358$ Å and $\lambda_2 = 5461$ Å the films investigated were of comparable thickness, where $d/\lambda \simeq 0.1$. At $\lambda_3 = 6438$ Å, $d/\lambda = 0.04$. At the red end of the visible spectrum, silver films show greater reflection and consequently transmit less, making it very difficult to work with thicknesses over $\simeq 250$ Å. This, however, could be seen as an advantage since the interferometric technique, dependent as it is on the high reflection coefficient of the interferometer coatings, could be used at lower thickness values with longer wavelengths.

Figure V.1 shows the variation of Δ vs θ for a silver film of 550 Å at $\lambda_1 = 4358$ Å. The crosses represent the experimental points, while the solid line is the 'theoretical' computed variations. Plate (12) shows the fringe shift caused by a step height of 550 Å. This was the thickness of the film. Plate (13) shows a series of photographically recorded fringes of equal thickness taken at angles of incidence 0° to 70°. At $\lambda_2 = 5461$ Å the experimental and computed variations of Δ vs θ for a film of 600 Å are shown in Fig.V.2. Plate (14) shows the fringe shift equivalent to the film thickness. Plate (15) gives the recorded fringe separation at various angles of incidence. At the longer end of the spectrum $\lambda_3 = 6438$ Å the film thickness was 250 Å. This gave enough transmission to facilitate photographic recording without unduly inhibiting the requirements of reflection coefficient. However, it is seen that the experimental points are significantly shifted from the computed curve. The latter was computed using constants determined for thicker films of $d \geq 500$ Å. Fig.V.3 shows the experimental and computed variations of Δ vs θ for $d/\lambda \simeq 0.04$. Plate (16) shows fringes of equal thickness taken at different angles of incidence at the wavelength $\lambda_3 = 6438$ Å.

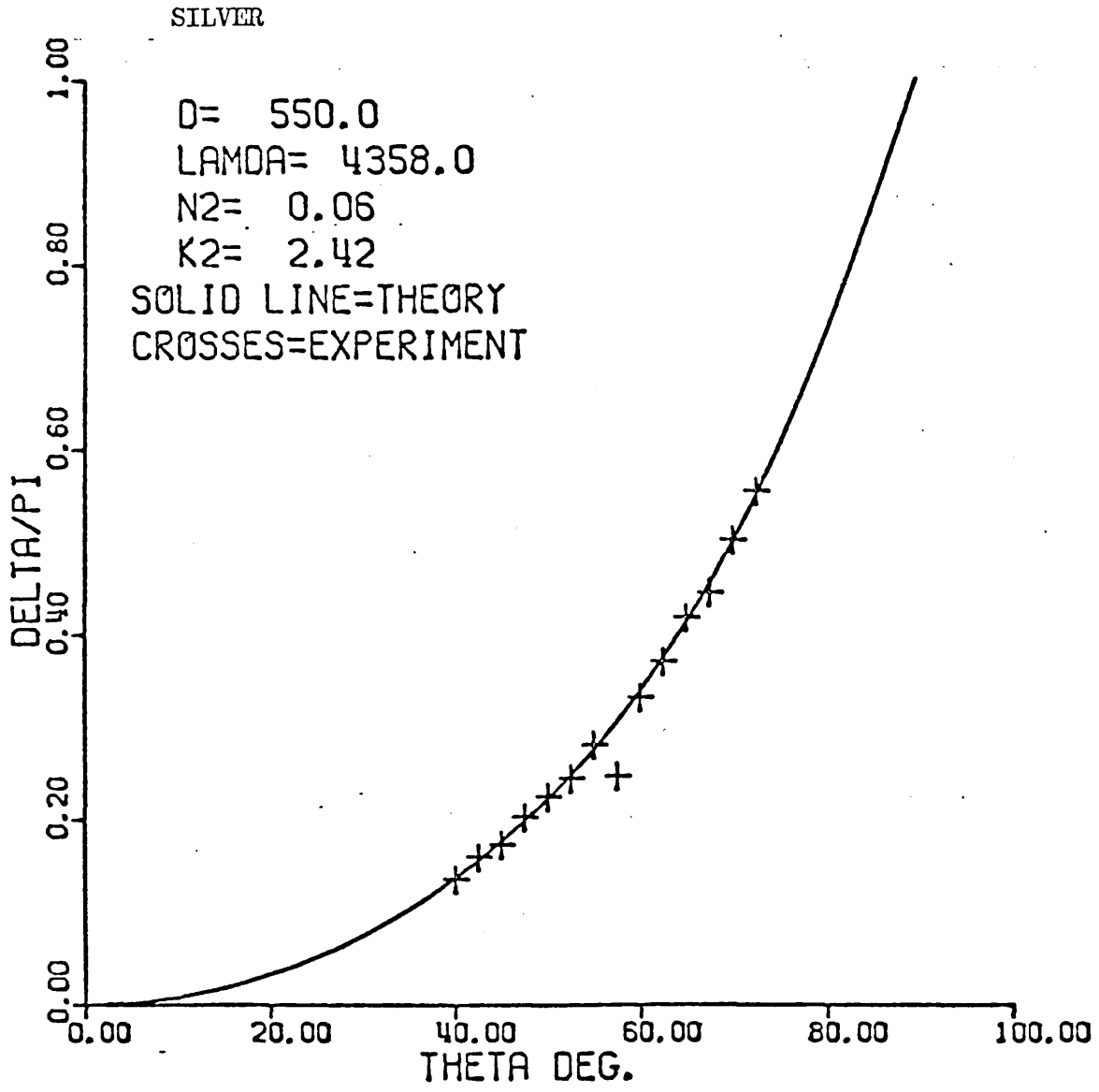
SILVER
D= 550.0
LAMDA= 4358.0
N2= 0.06
K2= 2.42
SOLID LINE=THEORY
CROSSES=EXPERIMENT
DELTA/PI
0.00
0.20
0.40
0.60
0.80
1.00
0.00
20.00
40.00
60.00
80.00
100.00
THETA DEG.

Fig.V.1

PLATE (12)

d_{Ag} = 550 Å

λ_1 = 4358 Å

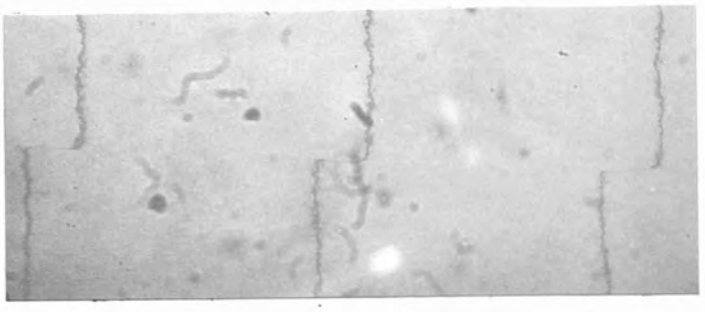

PLATE (13)

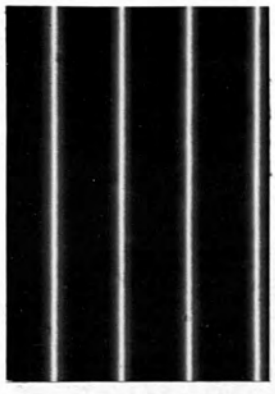

θ = 0°

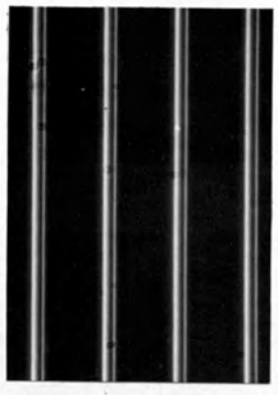

θ = 40°

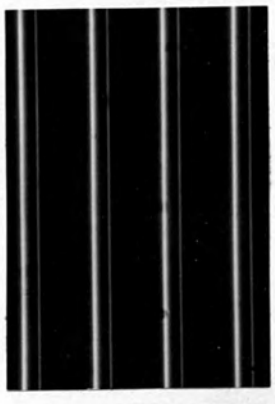

θ = 50°

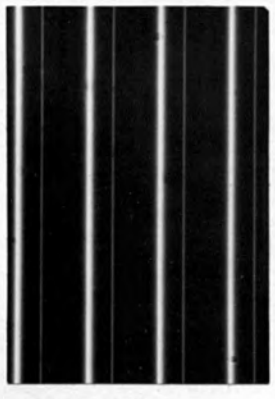

θ = 60°

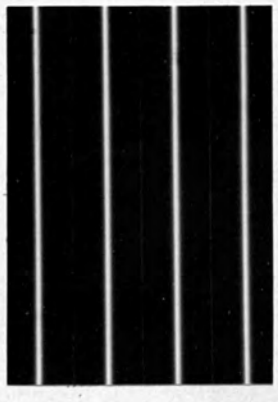

θ = 70°

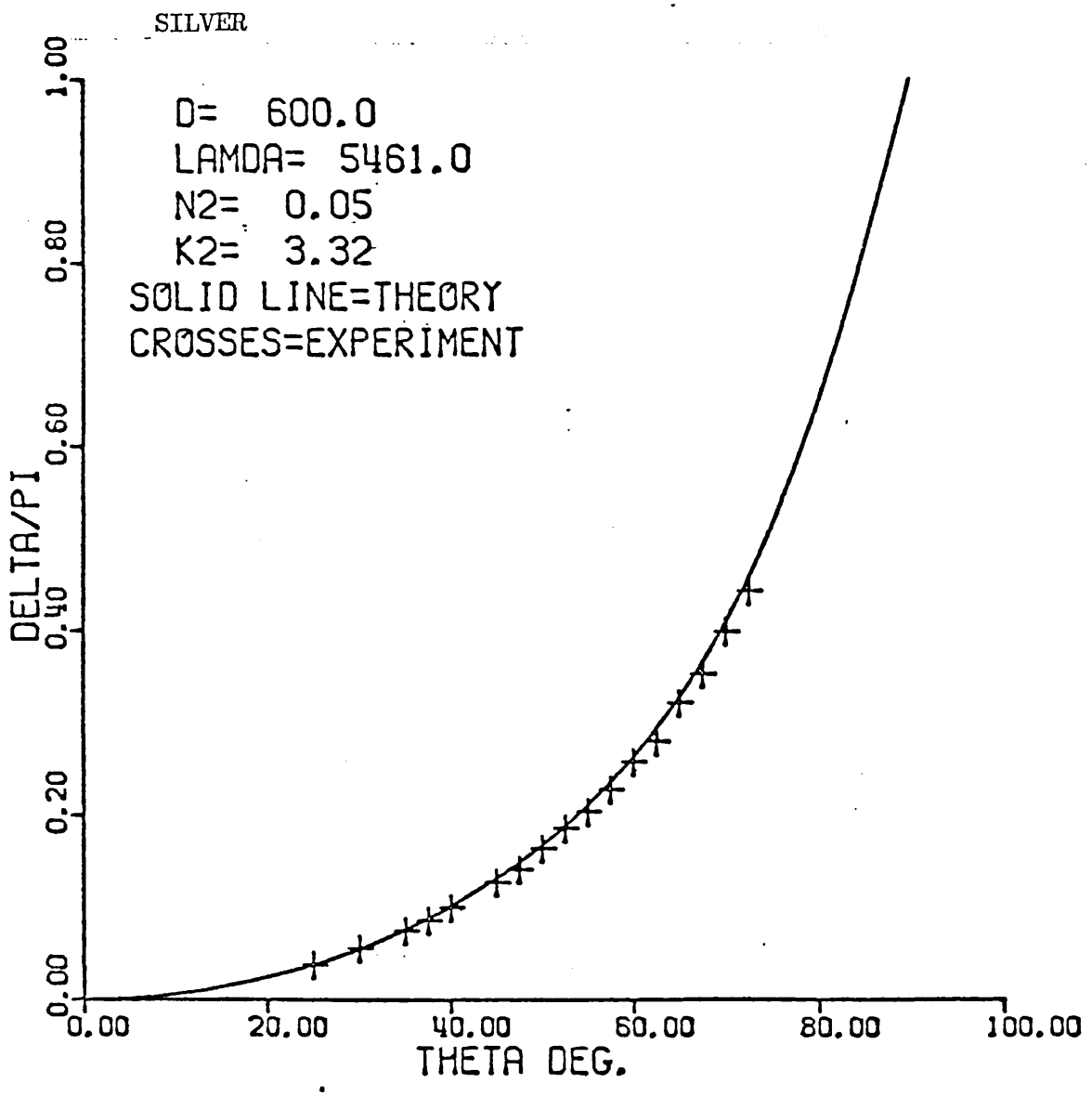
SILVER
D= 600.0
LAMDA= 5461.0
N2= 0.05
K2= 3.32
SOLID LINE=THEORY
CROSSES=EXPERIMENT
DELTA/PI
0.00
0.20
0.40
0.60
0.80
1.00
0.00
20.00
40.00
60.00
80.00
100.00
THETA DEG.

Fig.V.2

PLATE (14)

d_{Ag} = 600 Å

λ_2 = 5461 Å

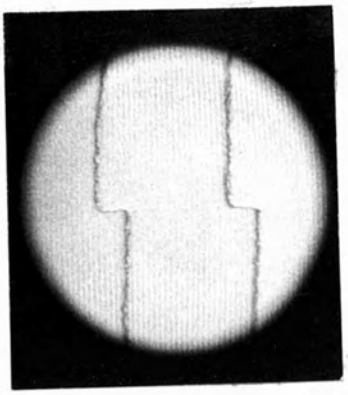

PLATE (15)

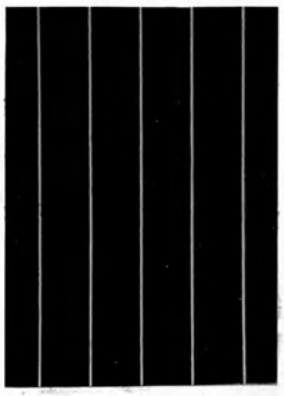

$\theta = 0^\circ$

$\theta = 30^\circ$

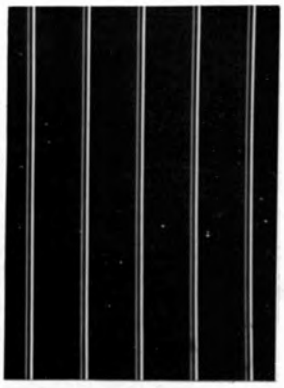

$\theta = 40^\circ$

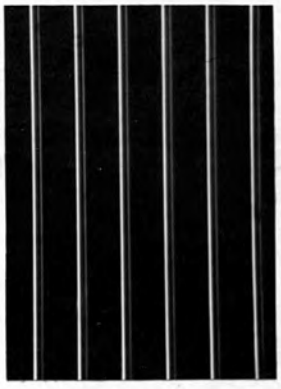

$\theta = 50^\circ$

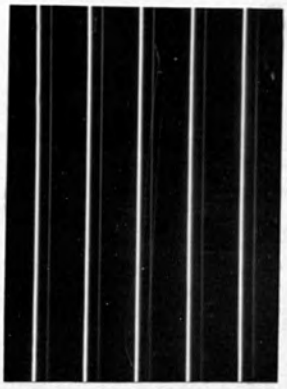

$\theta = 60^\circ$

$\theta = 70^\circ$

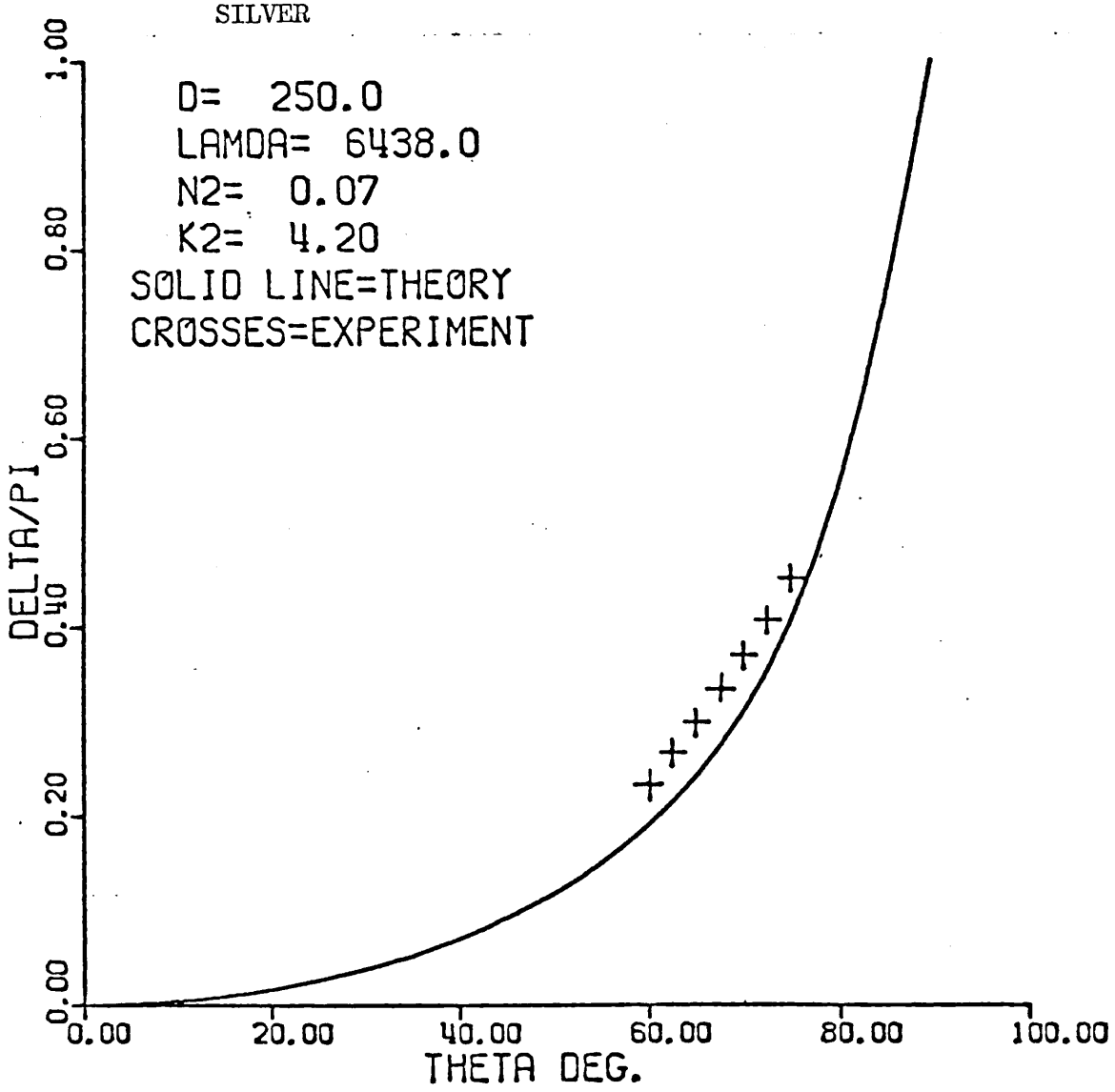
SILVER
D= 250.0
LAMDA= 6438.0
N2= 0.07
K2= 4.20
SOLID LINE=THEORY
CROSSES=EXPERIMENT
DELTA/PI
0.00
0.20
0.40
0.60
0.80
1.00
0.00
20.00
40.00
60.00
80.00
100.00
THETA DEG.

Fig.V.3

PLATE (16)

d_{Ag} = 250 Å λ_3 = 6438 Å

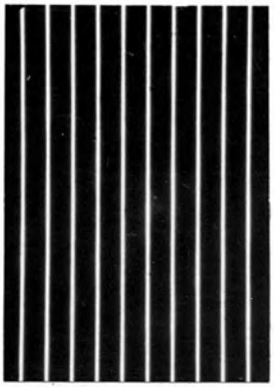

θ = 0°

θ = 50°

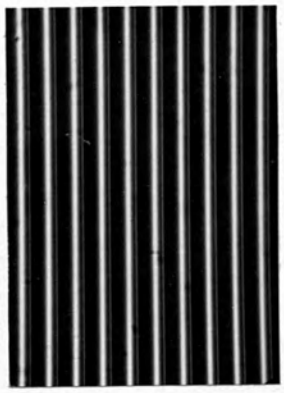

θ = 65°

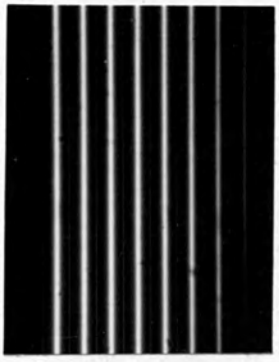

θ = 75°

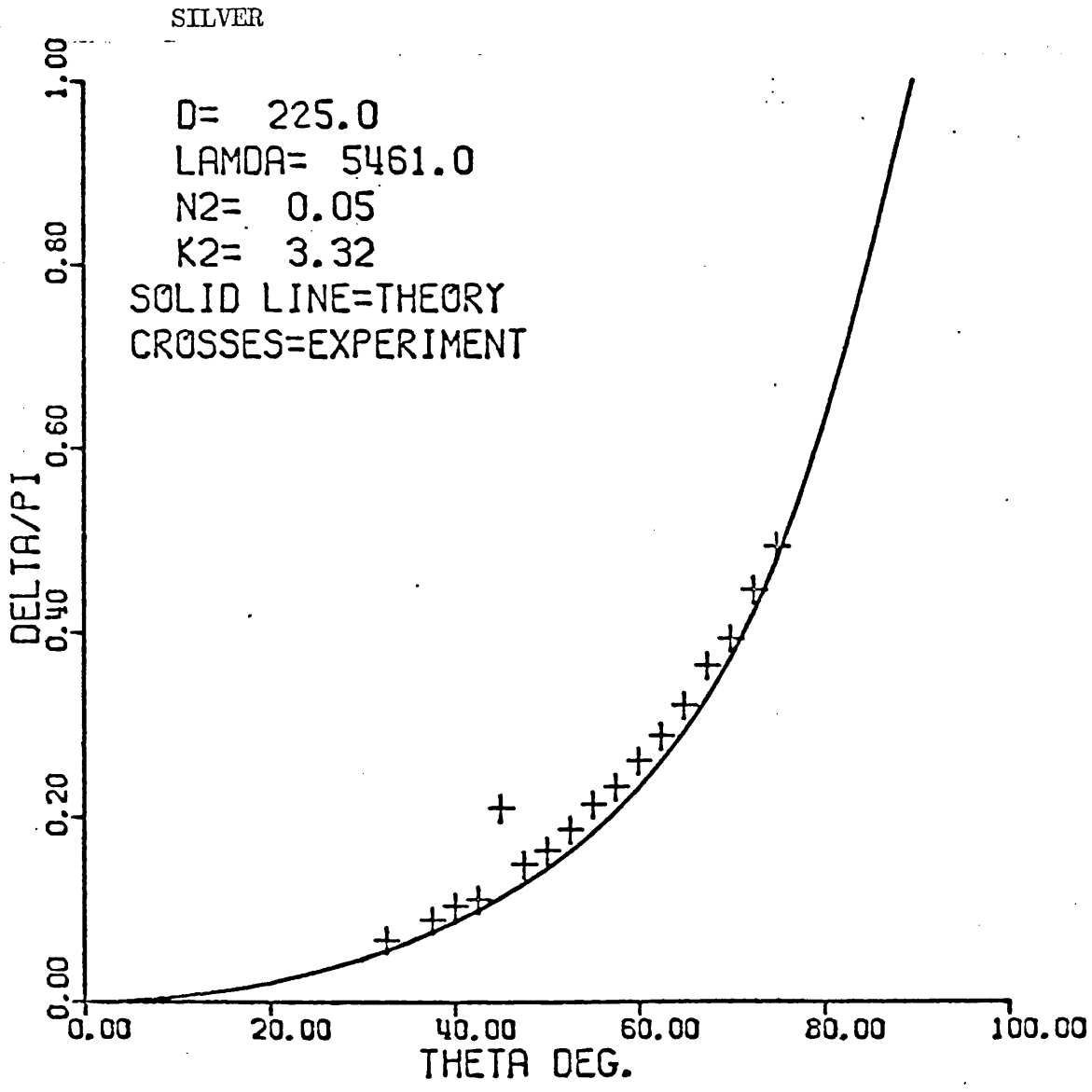
SILVER
D= 225.0
LAMDA= 5461.0
N2= 0.05
K2= 3.32
SOLID LINE=THEORY
CROSSES=EXPERIMENT
DELTA/PI
0.00
0.20
0.40
0.60
0.80
1.00
0.00
20.00
40.00
60.00
80.00
100.00
THETA DEG.

Fig.V.4

PLATE (17)

d_{Ag} = 225 Å

λ_2 = 5461 Å

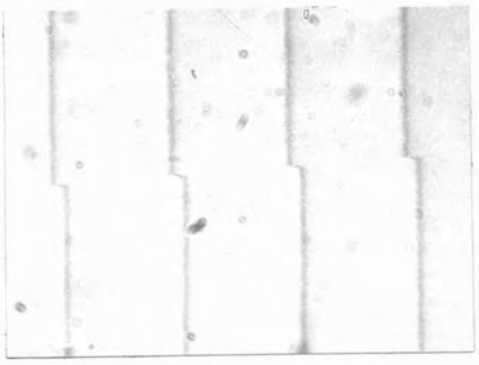

PLATE (18)

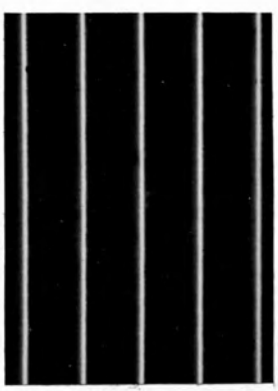

θ = 0°

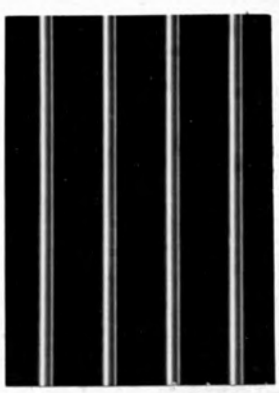

θ = 42.5°

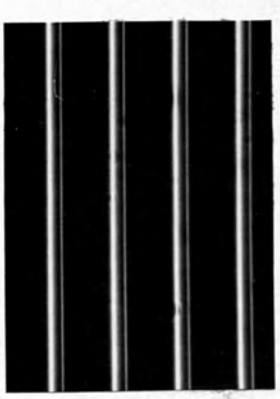

θ = 52.5°

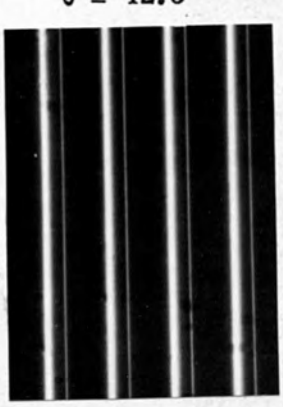

θ = 62.5°

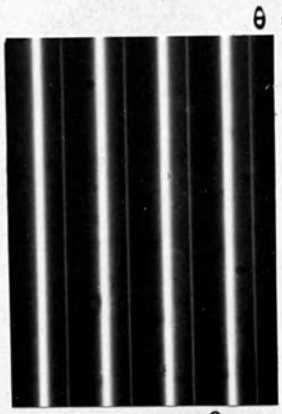

θ = 70°

To further illustrate the effect of thickness and to demonstrate the applicability of the technique, a film of silver of 225 Å was deposited and Fig.V.4 gives the variation of Δ vs θ for this film at $\lambda_2 = 5461$ Å. Plates (17) and (18) exhibit the fringe shift due to the thickness and the recorded fringes at different angles of incidence, respectively. It is again seen that computed variation with bulk constant is significantly departed from the experimental points.

V.4 EXPERIMENTAL RESULTS ON GOLD FILMS

In the case of gold, measurements were made at two wavelengths, $\lambda_2 = 5461$ Å and $\lambda_3 = 6438$ Å.

The reflectivity of gold films at these wavelengths is reasonable, while at $\lambda_1 = 4358$ Å it is poor and the visibility of the fringes in a gold coated air wedge interferometer is very poor. The thickness of the film, used at the two wavelengths, was 580 Å ± 20 Å. Plate (19) gives the fringe shift caused by a gold step of such height. Measurements were also made on thinner films of thickness $d \leq 200$ Å but widely differing values of d as deduced by the interferometric technique made any results obtained on such films highly suspect. The difficulties with measuring gold films thickness were referred to in the last chapter.

Figure V.5 shows the Δ vs θ computed and experimental variations at $\lambda_2 = 5461$ Å. Plate (20) shows the doubled fringes obtained at this wavelength. Fig.V.6 gives the variations of the same film at $\lambda_3 = 6438$ Å and Plate (21) illustrates the fringes shifts obtained at different angles of incidence. The agreement between the experimental points and computed curves show that thickness effects are irrelevant at this stage, since the Schulz constants were determined for films of thickness of $d \geq 700$ Å. However, for the longer wavelength there is some difference between the computed and experimental variations.

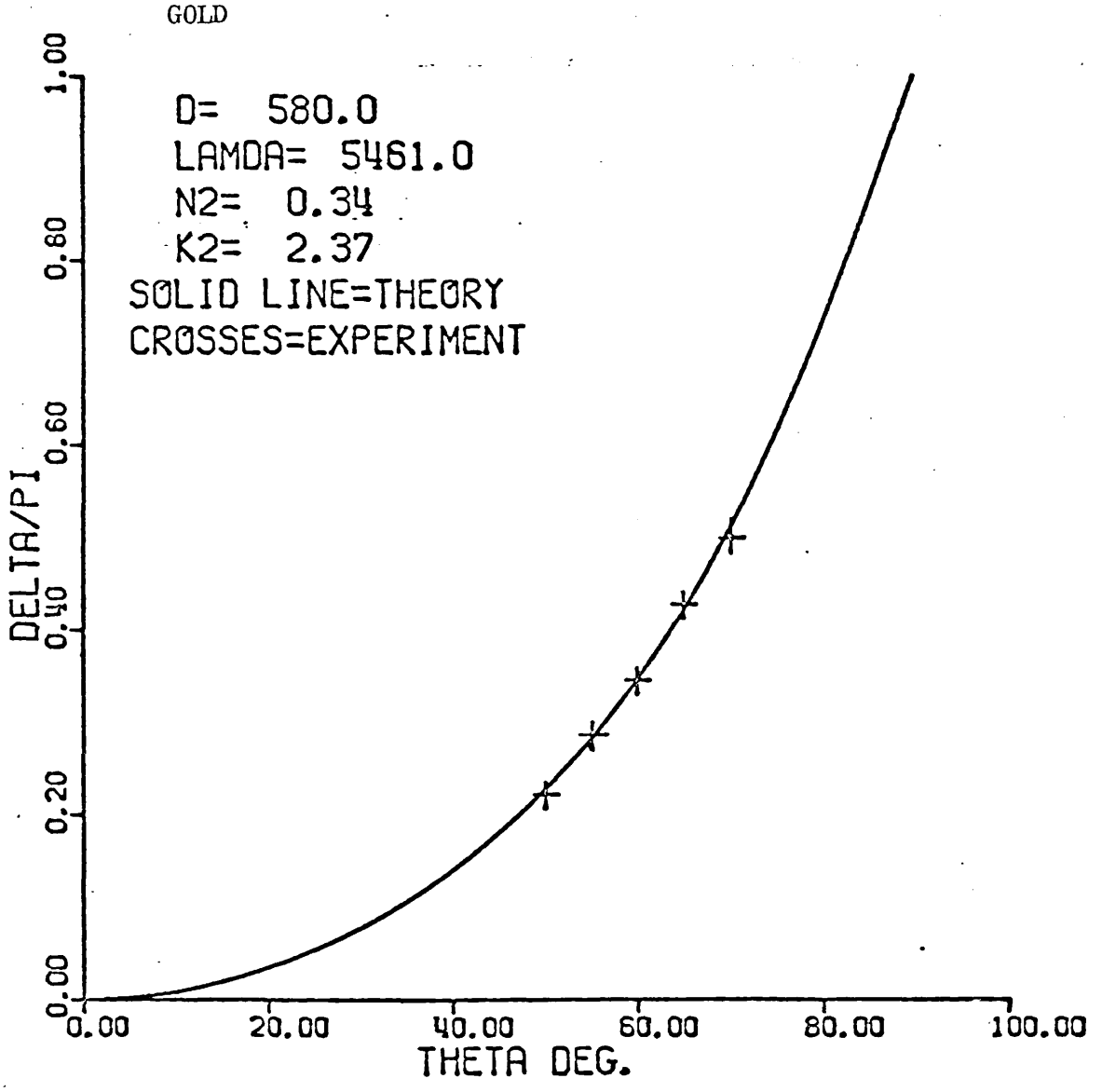
GOLD
D= 580.0
LAMDA= 5461.0
N2= 0.34
K2= 2.37
SOLID LINE=THEORY
CROSSES=EXPERIMENT
DELTA/PI
0.00
0.20
0.40
0.60
0.80
1.00
0.00
20.00
40.00
60.00
80.00
100.00
THETA DEG.

Fig.V.5

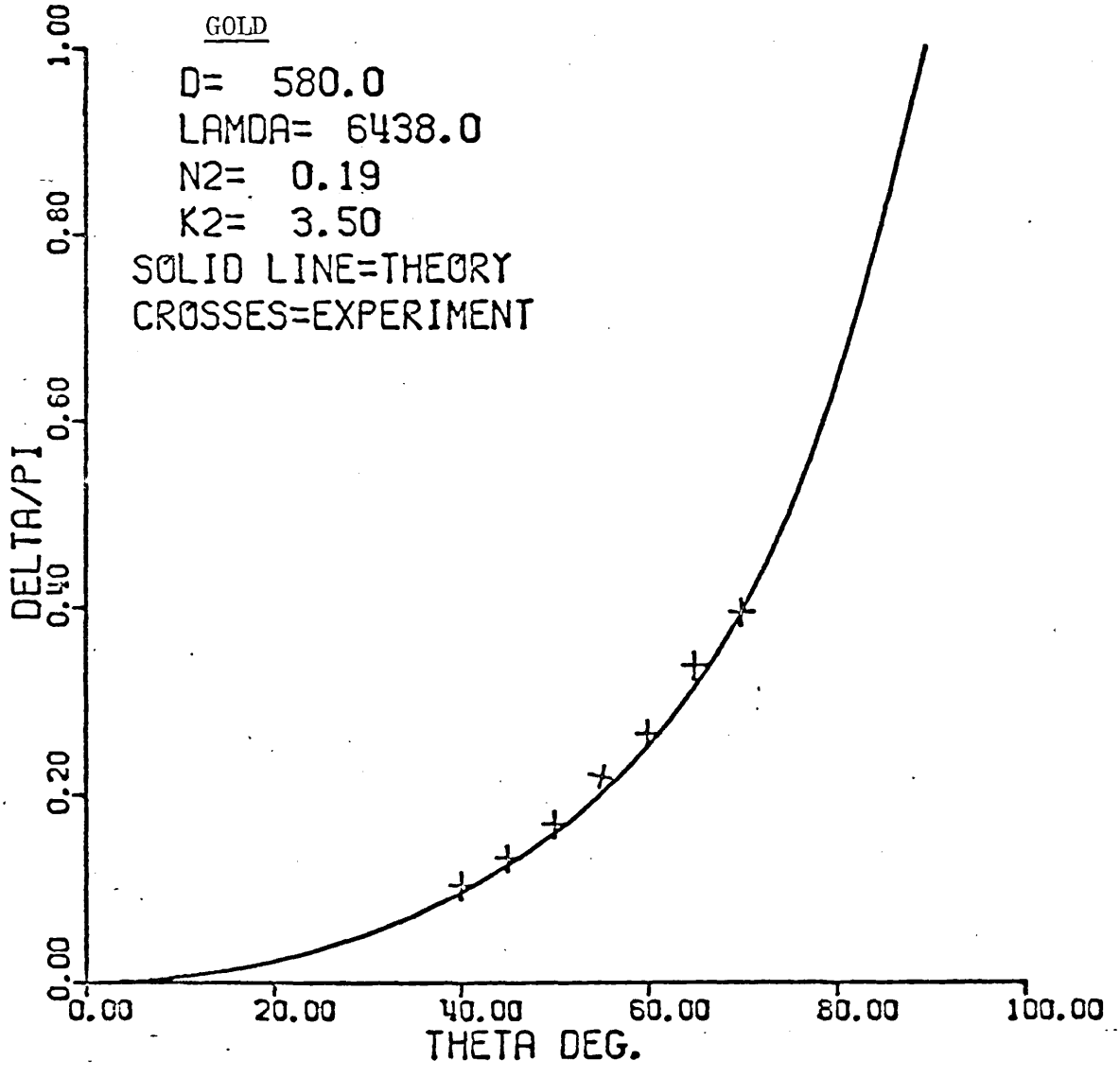
GOLD
D= 580.0
LAMDA= 6438.0
N2= 0.19
K2= 3.50
SOLID LINE=THEORY
CROSSES=EXPERIMENT
DELTA/PI
0.00
0.20
0.40
0.60
0.80
1.00
0.00
20.00
40.00
60.00
80.00
100.00
THETA DEG.

Fig.V.6

PLATE (19)

d_{Au} = 580 Å

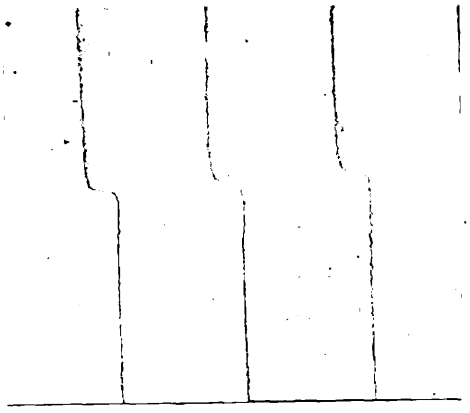

λ_2 = 5461 Å

PLATE (20)

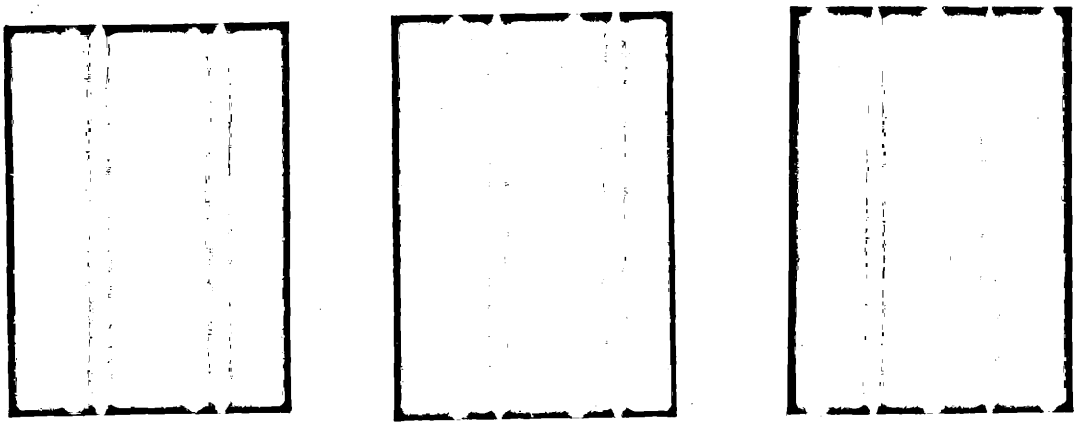

θ = 50° θ = 60° θ = 70°

λ_3 = 6438 Å

PLATE (21)

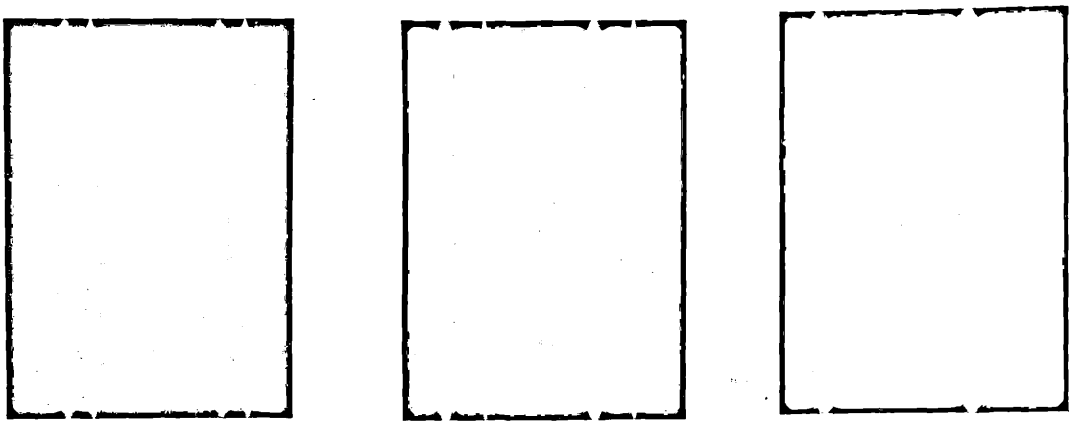

θ = 50° θ = 60° θ = 70°

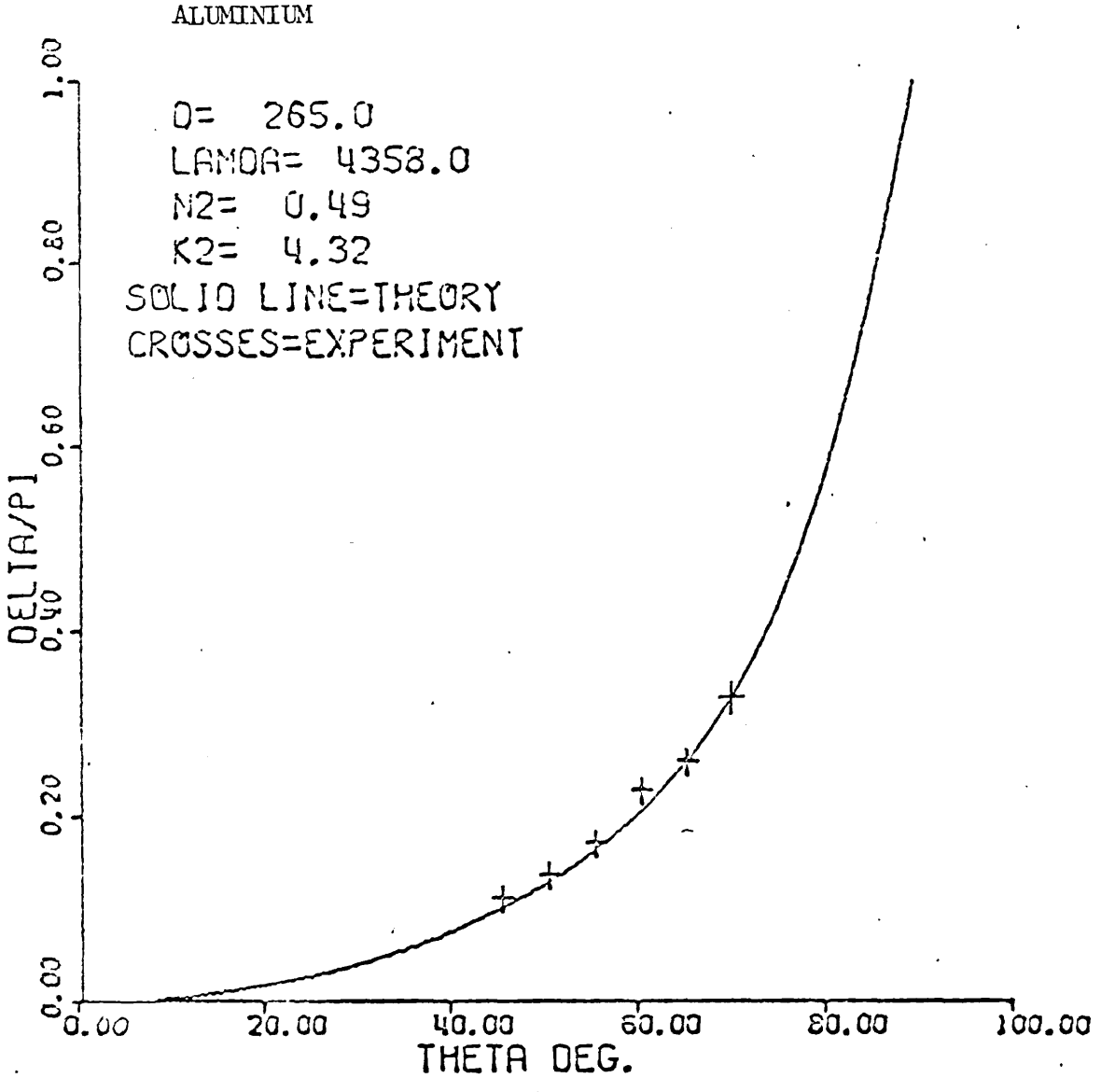
ALUMINIUM
D= 265.0
LAMDA= 4358.0
N2= 0.49
K2= 4.32
SOLID LINE=THEORY
CROSSES=EXPERIMENT
DELTA/PI
0.00
0.20
0.40
0.60
0.80
1.00
0.00
20.00
40.00
60.00
80.00
100.00
THETA DEG.

Fig.V.7

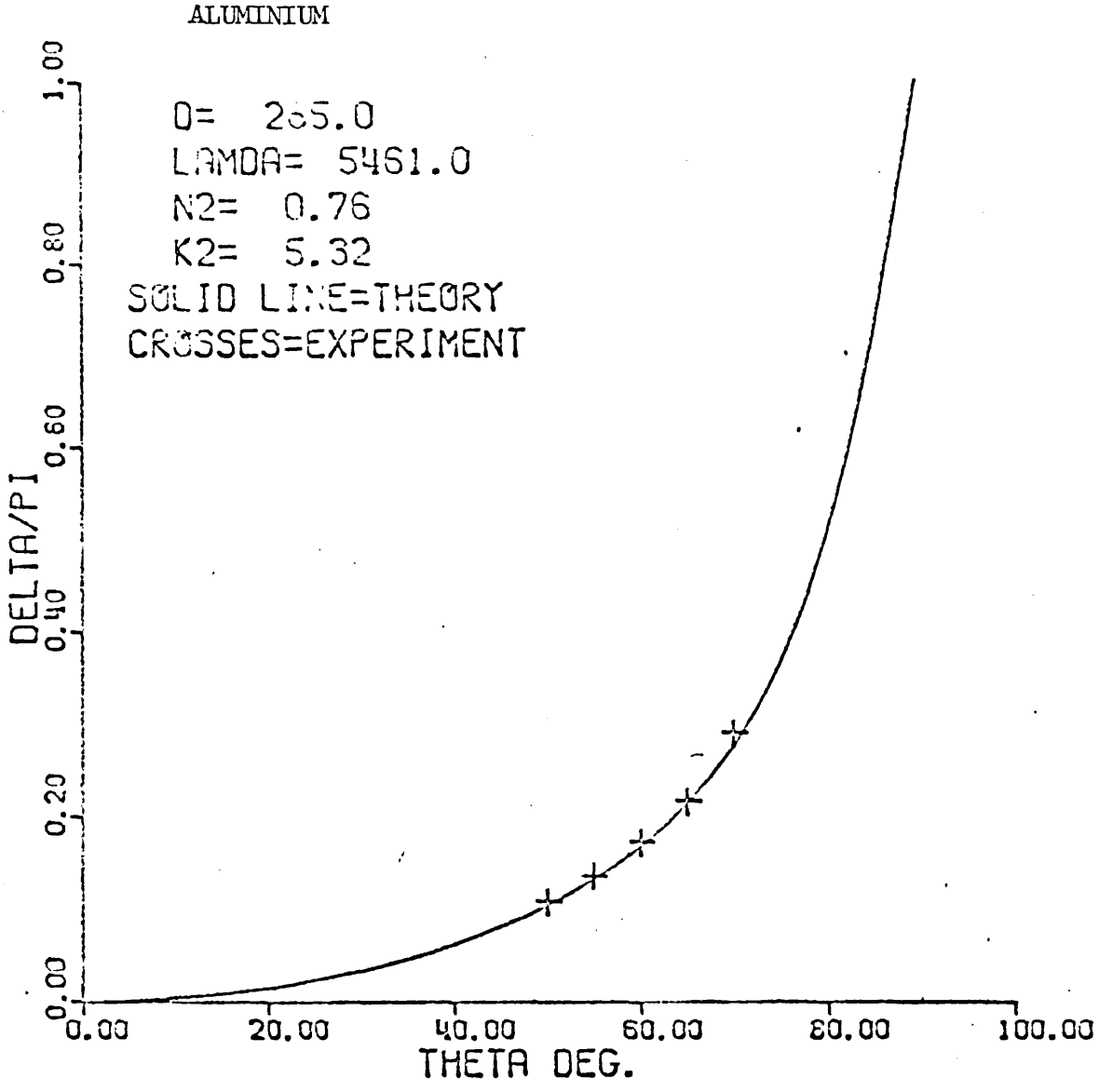
ALUMINIUM
O= 265.0
LAMDA= 5461.0
N2= 0.76
K2= 5.32
SOLID LINE=THEORY
CROSSES=EXPERIMENT
DELTA/PI
0.00
0.20
0.40
0.60
0.80
1.00
0.00
20.00
40.00
60.00
80.00
100.00
THETA DEG.

Fig.V.8

PLATE (22)

$d_{Al} = 265$ Å

$\lambda_1 = 4358$ Å

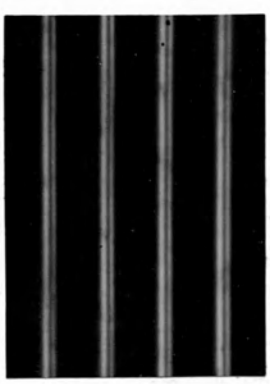

$\theta = 50^\circ$

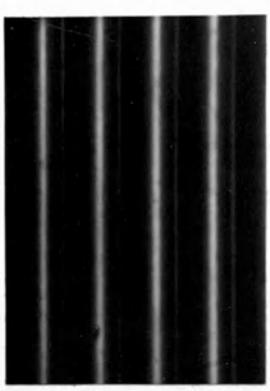

$\theta = 70^\circ$

$\lambda_2 = 5461$ Å

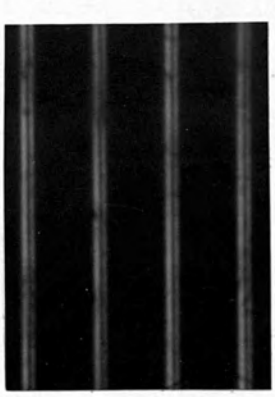

$\theta = 50^\circ$

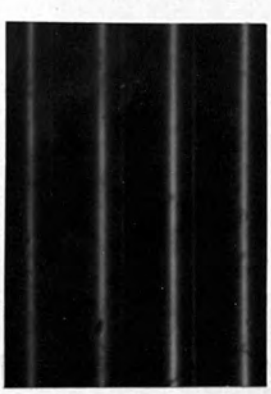

$\theta = 70^\circ$

V.5 EXPERIMENTAL RESULTS ON ALUMINIUM FILMS

Two experiments were performed on the same Aℓ film. The thickness of the film was 265 Å ± 20 Å .

The experimental and computed variations of Δ vs θ at $\lambda_1 = 4358$ Å and $\lambda_2 = 5461$ Å are shown in Figs.V.7 and V.8 respectively. The experimental points come close to the computed curve indicating close agreement with the optical constants used for computation. Plate (22) shows fringe separations at λ_1 and λ_2 for different values of θ the angle of incidence. The variation of Δ vs θ for Aℓ was not previously reported in the literature *.

V.6 DISCUSSION

The results obtained in this chapter represent experimental data in a direct manner, i.e. they give Δ as a function of θ. This seemed natural since the differential change of phase results from the non-normal reflection of light at the air/metal interface. They also confirm the general trend of optical properties of thinner films departing from those of thicker films approximating to the bulk case. The films were evaporated at a rate of 25 Å/second. This alone could account for any differences with previously measured values of Δ for films prepared at different rates. Avery[32], and Clegg[44] measured Δ for films of Ag, Au, Sn and Cu. Clegg's measurements were made in vacuum of the order of 2×10^{-5} mm Hg while Avery's, as in the present work, were made in air within a short time of their removal from the vacuum chamber. Clegg's measurements were made at $\theta = 65^{\circ}$, while Avery's were made at a range of incidence from normal to the highest possible incidence allowed by the interferometric technique.

---

* Private communication with Prof. O.S. Heavens, York University.

No comparable measurements, to the knowledge of the author, are made on Aℓ films, except at fixed angles as part of ellipsometric determination of the Aℓ optical constants. Avery's films ranged from 125 Å-500 Å in thickness and his measurements were made at more than one wavelength in the visible part of the spectrum. Table V.1 gives a comparison of results, obtained on silver films of comparable thickness at $\lambda = 5461$ Å, by Avery, Clegg and in the present work. The table also contains the computed values of Δ at the wavelength mentioned, based on 'bulk values' of n and k obtained by Schulz.

TABLE V.1

Author	Film Thickness	Δ_{exp} at $\theta = 65^\circ$	Δ_{comp} Schulz $\begin{matrix} n \\ k \end{matrix}$
Clegg	~ 400 Å	0.333π	$\hat{n} = 0.05 - i3.32$
Present	~ 600 Å	0.321π	$\lambda = 5461$ Å
Avery	~ 500 Å	0.320π	$\Delta_{65^\circ} = 0.326$

It is clear from the above table that Clegg's experimental value is higher than the values determined by Avery and in the present work. The latter two values agree remarkably well considering improved vacuum conditions used to prepare the films in this work. They are also in agreement with the computed value based on constants determined by Schulz. Clegg[44], explains the difference between his results and those of Avery on the account of the low rate of evaporation, 2 Å/sec, and to the effect of aggregated structure which is usually attached to films prepared at slow rates of evaporation.

It must be mentioned here that graphs giving Δ vs θ presented in this chapter, are directly calculated from the order separation of the doubled fringe patterns as explained in the previous chapter. They show $\Delta = 0^\circ$ for $\theta = 0^\circ$. However, it can be shown from theory given in the Introduction, Chapter I and references (1),(14),(15) and (16), that for

$\theta = 0^{\circ}$, $\Delta = \pi^{\circ}$, that if the values of Δ indicated in the graphs is transformed into regular measurement, then we will have

$$\Delta = (\pi - \Delta_{graph}) .$$

This is important if the values in the graphs are used to substitute in the formulae given in the Introduction. It may be noted, also, that the shift of the dark bands in a Babinet Compensator used in Drude's method for determining Δ, when transformed into an angle is in fact equal to $(\pi - \Delta)$. In this respect the interferometric technique as well as the polarimetric method are not able to differentiate between a differential change of phase (or relative phase shift) of zero or of π° .

CHAPTER VI

THE EXTINCTION COEFFICIENT OF Ag, Au AND Aℓ FILMS IN THE THICKNESS RANGE OF $d \geq 200$ Å IN THE VISIBLE SPECTRUM

VI.1 INTRODUCTION

In the first four chapters of this thesis the quantity $\Delta = (\delta_p - \delta_s)$ was studied both theoretically and experimentally. It has been shown a sensitive quantity to changes in the optical constants in various ranges. However its dependence on k in the lower regions of n and higher ranges of d is more prominent than its dependence on n. We also have shown how Δ could be determined as a function of θ for a certain film using an interferometric technique originally reported by Tolansky[5], The interferometric technique is shown to be simple, inexpensive and possessing reliable accuracy.

In this chapter we take the investigation a step further. We shall make use of the experimental data obtained in Chapter V to extract values of k the extinction coefficient of the films investigated. This is accompanied by obtaining graphs of Δ vs n for constant values of k. The value of k corresponding to a Δ_{exp} at certain θ, d and λ, could be found pretty accurately since interpolation at any point is nearly linear at higher d and θ values. In this way we shall have a complete 'interferometric technique' for the determination of the extinction coefficient of highly reflecting absorbing single layers. This together with interferometric determination of the film thickness seems to open a more comprehensive interferometric approach to the determination of the optical parameters of thin absorbing films. This is what we set out to do in the first place.

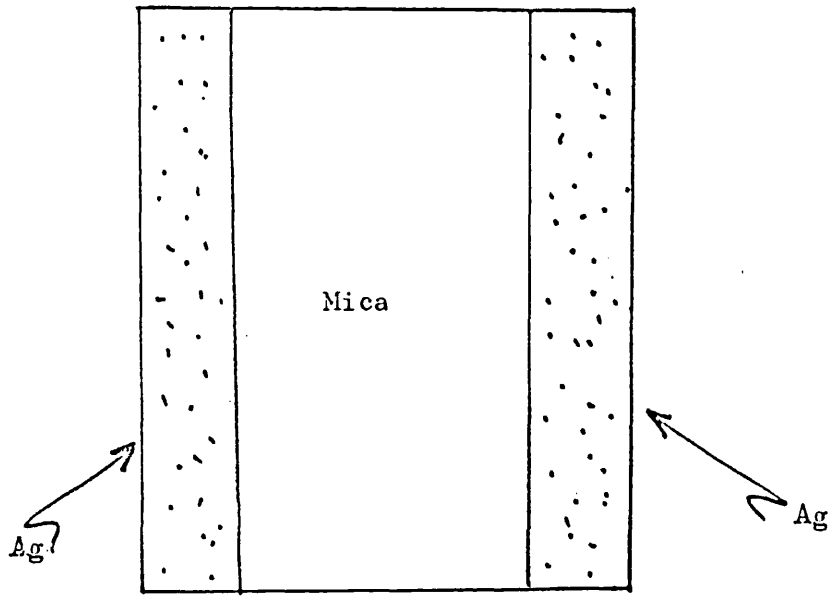

Fig.VI.1

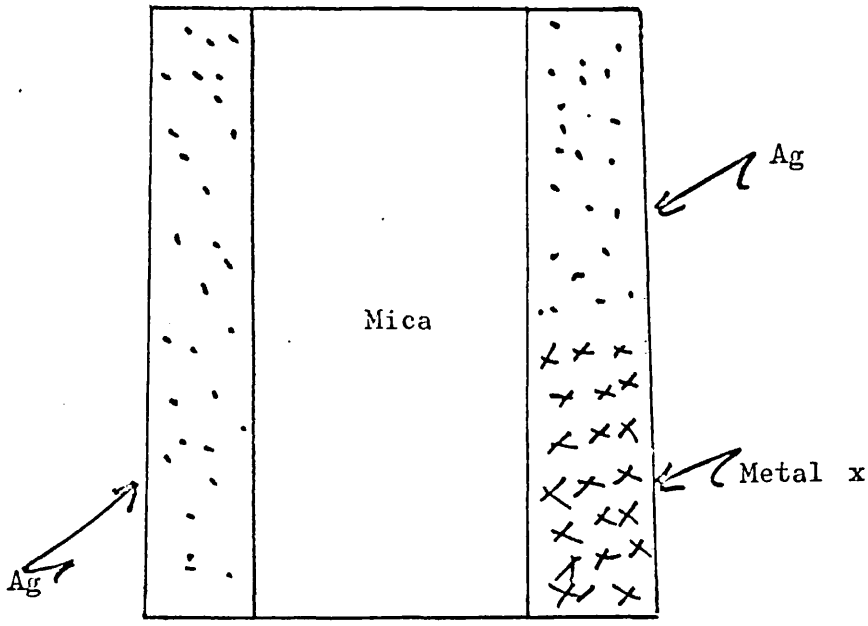

Fig.VI.2

VI.2 PREVIOUS WORK

Interferometry has been applied to study thin films mainly for determining their thickness, using either fizeau or f.e.c.o. fringes and also for the measurement of phase changes in reflection and transmission. However, Schulz[13,20,48,49] tried to extend the usefulness of interferometric techniques to find the optical constants. He used an interferometric assembly shown in Fig.VI.1. This consisted of silver-dielectric-silver transmission filter. The dielectric separating the two metallic layers was a freshly cleaved sheet of mica. He deduced the value of the normal incidence phase change at reflection at the mica-metal interface from the wavelength shift introduced as a result of such phase change taking place. Then he calculated k from the following equation

$$\tan \beta = \frac{2 k n_o}{n^2 + k^2 - n_o^2} \qquad \ldots (VI.1)$$

where n_o is the refractive index of the dielectric separating the two silver layers. In his paper[13] he used a more complicated arrangement, depositing silver on one side of the mica and silver and the x metal on the other side as shown in Fig.VI.2. In such cases there were two adjacent filters Ag-mica-Ag and Ag-mica-metal x, where the first filter was used as a standard or reference. The arrangement required knowledge of

(a) the mica dispersion which had to be measured in a separate experiment;

(b) the thickness of metal layers had to satisfy equation (VI.1) which assumes a single reflection;

(c) the method involved the measurement of wavelength at peak transmissions. This is not usually an easy task if the metallic film thickness is not thick enough to produce a highly reflecting surface and sharp fringes;

(d) the fact that mica is doubly refracting means getting two sets of fringes at each wavelength. This could lead to errors if care is not taken in measurements.

The interferometric arrangement used in this work was described in Chapter III. It is far simpler than that employed by Schulz. It possesses the advantages:

(a) the dielectric medium between the two reflecting surfaces of the interferometer is air, thus avoiding the complications arising from the mica dispersion;

(b) no wavelength measurements are involved;

(c) formulae employed to analyse the results take into consideration the multiple reflections within the film as opposed to using formula (VI.1) which apply only to the bulk case.

A discussion of the values of k yielded by different methods will be given later in this chapter.

VI.3 GRAPHICAL EXTRACTION OF k VALUES OF Ag, Au AND Aℓ FILMS

To extract the k value of the metallic films used as interferometer coatings in the interferometric determination of Δ, a computer program was run to produce a Δ vs n chart for constant values of k, for certain values of λ, d, θ and substrate index. The k values were in 0.1 steps. The experimental value of Δ, determined in the last chapter was then 'enclosed' between two values of k. In the case of films of $d \geq 200$ Å the line of variation of Δ vs n for a certain value of k over a limited range of n was almost a horizontal line parallel to the x-axis, the n-coordinate. A second graph of Δ vs n was constructed in which parallel lines, parallel to the n-axis, were drawn corresponding to the experimental value of Δ, and using data from the sensitivity study in Chapter II, they also were drawn according to the variation in k caused by variation in Δ equivalent to the maximum experimental error in Δ. All graphs were drawn except one, at $\theta = 70^{\circ}$ and for substrate index of 1.5. Figs.VI.3 - VI.17 correspond to the following cases respectively.

Ag	d = 550 Å	λ = 4358 Å	θ = 70°
Ag	d = 600 Å	λ = 5461 Å	θ = 70°
Ag	d = 250 Å	λ = 6438 Å	θ = 70°
Ag	d = 225 Å	λ = 5461 Å	θ = 70°
Au	d = 580 Å	λ = 5461 Å	θ = 60°
Au	d = 580 Å	λ = 6438 Å	θ = 70°
Aℓ	d = 265 Å	λ = 4358 Å	θ = 70°
Aℓ	d = 265 Å	λ = 5461 Å	θ = 70°

The values of k which emerged from these graphs are tabulated in the following table together with Schulz values for comparison.

TABLE VI.1

Metal	d	λ	k	Schulz values of d ≥ 500 Å
Ag	550	4358	2.42 ± 0.020	2.42 ± 0.05
Ag	600	5461	3.45 ± 0.030	3.32 ± 0.07
Ag	250	6438	3.35 ± 0.020	4.20 ± 0.08
Ag	225	5461	3.10 ± 0.020	3.32 ± 0.07
Au	580	5461	2.37 ± 0.020	2.37 ± 0.05
Au	580	6438	3.46 ± 0.040	3.50 ± 0.07
Aℓ	265	4358	4.011 ± 0.025	4.32 ± 0.08
Aℓ	265	5461	5.016 ± 0.025	5.32 ± 0.10

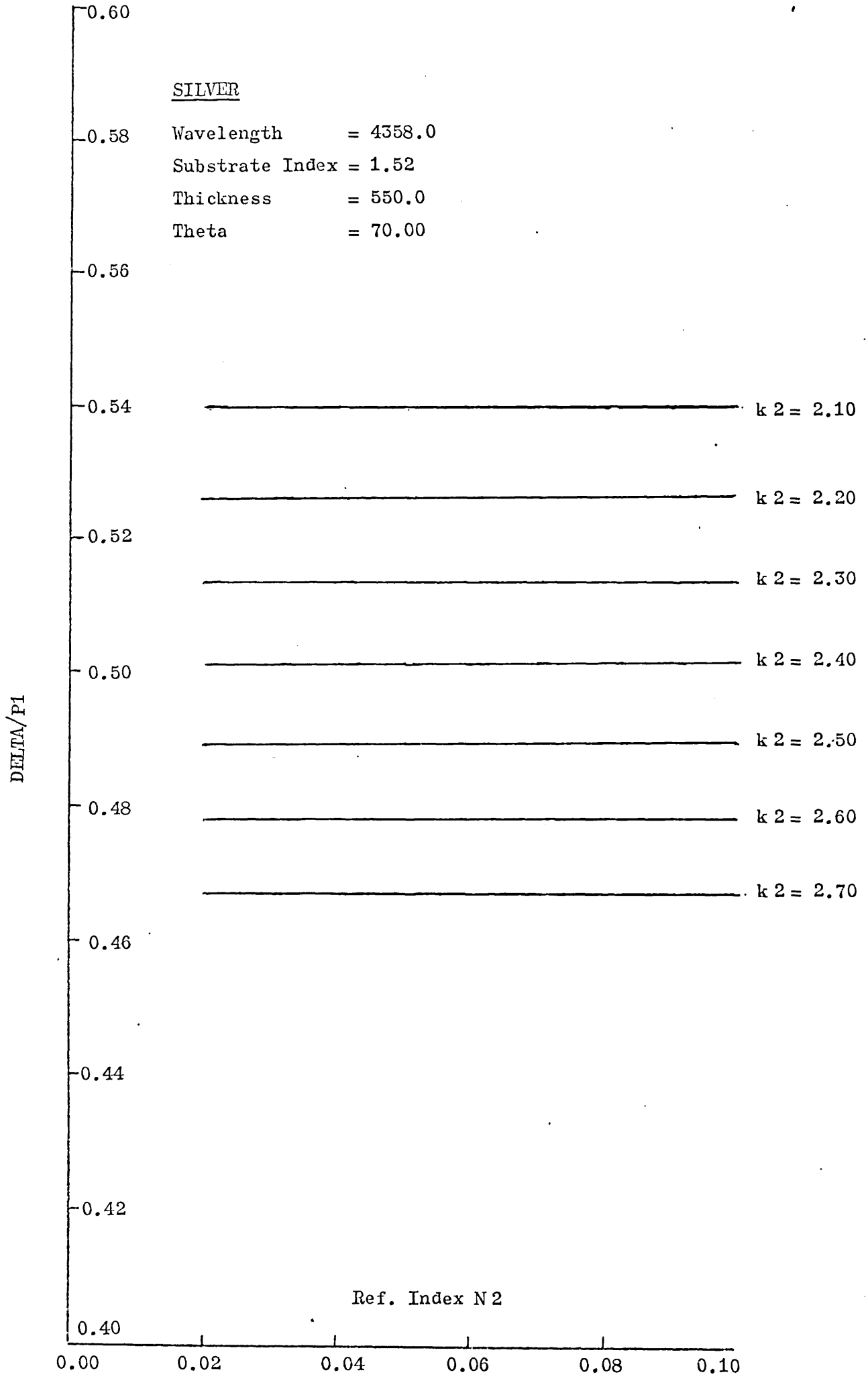
SILVER
Wavelength = 4358.0
Substrate Index = 1.52
Thickness = 550.0
Theta = 70.00
k 2 = 2.10
k 2 = 2.20
k 2 = 2.30
k 2 = 2.40
k 2 = 2.50
k 2 = 2.60
k 2 = 2.70
DELTA/P1
Ref. Index N 2
0.60
0.58
0.56
0.54
0.52
0.50
0.48
0.46
0.44
0.42
0.40
0.00
0.02
0.04
0.06
0.08
0.10

Fig.VI.3

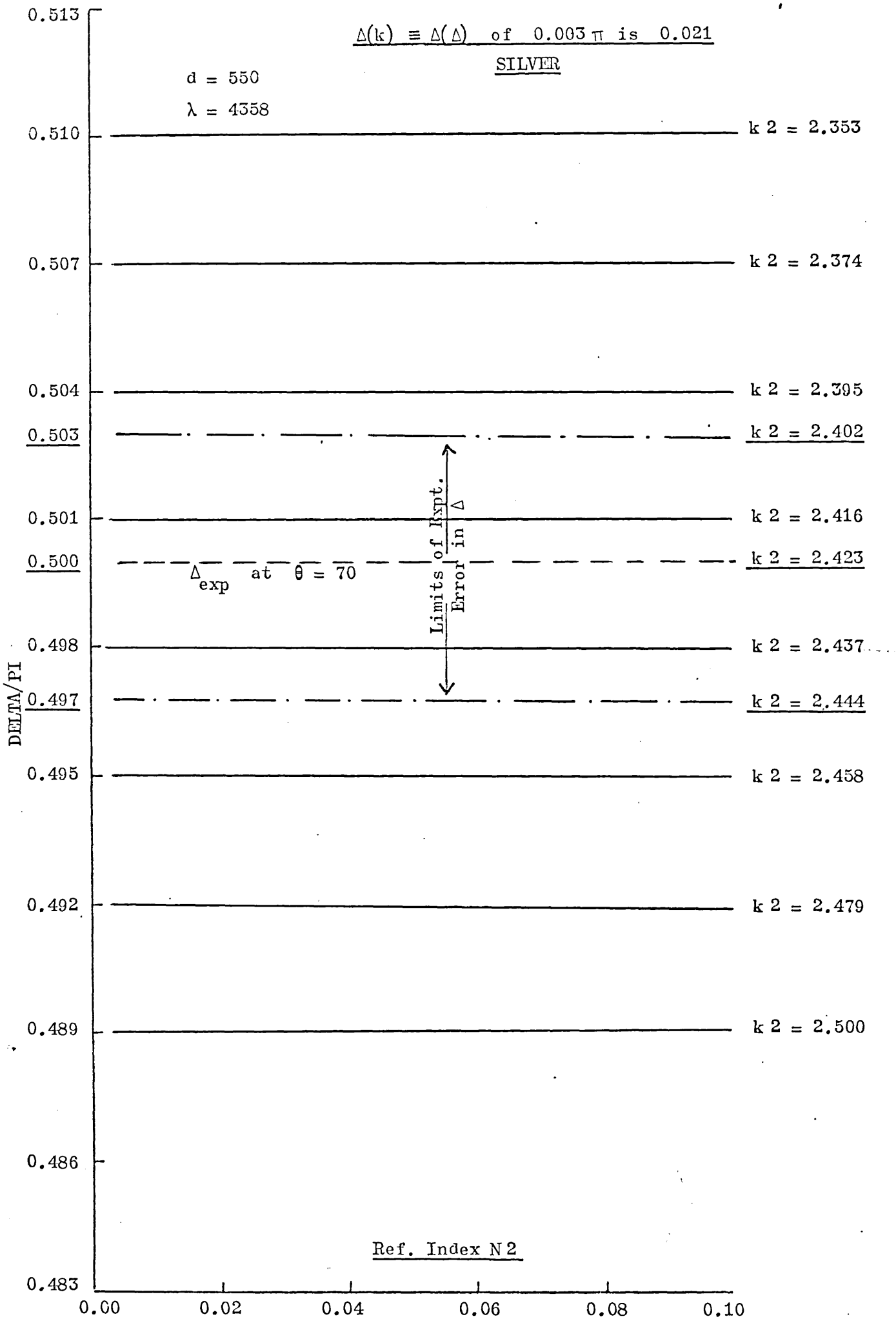
Δ(k) ≡ Δ(Δ) of 0.003 π is 0.021
SILVER
d = 550
λ = 4358
0.513
0.510
0.507
0.504
0.503
0.501
0.500
0.498
0.497
0.495
0.492
0.489
0.486
0.483
k 2 = 2.353
k 2 = 2.374
k 2 = 2.395
k 2 = 2.402
k 2 = 2.416
k 2 = 2.423
k 2 = 2.437
k 2 = 2.444
k 2 = 2.458
k 2 = 2.479
k 2 = 2.500
Limits of Expt. Error in Δ
Δexp at θ = 70
DELTA/PI
Ref. Index N 2
0.00
0.02
0.04
0.06
0.08
0.10

Fig.VI.4

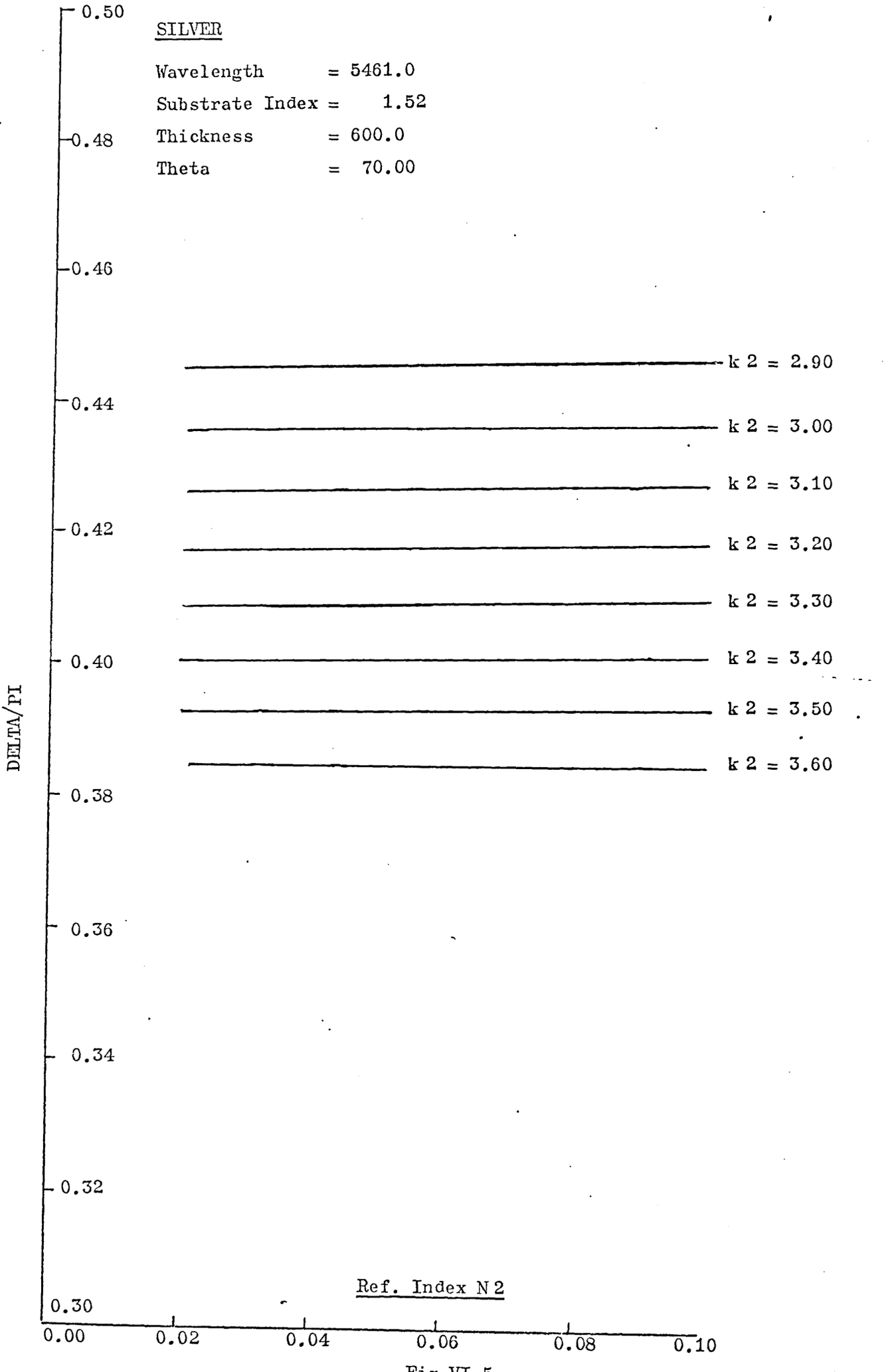
SILVER
Wavelength = 5461.0
Substrate Index = 1.52
Thickness = 600.0
Theta = 70.00
k 2 = 2.90
k 2 = 3.00
k 2 = 3.10
k 2 = 3.20
k 2 = 3.30
k 2 = 3.40
k 2 = 3.50
k 2 = 3.60
DELTA/PI
0.50
0.48
0.46
0.44
0.42
0.40
0.38
0.36
0.34
0.32
0.30
0.00
0.02
0.04
0.06
0.08
0.10
Ref. Index N 2

Fig.VI.5

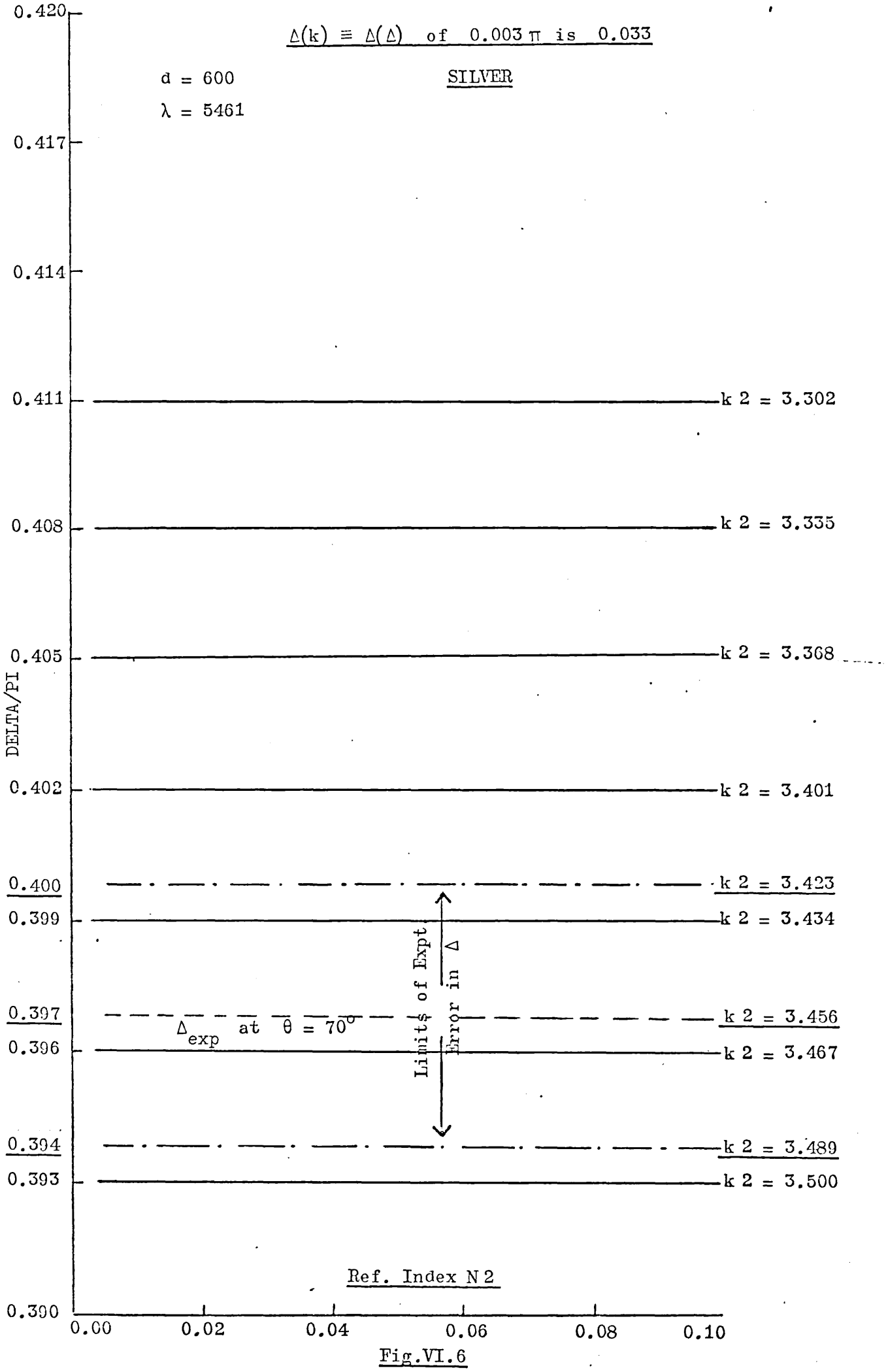
Δ(k) ≡ Δ(Δ) of 0.003 π is 0.033
d = 600
λ = 5461
SILVER
0.420
0.417
0.414
0.411
0.408
0.405
0.402
0.400
0.399
0.397
0.396
0.394
0.393
0.390
DELTA/PI
k 2 = 3.302
k 2 = 3.335
k 2 = 3.368
k 2 = 3.401
k 2 = 3.423
k 2 = 3.434
k 2 = 3.456
k 2 = 3.467
k 2 = 3.489
k 2 = 3.500
Limits of Expt. Error in Δ
Δexp at θ = 70°
Ref. Index N 2
0.00
0.02
0.04
0.06
0.08
0.10

Fig.VI.6

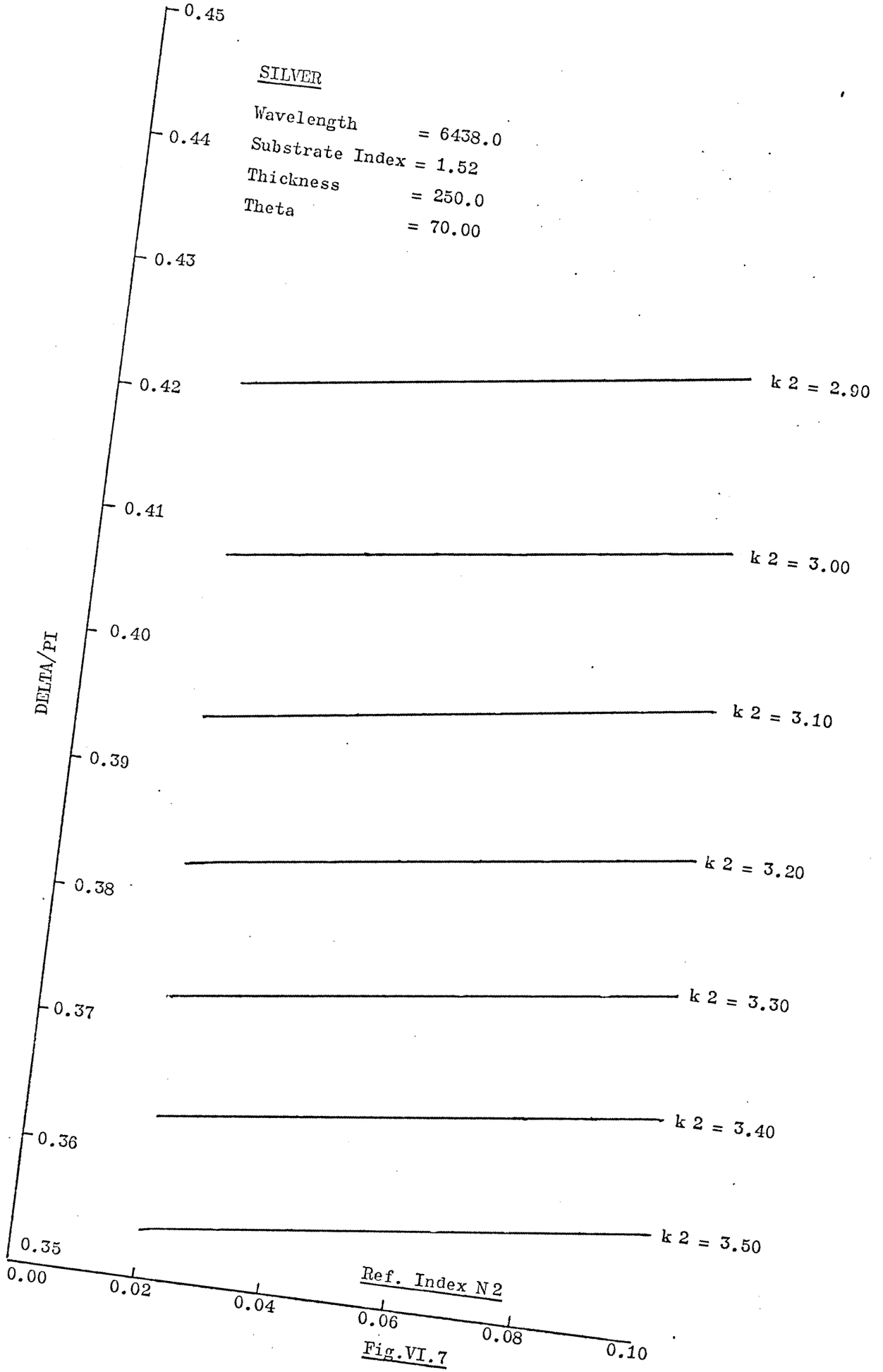
SILVER
Wavelength = 6438.0
Substrate Index = 1.52
Thickness = 250.0
Theta = 70.00
DELTA/PI
0.45
0.44
0.43
0.42
0.41
0.40
0.39
0.38
0.37
0.36
0.35
k 2 = 2.90
k 2 = 3.00
k 2 = 3.10
k 2 = 3.20
k 2 = 3.30
k 2 = 3.40
k 2 = 3.50
0.00
0.02
0.04
0.06
0.08
0.10
Ref. Index N 2

Fig.VI.7

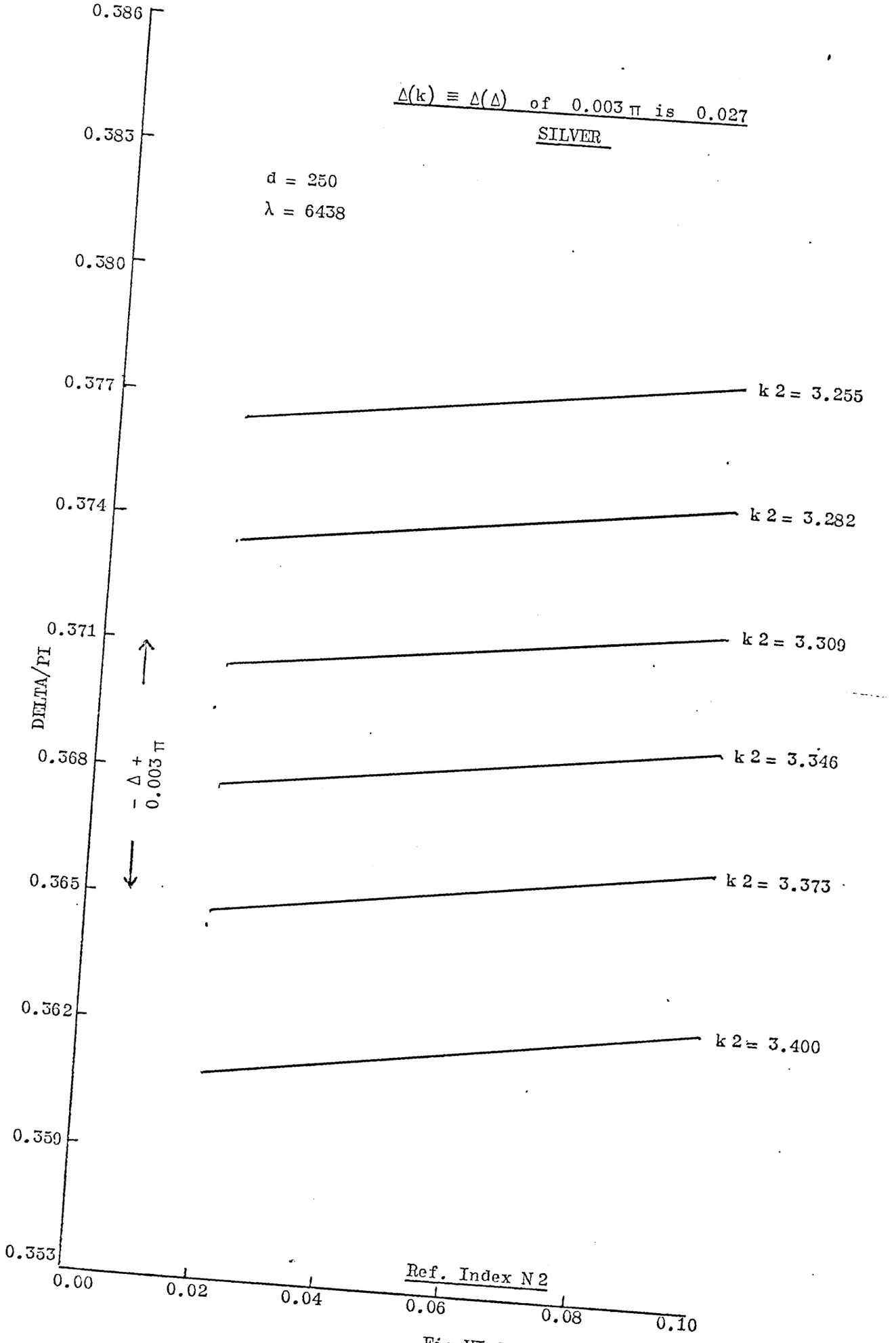
Δ(k) ≡ Δ(Δ) of 0.003 π is 0.027
SILVER
d = 250
λ = 6438
k 2 = 3.255
k 2 = 3.282
k 2 = 3.309
k 2 = 3.346
k 2 = 3.373
k 2 = 3.400
DELTA/PI
- Δ +
0.003 π
Ref. Index N 2
0.386
0.383
0.380
0.377
0.374
0.371
0.368
0.365
0.362
0.359
0.353
0.00
0.02
0.04
0.06
0.08
0.10

Fig.VI.8

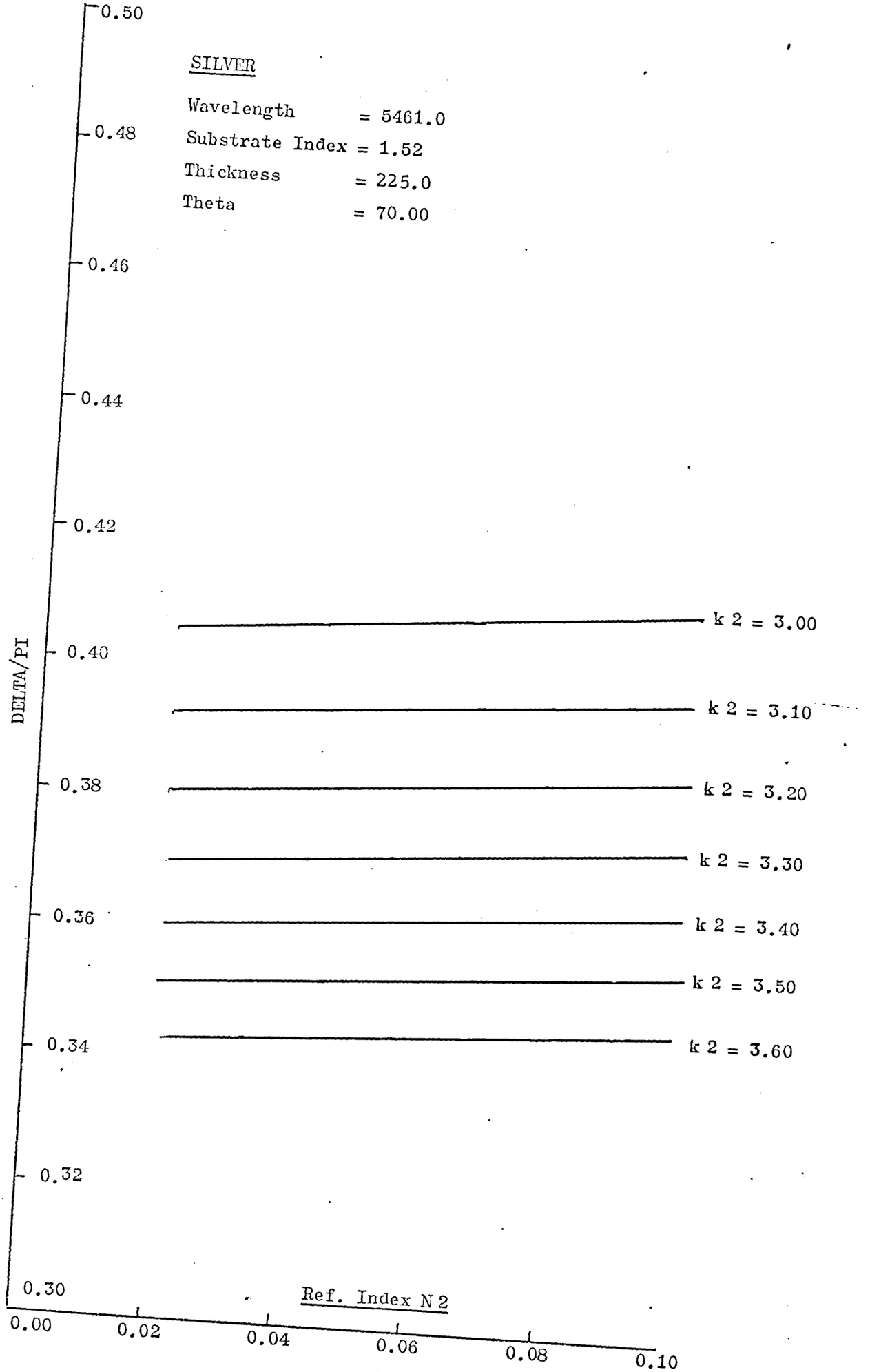
SILVER
Wavelength = 5461.0
Substrate Index = 1.52
Thickness = 225.0
Theta = 70.00
DELTA/PI
0.50
0.48
0.46
0.44
0.42
0.40
0.38
0.36
0.34
0.32
0.30
k 2 = 3.00
k 2 = 3.10
k 2 = 3.20
k 2 = 3.30
k 2 = 3.40
k 2 = 3.50
k 2 = 3.60
Ref. Index N 2
0.00
0.02
0.04
0.06
0.08
0.10

Fig.VI.9

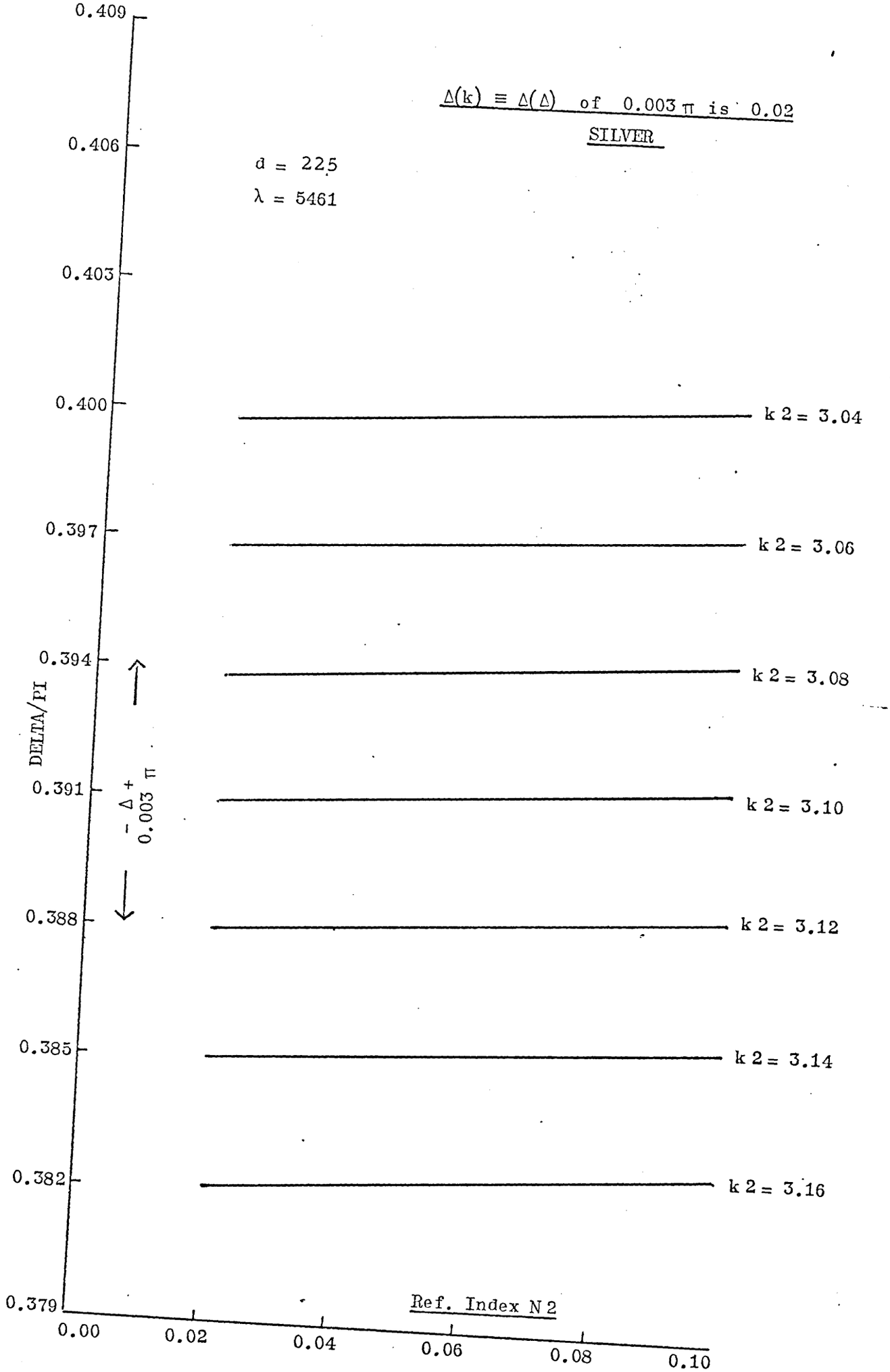
Δ(k) ≡ Δ(Δ) of 0.003 π is 0.02
SILVER
d = 225
λ = 5461
0.409
0.406
0.403
0.400
0.397
0.394
0.391
0.388
0.385
0.382
0.379
DELTA/PI
- Δ +
0.003 π
k 2 = 3.04
k 2 = 3.06
k 2 = 3.08
k 2 = 3.10
k 2 = 3.12
k 2 = 3.14
k 2 = 3.16
Ref. Index N 2
0.00
0.02
0.04
0.06
0.08
0.10

Fig.VI.10

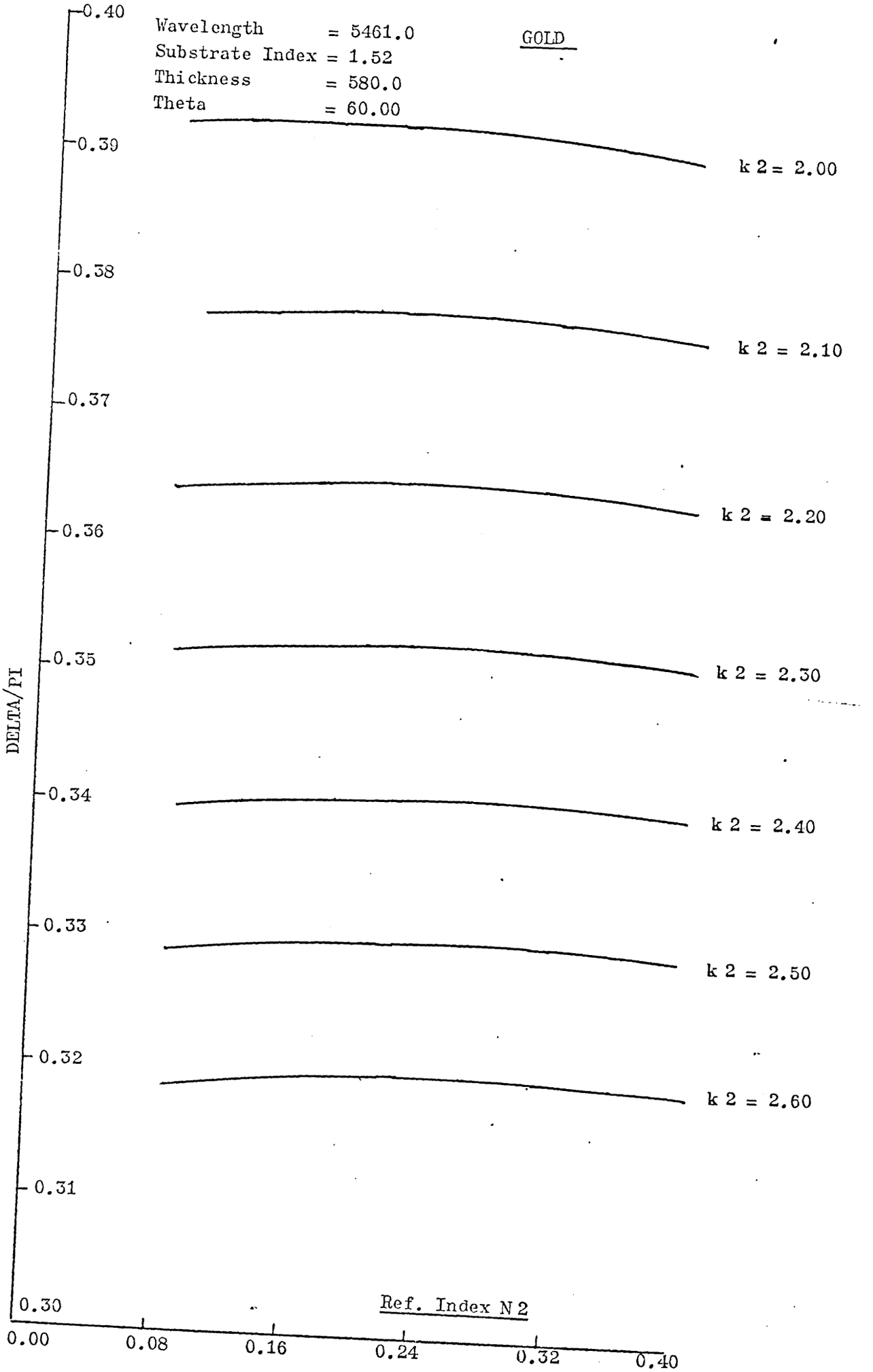
Wavelength = 5461.0
Substrate Index = 1.52
Thickness = 580.0
Theta = 60.00
GOLD
k 2 = 2.00
k 2 = 2.10
k 2 = 2.20
k 2 = 2.30
k 2 = 2.40
k 2 = 2.50
k 2 = 2.60
DELTA/PI
0.40
0.39
0.38
0.37
0.36
0.35
0.34
0.33
0.32
0.31
0.30
Ref. Index N 2
0.00
0.08
0.16
0.24
0.32
0.40

Fig.VI.11

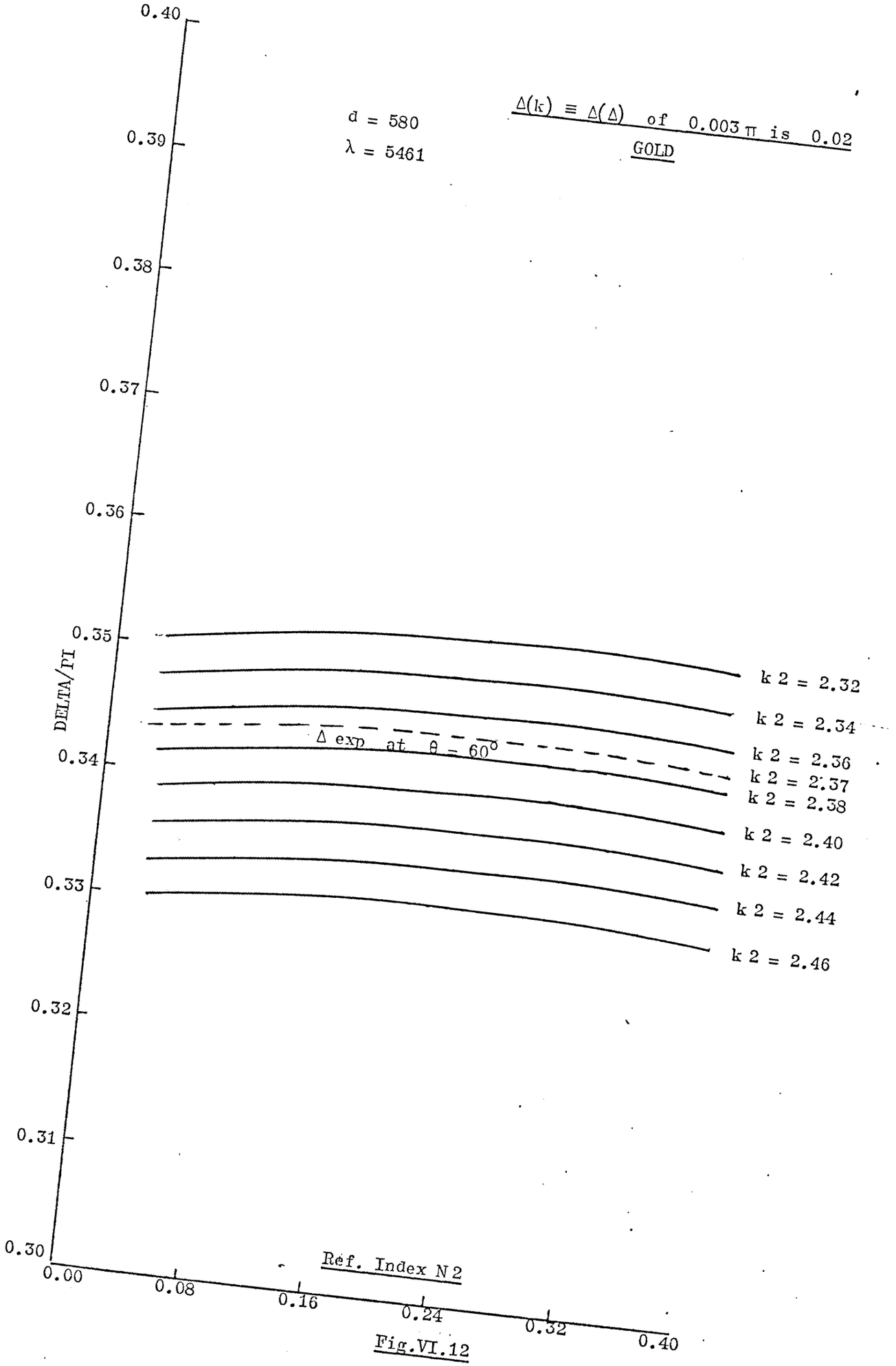
d = 580
λ = 5461
Δ(k) ≡ Δ(Δ) of 0.003 π is 0.02
GOLD
DELTA/PI
0.40
0.39
0.38
0.37
0.36
0.35
0.34
0.33
0.32
0.31
0.30
Δ exp at θ = 60°
k 2 = 2.32
k 2 = 2.34
k 2 = 2.36
k 2 = 2.37
k 2 = 2.38
k 2 = 2.40
k 2 = 2.42
k 2 = 2.44
k 2 = 2.46
Réf. Index N 2
0.00
0.08
0.16
0.24
0.32
0.40

Fig.VI.12

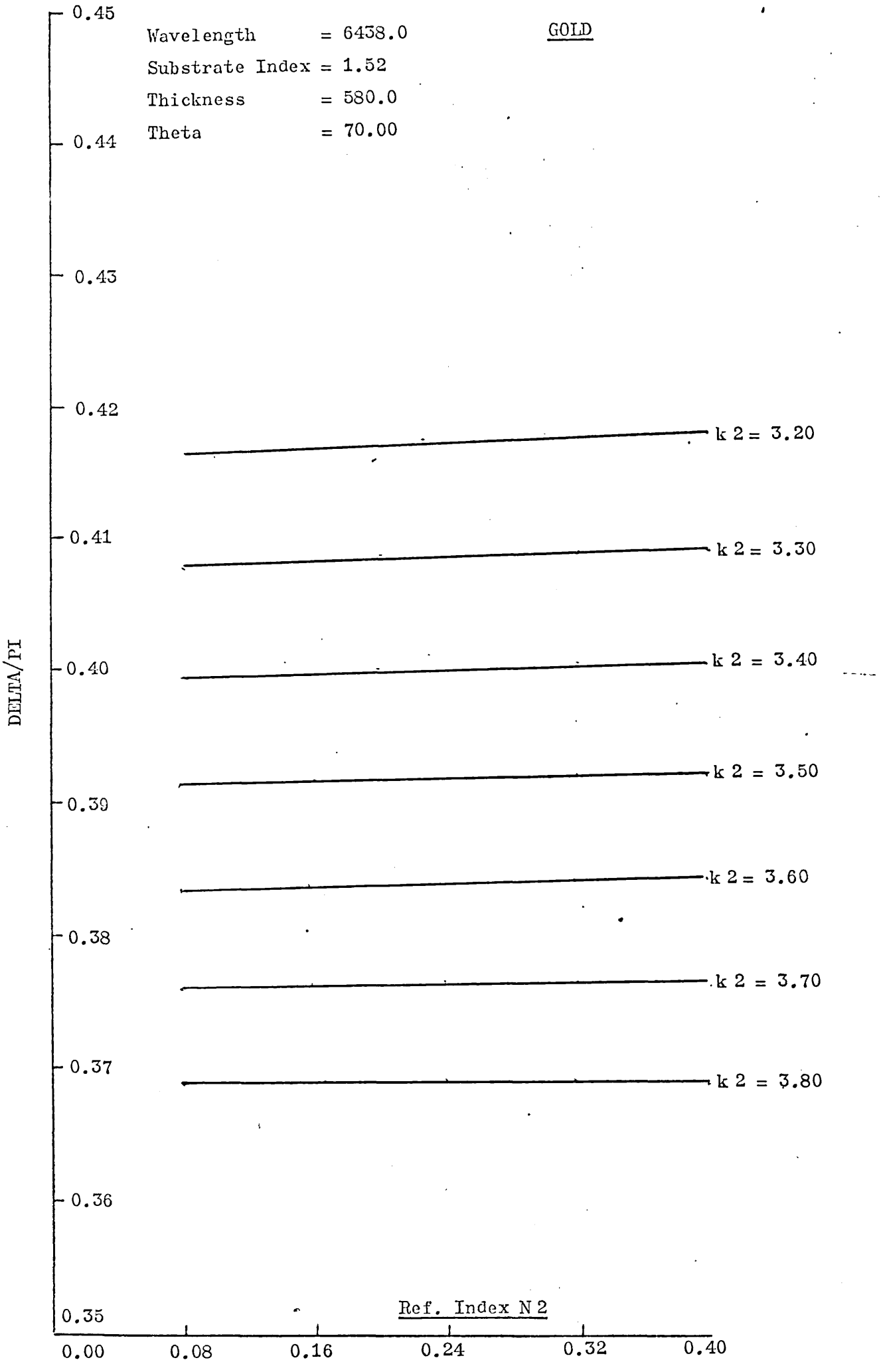
Wavelength = 6438.0
Substrate Index = 1.52
Thickness = 580.0
Theta = 70.00
GOLD
DELTA/PI
0.45
0.44
0.43
0.42
0.41
0.40
0.39
0.38
0.37
0.36
0.35
k 2 = 3.20
k 2 = 3.30
k 2 = 3.40
k 2 = 3.50
k 2 = 3.60
k 2 = 3.70
k 2 = 3.80
Ref. Index N 2
0.00
0.08
0.16
0.24
0.32
0.40

Fig,VI.13

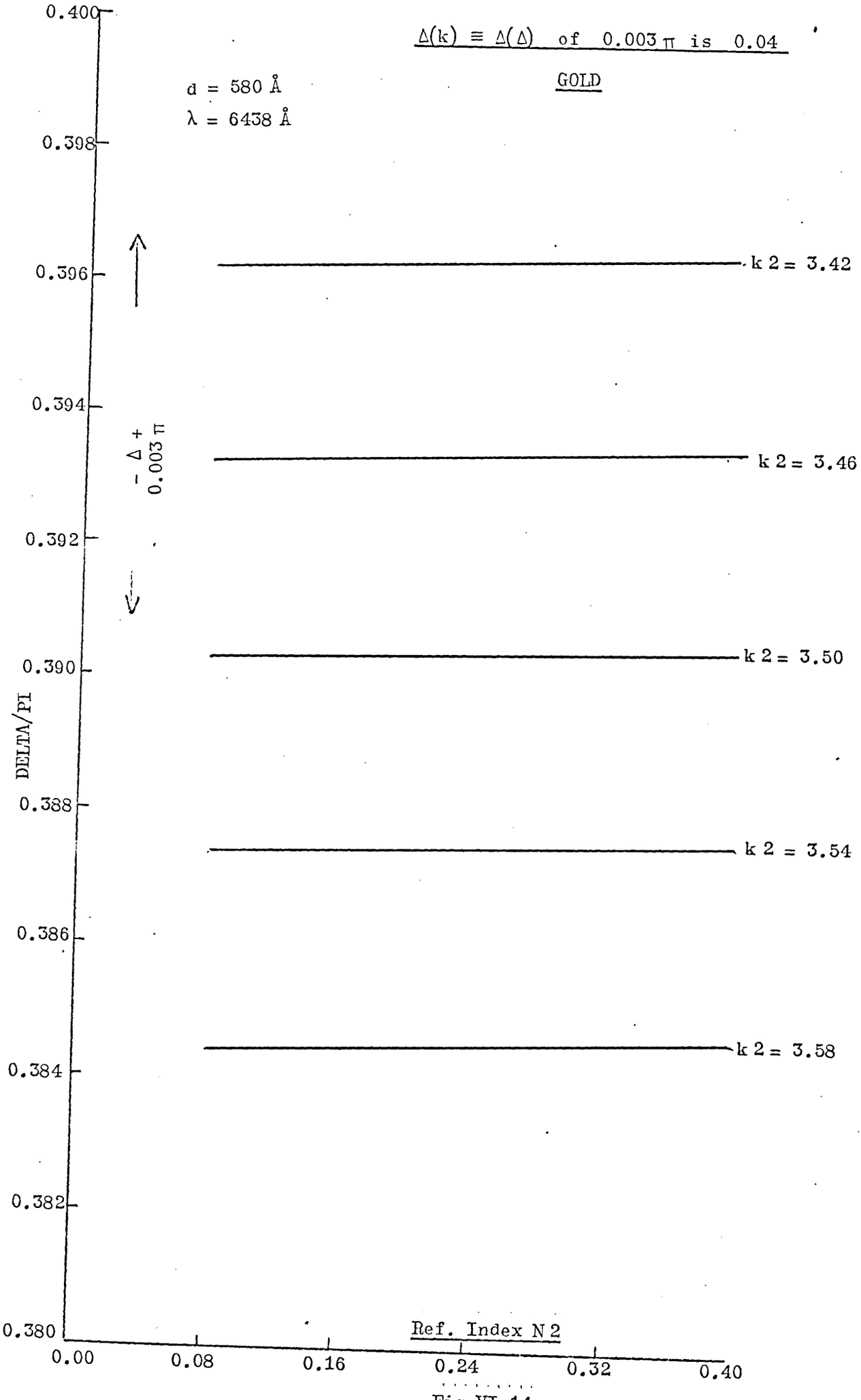
Δ(k) ≡ Δ(Δ) of 0.003 π is 0.04
GOLD
d = 580 Å
λ = 6438 Å
k 2 = 3.42
k 2 = 3.46
k 2 = 3.50
k 2 = 3.54
k 2 = 3.58
- Δ +
0.003 π
DELTA/PI
0.400
0.398
0.396
0.394
0.392
0.390
0.388
0.386
0.384
0.382
0.380
0.00
0.08
0.16
0.24
0.32
0.40
Ref. Index N 2

Fig.VI.14

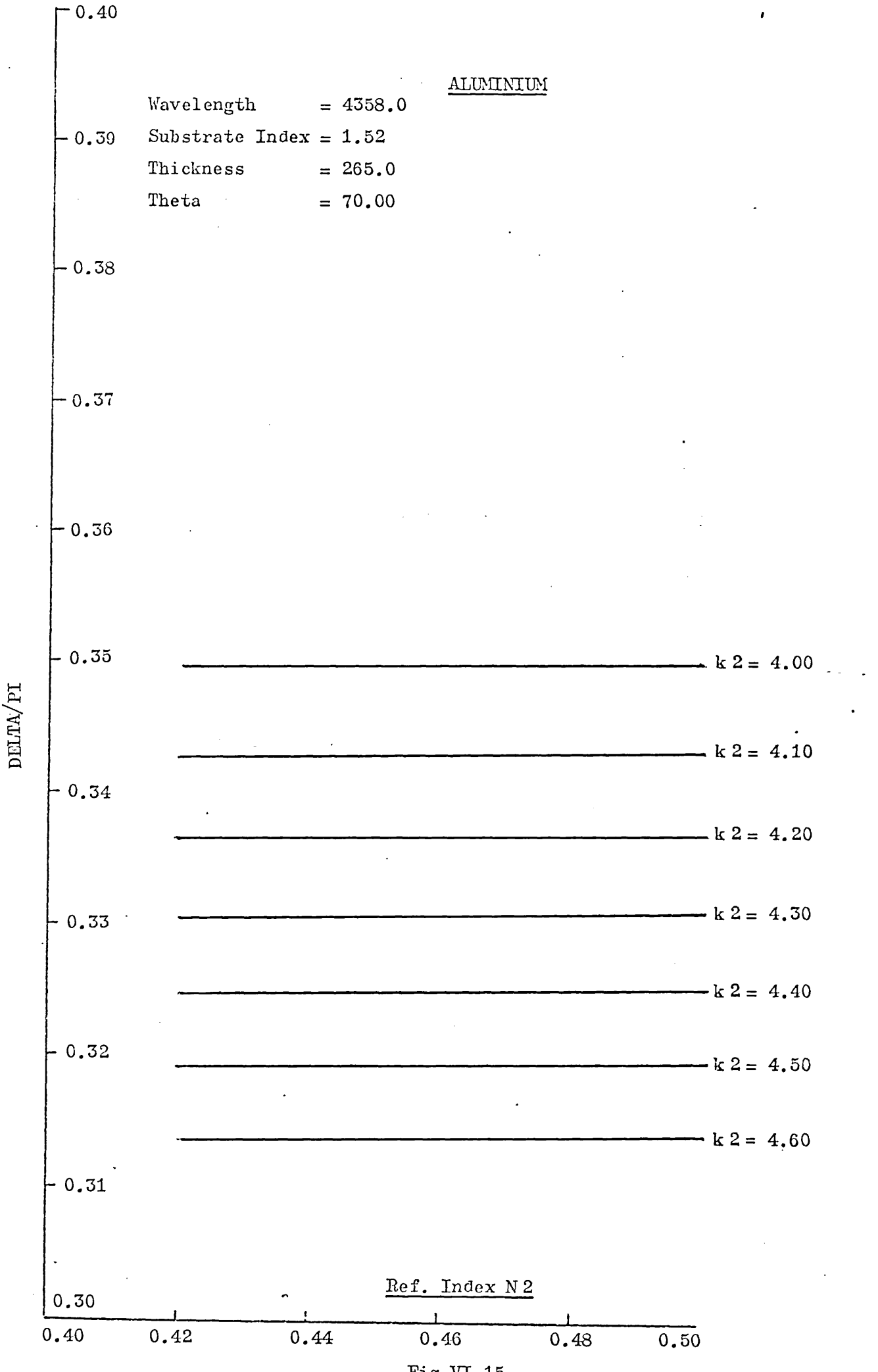
ALUMINIUM
Wavelength = 4358.0
Substrate Index = 1.52
Thickness = 265.0
Theta = 70.00
DELTA/PI
0.40
0.39
0.38
0.37
0.36
0.35
0.34
0.33
0.32
0.31
0.30
k 2 = 4.00
k 2 = 4.10
k 2 = 4.20
k 2 = 4.30
k 2 = 4.40
k 2 = 4.50
k 2 = 4.60
Ref. Index N 2
0.40
0.42
0.44
0.46
0.48
0.50

Fig.VI.15

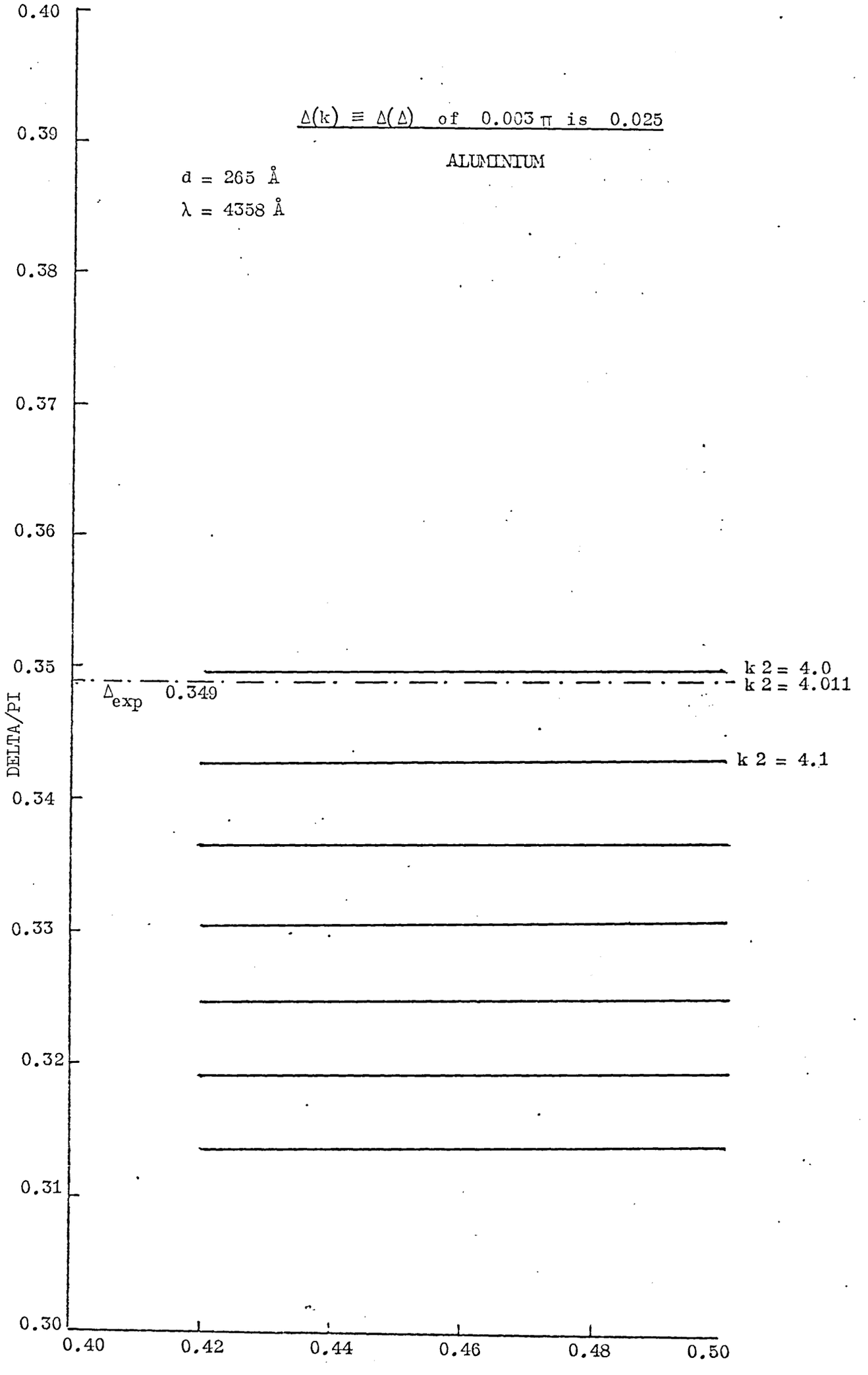
Δ(k) ≡ Δ(Δ) of 0.003 π is 0.025
ALUMINIUM
d = 265 Å
λ = 4358 Å
0.40
0.39
0.38
0.37
0.36
0.35
0.34
0.33
0.32
0.31
0.30
DELTA/PI
Δexp 0.349
k 2 = 4.0
k 2 = 4.011
k 2 = 4.1
0.40
0.42
0.44
0.46
0.48
0.50

Fig.VI.16

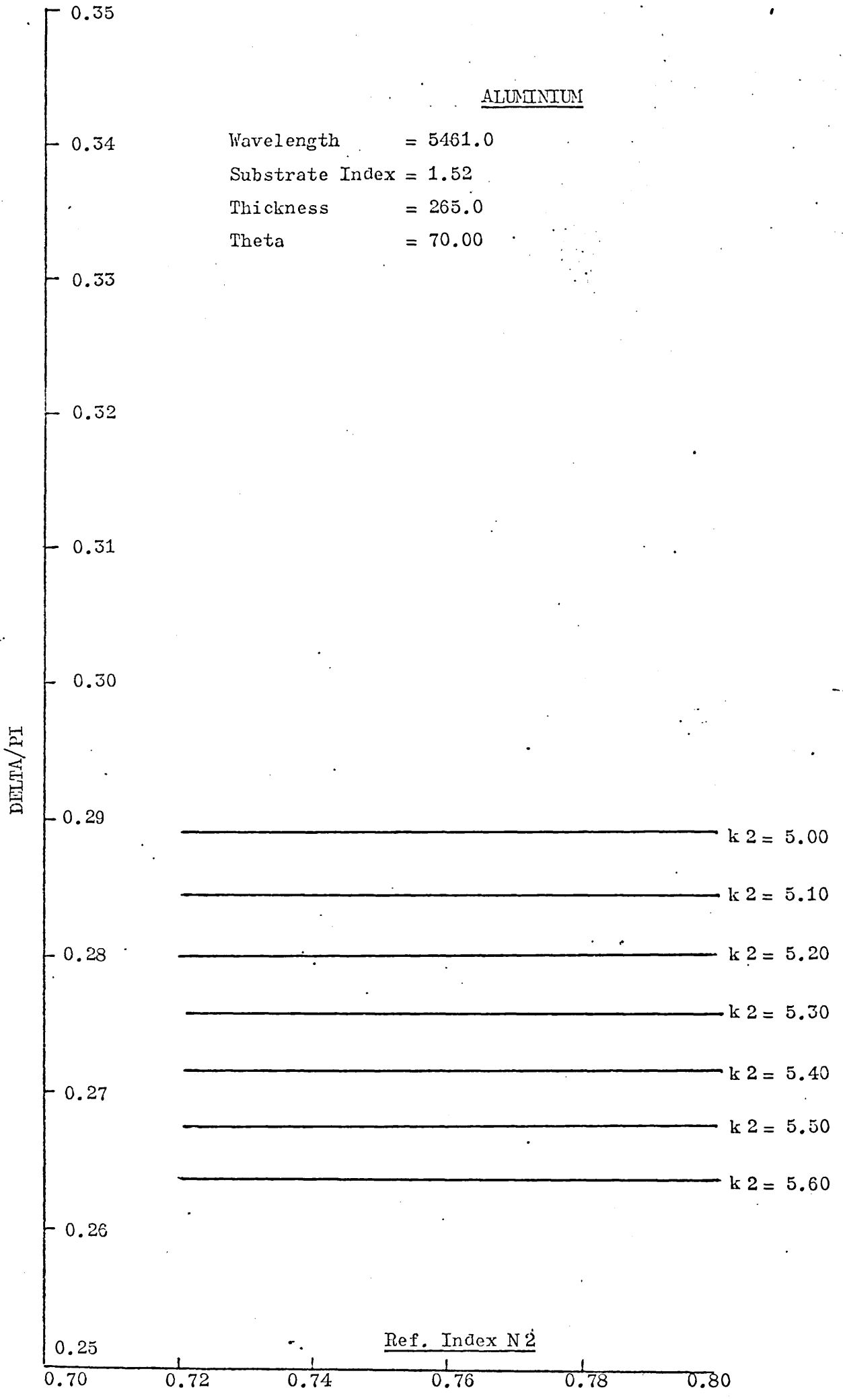
ALUMINIUM
Wavelength = 5461.0
Substrate Index = 1.52
Thickness = 265.0
Theta = 70.00
DELTA/PI
0.35
0.34
0.33
0.32
0.31
0.30
0.29
0.28
0.27
0.26
0.25
k 2 = 5.00
k 2 = 5.10
k 2 = 5.20
k 2 = 5.30
k 2 = 5.40
k 2 = 5.50
k 2 = 5.60
Ref. Index N 2
0.70
0.72
0.74
0.76
0.78
0.80

Fig.VI.17

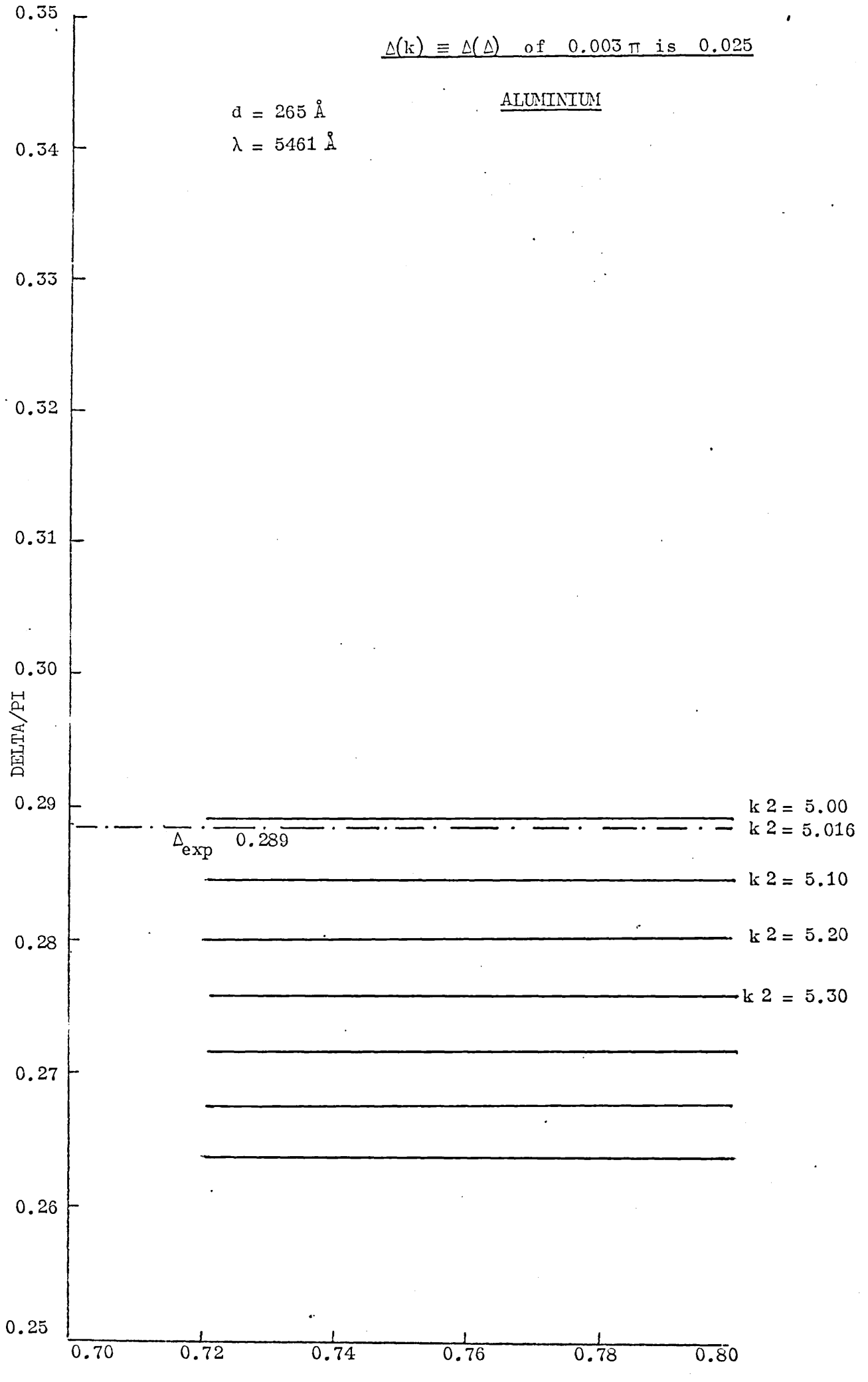
Δ(k) ≡ Δ(Δ) of 0.003 π is 0.025
ALUMINIUM
d = 265 Å
λ = 5461 Å
DELTA/PI
0.35
0.34
0.33
0.32
0.31
0.30
0.29
0.28
0.27
0.26
0.25
0.70
0.72
0.74
0.76
0.78
0.80
k 2 = 5.00
k 2 = 5.016
k 2 = 5.10
k 2 = 5.20
k 2 = 5.30
Δexp 0.289

Fig.VI.18

VI.4 DISCUSSION

The values of the extinction coefficient k for films of Ag, Au and Aℓ were determined by an interferometric technique based on establishing the experimental variation of Δ, the differential phase change at reflection air/metallic film interface as a function of θ the angle of incidence. The k values were, in general, 50% more accurate than those determined by Schulz[20]. This accuracy was achieved by prior theoretical study of the dependence of the quantity Δ on various factors namely, (d/λ) ratio, n and k. Good agreement was obtained in the present work and those previously determined by interferometric techniques. However, for silver films of $d \leq 250$ Å some disagreement is observed. For an Ag film of $d = 250$ Å at $\lambda = 6438$ Å the k value determined here is about 25% less than that reported by Schulz. This is not very surprising since Schulz values were determined for films of $d \geq 500$ Å. The experimental behaviour of Δ vs θ for the Ag film of $d = 250$ Å is shown in Fig.V.3 The experimental crosses are significantly shifted from the computed curve based on Schulz constants.

In this and the last five chapters it was shown that interferometry is capable of serving as a useful and accurate means for the determination of the extinction coefficient of thin highly reflecting films. The simplicity of the interferometric technique and the charted computed properties of Δ made this possible.

CHAPTER VII

THE FORMATION AND CHARACTERISTICS OF WHITE LIGHT MULTIPLE-BEAM INTERFERENCE FRINGES

VII.1 INTRODUCTION

In this and the next chapter a new technique, based on the formation of white light multiple-beam fringes, for the study of surface microtopographies is discussed. However, in this chapter the formation and characteristics of white light multiple-beam fringes are dealt with. This is necessary as an introduction to the next chapter where the application of the white light fringes is described.

White light fringes are, perhaps, the most commonly observed in nature. They form in thinly spread water pools and in oil films, they also occur in soap bubbles. Newton rings, formed between a lens and a plate, are very familiar to all who work in optics. In them one observes the famous dark spot in the centre and one or two coloured orders beyond which overlapping takes place. The darkness of the fringe in the centre, was concluded by Young to be due to a phase change of π when light is reflected from a rare medium at the boundary of a dense medium, i.e. an apparent alteration in the path of $\lambda/2$. This was confirmed by Fresnel's three mirrors experiment in 1819. However, the visibility of Newton rings is low since it is, effectively, a two beam interference set-up using glass surfaces of low reflectivity.

Tolansky, in the forties, developed the multiple-beam interference techniques and applied them to a wide range of surface studies[34,35,39]. He produced multiple-beam monochromatic Newton rings in transmission and applied them to the measurement of the differential change of phase on reflection air/metallic film interface. In 1972 he reported[58] the formation of multiple-beam white light fringes on mica surfaces. They were, in effect, the multiple-beam version of Newton's rings. The beautiful patterns had a much enhanced visibility and their colour dispersion was greatly increased due to the higher reflectivities of the surfaces involved.

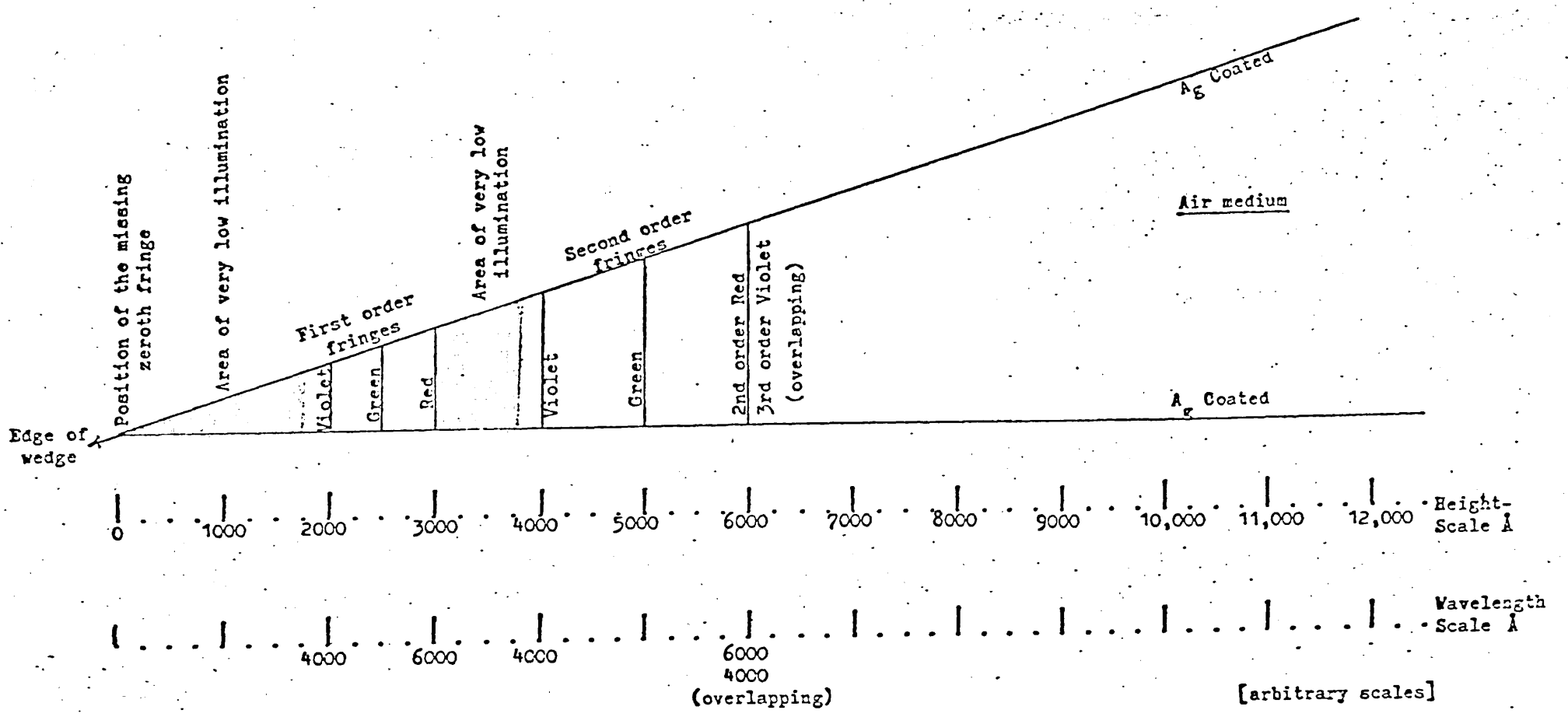
Edge of wedge
Position of the missing zeroth fringe
Area of very low illumination
First order fringes
Violet
Green
Red
Area of very low illumination
Second order fringes
Violet
Green
2nd order Red
3rd order Violet (overlapping)
Ag Coated
Air medium
Ag Coated
0
1000
2000
3000
4000
5000
6000
7000
8000
9000
10,000
11,000
12,000
Height-Scale Å
Wavelength Scale Å
4000
6000
4000
6000
4000
(overlapping)
[arbitrary scales]

Fig.VII.1

In the following, the technique involved in producing white light multiple-beam fringes in transmission is described, and their properties are investigated.

VII.2 THE FORMATION OF WHITE LIGHT MULTIPLE-BEAM INTERFERENCE FRINGES

It is important to realize that, unlike in the case of monochromatic multiple-beam fringes, white light multiple-beam fringes require very small path differences. This means in practice, that the surfaces involved will have to achieve a great degree of closeness. Newton's rings is a case in point, where the lens-plate combination achieves physical contact, or very nearly so, at centre point. In a wedge interferometer the point of contact would constitute the edge of the wedge. The condition for achieving physical contact at the edge of the wedge is important since it, as will be detailed later, defines where the first, second... etc. orders appear.

To enhance the visibility and colour dispersion the surfaces involved will have to be coated with highly reflecting contouring silver film. This introduces a new element, namely the effect of the phase change upon reflection, air/Ag , which is a function of both the wavelength and film thickness.

Figure VII.1 represents an air wedge of angle ϵ where, it is assumed, physical contact takes place at the edge of the wedge. The surfaces are assumed to be coated with an identical highly reflecting silver film of thickness d and R and T are its reflectivity and transmissivity respectively. According to Fig.VII.1, the appearance of fringes resulting from the interference of the transmitted multiply reflected beams. within the interferometer at normal incidence of parallel white light, will be governed by the following simple relation:

$$N\lambda = 2t \qquad \ldots (VII.1)$$

where N is the order number and t is the thickness of the interferometer at a particular point. However, the above relation, and Fig.VII.1 do not take into account the additional path difference introduced by the phase change on reflection air/Ag. To do so relation (VII.1) will be re-written as follows:

$$N\lambda = 2(t + \beta) \; . \qquad \ldots \text{(VII.2)}$$

This means that coloured transmitted fringes of maximum intensities will be expected to appear at contours satisfying the relation (VII.2) in the form:

$$N \cdot \lambda/2 = (t + \beta) \qquad \ldots \text{(VII.3)}$$

where $(\beta)_{d,\lambda}$ is the additional path difference due to the phase change on reflection air/Ag .

The intensity distribution in a transmitted multiple-beam fringe is governed by the Airy formula, i.e. the relation between the transmitted intensity and the phase difference between any two successive interfering beams contributing to a particular point in the fringe pattern. This latter quantity is $\delta = \frac{2\pi}{\lambda}$. (Path difference between any two successive beams) and we can write

$$\delta = \frac{2\pi}{\lambda} \cdot \left[2(t + \beta)\right] \qquad \ldots \text{(VII.4)}$$

This is for normal incidence and an air coated interferometer. The Airy formula would then be written as follows

$$I = \frac{T^2}{(1-R)^2} \cdot \frac{1}{1 + \frac{4R}{(1-R)^2} \cdot \sin^2 \delta/2} \cdot I_o \; , \qquad \ldots \text{(VII.5)}$$

when t is set to equal zero, i.e. there is physical contact, but not optical, the above relation will be written as follows:

$$I = \frac{T^2}{(1-R)^2} \cdot \frac{1}{1 + \frac{4R}{(1-R)^2} \cdot \sin^2\left[\frac{2\pi}{\lambda} \cdot \beta\right]} \cdot I_o \qquad \ldots \text{(VII.6)}$$

Now, examination of this last formula (VII.6) would show that, for each wavelength, there will be a small amount of light transmitted at the

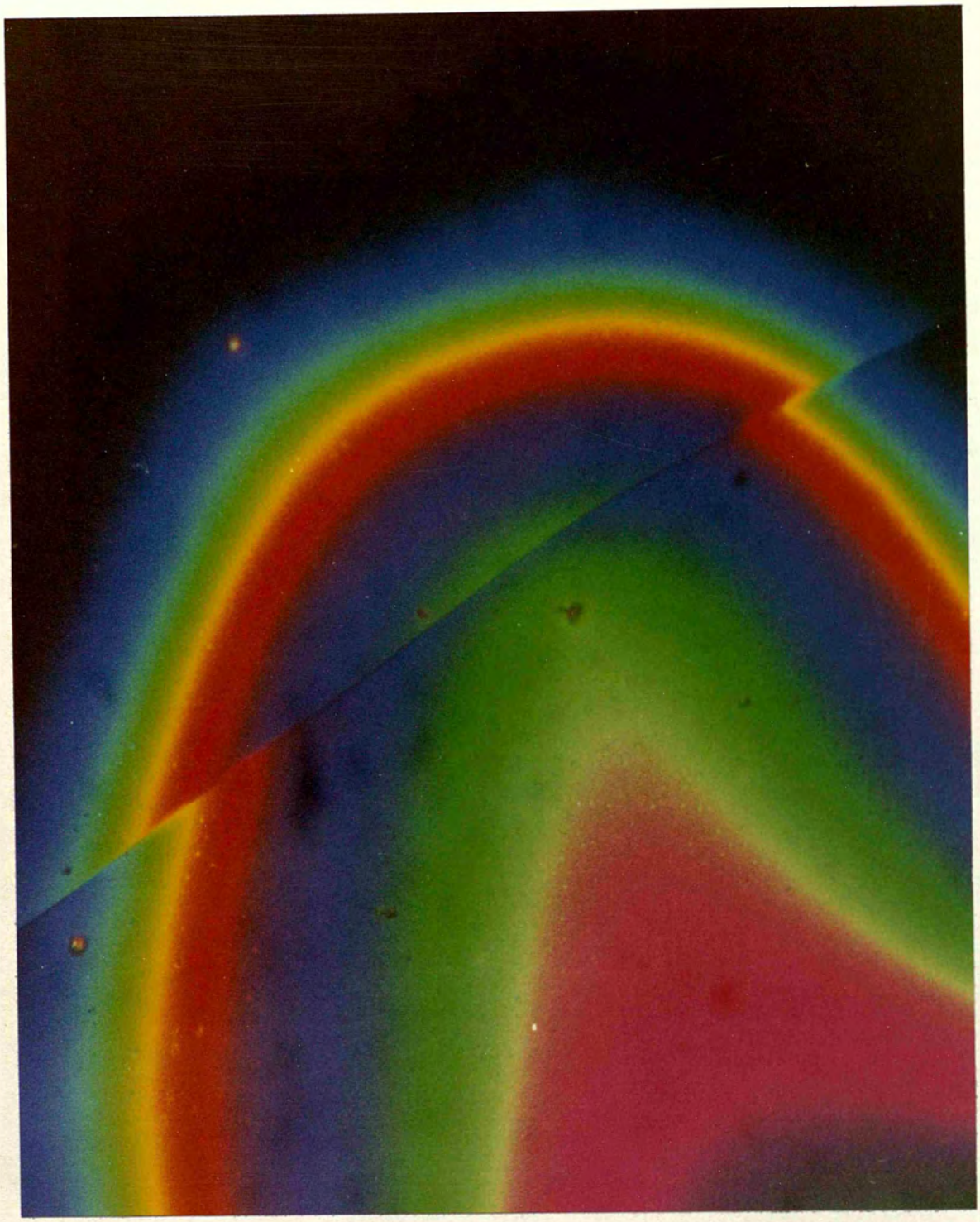

PLATE (23)

zero-order or contact point. The intensity transmitted will depend on the magnitude of T and R and on the value of $\left(\frac{\beta}{\lambda}\right) \cdot 2\pi$. A quick evaluation would show that for $\lambda = 5000$ Å the transmitted intensity is near to the minimum intensity of the corresponding monochromatic fringe pattern. The amount of light transmitted increases with decreasing wavelength. This is because the term (β/λ) decreases with increasing wavelength. This seems to be the explanation to the blue colouration which appeared in Tolansky's pattern[58]. The photographic emulsion is more sensitive in the blue where the system transmits most.

Now, the first visible fringe will appear in a region removed from the edge of the wedge. This would result in a band of no visible illumination separating the zeroth fringe from the visible fringes of the first order. In the second order overlapping would take place, and as a result the second order band of no visible illumination is much less in width compared with its correspondant in the first order. The colours of the third order suffer severe overlapping. The increased path differences involved in the higher orders prevents them being observed. However, these higher orders are observed if monochromatic light replaces the incident white light. Plate (23) shows white light multiple-beam fringes obtained in an interferometer where one component is a freshly cleaved mica surface, silver coated, the other is a microscope slide coated with an identical silver film. The features described above are clearly distinguished in the plate.

VII.3 THE TECHNIQUES FOR PRODUCING WHITE LIGHT MULTIPL-BEAM FRINGES ON MICA SURFACES

As pointed out earlier, the path differences involved in the formation of white light multiple-beam fringes are very small. Hence any arrangement which may be used to house the two components of the interferometer will have to facilitate bringing the surfaces as close as possible. The other problem, encountered when dealing with a mica surface, is the marked wrinkling with ups and downs often many light waves in height and depth.

A technique to solve these problems was described by Tolansky[58] and was used in this work. The freshly cleaved sheet was placed in the chamber of the evaporation plant, together with a microscope cover slip. They were both coated, simultaneously, with a highly reflecting silver film of thickness $d \simeq 350$ Å. This corresponds to a reflection coefficient of $R \simeq 0.80$ for the green line of mercury where $\lambda = 5461$ Å. After they were removed from the chamber, a small drop of Canada balsam was placed on the rear (unsilvered) face of the mica sheet. Against this a clean glass microscope cover slip was placed. The other component of the interferometer was placed with this assembly where the two silvered surfaces were brought together and pressed down hard. The two components were clipped together. In this manner many areas of very close approach were realized, and the Canada balsam when spread to a thin film, the forces of surface tension helped to flatten the wrinkling in the mica sheet.

The optical system used to observe and record the white light multiple-beam fringes was similar to that described in Fig.III.1 of chapter III. The fringes were recorded on a 35 mm colour negative Fuji film of 100 ASA. Exposures were determined by trial and error.

It must be said here that the commercially available services to process colour material leave quite a lot to be desired! There seems to be no realization that some of us do not use cameras for the just the occasional snap shot!

CHAPTER VIII

A NEW INTERFEROMETRIC TECHNIQUE FOR THE STUDY OF SURFACE MICROTOPOGRAPHY

VIII.1 INTRODUCTION

In the last chapter the formation and characteristics of multiple-beam white light fringes were described. The most important characteristics are (a) the knowledge of the order number, and (b) the heightened topographical dispersion. The latter property is a consequence of the fact that the topographical height of the isolated spectrum in the first order is ~ 1500 Å. In monochromatic Fizeau fringes the order separation $\lambda/2$ is 2730 Å for the green line of mercury.

However, little, if any, quantitative information about the surface microtopography could be derived from the attractive white light fringes described in the last chapter. Tolansky[58] contended that a "... normally colour sensitive eye should be able to divide the spectral colour range in the visible into a hundred parts". This, in fact, is to suggest the 'scaling' of the first order spectrum. Herriot, 1961 [59], produced a system of multichromatic multiple beam Fizeau filling the orders. His low-order fringes belonged to 10 wavelengths to the order.

In this chapter a new optical system is described in which a 'sweeping' fringe of variable chromaticity 'moves' into alignment with a 'stationary' fringe of a fixed wavelength at a feature in the surface under study. This dynamic arrangement helps surveying the order span and does away with the need to measure step heights in form of fringe displacements. Only wavelengths are measured using a spectrometer drum. This is far more accurate and direct method than the usual employment of a travelling comparator to measure fringe displacements on photographic plates.

In the following experimental details of the optical system and some measurements on mica surfaces will be given. Also an assessment of the errors involved in the technique and their likely effect on the accuracy of measurements are discussed.

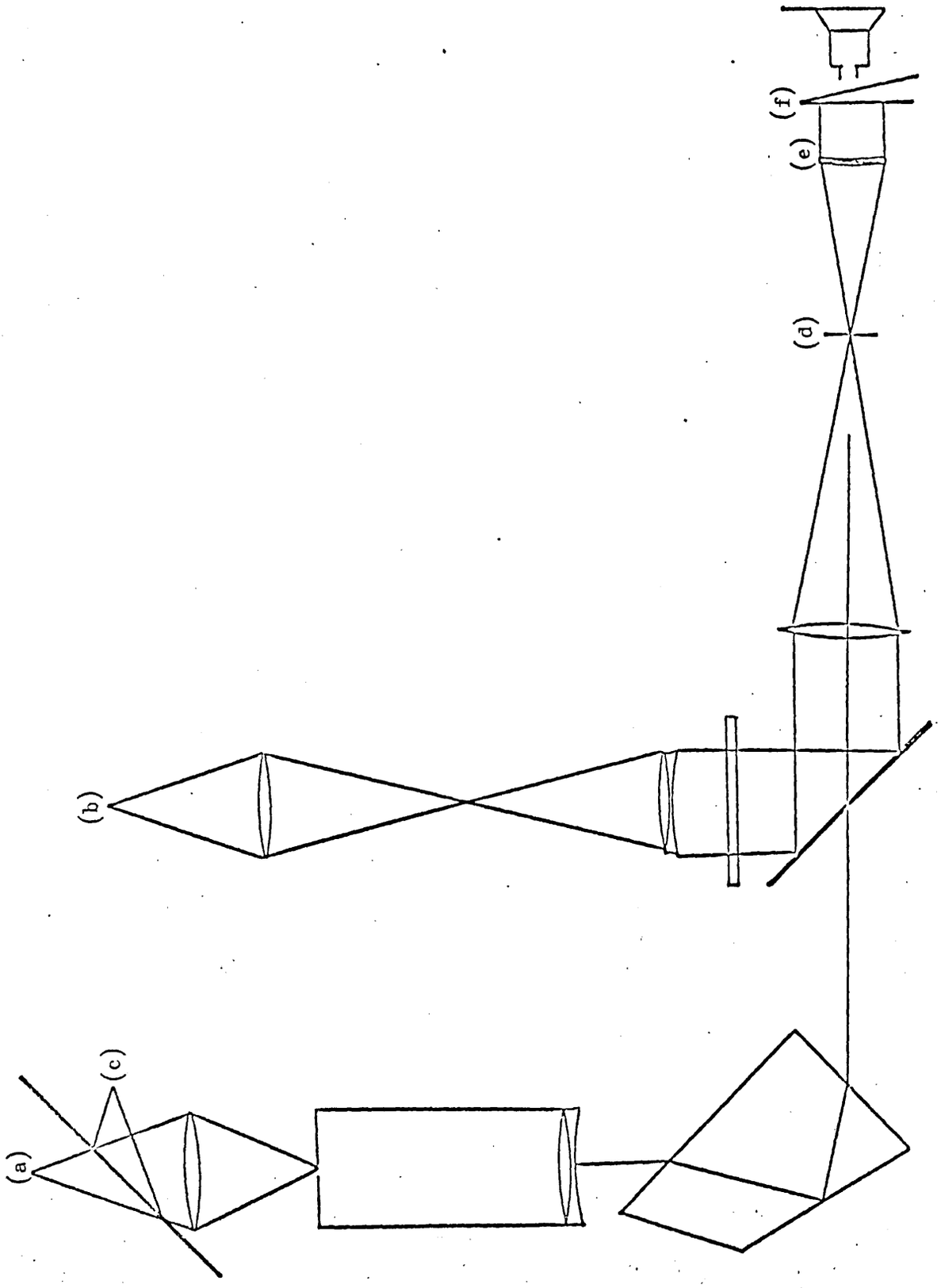

Fig.VIII.1

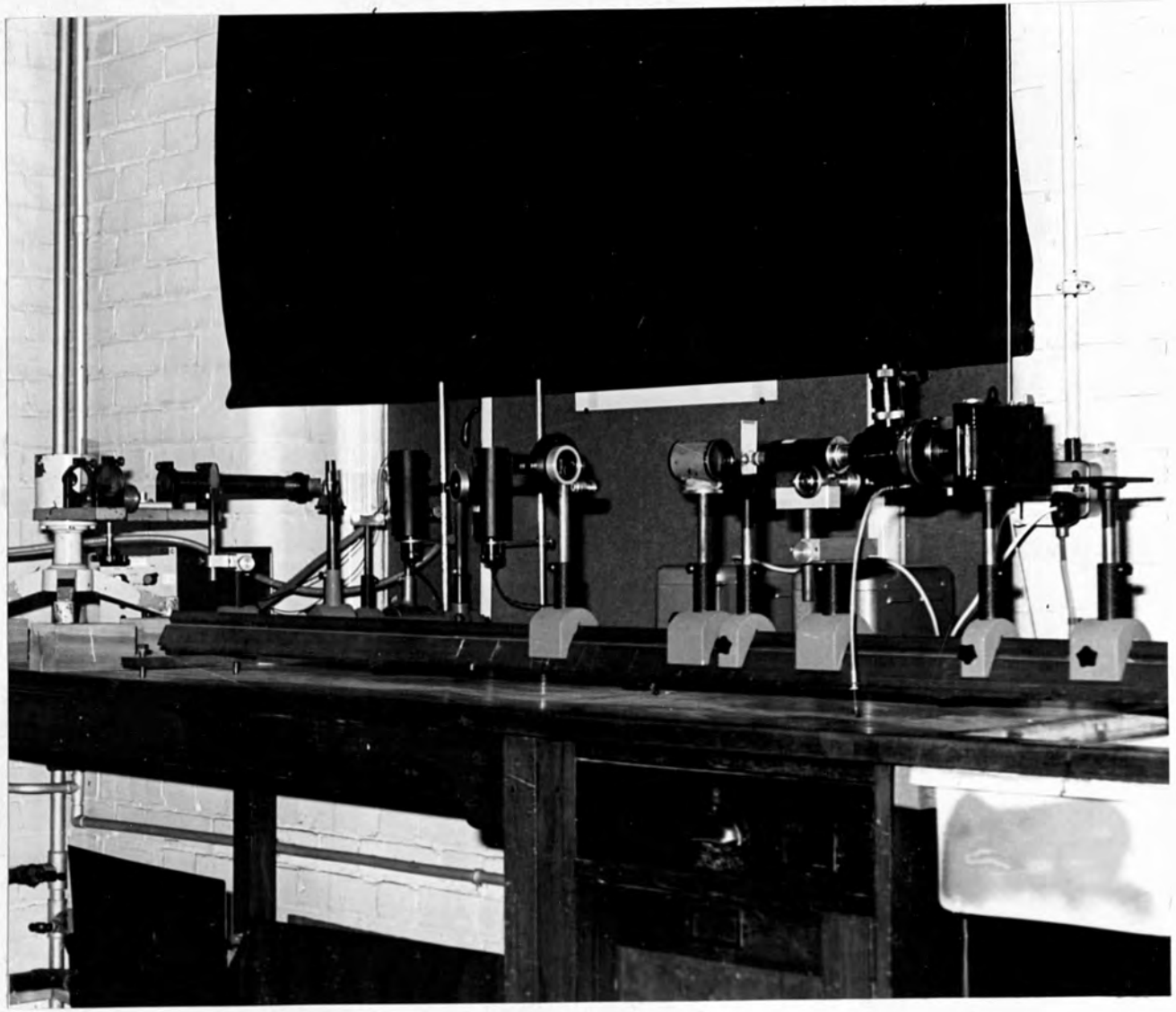

PLATE(24)

VIII.2 THE OPTICAL SYSTEM

The optical arrangement is shown, schematically, in Fig.VIII.1. Light from two sources falls, simultaneously, onto the test specimen via a rectangular slit. Source (a) was a white light quartz-iodine lamp. The white light was condensed onto the slit of a Hilger constant deviation spectrometer. The telescope arm of the spectrometer was removed and replaced by a simple bi-convex lens of focal length 100 cm. This arrangement produced a pure white light spectrum dispersed over a length of about 150 mm in the focal plane of the lens. A slit was placed in the plane of the spectrum and its width adjusted to 1 mm.

The extended spectrum contained some 3000 Å between its visible ends, and the slit selected a band of approximately 20 Å width. The wavelength of the light emerging from the slit was determined by reading, and varied by moving the calibrated drum of the constant deviation spectrometer. This arrangement allowed the formation of the 'sweeping fringe' to be moved from one end of the spectrum to the other, producing a variable colour fringe in the first order. The calibration of the spectrimeter drum was carried out with the aid of source (c) which emitted line spectra of known wavelengths covering the visible range. Light from the multichromatic source (b) was filtered, using a high quality narrow band all dielectric interference filter. This latter arrangement provided the 'stationary reference' fringe having a fixed wavelength determined by the peak transmission λ of the filter used.

When the drum calibration was carried out and thus rendering the length of the dispersed white light 'readable', the calibration source (c) was cut off. Now we would have the two sources (a) and (b) focused down on the slit (d) and a lens (e) rendered the emerging mixture parallel when it falls onto the test speciment (f). A microscope with a camera attachment were used to record the fringes. Plate (24) shows the actual experimental set-up.

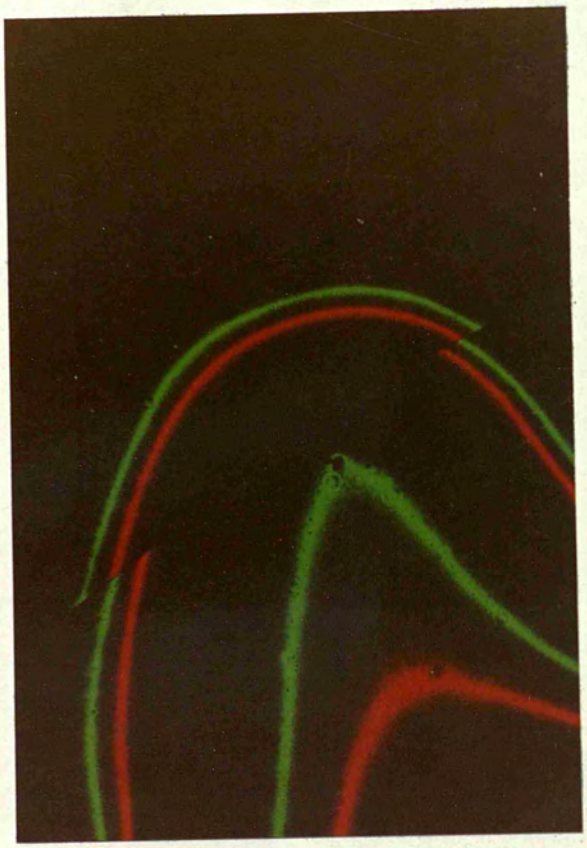

PLATE (25)

VIII.3 MEASUREMENTS ON MICA SURFACE

A clean freshly cleaved mica sheet was silvered on one side in the work chamber of the evaporation plant described in Chapter III. Simultaneously a microscope cover slip was introduced in the plant and was silvered to the same extent as the mica surface. This ensured that the two reflecting surfaces of the interferometer had the same reflectivity. The reflecting silver film had a thickness of the order of 380 Å giving reflectivity of about 0.85 for green mercury line 5460 Å.

Multiple-beam white light interference fringes were secured in the manner described in the last chapter. When the areas of close approach and the different orders were recognized, the test etalon was mounted in front of the microscope as in Plate (24) and Fig.VIII.1.

First, the test etalon was allowed to receive light from the multichromatic source (b) only. The filter used was a Barr and Stroud all dielectric interference filter with peak transmission at λ_1 5461 Å. The green 'stationary' fringe belonging to this wavelength was observed in the first and second orders. The first order fringe was a discontinuous contour ending abruptly at the edge of a cleavage step. Beyond the step the fringe continued, but was displaced at the edge of the step because of the sudden change in wedge thickness t. When light from source (a) was also, simultaneously, allowed to fall onto the interferometer and the drum of the constant deviation spectrometer was rotated, the resulting 'sweeping' fringe was made to join the 'stationary' fringe at the step edge. The final appearance was a continuous but two coloured contour. The wavelength at which the 'sweeping' fringe was made to align with the 'stationary' fringe was read on the spectrometer drum. This was found to be 6010 Å. Plate (25) shows the situation just described. The alignment was carried out with the aid of a cross-wire eyepiece.

The measurement of the height of the cleavage step could have, happily, ended here ! However, as shown in the last chapter, the considerations of the additional path difference introduced by the change of phase upon reflection at the Air/Ag interface inside the etalon, must be taken into account.

Schulz[57] measured the change of phase on reflection Air/Ag, as a function of the wavelength in the visible spectrum. His measurements were made on a silver film of thickness $d > 350$ Å which closely approximates to bulk properties. The equivalent path difference at the wavelengths λ_1 5461 Å and λ_2 6010 Å due to the change of phase at reflection Air/Ag, as taken from Schulz measurements, are 1020 Å and 980 Å respectively. These values will be adopted here for the purpose of calculating the mica cleavage step.

Now, we may write the following two relations for the heights of the interferometer contoured by the 'stationary' green fringe and the 'sweeping' orange-red fringe respectively:

$$t_{\lambda_1} = \frac{\lambda_1}{2} - \beta_{\lambda_1, d} \quad , \qquad \ldots \text{(VIII.1)}$$

$$t_{\lambda_2} = \frac{\lambda_2}{2} - \beta_{\lambda_2, d} \quad . \qquad \ldots \text{(VIII.2)}$$

The height of the mica cleavage step in plate (24) will be given by

$$t_{\lambda_2} - t_{\lambda_1} = \frac{\lambda_2 - \lambda_1}{2} - \left(\beta_{\lambda_2, d} - \beta_{\lambda_1, d}\right) \qquad \ldots \text{(VIII.3)}$$

where $\beta_{\lambda_1, d}$ and $\beta_{\lambda_2, d}$ are the equivalent path differences caused by the change of phase on reflection Air/Ag at the wavelengths $\lambda_1 = 5461$ Å and $\lambda_2 = 6010$ Å respectively.

$$\therefore \qquad (\Delta)t = \frac{6010 - 5461}{2} - (980 - 1020)$$

$$= \frac{549}{2} + 40$$

$$(\Delta)t = 314.5 \text{ Å}.$$

VIII.4 DISCUSSION

A new optical arrangement for producing multiple-beam fringes of variable chromaticity has been described. Since the order of interference is known to be unity, the ambiguity usually associated with order number in this kind of investigation has been removed. The use of a monochromator to provide variable chromaticity enables the contour to scan the whole visible spectral range within a known order. It might be useful to indicate here that the fringes described in this paper are Fizeau multiple-beam fringes in the first order. The principal advantage of these fringes over f.e.c.o. fringes, for example, is that a surface feature covered by a first or second-order white light system, can be explored visually in minute detail. In f.e.c.o. fringes, the system is essentially static and the order number has to be determined before the fringes could be interpreted. Another feature of the present system of fringes is that the shape of the topographical feature is detectable at a glance because the spectra tend to contour the narrower part of the wedge in the shorter wavelength region and the wider parts in the longer wavelength region.

The degree of precision which is to be expected from this technique depends on several factors:

(a) The quality of the fringes, i.e. their sharpness and visibility. This in turn depends on the high reflectivity of the surfaces involved.

(b) The width of source lines employed.

(c) The accuracy associated with the measurement of the quantity β.

(d) The accuracy with which the alignment of the two coloured parts of the fringe and the consistency of the drum readings at this point.

In the present work the fringe width was about $1/25$ of the order separation between orders one and two. As for the line width, the filter

used in connection with source (b) had a half-width of the order of 20 Å while the width of the line selected from the dispersed white light was determined by the width of the slit (d). The slit could select a band of approximately the same width as that transmitted by the filter as explained earlier in this chapter. The error in the quantity $\left(\beta_{\lambda_{2,d}} - \beta_{\lambda_{1,d}}\right)$ is not likely to be very much greater than ±7 Å. Schulz[57], mentions a probable uncertainty of ±15 Å in the measurement of individual values of β.

It was found to be possible to reset the drum of the monochromator (the modified Hilger constant deviation spectrometer) to better than ±8 Å. The maximum variability therefore associated with the term $\frac{\lambda_2 - \lambda_1}{2}$ was ±4 Å. It is therefore fair to say that the overall error in the measurement of the step height is not likely to exceed ±10 Å.

CHAPTER IX

FUTURE WORK

This is a short account of some ideas projected for future work.

It was the main target of this thesis to show that interferometric techniques could be still extended to cover new grounds and applications both in thin film optics and surface microtopography. The study of the sensitivity of the differential change of phase on reflection Air/Metallic film, Δ, showed that for thin films of $d \leq 200$ Å, Δ was sensitive to both n and k. This gives grounds to believe that a similar study on the more readily measurable quantities β and β' by techniques similar to those used by Baraket et al[55]. The author was a member of this research group at Egypt's National Research Centre when a wide range study was carried out on the optical phase properties of thin films. It is the intention to carry out these studies some steps further and use measurements of β and β' to deduce the optical constants of films studied in light of sensitivity charts. Quartz optics may be useful to extend the interferometric technique described in Chapter III to the ultra violet parts of the spectrum. In the sphere of surface microtopography it is envisaged that the optical system described in Chapter VII may be developed into an instrument using two dispersing elements, may be reflection gratings, to provide instant surveying at the exit slit of surface features of a specimen.

At this stage it may be proper to close this investigation with an Arabic phrase, which, I am sure, its English translation would not be very far from an existing English equivalent:

"Thou shall not say I know for you only try"

REFERENCES

(1) ARCHER, R.J., 'Manual of Ellipsometry', Gaerten Scientific Corporation, Chicago, U.S.A.

(2) DRUDE, P., 'Bestimmung der Optischen Konstanten der Metalle', Wied. Ann. Phys., 39, 481 (1890).
'Uber Oberflachenschichten, I und II' Wied. Ann. Phys., 30, 532,865 (1899).

(3) ABELES, F., 'Methods for Determining Optical Parameters of Thin Films', In Progress in Optics, 2, 250; edited by E. Wolf, North Holland Publishing Co., Amsterdam (1963).

(4) HEAVENS, O.S., 'Measurement of Optical Constants of Thin Films', In Physics of Thin Films, 2, 193; edited by G. Hass and R. Thun, Acad. Press, (1964).

(5) TOLANSKY, S., Phil. Mag., 35, 120 (1944).

(6) PHILIP, R. and TROMPETTE, J., C.R. Acad. Sci. Paris, 241, 627 (1955).

(7) AVERY, D., Phil. Mag., 61, 1018 (1950).

(8) TOLANSKY, S., J. de Phys. et le Radium, 11, 373 (1950).

(9) KOESTER, C.J., J. Res. Nat. Bur. Std., 64A, 191 (1960).

(10) BRUCE, C.F. and CIDDOR, P.E., J. Opt. Soc. Am., 50, 295 (1960).

(11) BOUSQUET, P., DELEUIL, R. and GASTAUD, A., J. Phys. (Paris), 25, 31 (1964).

(12) BARAKAT, N. and NOKHTAR, S., J. Opt. Soc. Am., 53, 1153 (1963).

(13) SCHULZ, L.G., J. Opt. Soc. Am., 44, 357 (1954).

(14) DRUDE, P., 'Theory of Optics', (1902), Dover Edition (1959).

(15) HEAVENS, O.S., 'Optical Properties of Thin Solid Films', Butterworth Scientfic Publications Ltd., (1955).

(16) BORN, H. and WOLF, E., 'Principles of Optics', Pergamon Press, (1970).

(17) SENNETT, R.S. and SCOTT, G.D., J. Opt. Soc. Am., 40, 203 (1950).

(18) RASIGNI, G. and ROUARD, P., J. Opt. Soc. Am., 53, 604 (1963).

(19) HADELY, L.N. and DENNISON, D.M., J. Opt. Soc. Am., 37, 451 (1947).

(20) SCHULZ, L.G., Adv. Phys. (Phil. Mag. Supp.), 6, 102 (1957).

(21) VASICEK, A., 'Ellipsometry in the Measurement of Surfaces and Thin Films', Nat. Bur. Std. Misc. Publ., 256, U.S. Government Printing Office, Washington, D.C., (1964).

(22) MEYER, G., Z. Physik, 168, 169 (1962).

(23) BERREMAN, D.W., J. Opt. Soc. Am., 60, 499 (1970).

(24) BERREMAN, D.W., Phys. Rev., 1B, 381 (1970).

(25) BENNET, H.E. and BENNET, J.H., 'Precision Measurements in Thin Film Optics', In Physics of Thin Films, 4, Acad.Press, (1967).

(26) McCRACKEN, F.L. and COLSON, J.P., In 'Ellipsometry in the Measurement of Surfaces and Thin Films', Nat. Bur. Std. Misc. Pub. 256. U.S. Government Printing Office, (1964).

(27) HUMPHREYS-OWEN, S.P.F., Proc. Phys. Soc. (London), 77, 949 (1960).

(28) WARD, L. and NAG, A., Brit. J. Appl. Phys., 18, 277 (1967).

(29) WARD, L. and NAG, A., Brit. J. Appl. Phys., 18, 1629 (1967).

(30) SHAALAN, M.S. and TAYLOR, A.J., 'Conference on Optical Properties of Thin Films', 24-26 September, 1973, University of Southampton.

(31) CAREY, R. and THOMAS, B.W.J., Phys. Bul., 24, July (1973).

(32) AVERY, D., Ph.D. Thesis, University of London, (1951).

(33) BARAKAT, N. and SHAALAN, M.S., Opt. Acta., 16, (3), 363-370 (1969).

(34) TOLANSKY, S., 'Introduction to Interferometry', Longmans, (1955).

(35) TOLANSKY, S., 'Multiple Beam Interferometry of Surfaces and Films', Oxford University Press, (1949).

(36) BROSSEL, J., Proc. Phys. Soc., 59, 226 (1947).

(37) BARAKAT, N. and MOKHTAR, S., J. Opt. Soc., 53, 300-301 (1963)

(38) HOLLAND, L., 'Vacuum Deposition of Thin Films', Chapman and Hall, (1956).

(39) TOLANSKY, S., 'Surface Microtopography', Wiley, (1960).

(40) LAURENT, Journ. de Physique, 2, 1892.

(41) HEAVENS, O.S., 'Optical Properties of Thin Film', In Rept. Prog. Phys., 23, 1, (1960).

(42) GEHRCKE, E., Interferenzen, p.39 (1906).

(43) HOLDEN, J., Proc. Phys. Soc., 62 B, (1949).

(44) KINOSITA, K., J. Phys. Soc. Japan, 8, (1953).

(45) MacLAURIN, R.C., 'The Theory of Light I', 241-250 (1908).

(46) SCANDONE, F. and BALLERINI, L., Nuovo Cimento, pp.81-115 (1945).

(47) CLEGG, P.L., Proc. Phys. Soc. B., 65, 774 (1952).

(48) SCHULZ, L. and SCHEINBER, E., J. Opt. Soc. Am., 40, 761 (1950)

(49) SCHULZ, L., J. Opt. Soc. Am., 41, 1047 (1951).

(50) KOEHLER, W., J. Opt. Soc. Am., 43, 738 (1953).

(51) KOESTER, C., J. Opt. Soc. Am., 48, 255 (1958).

(52) WEAVER, C., et al., J. Opt. Soc. Am., 49, 994 (1959).

(53) BRUCE, C. and CIDDOR, P., J. Opt. Soc. Am., 50, 295 (1960).

(54) CIDDOR, P., Opt. Acta, 7, 399 (1960).

(55) BARAKAT, N. et al., J. Opt. Soc. Am., 54, 213-216 (1964).

(56) PHILIP, R., C.R. Acad. Sci., Paris, 243, 365 (1956).

(57) SCHULZ, L., J. Opt. Soc. Am., 41, 261, (1951).

(58) TOLANSKY, S., Lab. Practice, 21, 621-623 (1972).

(59) HERRIOT, D.R., J.O.S.A., 51, 1142-1145 (1961).

The material contained in Chapters VII and VIII was accepted for publication in Journal 'D' of the Institute of Physics.

ABSTRACT OF PAPER PRESENTED

AT

THE INSTITUTE OF PHYSICS CONFERENCE

ON

THE OPTICAL PROPERTIES OF THIN FILMS

UNIVERSITY OF SOUTHAMPTON 1973

INTERFEROMETRIC DETERMINATION OF THE EXTINCTION COEFFICIENT k OF HIGHLY REFLECTING METALLIC FILMS

M S Shalaan and A J Taylor
Department of Physics
Royal Holloway College
University of London
Egham Hill, Egham
Surrey, TW20 0EX

ABSTRACT

Tolansky (1944) used multiple beam interference fringes produced by an air wedge to determine the differential phase change at reflection Δ ($\Delta = \delta_p - \delta_s$). The method is used to find k, the extinction coefficient of the coating films of the interferometer. A computer programme is used to draw curves of Δ versus refractive index n for constant values of k, (n and k are defined by $\hat{n} = n - ik$), for a given film thickness, wavelength and angle of incidence.

The quantity Δ is obtained at a number of angles of incidence, and values of k may be deduced from the computed curves. If Δ is accurate to $\pm$ 0.003 π then k may be determined to within $\pm$ 0.03 . for values of $2.0 < k < 5.0$, providing n is in the range $0.05 < n < 3.0$. The method is suitable for film thicknesses greater than 300 Å.

This technique is not suitable for determining accurate values of n because of the insensitivity of Δ to n. To demonstrate the method, values of k for films of silver, aluminium and gold have been obtained for wavelengths in the visible region.

OPTICA ACTA, 1969, VOL. 16, NO. 3, 363–370

Phase modulation of the first beam in multiple-beam transmitted systems

N. BARAKAT
Ain Shams University, Cairo, U.A.R.

M. S. SHAALAN
National Standardization Centre, Cairo, U.A.R.

(*Received* 30 *April* 1968; *revision received* 21 *October* 1968)

Abstract. The phase of the first beam in multiple-beam fringes in transmission has been altered by introducing a phase plate in its path. Reflection-like fringes in transmission result when the phase angle introduced is close to π.

The resulting fringes which appear as sharp dark lines with I_{min} close to zero on a bright background are found suitable for determining the differential change of phase at reflection of the P and S components of light vibrations, for metallic films whose reflectivities range from 35 per cent to 60 per cent. Differential change of phase at reflection has been determined for Ag films whose thicknesses range from 100 to 200 Å.

1. Introduction

Multiple-beam fringes are altered by introducing an additional phase delay in one of the beams contributing to the formation of the fringes. This may be accompanied by a change in amplitude. This alters the intensity distribution of the fringe system in a way which depends upon the value and sign of the phase angle introduced, the order of the beam modulated and the accompanying change (if any) in its amplitude. Modulation of multiple-beam interference fringes at reflection was performed [1] and applied to determine the change of phase in transmission through very thin layers of silver.

In this work the first beam contributing in the formation of multiple-beam fringes in transmission has been modulated by introducing a phase plate in the path of the first beam. The resulting fringe system appears as sharp dark lines on a bright background, which is termed ' reflection-like fringes in transmission '. These fringes are found to be superior in sharpness and visibility to the unmodulated transmitted system when metallic coatings of low reflectivity are used. Interferometric methods using ordinary multiple-beam fringes for differential change of phase measurement are applicable only when the resulting fringes are sharp. This takes place only when highly reflecting metallic films of reflectivity more than 80 per cent are under investigation. This is why all previous investigators using interference fringes were restricted to absorbing films of reflectivity more than 80 per cent. This also explains why no reliable previous data on the determination of differential change of phase for thin metallic films of reflectivity range 35–60 per cent have been reported in the literature.

2. Theory

In the following the effect of adding a phase angle ϕ to the first transmitted beam, on the distribution of intensity in a multi-beam transmitted system, is discussed. The case considered is the case of an Airy summation.

R_T = resultant wave of multiple beams in the case of a Fabry–Perot interferometer,

$$= T \exp i(\omega t + 2\gamma) + TR \exp i(\omega t + 2\gamma - \delta) + \ldots$$

$$= A_T \exp i(\omega t + 2\gamma - \Delta),$$

where δ is the phase difference between any two successive beams, γ is the phase change due to transmission through *one* film, Δ is the phase difference of resultant w.r.t. the first transmitted beam and

$$\tan \Delta = \frac{R \sin \delta}{1 - R \cos \delta}.$$

In figure 1 OC represents the resultant of all beams, O*b* represents the first transmitted beam and *bc* represents the resultant of all beams except the first.

$$\overline{bc}^2 = A_T^2 + T^2 - 2A_T \cdot T \cos \Delta.$$

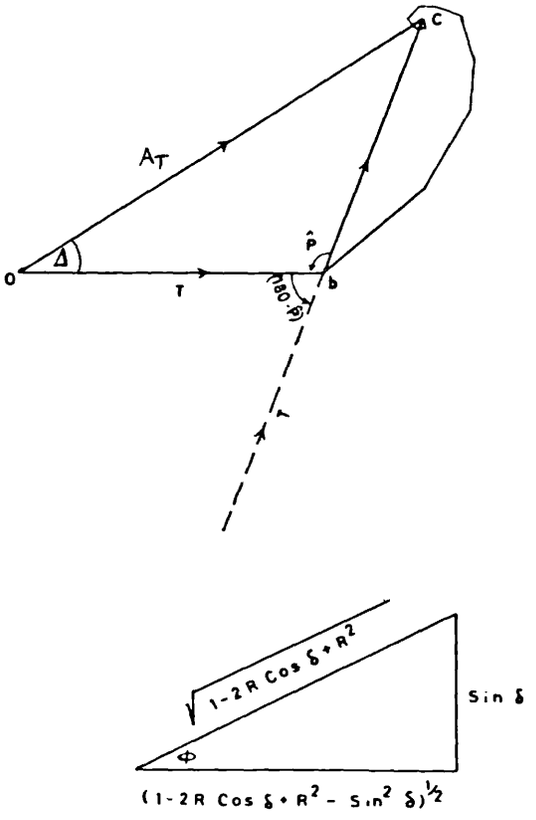

Figure 1.

The amplitude of the resultant of all beams other than the first is:

$$\frac{TR}{\sqrt{(1-2R\cos\delta+R^2)}}.$$

Now in the triangle Obc:

$$\sin cbO=\sin P=\frac{\sin\delta}{\sqrt{(1-2R\cos\delta+R^2)}}.$$

It is clear from the diagram that the maximum intensity is achieved from an angle δ when the phase of the first transmitted beam is altered by $(180-P)°$, while alteration by $(360-P)°$ brings the two vectors along the same line but with opposite directions giving minimum intensity.

If the phase of the first transmitted beam is delayed by an angle ϕ, the resultant transmitted intensity is given by:

$$\left.\begin{aligned} I_R&=T^2+\frac{T^2R^2}{1-2R\cos\delta+R^2}-\frac{2T^2R}{\sqrt{(1-2R\cos\delta+R^2)}}.\cos(P+\phi),\\ I_R&=T^2+\frac{T^2R^2}{1-2R\cos\delta+R^2}-\frac{2T^2R}{1-2R\cos\delta+R^2}(\cos\phi(R-\cos\delta)-\sin\phi\sin\delta). \end{aligned}\right\} \quad (1)$$

This equation gives the intensity distribution for any value of the angle of modulation ϕ for all values of δ when T and R are known from the properties of the coating layers when $\phi=180°$.

Therefore

$$I=2T^2-\frac{2T^2R^2-T^2}{1-2R\cos\delta+R^2}. \quad (2)$$

Accordingly, if $(A+B)=2T^2$ and $C=T^2(1-2R^2)$, then

$$I=A+B-\frac{C}{1-2R\cos\delta+R^2}.$$

Now if

$$A+B\geqslant\frac{C}{(1-R)^2},$$

C being positive, we get an intensity distribution similar to the reflected system in multiple-beam fringes, with

$$I_{\min}=A+B-\frac{C}{(1-R)^2},\quad \delta=2n\pi,$$

$$I_{\max}=A+B-\frac{C}{(1+R)^2},\quad \delta=(2n+1)\pi.$$

Intensity distribution and visibility of fringes

The conditions for having a reflected system are:

$$2T^2\geqslant T^2\frac{(1-2R^2)}{(1-R)^2}\quad\text{and}\quad R^2<\tfrac{1}{2}.$$

For such a system of reflection-like fringes in transmission:

$$I_{\min}=T^2\left(\frac{1-2R}{1-R}\right)^2.$$

An interesting case arises, giving $I_{\min}=0$; the condition is:

$$A+B=\frac{C}{(1-R)^2}.$$

The value of R satisfying this condition is equal to $\frac{1}{2}$:

$$I_{\max}=T^2\left(\frac{1+2R}{1+R}\right)^2.$$

The visibility of fringes in the particular case of $R=\frac{1}{2}$ will be equal to unity. As R increases, C decreases and is equal to zero as $R=1/\sqrt{2}$. In this case equation (2) becomes $I=A+B=2T^2$, i.e. independent of the phase angle δ. A uniform background (of magnitude equal to $2T^2$ for $R=71$ per cent) appears in the field of view. As R increases further, C is no longer positive and the equation of intensity becomes

$$I=A+B+\frac{|C|}{1-2R\cos+R^2},$$

$|C|$ being the numerical value. This is the intensity distribution of a transmitted system of

$$I_{\max}=\frac{|C|}{(1-R)^2} \quad \text{and} \quad I_{\min}=\frac{|C|}{(1+R)^2}$$

at $\delta=2n\pi$ and $(2n+1)\pi$ respectively. This will be superimposed on a background of magnitude equal to $(A+B)$.

3. Production of reflection-like fringes in transmission

The optical set-up used to investigate the effect of introducing an additional phase to the first beam is shown in figure 2. Two optical flats of diameter 60 mm and thickness 11 mm were coated with thin evaporated silver layers of reflectivities R_1 and R_2 where $\sqrt{(R_1R_2)}=63$ per cent. The two optical flats were used to form a silvered air wedge of angle $\epsilon=0{\cdot}0002$ rad. The wedge was adjusted with its edge parallel to the vertical slit S'. A monochromatic source of $\lambda=5461$ Å was used to illuminate the wedge with parallel light. At the focal plane of the projection lens L_3 successive images of the slit S' appeared.

Plate 1 shows the appearance of these images. The microscope objective was moved back to position B until the usual multiple-beam transmitted system was in focus. Plate 2 shows the transmitted system of bright fringes on a dark background. To investigate the effect of introducing an additional phase to the first beam, a MgF_2 layer of thickness 6687 Å on a glass substrate was introduced in the path of the first image and adjusted to make an angle of 45° with the optical axis. The phase angle introduced was calculated using the formula

$$\phi=\frac{2\pi}{\lambda}(\mu_\lambda-1)\frac{t}{\cos 32^\circ},$$

where t is the thickness of the MgF_2 layer and μ_λ is its refractive index. A change in the intensity distribution of the transmitted system was observed and recorded photographically as shown in plate 3. It is a reflected system with relatively sharp dark lines on a bright background. They are termed here 'reflection-like fringes in transmission'.

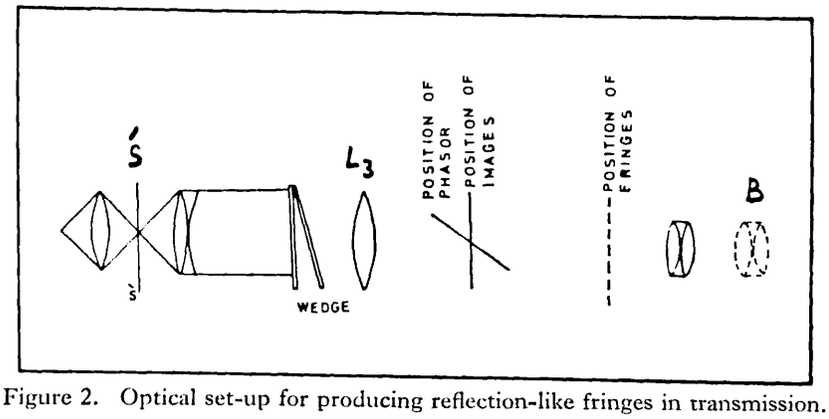

Figure 2. Optical set-up for producing reflection-like fringes in transmission.

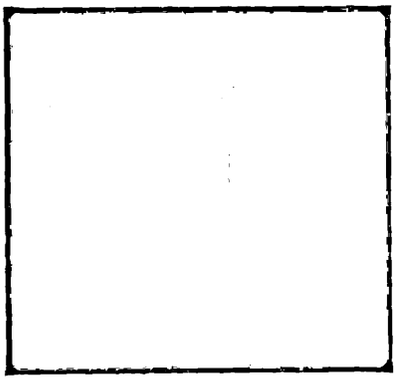

Plate 1.

Plate 2.

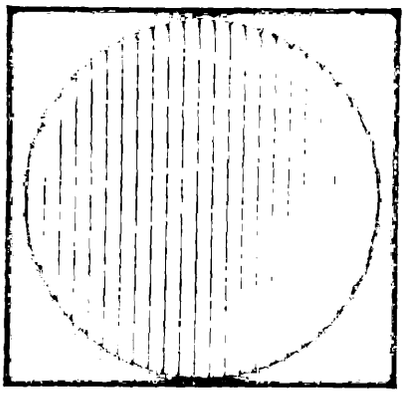

Plate 3.

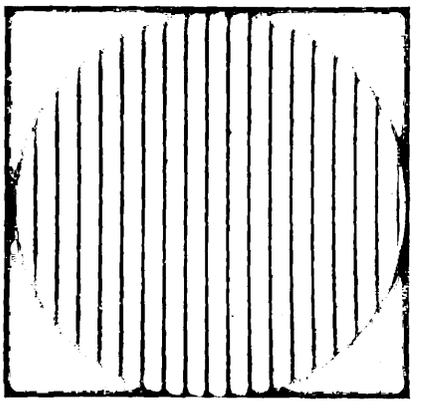

Plate 4.

The effect of reflectivity of the coating layer on the intensity distribution of reflection-like fringes has been investigated experimentally using silvered air wedges of reflectivities ranging from 40 per cent to 80 per cent. Observations are found to be in complete agreement with theoretical deductions reached before. In the previous experiments the phase plate was adjusted so that only the first image passed through it while the rest of the images were viewed through glass. The condition for maximum visibility in reflection-like fringes in transmission has been verified experimentally. In this experiment two optical flats were coated with silver layers of reflectivity = 50 per cent. Plate 4 shows the reflection-like fringes in transmission resulting. The experimental value of visibility was 0·98.

4. Determination of differential change of phase at reflection for silver layers over the range 100–200 Å thick

Tolansky [2] applied multiple-beam fringes for the measurement of differential change of phase at reflection. He used a silvered lens/plate interferometer and multiple-beam fringes in transmission. The thickness of the Ag layer was over 350 Å. His results were in accordance with theoretical calculations based on

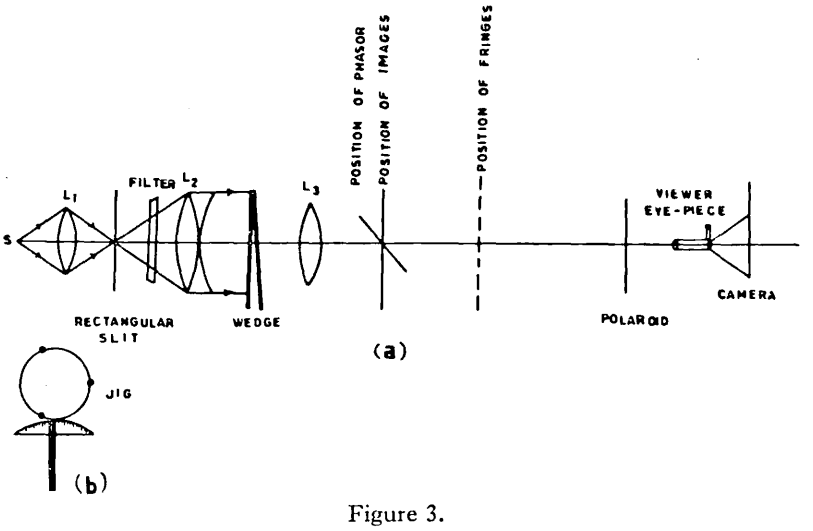

Figure 3.

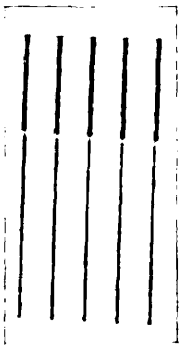

Plate 5.

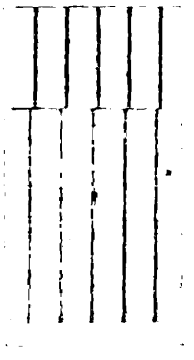

Plate 6.

assuming the Ag layer to be of the same optical constants as the bulk metal. The formulae were deduced from the electromagnetic theory. Avery [3] extended the interferometric method for measuring the differential change of phase at reflection to a number of layers, namely silver, copper and tin. He used an air wedge coated with evaporated layers of the metals previously mentioned. His technique was applied only to multiple-beam Fizeau fringes and fringes of equal chromatic order in transmission. His measurements included the differential change of phase at reflection for Ag layers of high and low reflectivities. He claimed that displacements between resolved components for R as low as 30 per cent, at high angles of incidence, were measurable using the transmitted system.

In this work the differential change of phase at reflection air/Ag is measured for Ag layers of low reflectivity with thickness between 100 and 200 Å. The low reflectivity made it necessary to modify the interferometric method. The solution was found in applying multiple-beam reflection-like fringes in transmission obtained by the method described above. The optical arrangement for recording the fringe shift of reflection-like fringes due to differential change of phase over the incidence range 0–50° is shown in figure 3. Two optical flats were coated with identical silver films of $R=60$ per cent and thickness 185 Å. Thickness measurement was carried out using multiple-beam Fizeau fringes at reflection. The wedge was adjusted with its edge parallel to the rectangular slit S. The usual fringes in transmission were then obtained. When the phase plate was introduced in the path of the first beam, the result was a reflection-like system of fringes.

Plates 5 and 6 show reflection-like fringes due to the P and S components of angles of incidence at 25 and 35° respectively.

At angle 25° no shift was observed. A double shutter was used to record each component separately. The same steps were carried out for silver films of thickness 155, 135 and 105 Å. The fringe shift $\Delta y/y$ was measured using an Abbé comparator. The differential change of phase was then calculated as a fraction of λ using the relation:

$$\Delta=(\delta_p-\delta_s)=\frac{\Delta y}{y}\cdot\frac{\lambda}{2},$$

where y is the distance between any two successive fringes.

5. Results and discussion

Figure 4 shows the variation of the differential change of phase at reflection as a function of λ with the angle of incidence. The main features of the curves are:

(*a*) Minima at angle of incidence 25° appeared in the four Ag films examined and reached almost zero shift.

(*b*) Maxima at angle of incidence 35° appeared in the four cases. The experimental curves of the differential change of phase Δ versus the angle of incidence for evaporated Ag films of thickness range 100–200 Å showed the presence of zero value at $\theta=25°$ followed by a maximum value of Δ at $\theta=35°$ followed by a maximum then gradual increase of Δ with θ. Such behaviour of Δ of this type of film is completely different from that of thick films of thickness more than 350 Å for the case of Ag. The experimental curve for Δ versus θ

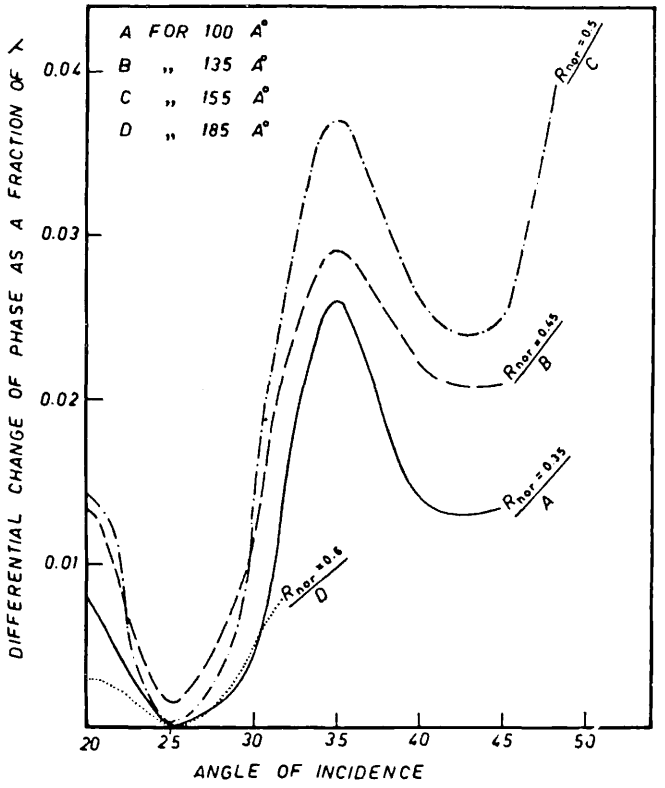

Figure 4.

carried out by previous investigators showed a gradual but slow increase of Δ with θ up to some 40° then a quicker increase continues up to $\theta = 80°$ for evaporated Ag films of thickness > 350 Å. No maxima or minima were reported.

On peut modifier la phase du premier rayon dans le cas des interférences à ondes multiples par l'introduction d'une lame de phase sur son trajet. Lorsque le déphasage ainsi introduit est voisin de π, on obtient par transmission un système de franges analogue aux franges par réflexion.

Les franges ainsi obtenues, qui apparaissent comme des lignes obscures et fines avec I_{min} voisin de zéro sur fond clair sont utiles pour déterminer la variation de phase différentielle des composantes P et S des vibrations lumineuses pour des couches métalliques dont les réflectances sont comprises entre 0,35 et 0,60. Le déphasage à la réflexiona été déterminé pour des couches d'argent dont les épaisseurs sont comprises entre 100 et 200 Å.

Durch Einführen einer Phasenplatte in das erste Strahlenbündel eines Vielstrahl-Interferometers werden die Phasen der Streifen verschoben. Es entstehen in Transmission Streifen, die denen in Reflektion ähneln, wenn der eingeführte Phasenwinkel nahe bei π liegt.

Die erhaltenen Streifen erscheinen als scharfe dunkle Linien mit einem I_{min} nahe bei Null auf hellem Grunde und eignen sich gut zur Bestimmung der Phasenverschiebung in der P- und S-Komponente der Lichterregung für metallische Schichten mit einem Reflektionsvermögen zwischen 35 und 60 Prozent. Man kann auch die Phasenverschiebung bei der Reflektion an Silberschichten mit Dicken von 100 bis 200 Å bestimmen.

References

[1] Barakat, N., and Abu Zakham, F. G., 1965, *Optica Acta*, **12**, 321.
[2] Tolansky, S., 1944, *Phil. Mag.*, **35**, 120.
[3] Avery, D., 1950, *Phil. Mag.*, **61**, 1018.

E R R A T A

Page	Line	Reads	Should read
9	29	differen-	differential
17	10	micritopography	microtopography
19	14	change	charge
19	26	(I.5)	(I.8)
20	1	delete [k = (nk) ..... coefficient]	
25	29	wavelengths	wavelength
26	3	$k \gg n$	$k > n$
26	9	delat	dealt
29	6	dscribe	describe
74	24	dimater	diameter
83	14	belinging	belonging